STREAMFLOW MODELLING

by

P. KOLOVOPOULOS

Water Systems Research Group
University of the Witwatersrand
Johannesburg, 2000, South Africa

Water Systems Research Group
Report No. 7
1990

Report to the Water Research Commission on the Project
"Effects on Urbanization on Catchment Water Balance"

Head of Department
and Project Leader : Professor D. Stephenson

WRC REPORT NO. 183/7/93
ISBN 1 86845 035 X
ISBN SET NO. 1 86845 040 6

WATER RESEARCH COMMISSION

EFFECTS OF URBANIZATION ON CATCHMENT WATER BALANCE

LIST OF REPORTS

Report No.	Title	By
1	Analysis of effects of urbanization on runoff	D. Stephenson
2	Description of catchments and methodology	J.J.Lambourne T. Coleman
3	Geohydrology of Catchments	W.A.J. Paling D. Stephenson
4	A hydrometeorological data management package Wits Data Management System WITDMS	J.J. Lambourne
5	The effect of storm patterns on runoff	N. Patrick
6	Runoff Modelling	A. Holden
7	Streamflow modelling	P.Kolovopoulos
8	Runoff management modelling	T. Coleman D. Stephenson
9	Catchment water balance	J.J. Lambourne F. Sutherland
10	Urban Runoff Quality & Modelling Methods	T. Coleman
11	Compendium of papers published on the research	
12	Executive Summary	D. Stephenson

ABSTRACT

The recent floods in South Africa emphasised the need for research into a reliable model for flood routing, general flood plain modelling and a more accurate method for the determination of flood lines. The objectives of this dissertation were therefore set as:

- The development of an operational system for the simulation of unsteady flow in open channels.
- The study of wave propagation in channels and the identification of the pertinent parameters that affect it.
- The assessment of the applicability of existing flood routing models and development of a model for the accurate routing of floods in compound channels. The channel-flood plain interaction must be taken into account.

A one-dimensional model for the general simulation of flow in looped or branched open channels has been developed. It enables hydrologists to model a river with its tributaries, inundated plains, diversions etc. This resulted in a suite of programs, which concentrate on micro-computer compatibility, operational data-handling structure, a user-friendly interface, and interactive operation.

The algorithm structure of the model was developed after a variety of procedures were tested in terms of accuracy, computational speed , storage requirements and flexibility. A new, stable discretization scheme has been developed based on the solution of a box scheme of the Preismann type. A looped algorithm technique coupled with the double sweep method is employed to reduce machine memory and execution time requirements. Practical applications demonstrated the capability of the model to handle different types of flow and complicated river configurations both in South Africa and abroad. The model proved to be capable of simulating, with minimal distortion, a wide range of unsteady flows, tidal flows and regulated flows encountered in prototype channels.

The model is used as a tool for the study of flood propagation in prismatic and compound channels. Methods for the routing of hydrographs, when the downstream boundary condition is not available, were tested and compared in terms of speed and range of applicability. The suite of models was coupled with a non-linear kinematic model and the developed wave models were tested against published data.

Wave subsidence was extensively studied. Applying the small perturbation analysis the spectrum of shallow water waves was divided into bands, taking into account the predominant physical mechanisms and the attenuation characteristics of the waves. The theoretical findings were tested using the newly developed model and practical criteria for determining the applicability of each wave model were derived. Graphs were developed which assist the analyst in identifying, prior to the routing, the dominant mechanisms responsible for wave subsidence, the appropriate approximation model, or provide a qualitative knowledge of the quantity of subsidence expected.

A parametric study was applied in order to investigate the effect of the wave parameters on the damping of flood waves in prismatic channels in conjunction with the defined practical criteria. From the analysis it was concluded that the pertinent parameters that affect the wave subsidence are the wave duration and the slope. Other factors such as the wave amplitude and the time to peak, have only a minor influence on subsidence. It was also shown that wave damping is affected by the model's numerical solution and the truncation errors.

The research was extended to compound channels, with emphasis on the evaluation of the dynamic effect of the flood plain flow, and the modelling of momentum transfer between the main channel and the flood plain. The mechanism of momentum transfer was initially analysed under steady-state conditions. From the evaluation of various methods, it was concluded that the area method is the most promising discharge computation method and that the Prinos model gives the most accurate results for the apparent shear force at the 'main channel-flood plain' interface. The two models were modified and the results of the analysis were extrapolated under unsteady flow conditions. The unsteady flow model facilitated the investigation of the significance of the momentum transfer phenomenon in natural channels and the specific parameters that affect it. The analysis showed that the momentum exchange, results in a shift of the loop rating curve, a delay in the falling of water levels, an increase in the flood plain flow and a decrease of the main channel carrying capacity.

A parametric analysis was used to study the effect of the momentum transfer mechanism in relation to the channel parameters. The analysis indicated that in most natural channels, the phenomenon of the 'main channel-flood plain' interaction can safely be ignored and any of the conventional flood routing models can be used. However, for flat rivers with smooth boundaries and relatively small main channel, width to depth ratios, conventional models can give erroneous results.

An analysis of the existing conventional models was also performed. The separate channel model and the off-channel model were compared in terms of computed hydrograph peaks and attenuation times. It was concluded that the storage method may overestimate the peak water levels considerably while flowrates are underestimated. The findings of this dissertation provide a reliable model and guidelines for more accurate modelling of flood routing in natural rivers.

TABLE OF CONTENTS

VOLUME II

LIST OF ILLUSTRATIONS

1.0 INTRODUCTION

1.1 GENERAL REVIEW OF THE DEVELOPMENT OF UNSTEADY FLOW MODELS

The ability to accurately predict the movement of flood waves is of importance to river engineers and managers. In the design of hydraulic structures, river improvement works and flood protection and warning schemes, a knowledge of the water levels and discharge is essential. In many streams and rivers, flows can be accurately and economically determined using steady-flow concepts. This involves simplifications which while conceptually and analytically appealing, fails to provide a sound basis from which to fully analyse and accurately determine the flows or water levels. These flows are in fact, transient in nature, as is the case for the regulated flows occurring in some rivers and the periodic, unsteady flows prevailing in estuaries. The increasing demand for accurate information has focused attention on the need for thoroughly understanding the dynamics of unsteady flows in such waterways. This is reflected in the large amount of research effort which has been expended over many years in the area of flood routing and river modelling.

Although the subject of unsteady open-channel flow covers many disciplines, it involves four major fields of study: open channel flow, unsteady-flow hydrodynamics (or hydraulic transients), mathematics and numerical analysis, and computer modelling and simulation. The terms 'unsteady flows' and 'transient flows' are used interchangeably to denote both temporal and spatial variations in depth and in the velocities of the water particles.

The early development of mathematical models was limited to relatively simple types, primarily to avoid the complicated analytical techniques associated with the use of more complex methods. Thus, approximate numerical solution methods were introduced, thereby resulting in the **numerical simulation model** or the **computational model**. However, the amount of labour involved with such iterative methods generally exceeded the feasible capabilities of manual calculation and barred further progress. The advent of efficient high speed digital computers removed this barrier and allowed a fuller application of the simpler models.

Advances in the theory and application of numerical methods for solving the systems of partial differential equations of flow and transport have also had a profound impact on modelling techniques during the past two decades. As a consequence, numerical simulation modelling today, is synonymous with **computer simulation modelling** or simply computer modelling (Lai et al., 1978). Thus modelling and simulation are the relationships which link three major elements: prototype, model, and computer. Modelling is primarily concerned with the relationship between the prototype and the model, while simulation refers mainly to the relationship between the model and the computer (Clarke, 1973).

Computer modelling and simulation begins with the selection, examination, or derivation of basic partial differential equations to properly describe the unsteady flow of interest. The one-dimensional, gradually varied, unsteady flow equations, commonly referred to as **Saint Venant equations** constitute a set of quasilinear partial differential equations, and have been known for over 100 years. Flood routing involves, essentially, a solution of these equations and the methods proposed for this have been many and varied. The complexity and mathematical intractability of the equations, led many researchers to investigate them in simplified forms, observing that in most instances certain of the terms in the dynamic equation were much smaller than others and could be ignored. These approaches, which include the storage routing methods (based upon the continuity equation) and diffusion methods, generally have the advantage of ease of solution and rapid analysis. They are, however, approximate, and in many instances the assumptions upon which they are based are not valid. Sufficiently accurate solutions can therefore not always be obtained.

With the development of the modern computer, solution of the complete Saint Venant equations by numerical methods has become a more practical proposition. Much research has been directed towards this end in recent years, and this has led to the development of a number of well tested and understood methods of solution. In the field of flood waves, Stoker pioneered the use of finite difference equations in the study of floods on the Ohio river (Stoker, 1953; Isaacson et al.,1958).

Until the seventies there was a spate of publications on the use of numerical analysis in flood routing. Examples of these works are: Flood waves in natural waterways (Baltzer and Lai, 1968);flood routing in an irregular channel (Fletcher et al., 1967); finite-difference solutions of the shallow water equation (Ligget and Woolhiser, 1967);the stability of finite difference equations (Perkins, 1967) etc. All of these efforts had been directed toward gradual variations in flow. Martin and DeFazio (1969) demonstrated that the simple finite-difference equation developed by Stoker could be adapted to many open-channel wave problems involving flows from gradually-varied to rapidly varied form.

During the seventies the science of mathematical modelling in hydraulics was dominated by the work of the Grenoble school, the Danish Institute and the Delft Institute. Preismann and his associates in Grenoble, Abbot in the Danish Institute and researchers such as Cunge at the Delft Institute developed 'schemes', 'tricks' and methods that formed the basis for many of the solutions of unsteady flow problems. Their experience on the simulation of unsteady flows led to the development between 1972 and 1980 of **modelling systems**. As Cunge et al. (1981) define it, such systems comprise all the programmed procedure (software) necessary to construct and operate models of a river with its tributaries, inundated plains, and existing and future structures including dykes, dams, canals etc The engineer using such a system would only be concerned with the physical aspect of the problem, just as the user of a scale model would be. Two very well known systems are: SOGREAH'S CARIBA system (SOGREAH, 1978) and the Danish Hydraulic Institute's SIVA System 21 (Abbot, 1979).

In South Africa, Weiss and Midgley (1978) developed a similar system which comprised of a suite of mathematical flood-plain models. The suite of models can be used to simulate the rise and fall of flood waters, the flow velocities and the degree of scour or sediment deposition at any part of the flood plain during events covering a wide range of severity. In North America the U.S. Geological Survey developed an operational system for simulation modelling (Lai et al., 1978). The system is designed so that it may be used with a variety of one-, two-, and three- dimensional models. During the eighties numerous mathematical models have appeared, the modelling capability has expanded, and the types of analysis of the various flow problems have been greatly altered since the advent of the modern computer. In spite of the rapid advancement of the capability and capacity of today's micro-computers, the majority of the systems for the simulation of unsteady flow are operating on main-frame computers.

1.2 FLOOD ROUTING METHODS

The wide variety of hydraulic methods of channel routing provide a bewildering choice for the potential user. These methods can be classified into three groups:

- (a) **Hydrological** or **storage** methods.
- (b) **Approximation** methods or simplifications of the full Saint Venant equations.
- (c) Methods using a numerical solution of the full Saint Venant equations for gradually varying flow in open channels.

The term **hydrological methods** is applied to all methods of channel routing in which a channel reach is treated as a lumped system and the momentum equation replaced either by a 'black box' representation or by a conceptual model. They are termed 'hydrological methods' because they concentrate on the concept of storage for the flood water and do not directly include the effects of resistance to the flow. Such methods can be used even when nothing is known about the topographical or roughness characteristics of the intermediate channel sections. One of the most popular methods of this type is known as the **Muskingum method,** which was developed by McCarthy (1938). The method uses the linear relationship:

$$S = K\ \{\varepsilon Q_1+(1-\varepsilon)Q_0\} \tag{1.1}$$

where

K , ε : Muskingum parameters

Q_1, Q_0: inflow and outflow at the downstream and upstream sections respectively

S : storage

Despite the popularity of the method, it has many disadvantages such as:

- The equations of motion do not strictly justify the belief that the storage is determined by inflow Q_I and outflow Q_0 alone. It can be shown (Henderson, 1966) that the method is justified only in very steep rivers. In this case, the flood wave has certain very simple properties and all the terms, except the slope, in the momentum equation can be ignored.

- All the hydrological methods assume a unique relationship between the stage and the discharge along the reach (Natural Environmental Research Council, 1975). This is contrary to observations of natural floods which show that the discharge for a particular stage, when the flood-level is increasing, is greater than the discharge for the same stage, when the flood-level is decreasing. The phenomenon will be analysed in more detail in Chapter 7 and illustrated graphically in the model applications section by plotting the well-known loop-rating curves.

Because of the inaccuracies due to the approximations of the hydrological methods, engineers turned to the Saint Venant equations. These equations are, however, too complicated for an analytical solution of flood in a natural river. Thus, the Saint Venant equations have in turn been simplified by omitting various terms such as the acceleration in time and space. The resulting equations are designated the **diffusion equations** and the **kinematic equations** respectively. The kinematic and diffusion wave models have found wide application in engineering practice. The diffusion model assumes that the inertia terms in the equation of motion are negligible as compared with the pressure, friction and gravity terms. The kinematic model assumes that inertia and pressure terms are negligible as compared with the friction and gravity terms. Although approximate, both the kinematic and diffusion models have been shown to provide good representations of the physical phenomenon in a variety of cases. Lighthill and Whitham (1955) were able to show that flood propagation can be described in terms of kinematic rather than dynamic waves. The kinematic model has been successfully applied to overland flow, as well as to the description of the travel of slow-rising flood waves. The subsidence of the flood wave, however, is better described by the diffusion model since the kinematic model, by definition does not allow for subsidence. Hayami (1951) first produced a flood-routing method based on a linear convection-diffusion equation. He argued that floods in natural rivers channels are affected by the irregularities in the channel geometry.

In natural channels, however, a wider range of unsteady flows (gravity waves, bores, tidal waves, regulated flows etc.) are encountered, which cannot be simulated accurately by the diffusion model. Open channel gravity waves are generated by rapid or gradual variation in either the flow-rate or the depth of flow. Gravity waves generated by sudden or rapid variations are called **surges**, whereas more gradual variations produce a smooth free surface, as exhibited by flood waves in rivers. On occasion, waves possessing severe water-surface profile variations produce a breaking front, commonly called a **bore** or a moving hydraulic jump. Bores are occasionally formed in open channel conveyance structures connected to pumps or turbines due to the frequent rapid changes in the flow rate through the prime mover. **Tidal waves** in estuaries are more often of the gradually-varied type, but in some parts of the world tidal bores are common.

To avoid the limitations of the first two groups of routing methods, the hydraulic computations can be based on numerical solution of the full Saint Venant equations. The improvements in the techniques of numerical analysis have led to the understanding of the problems of instability and numerical diffusion in the analysis of complicated models. These problems can therefore be minimised.

The decision as to which type of model to use for a particular problem must be determined by the engineer. The advantages and disadvantages of the three groups can be summarised as follows:

- Groups (b) and (c) have the following advantages; (1) a sound theoretical base, (2) the ability to simultaneously produce stage and velocity information which is normally lost in the hydrological models. The primary disadvantages are stability, mass conservation problems, the complexity and the volume of data input required.

- The hydrological models advantages are; (1) they are inexpensive, (2) they are simple, as only a few parameters are required (e.g. Muskingum type models have only two parameters), (3) they are unconditionally stable and mass conservation is guaranteed. Primary drawbacks are the fact that stage and velocity cannot be determined directly, the accuracy of the model is limited and backwater conditions must be avoided. In most cases the hydrological models cannot account for a changing of the downstream boundary condition.

In general, the two major factors affecting the choice of a routing model, are:

- The type information required as output from the method. If stage and discharge information are required, models from group (b) or (c) can be used. If the flow peaks are the primary concern and phasing errors are not critical, hydrological models are the best choice.

- The quantity of data available concerning the geometry of the natural river course and the effect of previous floods. If no data are available the user is again limited to the hydrological methods. This is not, however, a critical factor as cross-sectional data can, in most cases, be extracted from maps. Inflow hydrographs can then be generated by well tested and accepted catchment simulation models (Kolovopoulos, 1986).

The factors mentioned above make the selection of the routing model between the storage methods and the hydrological models in most applications quite obvious. The selection of the appropriate routing model between groups (b) and (c), however, is difficult as the range of applicability of each wave model is not clearly defined. This is one of the research topics addressed in this dissertation.

1.3 DEVELOPMENT OF A HYDRODYNAMIC MODEL OF RIVER FLOW ON A MICRO-COMPUTER

The advent of efficient, large capacity, high speed, digital computing systems dramatically reduced the computational burden of numerical simulation modelling. Among the first of the hydraulic problems to attract the attention of scientists and engineers using computer techniques, was the computation of various unsteady flows, particularly unsteady open-channel flow. Studies for more than two decades into the various aspects of unsteady open channel flow have resulted in the development of many computer flow simulation models. These unsteady flow simulation models have thus far been predominantly based on main-frame computer architecture. The reasons for this were twofold:

- **Storage requirements**: Hydrological models and especially unsteady flow simulation models, have extensive data capture and storage requirements (topography data, boundary values etc.).
- **Processing speed**: The solution of the Saint Venant equations involves the iterative solution of large matrices. Most main-frame computers are equipped with 32-bit processors

while micro-computers have in the past contained 8-bit and 16-bit processors. The main-frame computers can therefore carry out the required calculations at a much faster rate than any of the micro-computers available.

The majority of the unsteady open channel flow simulation programs are therefore based on computer hardware and software dating back one or two generations. During this period, the main thrust of the work has been concentrated on the development of new more efficient algorithms in order to solve the large system of equations which arose. Many of the resultant programs are large and unwieldy. Main-frame computing practices also suffer from a number of disadvantages such as:

- **Accessibility**: Very few consulting firms in South Africa have access to main-frame computers.

- **Cost**: The capital cost of acquiring a main-frame computer is beyond the means of most engineering firms. Alternatively, should one subscribe to a main-frame computer bureau, the running of a simulation program may prove to be expensive in terms of processing costs.

- **Interaction with user**: Main-frame operating systems tend to be more complicated and rigorous than 'user friendly' micro computer operating systems. Main-frame programs are usually designed to accept instructions and data as a pre-processed input package, operate on the data, and output results with little or no communication with the end user. This type of batch program execution allows for many users to access the computer at the same time. The micro-computer, being dedicated to one user, allows for greater interactive communication with the user during program execution. A program designed for implementation on a main-frame generally, does not allow for this interaction.

- **Graphics:** Modern developments in micro computer graphics allow the analyst to observe the simulation taking place in order, for example, to study the variations in water level as the flood increases and subsides. In addition, the graphic representation assist in the handling of the input and output data in an easily understandable form and for the interaction with the user. This is not possible on a mainframe computer. Colour graphics are in fact comparable with hydraulic type models costing many times more than numerical models.

Over the past two decades the power and capacity of micro-computers has been continually enhanced and expanded by new advances in micro-computer technology. Current small computer systems are based on 16-bit microprocessors, which are two to eight times faster than the previous 8-bit microprocessors, and have twice the storage capacity of their predecessors. These developments have demonstrated that is not only possible but also feasible to develope a system for implementing an unsteady open-channel flow simulation model on a micro-computer. The following attributes are necessary in order for the system to be operational:

- **Simplicity:** Features that are too complex for the user to understand should not be used. (Anything difficult to explain will almost certainly be difficult to use).
- **Consistency:** The package must behave in a generally predictable manner. All aspects of such a package should follow simple and consistent patterns without exception.
- **Completeness:** There should be no irritating omissions in the set of functions provided by the package. Small function set should be provided which is able to handle a wide range of applications.
- **Robustness:** Misuse of the package should be detected and reported in the most helpful manner possible. Only in extreme circumstances should errors cause program termination.

- **Economy**: The package should be small and economical to use in order that it be seen as a viable addition to an existing program.
- **Independence**: The package should not be unduly restricted by the hardware configuration of a particular micro-computer, or by highly specialised applications requirements.

1.4 CONCLUSIONS

In spite of the rapid spread of micro-computers among all Civil and Structural engineering firms in South Africa (Mayne, 1984) the availability of comprehensive hydrological software on micro-computers for the simulation of a wide range of unsteady flows, was, at the time of writing, extremely limited. In practice steady state backwater programs such as HEC-2 (Corps of Engineers, 1976) are commonly used in South Africa for the computation of water-surface profiles. In cases where the full hydrograph must be routed, Muskingum flood routing methods or kinematic simplifications are employed (WITWAT model -Green, 1985; SWMM model -Huber et al., 1982). Advanced models such as the one developed by Weiss and Midgley (1978), are large, unwieldy, main-frame orientated and outdated in their computational procedures. South Africa also suffers from severe problems of river flooding. The recent flood disasters in Natal, the Free State and Northern Cape have cost the country dearly.

It therefore becomes clear that a comprehensive, micro-computer orientated suite of programs based on the solution of the full Saint Venant equations could be a viable aid in the analysis of the effects of periodic flooding (Kolovopoulos and Stephenson, 1988). It will enable the engineers to carry out better planning and flood management and to control flood plain development. The model must however be, flexible enough to be used as a tool in theoretical studies. In the development of the suite of models, emphasis was focused on two additional problems:

- Often the approximation models are used by engineers without an understanding of their range of applicability. A suite of models based on the full Saint Venant equations must be flexible enough to allow for the diffusion and kinematic models and the limitations in the use of each model must be specified.

- The complexity of river flow in irregular channels, which is associated with the interaction between the main channel and the flood plain. The problem has received attention only in recent years, and only during steady-state conditions. Therefore, the suite of models must allow for the different flood routing theories and provide the option in order that the appropriate flood plain model can be used for each specific application.

In view of the above and the natural processes involved, the aims of this study were set out as follows:

1. The development of an operational system for the simulation of unsteady flow in open channels.

2. The suite of models should be micro-computer compatible, making it more accessible to practising engineers.

3. The models should be able to simulate, with minimal distortion, the wide range of unsteady flows, tidal flows, and regulated flows encountered in prototype channels. They should generate accurate results by means of a stable, convergent, and numerically reliable computational scheme.

4. The models should permit schematization of a diversity of complex prototype conditions; for example, variable channel

conveyance and cross-sectional properties, channel overbank storage, lateral inflows, branching channels and networks of channels etc.

5. The suite of models should incorporate all the attributes discussed earlier: simplicity, consistency, completeness robustness, performance and independence. The system must have an operational data-handling structure, must be user friendly, and interactive.

6. The existing theories on the range of applicability of the approximation models will be combined in order to study the wave propagation in channels and to identify the pertinent parameters which affect it. The engineer will therefore have available practical criteria as to which model to apply, the kinematic or diffusion model, in which situation and will obtain an initial rough and quick determination of the main characteristics of the flow wave.

7. To assess the applicability of the existing flood routing models and to develop a new model for the accurate routing of floods in compound channels, taking into account the channel-flood plain interaction.

The methodology used to achieve the above-mentioned objectives is outlined below:

- In Chapter 2 the Saint Venant equations for one-dimensional unsteady flow in open channel are presented.

- Chapter 3 gives a brief account of the various numerical methods for the solution of the Saint Venant equations. The efficiency of different numerical algorithms is analysed in terms of stability, diffusion and convergence.

- In Chapter 4 the algorithm of the implicit flow model for the simulation of flow in looped and branched channels is outlined.

- In Chapter 5 a rational calibration and adjustment strategy is developed. Criteria of the accuracy of the simulation are defined as a set of goodness-of-fit techniques, the model parameters for a sound model calibration are analysed, and a statistical package to aid in model verification is developed.

- In Chapter 6 the model's ability to handle different types of flow is demonstrated through a series of seven diverse flow situations.

- Chapter 7 deals with the propagation of waves in prismatic channels. The applicability of the approximation models is examined, and the pertinent parameters that affect the waves are identified and analysed.

- In Chapter 8 the available techniques for the modelling of the unsteady flow in compound channels are examined, with emphasis on the evaluation of the dynamic effect of the flood plain flow and the modelling of the momentum transfer between main channel and flood plain.

This suite of models, called **OSYRIS** (Operational SYstem for RIver flow Simulation), and the research findings in prismatic and compound channels, have been developed in an attempt to provide a comprehensive treatise on open channel flow and a framework for practical use on South African river applications.

2.0 MATHEMATICAL FORMULATION OF THE ONE-DIMENSIONAL OPEN CHANNEL FLOW EQUATIONS

2.1 EQUATIONS REPRESENTING ONE-DIMENSIONAL UNSTEADY FLOW IN OPEN CHANNELS

One-dimensional flow implies flow along a single axis only, while two-dimensional flow refers to flow with components in two directions perpendicular to one other. In open channel flow, the system is often treated as one-dimensional (1-D), although truly one-dimensional flow is not possible in nature. Two-dimensional (2-D) flow analysis is sometimes required in a very wide estuary or an irregular channel. The analysis in the following chapters is based on what is termed a "one dimensional situation". The extent to which a natural river's flow can be modelled in this manner without violating the basic concepts of the one-dimensional flow equations will be investigated.

The derivation of (1-D), shallow-water, unsteady flow equations has appeared in many textbooks and scientific articles (e.g. Stoker (1957), Chow (1959), Dronkers (1964), Henderson (1966)) and it will not be repeated in this text. The set of equations representing unsteady, open channel flow are commonly known as the **Saint Venant equations**. The Saint Venant equations are a simplified version of the more general equations of motion known as the **Navier-Stokes equations**. Yen (1973) derived the general equations of motion for unsteady, spatially varied, turbulent flow for a viscous, compressible, non-homogenous fluid in a channel with arbitrary alignment and arbitrary cross-sectional area. Three partial differential equations were derived. Namely, the continuity equation, the momentum equation and the energy equation. The Saint Venant equations can be derived using the general equations of motion in two ways: firstly by reducing the general equations of flow through the use of suitable assumptions, secondly by making similar assumptions and thereafter applying the principles of continuity and momentum balance. The first method is the more rigorous while the second method can be found in the major reference works, e.g. Chow (1959).

In both methods the following assumptions are made (Constantinides, 1982):

- The fluid is homogeneous and incompressible.
- Variation of the internal normal stresses acting on the cross-section of flow is negligible. These stresses are caused mainly by the effect of compressibility and the change in viscosity of a non-homogeneous liquid.
- Flow is one-dimensional, i.e. fluid acceleration in all directions other than the direction of flow is negligible.
- Flow must be gradually varied, i.e. no rapid change in the flow cross-section should exist.
- The friction slope is approximated by the energy slope.
- Velocity is constant across any section.
- Pressure distribution across any section is hydrostatic.
- Lateral flow into or out of the main flow carries no appreciable momentum.
- The bed gradient is small so that $\theta \approx \sin\theta \approx \tan\theta$

One-dimensional unsteady flow in channels, assuming that the density is constant, can be described by two dependent variables; for instance the water-stage (Z) and the discharge (Q), at any given cross-section. These dependent variables define the state of the fluid motion along the water course in time, i.e. as a function of two independent variables (x for space and t for time). Although the independent variables are always the same, there are four principal combinations of dependent variables. These include the following pairs: depth and velocity (y,u), depth and discharge (y,Q), stage and velocity (Z,u), and stage and discharge (Z,Q).

The choice of the form of the differential equations depends on the pair of dependent variables, the type and condition of flow, the complexity of channel geometry, and the purpose of simulation. For example, when the river is steep and its cross-sectional variations are small, the use of Z(x,t) rather than y(x,t) as a dependent variable is recommended since Z and $(\partial A/\partial x)_{Z=const}$ vary slowly from one point to the next (Cunge et al., 1981). On the other hand, flat slopes and large cross-sectional variations favour the use of y(x,t). In this study the water-stage Z(x,t) and the discharge Q(x,t) were selected as dependent variables. The partial differential equations which were employed are:

a. Continuity equation

$$\frac{\partial Q}{\partial x} + B(Z)\frac{\partial Z}{\partial t} = 0 \tag{2.1}$$

where

Q : discharge in x direction (m^3/sec)

x : distance along the longitudinal axis of flow (m)

B(Z) : water surface width (m)

t : time (sec)

b. Momentum equation

$$\frac{\partial Q}{\partial t} + \frac{\partial}{\partial x}\left(\frac{Q^2}{A(Z)}\right) + gA(Z)\frac{\partial Z}{\partial x} + gA(Z)S_f = 0 \qquad (2.2)$$

where

$A(Z)$: cross-sectional area

S_f : friction slope due to flow resistance

The channel cross-section properties are shown in Figure 1.

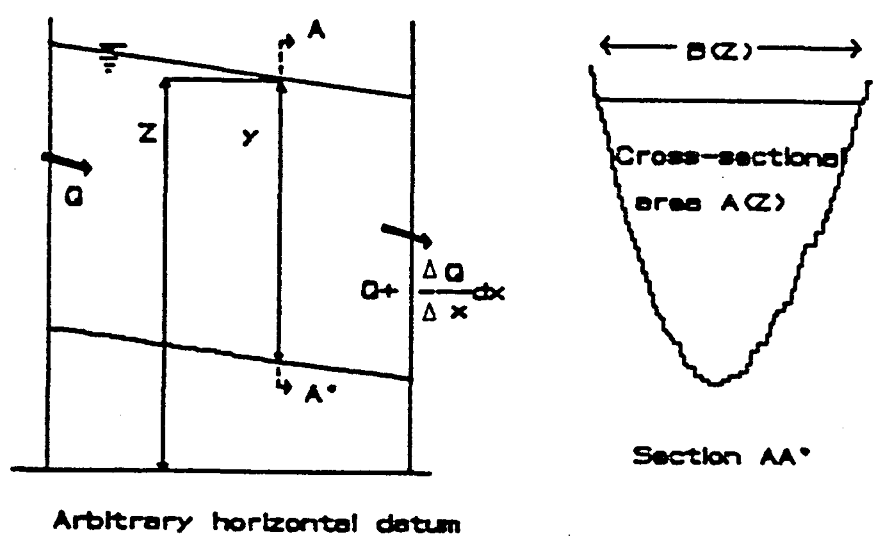

Figure 1. Definition sketch of a typical channel cross-section

The abovementioned set of equations are the most often employed in engineering practice. They were first presented by Baltzer and Lai (1968) and have been used in the majority of analysis since then (Preissmann, 1961; Vasilief, 1970). These equations do not account for lateral inflow. The reasons are:

- Inflow (or outflow) continuously distributed along the river course is seldom encountered in mathematical modelling of rivers.

- Tributaries and effluents are represented by the model as point inflows or outflows (boundary or connectivity conditions) and not as continuous lateral discharge.

- The possible error introduced from uncertainties regarding the velocity of the lateral flow vector might be greater than those introduced by neglecting lateral inflow.

Each term in the dynamic equation can be considered to represent a particular slope, i.e.

$\frac{\partial}{\partial x}\left(\frac{Q^2}{A}\right)$, $\frac{\partial Q}{\partial t}$: are the 'inertia' or 'acceleration' terms

$\partial Z/\partial x$: is the slope of the water surface itself

S_f : is the friction slope

The first term represents the slope of the energy grade line due to the variations of velocity in time (acceleration). The second is the slope which corresponds to the variations of velocity head $u^2/2g$ (in steady flow in space). These interpretations become more evident if the dynamic equation is written with dependent variables stage $Z(x,t)$ and velocity $u(x,t)$ as:

$$\frac{1}{g}\frac{\partial u}{\partial t} + \frac{u}{g}\frac{\partial u}{\partial x} + \frac{\partial z}{\partial x} + S_f = 0 \qquad (2.3)$$

The equation (2.3) can be rearranged to compare the effect of steady with unsteady flow and uniform with non-uniform flow, uniformity being related to the variation of flow properties in space (Henderson, 1966).

$$S_f = S_0 - \frac{\partial Z}{\partial x} - \frac{u}{g}\frac{\partial u}{\partial x} - \frac{1}{g}\frac{\partial u}{\partial t} \qquad (2.4)$$

Steady uniform flow

Steady non-uniform flow

Unsteady non-uniform flow

2.2 ENERGY EQUATION

Since two dependent variables are sufficient to describe one-dimensional flow, only two equations are needed, each of which must represent a physical law. Three physical laws can be formulated namely the conservation of mass, momentum and energy. The energy equation may be written as:

$$\frac{dZ}{dx} + \frac{d}{dx}\left(\frac{u^2}{2g}\right) + S_f = 0 \qquad (2.5)$$

The basic differences between the energy and the momentum equations are as follows:

- The two equations illustrate the difference between the friction slope and the dissipated energy. The friction slope accounts for the resistance due to external boundary stresses while the dissipated energy gradient accounts for the energy dissipation due to internal stresses working over a velocity gradient field. Only for steady uniform flow of a homogeneous incompressible fluid are these two gradients equal.

- When the flow variables are continuous, either of the two representations may be used, and they are regarded as equivalent (Abbot, 1979).

- When the flow variables are not continuous (hydraulic jump, bore) the two equations are not equivalent and only one of them is correct.

- The momentum equation describes the dynamic behaviour of fluid mass while the energy equation relates to steady state flow conditions. Application of the energy equation to a particular reach therefore neglects inertial effects (Hutchison, 1976).

Since the mass-momentum couple of conservation laws is applicable to both discontinuous and continuous situations while the mass-energy couple is not, the momentum equation should in general be applied. The dynamic equation becomes inaccurate when the Froude number of the flow approaches unity, and unreliable in highly curvilinear flows or highly prismatic channels. For example under sluice gates, around entrances, drop outlets, junctions, weirs and other similar structures. In estuary reaches with sudden constrictions, the momentum equation is no longer valid, as it does not reproduce the Bernoulli effect. In this case the energy equation (2.5) should be used. This occurs as the Bernoulli term;

$$\frac{\partial}{\partial x}\left(\frac{Q^2}{A}\right)$$

when expressed in finite differences, is highly inaccurate for significant values of $\partial A/\partial x$ (Hutchison, 1976). Use of the energy equation should be limited to severe constrictions in which the Bernoulli effects dominate.

2.3 ENERGY AND MOMENTUM CORRECTION FACTORS

In the derivation of the Saint Venant equations one of the basic assumptions is that of uniform velocity across the cross-section. In practice, however, the velocity varies from zero at the boundaries to a maximum somewhere in the upper middle section of the channel cross-section. Since the velocity distribution across a section is not always known, the mean velocity U (defined as the discharge divided by the area) should be corrected by introducing a coefficient α to correct the velocity head. A similar coefficient β is introduced in the momentum equation to correct the momentum term and to satisfy the assumption that the water-surface and the energy slope are the same over the entire cross-section. Equations for calculating these correction factors are derived in most standard text books. The formulae for the correction factors are:

$$\alpha = \frac{\int u_z^3 \; y_z \; dz}{U^3 \; A} \tag{2.6}$$

$$\beta = \frac{\int u_z^2 \; y_z \; dz}{U^2 \; A} \tag{2.7}$$

where

y_z : water depth

u : velocity at any point in the cross-section (m/s)

U : average cross-sectional velocity (m/s)

A : area of the flow region in a cross-section (m^2)

The subscript z denotes local values of depth and velocity averaged at position z in the cross-section.

The dynamic equation becomes:

$$\frac{\partial Q}{\partial t} + \frac{\partial}{\partial x}\left(\beta \frac{Q^2}{A(Z)}\right) + gA(Z)\frac{\partial Z}{\partial x} + gA(Z)S_f = 0 \tag{2.8}$$

For channels of regular cross-section and fairly straight channel alignment, it is reasonable to neglect the minor effects due to the nonuniform velocity distribution by setting the momentum coefficient equal to one. In reality, the momentum coefficient for flows in natural rivers will however always be greater than unity. It is found that the value of β for fairly straight prismatic channels ranges from approximately 1,01 to 1,12 (Chow, 1959). Generally, the coefficient is larger for small channels and smaller for large channels of considerable depth. As a result, the above equation of motion for a nonuniform velocity distribution is used to generalise the applicability of the flow equations.

2.4 RESISTANCE LAWS

In unsteady open channel flow friction forces arise mainly from the bed friction and the influence of the wind. These effects are introduced into the equation of motion.

In the momentum equation the term friction slope 'S_f' may represent any one of a number of empirical resistance laws. Most of these empirical laws are based on a relationship between discharge and friction losses of the type:

$$Q = K(Z)\, S_f^{1/2} \tag{2.9}$$

where

$K(Z)$ is the conveyance factor of the channel

S_f is the slope of the energy line in steady flow

Information regarding the effect of boundary-shear resistance under unsteady flow conditions is sparse. Thus, the energy dissipation relationship is an approximation borrowed from the steady, uniform flow theory. One of the most frequently used steady-state empirical relations is the Manning's equation:

$$Q = \frac{1}{n} A\, R^{2/3}\, S_f^{1/2} \tag{2.10}$$

where

Q = flow-rate

n = constant value known as Manning's n

S_f = friction slope

A = cross-sectional area

R is the hydraulic radius defined by the relation $R=A/P$ where P is the wetted perimeter of the cross-section

Manning's formula is simple and is reputed to provide reasonably accurate results for a large range of natural and artificial channels. This assumes that the flow is in the rough turbulent zone and that an accurate assessment of Manning's n has been made. In this study the Manning's equation is employed. The bed friction slope is therefore written as:

$$S_f = \frac{Q|Q|}{K^2(Z)} \qquad (2.11)$$

The factor $Q|Q|$ is introduced to account for tidal flows (reversal of the flow from flood tide to ebb tide).

For the surface stress τ_s, due to wind, the formula usually adopted is:

$$\tau_s = \xi B(Z)\, V^2_w \cos(w) \qquad (2.12)$$

where

ξ : dimensionless wind stress coefficient

$B(Z)$: top width

V_w : wind velocity vector making an angle (w) with the positive x-axis

The dimensionless wind-resistance coefficient (ξ) can be expressed as a function of the water-surface drag coefficient, c_d, the water density, p, and the air density, p_α, as:

$$\xi = c_d \frac{p_\alpha}{p} \qquad (2.13)$$

Combining equation (2.9) with equation (2.12) the momentum equation finally becomes:

$$\frac{\partial Q}{\partial t} + \frac{\partial}{\partial x}(\beta \frac{Q^2}{A(Z)}) + gA(Z)\frac{\partial Z}{\partial x} +$$

$$+ gA(Z)\frac{Q|Q|}{K^2(Z)} - \xi B(Z)V^2_w \cos(w) = 0 \qquad (2.14)$$

In lakes and seas where strong waves are generated by the wind, the coefficient c_d is also influenced by the height, the steepness and the velocity of propagation of these waves (Gerritsen, 1955). Thus, the wind effects on the water surface will also influence the vertical velocity distribution. If the channel is very wide, the y components of many quantities, which may include the wind effect, the Coriolis effect, and the secondary flow effect, become more significant. The transverse direction of the equations of motion then has to be considered in the flow analysis. A set of partial differential equations for (2-D) unsteady shallow-water flow can be developed from the general Navier-Stoke equations, with additional terms to account for the wind, Coriolis, and other effects if necessary. In shallow waters, however, with relatively small widths, we may neglect the influence of the Coriolis force, and all wind effects and use the momentum equation as in (2.14).

2.5 DEPENDENT VARIABLES

In the one-dimensional flow equations three coefficients are functions of the water-stage and actually represent the geometric and hydraulic characteristics of a river. These are:

- Width B(Z)
- Wetted area A(Z)
- Conveyance K(Z)

These functions provide an appropriate representation of all the relevant physical influences at any river cross-section, as long as the flow resistance may be represented by the same conveyance factor as in the uniform steady flow. If the cross-section is irregular (e.g. compound channel), the same value of the friction slope S_f, is considered to apply to the main channel as applied to the flood plains, over any river section. In this case, the common practice involves dividing the cross-section into several distinct sub-sections (vertical slices) with each subsection having different roughness from the others (Figure 2).

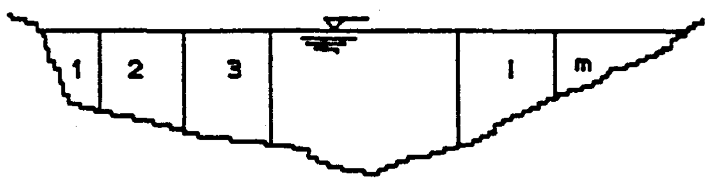

Figure 2. Division of natural cross-section into discrete elements

The value of the friction slope is assumed to be the same as that for steady flow and can be evaluated as:

$$S_f^{1/2} = \frac{Q_1}{K_1} = \frac{Q_2}{K_2} = \ldots\ldots = \frac{Q_i}{K_i} = \frac{\sum_{i=1}^{m} Q_i}{\sum K_i} \qquad (2.15)$$

The conveyance K_i in the ith subsection is defined as:

$$K_i = \frac{1}{n_i} A_i R_i^{2/3} \qquad (2.16)$$

where

A_i, R_i, and n_i are the area, hydraulic radius and roughness of the ith subsection respectively

As described by Chow (1959), the total section conveyance can be considered to be the sum of the conveyances in the subsections.

$$K(Z) = \sum_{i=1}^{m} K_i \qquad (2.17)$$

where m = number of subsections

Flood-plain modelling is extensively analysed in chapter 8, as the abovementioned model analysis does not accurately represent the process in reality. (Tingsanchali and Ackerman, 1976).

Two points must be emphasised:

- The Manning's roughness which is used in equation (2.9) for the calculation of the conveyance is not a roughness at all, but numerical coefficients which relate the overall section properties (hydraulic radius, cross-sectional area) to the discharge and the energy slope. In a constant section, the roughness can be considered to represent the physical roughness. But in a typical composite (natural) channel section, containing zones of varying bed roughness and/or overbank flow areas, the roughness reflects only the hydraulic radius and roughness effects. The implications of this on modelling will be further discussed in the model calibration and verification process, Chapter 5.

- Equation (2.17) defines a global conveyance factor for the cross-section. This is based upon the assumption that the friction slope S_f is constant across the cross-section width. If S_f is assumed to be constant and the horizontal velocities to be nonuniform, the free water surface can no longer be horizontal. It is only if the Saint Venant hypothesis of a uniform velocity distribution is valid that no contradiction arises. In practice it is always assumed that both S_f is constant and that the free surface is horizontal; the error thus committed is a measure of how the 'one dimensional situation' represents the real flow (Cunge et al., 1981).

3.0 NUMERICAL SOLUTION OF THE SAINT VENANT EQUATIONS

3.1 GENERAL

As it was shown in chapter two, there are many forms of the basic hydraulic laws, often having different domains of validity. The Saint Venant equations are a set of non linear partial differential equations. As they cannot be solved analytically for most cases, numerical techniques are employed. It is possible to find approximate solutions, i.e. stage and discharge at a certain number of points in the time-space domain, in such a way as to satisfy the basic laws as for as is possible.

Discretization is the procedure of representing a continuous variable by discrete values at specific points in space or time, or both (ASCE, Task Committee on Glossary, 1982). Considerable research has gone into the solution techniques for the Saint Venant equations. All available techniques are based on a procedure of discretizing the flow laws and then numerically solving the equations to furnish solutions. There are three classes of numerical solution methods:

1. Method of characteristics

2. Finite element method

3. Finite difference method

An introduction to these methods is given in the next paragraphs. Only the finite difference method will be evaluated, as it is the most widely used.

3.2 METHOD OF CHARACTERISTICS

The method of characteristics utilises the fact that flow conforms with certain relationships along characteristic curves, therefore the solution is evaluated along the characteristic curves. The partial differential equations of the mathematical model are transformed into characteristic (ordinary differential) equations and solved on a grid.

Movement along each characteristic line represents possible wave motion across the water surface. The physical significance of the characteristic lines is the most important feature of the theory. A small disturbance in an open channel propagates with celerity $c=(gy)^{\frac{1}{2}}$ relative to the water. The celerity c, depends on the gravitational acceleration g and the depth y. Because a disturbance in still water can travel in both directions along the channel, an observer on the shore witnesses two fronts moving with velocity:

$$\frac{dx}{dt} = u \pm c = u \pm (gy)^{\frac{1}{2}} \tag{3.1}$$

where

y = hydraulic depth
u = average velocity at section

One front clearly moves in the flow direction, while the other moves either in the opposite or same direction, depending on whether the flow is subcritical ($|u|<c$) or supercritical ($|u|>c$). The family of curves described by dx/dt in the x-t plane are called **characteristics** (Figure 3). The upper sign in Figure 3 describes the forward (c^+) characteristic while the lower sign describes the receding (c^-) characteristic. The flow properties,

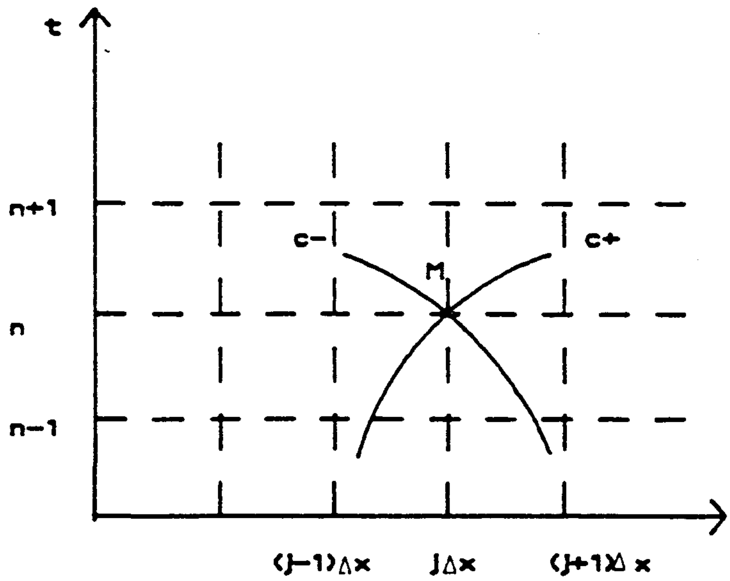

Figure 3. Computational grid for characteristic flow (subcritical flow)

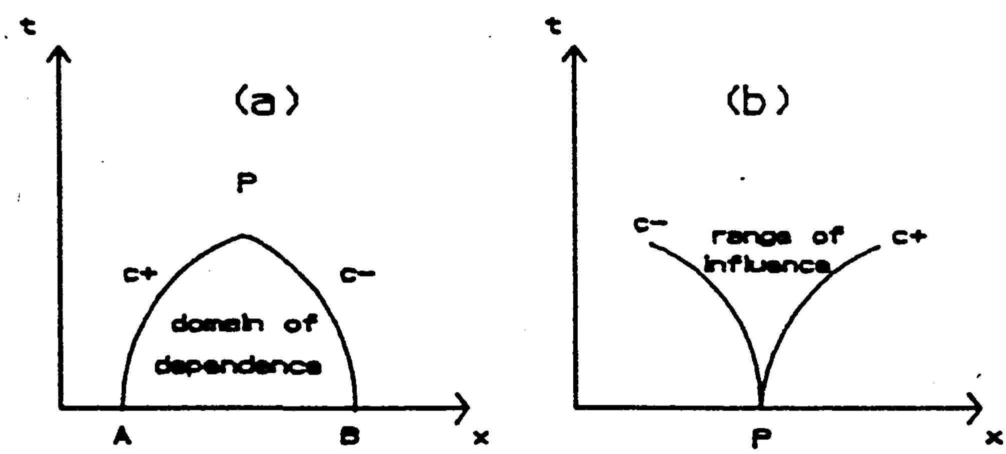

Figure 4. Domain of dependence (a) and range of influence (b) of a point P, as defined by the characteristics c^+ and c^-

depth and discharge, along each characteristic are described by relationships obtained from the unsteady flow equations using the equation (3.1). Stated differently, the flow equations describe the flow properties as seen by an observer travelling along the flow at a velocity defined by the characteristics.

Two terms, explained by the theory of characteristics, with considerable physical significance are the **domain of dependence** and the **range of influence**. The concepts are illustrated in Figure 4 for a point P.

The determination of the flow conditions at point P(x,t) depends wholly on conditions within the triangular area APB. Such an area is called the domain of dependence of P. The point P cannot be influenced by any information outside of the domain as no characteristic is available to carry the information inside. It can be seen that the characteristics PA and PB (Figure 4.b) limit the domain which is controlled by any particular boundary condition. The characteristics PA and PB then behave as the limits of direct application of data on AB, P is the furthest point to which this data can be independently utilised. Thus the pair of characteristics c^+ and c^- which originated from the point P will define the range of influence of P.

The method of characteristics can be based either on a grid of characteristics or a fixed grid. While the method which is based upon a grid of characteristics is theoretically appealing, one encounters difficulties in handling grid points, efficiently and rationally when they are irregularly spaced on the x,t plane. For practical application, one is forced to go through a series of interpolations in order to derive useful results at desired locations on the x,t plane. When using the method of specified time intervals, the interpolation process is simpler and is performed along the current time-line first, after which solutions are sought on the advanced time-line, by following the characteristic curves. As both methods require repeated interpolations at some point in their solution processes, the difference between them in this regard is not too significant.

The method will not be examined analytically as it is used primarily in exceptional cases. The principal advantage of characteristic methods would seem to be their capability of dealing easily with supercritical flow, which is however, rarely encountered in river modelling systems (Abbot, 1979). Abbot and Verwey (1970) used a four point method of characteristics to overcome some of the disadvantages of the method, i.e. utilising three different points in fixing the properties of a fourth point. A further exception is the study of dam break waves for which the variable-grid characteristic method is often used (Chervet and Dalleves, 1970).

In conclusion, the method has the following advantages:

- Relatively easy to implement; partial differential equations yield to straightforward ordinary differential equations.

- The mathematics of the method of characteristics underlines the essential physical wave behaviour. Characteristic directions are the time-space paths of information flow in the physical system.

- The method easily accommodates supercritical flows and can be used in dam break problems.

Despite these features the method is criticised for two major shortcomings in implementation:

- In most characteristic based techniques the time-steps are limited by stability criteria that restrict the relationship between time and space-mesh parameters.

- The need for a common time-step during non-linear events and at element boundaries, necessitates the use of either interpolation or geometric adjustments, which introduce errors into the solution.

- The application of the method to a two dimensional problem becomes even more difficult.

In this study the characteristic method will be used in conjunction with the difference methods to represent the boundary conditions in cases which cannot compute all flow variables at exterior boundary points of the model (e.g. routing problem).

3.3 FINITE ELEMENT METHODS

In recent years, the finite element method (FEM) has become increasingly popular in almost every engineering field. In fluid mechanics and groundwater hydraulics the method has been extensively applied. The method has also found application in various problems of surface waters, such as lake circulation, thermal loading and flows in others shallow waters (Cheng, 1978; Connor and Brebbia, 1976).

The application of the finite element method has been extended to unsteady open channel flows (Cooley and Moin, 1976; Smith and Cheng, 1976). Using this method the equations of a numerical model are solved by dividing the spatial domain into elements in each of which the solution of the governing equations is approximated by continuous functions. The most promising FEM method is the improved dissipative Galerkin method (Katopodes, 1984).

The method has not however, found widespread application in mathematical modelling of river flow. As far as one-dimensional problems are concerned, the method does not show any advantage over the two others and the legitimacy of its application to time dependent problems is not always clear cut (Cunge et al., 1981). The majority of the schemes developed for the FEM use finite differences for the time derivatives. The advantage of the 1-D flow simulation appears doubtful to many engineers. For the above reasons a finite-element method will not be developed in this report. An additional constraint, is the extensive memory requirement of mounting the finite-element method, within a suite of micro-computer models.

3.4 FINITE DIFFERENCE METHODS

3.4.1 GENERAL

This method is based on the representation of the continuously defined functions and its derivatives, in terms of approximate values defined at particular, discrete points called grid-points. Thus the differential equations are replaced by algebraic finite difference relationships. The different ways in which derivatives and integrals are expressed by discrete functions are called finite difference schemes.

The solution domain in the x-t space is covered by a rectangular grid spacing of Δx, Δt in the x,t directions respectively as shown in Figure 5.

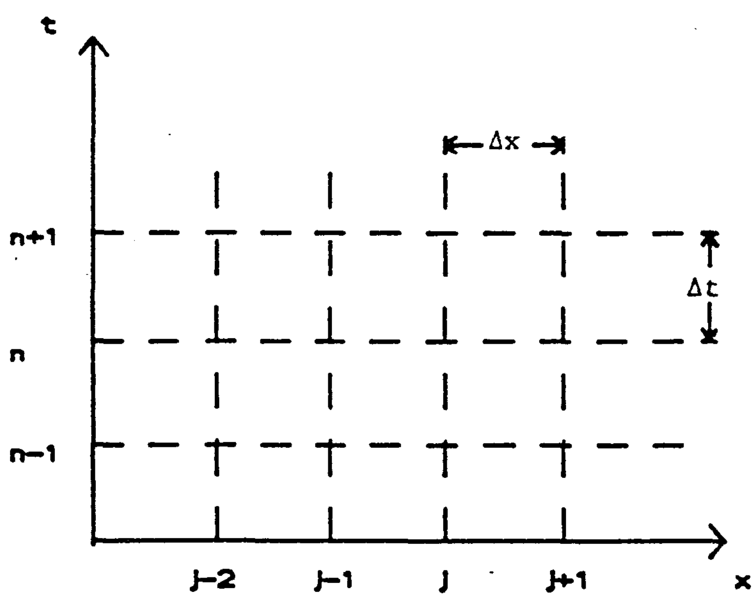

Figure 5. Finite difference grid

The error introduced by replacing the differentials of the Saint Venant equations by finite differences is called the **truncation error**. The truncation error can be established using Taylor's expansion. For an analytic function $f(x,t)$ the value at a point $(x_j+\Delta x)$ knowing the value at point x_j is:

$$f(x_j+\Delta x,t_n) = f(x_j,t_n) + \frac{\partial f}{\partial x} dx+.$$

$$+ \frac{\partial^2 f}{\partial x^2} \frac{\Delta x^2}{2} + \frac{\partial^3 f}{\partial x^3} \frac{\Delta x^3}{3!} + O(\Delta x^4) \qquad (3.2)$$

The term $O(\Delta x^4)$ contains all the remaining terms. These terms are called **'higher order terms'** and in this case 'fourth order terms'. Defining the grid functions as $f_j = f(x_j,t_n)$, the derivatives from equation (3.2) can be expressed as:

$$\frac{\partial f}{\partial x} = \frac{f^n_{j+1}-f^n_j}{\Delta x} - \frac{\partial^2 f}{\partial x^2} \frac{\Delta x}{2} - \frac{\partial^3 f}{\partial x^3} \frac{\Delta x^2}{3!} - O(\Delta x^3)$$

or

$$\left(\frac{\partial f}{\partial x}\right)_Z = \frac{f^n_{j+1}-f^n_j}{\Delta x} = \frac{\partial f}{\partial x} + \frac{\partial^2 f}{\partial x^2} \frac{\Delta x}{2!} + \frac{\partial^3 f}{\partial x^3} \frac{\Delta x^2}{3!} + O(\Delta x^3)$$

or

$$\left(\frac{\partial f}{\partial x}\right)_Z = \frac{f^n_{j+1}-f^n_j}{\Delta x} = \frac{\partial f}{\partial x} + O(\Delta x) \qquad (3.3)$$

In this case the approximation of the derivative $\partial f/\partial x$ by the difference operator $(\partial f/\partial x)_Z$ is of the first order, i.e. the first of the neglected terms is a derivative multiplied by Δx.

The following points should be noted:

- The greater the power n in the expression (Δx_n) the smaller the truncation error and the better the approximation if Δx is small.

- The grid spacing affects the truncation error. If the number of grid intervals is doubled (Δx divided by two), the error of approximation will be reduced by a factor of two for a first-order scheme and by a factor of four for a second order scheme.

- The exact magnitude of the error cannot be obtained since the Saint Venant equations cannot be solved analytically.

The replacement of the derivative $\partial f/\partial x$ by a ratio of finite differences such as $\Delta f/\Delta x$, implies that the numerical model must satisfy requirements of stability, accuracy and convergence. These are defined as follows:

- **Stability (numerical or computational)**: The ability of a scheme to control the propagation or growth of a small disturbance introduced in the calculations.

- **Accuracy**: The ratio of the difference between the approximate solution obtained using a numerical model and the exact solution of the governing equations, divided by the exact solution.

- **Convergence**: State of tending to a unique solution. A given scheme is convergent if an increasingly finer computational grid leads to a more accurate approximation of the unique solution. However, a numerical method may sometimes converge on the incorrect solution.

The convergence is governed by discretization errors. In practice, stability is a necessary condition for model operation since an unstable model is of little or no use. In an unstable scheme small disturbances grow without bound and soon completely dominate the solution. Shortening the time-step does not improve a truly unstable scheme. It is difficult to separate the concepts of stability and accuracy. A difference scheme which is a poor approximation of a particular differential equation will approach a different equation as the step size approaches zero. Such a scheme may be stable according to the definition, but the solution of the difference equation does not converge to the solution of that particular differential equation. Conversely, a scheme that is a good approximation of the differential equation may be unstable.

The Saint Venant equations constitute a set of quasi-linear partial differential equations. At present, there exists no method for analysing the stability of equations of this type. On the other hand, there are various methods for analysing the stability and convergence of linear partial differential equations (Roache, 1972) among them, notably, the Von Neumann approach (O'Brien et al., 1950). Traditionally, a way out of the mathematical difficulty imposed by the quasi-linear nature of the Saint Venant equations has been to linearize them, assuming that the behaviour of the linear system approximates that of the more complex quasi-linear system. In practice, the linear analysis serves, if not as a quantitative, at least as a qualitative description of the non-linear phenomena.

In conclusion, the finite-difference approach to the Saint Venant equations, or other similar equations, consists of the following steps (Dooge, 1986):

- Choice of the type of finite difference approximation to replace the derivatives in the original equation by finite differences.

- The choice of a method for linearizing the resulting algebraic equations.

o The choice of a method for the solution of the resulting linear algebraic equations.

The steps of the finite difference approach, the implications of each step on the stability and the accuracy are shown in Figure 6.

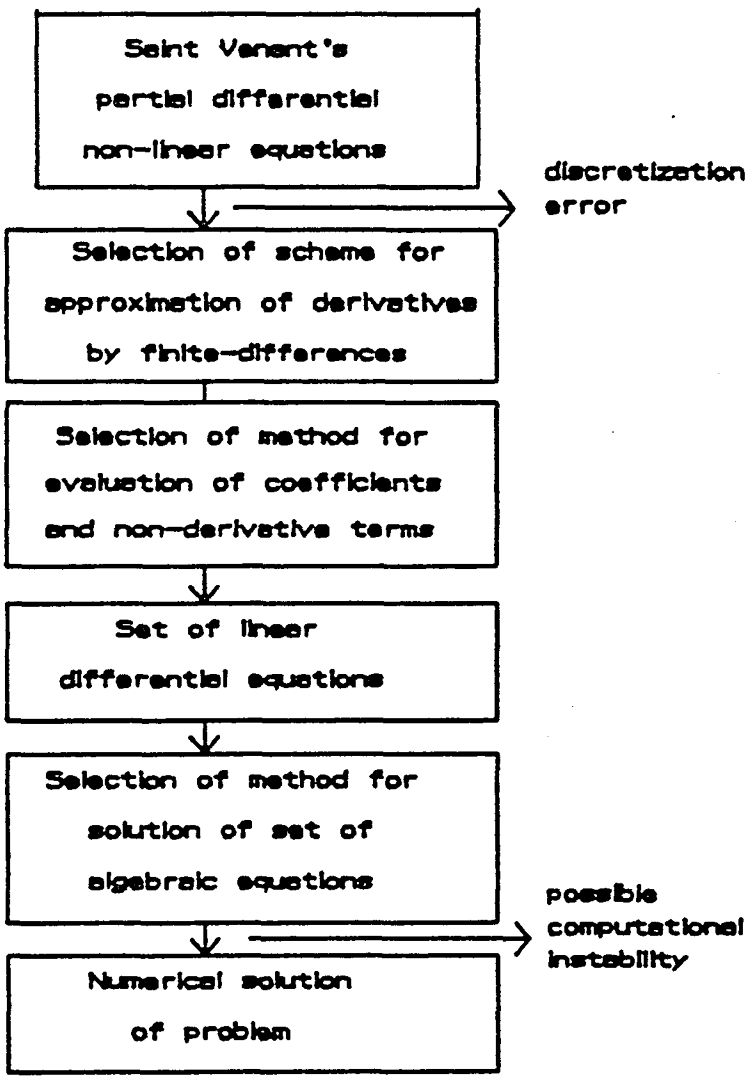

Figure 6. The finite difference approach

3.4.2 IMPLICIT VERSUS EXPLICIT SCHEMES

In the explicit finite difference methods, the dependent variables at a rectangular grid point on an advanced time-line are determined one point at a time, from the known values and conditions at grid points on the present time line or present and previous time lines. In the implicit methods, a number of unknowns at the advanced time level are related to less-weighted known values at the current time level. Since there are more than one unknown in the finite difference equation, a full set of simultaneous equations must be solved.

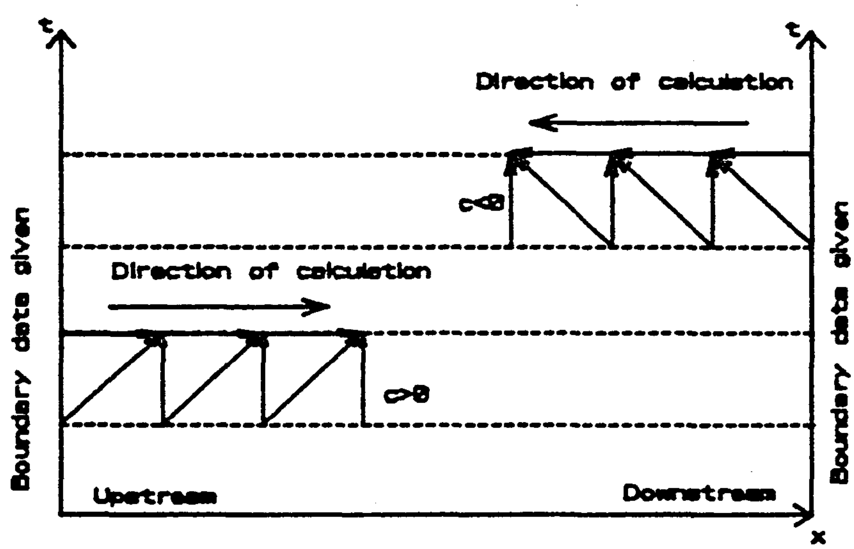

Figure 7. Different algorithmic structures for implicit schemes-Arrows indicate the direction of information transfer (Abbot, 1979)

A different definition is given by Abbot (1979) and highlights an important difference of the two methods, which is rarely pointed out. The explicit scheme is indifferent to the order or direction of computations in the space of independent variables, while any scheme that has a definite order or direction of computation in the space of the independent variables is called an implicit scheme (Figure 7).

Thus, the implicit schemes have two definite orders of computation, defining two "algorithmic structures". The first is used when $c>0$, the second when $c<0$. Important implications arising from these definitions are:

1. The implicit schemes are sensitive to boundary data structures that are in turn transmitted through the implicit scheme to appear at all points within the domain of the solution. Thus, the implicit schemes must be provided with alternative algorithmic structures for subcritical and supercritical flow respectively.

2. In practical river applications supercritical flows are not often encountered. However, when subcritical flow transforms to supercritical flow, the use of an inappropriate structure will result in instability.

3. Implicit schemes are far more complicated to program than explicit schemes, and the provision of alternative structures especially in multiconnected systems is very complicated. In this case through a form of 'control function' that recognises the supercritical regime, the solution is better performed by an explicit method, i.e. schemes with no algorithmic structure.

The concepts are better represented by drawing the characteristics in the x-t plane (Figure 8).

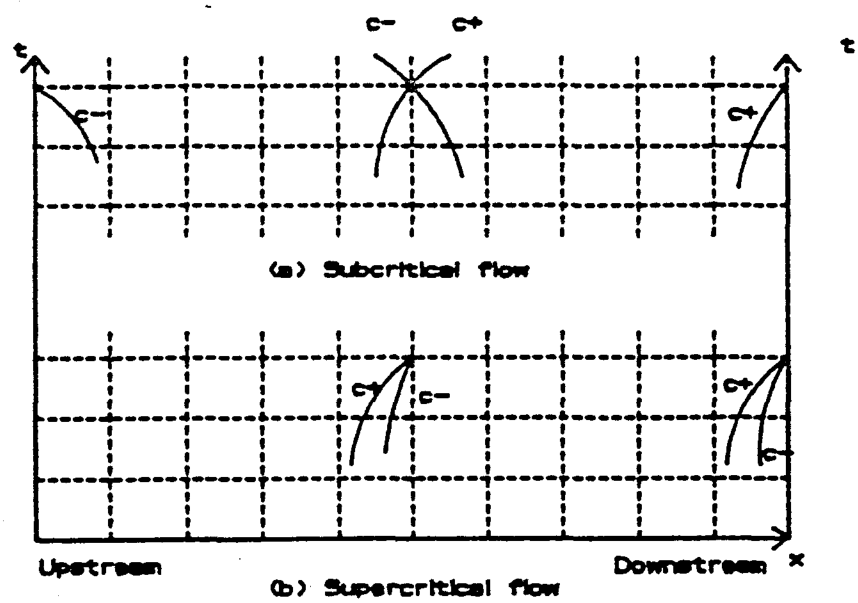

Figure 8. Subcritical versus supercritical flow in the x-t plane

As can be seen from Figure 8, under supercritical flow no c^+ characteristics can reach the upstream end, and two boundary conditions must be given. On the other hand, as both c^+ and c^- characteristics reach the downstream end, no condition is needed.

The characteristics also help in identifying a further important difference between explicit and implicit methods. In Figure 9(a) the flow properties at point P are to be calculated from known information of the previous time-step (explicit schemes). The numerical propagation lines have a slope $\Delta x/\Delta t$ in the x-t plane while the true propagation lines (characteristics KP, LP) have a slope dx/dt in the x-t plane.

In Figure 9 (a) the domain of dependence of P (area PKL) lies wholly within the domain bounded by the segment AC, the c^+ issuing from A and the c^- issuing from C. However, in Figure 9 (b) information is sought by the characteristics outside the computational domain (PAC). Since information outside this range

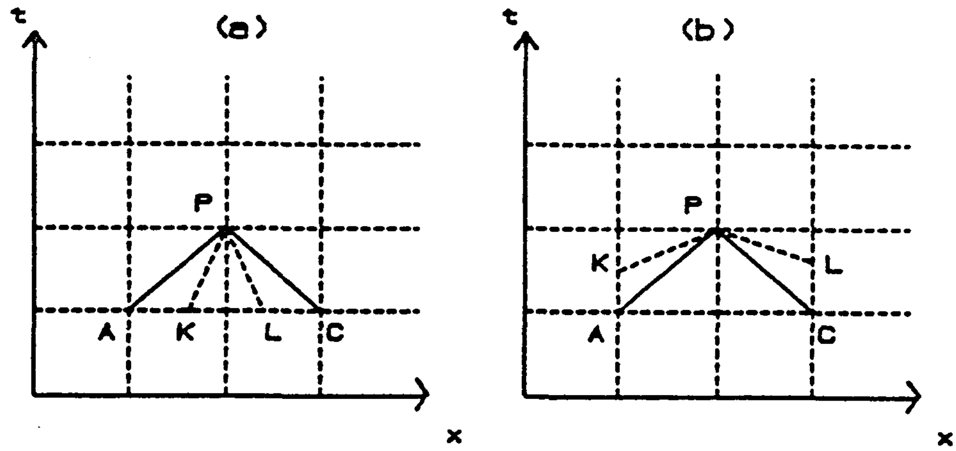

Figure 9. Propagation of information numerically and theoretically

is not propagated by the numerical scheme, instability will result. In other words, for stability to occur the physical speed of the moving wave front ($u \pm c$) must not exceed the computational celerity $\Delta x/\Delta t$. This is referred as the **Courant Criterion**, after Courant et al. (1928) and it limits the possible time-step for explicit methods. The Courant restriction can be written:

$$\frac{\Delta t}{\Delta x} < \frac{1}{(u \pm c)_{max}} \tag{3.4}$$

where

Δt : the time-step

Δx : the reach length

u : the mean flow velocity

c : the wave celerity

The effect on the accuracy and the stability of different space (Δx) and time increments (Δt) is summarised in Figure 10.

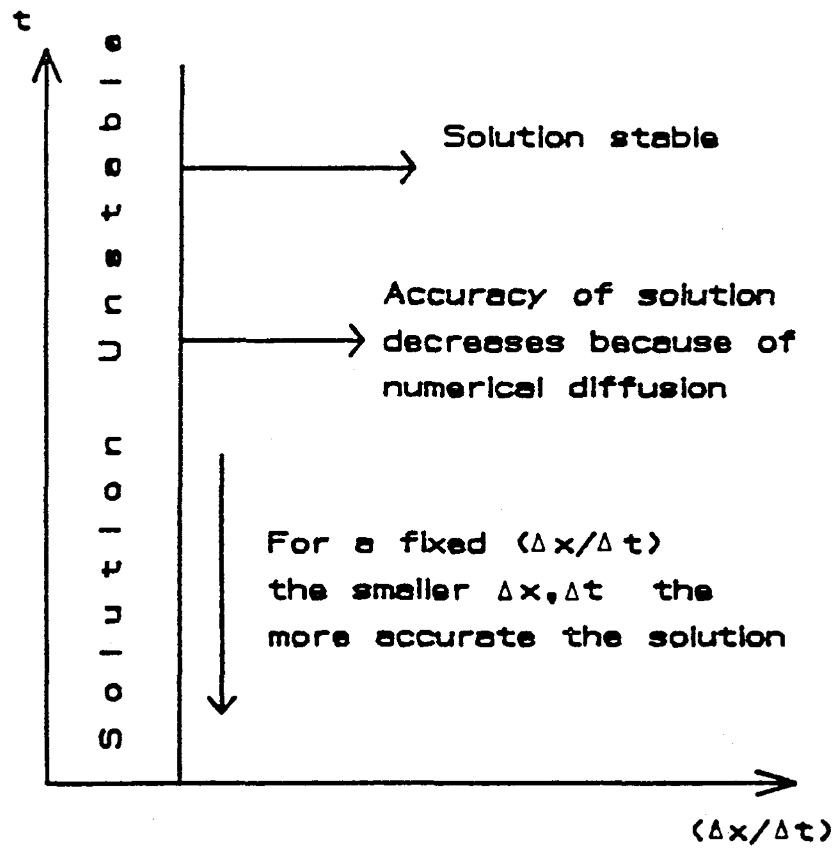

Figure 10. Effects of values of Δx and Δt on stability and accuracy for explicit finite difference schemes

From Figure 10 it can be seen that to minimise diffusion errors and obtain optimal accuracy the computational $\Delta x/\Delta t$ must be close to $(\Delta x/\Delta t)_{cr} = |u+(gy)^{\frac{1}{2}}|$. Since the space length increment (Δx) in practical applications is always fixed (reach length) the Courant criterion restricts the time increment in the explicit schemes to:

$$\Delta t < \frac{\Delta x}{|u+(gy)^{\frac{1}{2}}|} \qquad (3.5)$$

In implicit schemes the time-step may safely exceed the Courant limitation without affecting the stability of the solution. However, this is at the expense of the accuracy due to numerical diffusion. Thus, for large time increments the simulation results could be meaningless. This is even more dangerous since numerical diffusion is difficult to detect, while numerical instability automatically terminates the simulation. Ligget and Woolhiser (1967) reported that they were unable to make practical use of the "advantage" of the implicit schemes. If they increased the $\Delta x/\Delta t$ ratio more than would be allowed for in an explicit finite difference scheme, inaccuracy resulted and stability problems would sometimes occur. Therefore, even if the implicit schemes are not limited by the stability limitations, the Courant criterion remains a valuable indicator when selecting the simulation time-step.

The explicit schemes are much simpler to program and use. They follow the variation of the flow properties along the reach easier as the solution is performed explicitly. They have been found to be accurate and economical when correctly used (Strelkoff, 1970; Ligget and Woolhiser, 1967). On the other hand, implicit methods are considerably more stable than explicit schemes, for any choice of Δx and Δt. This is due to the fact that the implicit schemes make the solution at any point (j,n+1) dependent upon all other points. The computed point will therefore always lie within a domain of dependence of the point of intersection of two characteristics issuing from the previous time-level.

From the abovementioned pro's and con's of the implicit and explicit schemes, it becomes apparent that the adoption of the implicit schemes is not always justified. In river simulation problems, where time-steps of hours might have to be adopted, the implicit method is generally preferable. Most of the river modelling systems which are presently in use are based on implicit schemes. The possible unconditional stability and the aim to make the developed model easy to implement and micro-computer orientated dictate the use of an implicit algorithm. All the abovementioned arguments are nevertheless important in order that the modeller be aware of the limitations of the implicit algorithms.

4.0 IMPLICIT FLOW MODEL FOR THE SIMULATION OF FLOW IN BRANCHED AND LOOPED CHANNELS

4.1 GENERAL

Implicit schemes involve the solution of sets of simultaneous equations and thus the inversion of large matrices or, iteration methods. The large storage requirements coupled with the more complicated computational procedures resulted in most known implicit models being only suitable for use on mainframe computer systems. Thus, the formulation of a generally applicable one-dimensional flow model capable of executing on a personal computer such as the IBM AT, while maintaining computational efficiency becomes a difficult task. Different computational procedures were tested and methods for inversion of matrices were evaluated in terms of accuracy, computational speed, storage requirements and flexibility.

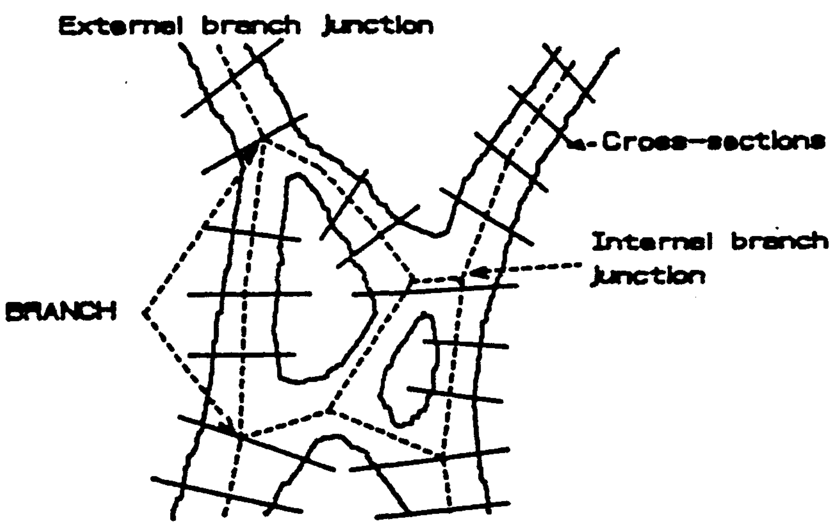

Figure 11. Hypothetical looped network

The developed implicit model, as it will be shown, has all the capabilities of standard mainframe models and at the same time is computationally efficient and accurate. It is applicable to any channel (branch) or system of channels (network of branches), interconnected (looped) or not, subject to backwater flow, unsteady flow, or both, whether caused by ocean tides or flood waves. A typical network composed of branches and reaches is illustrated in Figure 11.

4.2 DISCRETIZATION OF THE BASIC TERMS OF THE FLOW EQUATIONS

As stated in the second chapter the flow equations employed are:

a. Continuity equation

$$\frac{\partial Q}{\partial x} + B(Z)\frac{\partial Z}{\partial t} = 0 \qquad (4.1)$$

b. Momentum equation

$$\frac{\partial Q}{\partial t} + \frac{\partial}{\partial x}\left(\beta \frac{Q^2}{A(Z)}\right) + gA(Z)\frac{\partial Z}{\partial x} +$$

$$+ gA(Z)\frac{Q|Q|}{K^2(Z)} - \xi B(Z)V^2_w \cos(w) = 0 \qquad (4.2)$$

where the dependent variables are the surface elevation, $Z(x,t)$, and the channel discharge $Q(x,t)$.

The applicability of these equations is governed by the assumptions listed in the second chapter. Furthermore the slope of the channel bottom must be mild and reasonably constant over the reach length, so that the flow remains subcritical. Lateral flow into or out of the channel should be negligible between channel junctions.

Among the many implicit finite difference schemes the box schemes are the most widely used (Figure 12). The most popular box scheme is the Preismann scheme which was developed in France (Preismann, 1961; Preismann and Cunge, 1961). Many variations such as the Verwey's variant (Verwey, 1971) were based on this scheme. The major advantage of the box schemes is the simplicity in the basic computational grid-point structure and the applicability to unequal distance intervals.

In the box schemes, the space and time derivatives of any functional values, f(I), are respectively approximated, as follows:

$$\frac{\partial f(I)}{\partial t} \simeq \psi \frac{f_{j+1}^{n+1} - f_{j+1}^{n}}{\Delta t} + (1-\psi) \frac{f_{j}^{n+1} - f_{j}^{n}}{\Delta t} \tag{4.3}$$

and

$$\frac{\partial f(I)}{\partial x} \simeq \theta \frac{f_{j+1}^{n+1} - f_{j}^{n+1}}{\Delta x_j} + (1-\theta) \frac{f_{j+1}^{n} - f_{j}^{n}}{\Delta x_j} \tag{4.4}$$

where

$\Delta x = x_{j+1} - x_j$

$\Delta t = t_{n+1} - t_n$

θ = weighting factor determining the time between the t_n and t_{n+1} time-lines at which the spatial derivatives are evaluated

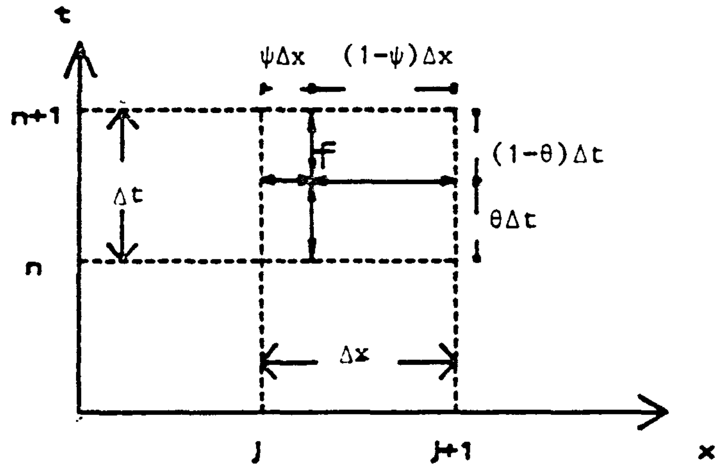

Figure 12. Box space-time grid system for implicit finite-difference schemes

ψ = weighting factor for space derivatives

The significance of different θ and ψ values is analysed in the following section of this Chapter. Usually space weighting ψ is equal to 0,50 but θ can vary in the range $0,60<\theta<1$.

The discretization of the Bernoulli and the friction terms is very important, since these terms influence the stability of the entire scheme. The Bernoulli term can be written as:

$$\frac{\partial}{\partial x}\left(\frac{Q^2}{A}\right) = \frac{2Q}{A}\frac{\partial Q}{\partial x} - \frac{Q^2}{A^2}\frac{\partial A}{\partial x} \tag{4.5}$$

Cunge et al. (1981) found that the correct discretization of the term Q^2/A^2 influences the stability of the difference scheme. They initially discretized the Bernoulli term as:

$$\left[\frac{1}{2}\left(\frac{Q^2}{A^2}\right)_j + \frac{1}{2}\left(\frac{Q^2}{A^2}\right)_{j+1}\right] \tag{4.6}$$

but this resulted in instability. They therefore proposed:

$$\frac{Q^2}{A^2} = \frac{\theta}{4}\left[\left(\frac{Q}{A}\right)_{j+1}^{n+1} + \left(\frac{Q}{A}\right)_{j}^{n+1}\right]^2 + \frac{1-\theta}{4}\left[\left(\frac{Q}{A}\right)_{j+1}^{n} + \left(\frac{Q}{A}\right)_{j}^{n}\right]^2 \tag{4.7}$$

The term for the friction slope $|Q|Q/K^2$ was discretized similarly. Verwey (1971) discretized the terms as follows:

$$\frac{\partial}{\partial x}\left(\frac{Q^2}{A}\right) = \frac{1}{\Delta x}\left(\frac{Q_{j+1}^{n}\, Q_{j+1}^{n+1}}{\bar{A}_{j+1}} - \frac{Q_{j}^{n+1}\, Q_{j}^{n+1}}{\bar{A}_{j}}\right) \tag{4.8}$$

where the superscript (-) denotes that the function A(Z) is evaluated within the time-step Verwey (1971) also denoted it as (n+1/2).

All the abovementioned discretizations were tested with different sets of data. The final discretization which was adopted and proved to be the more stable, is a variation of Verwey's discretization. For the Bernoulli term:

$$\frac{Q^2}{A^2} = \frac{\theta}{2}\left[Q_j^{n+1}\frac{(Q_j^n)}{(\bar{A}_j)^2} + Q_{j+1}^{n+1}\frac{(Q_{j+1}^n)}{(\bar{A}_{j+1})^2}\right] + \frac{1-\theta}{2}\left[\frac{(Q_j^n)^2}{(A_j^n)^2} + \frac{(Q_{j+1}^n)^2}{(A_{j+1}^n)^2}\right] \tag{4.9}$$

and for the friction slope:

$$S_f = \frac{Q|Q|}{K^2} = \frac{\theta}{2}\left[Q_j^{n+1}\frac{|Q_j^n|}{(\bar{K}_j)^2} + Q_{j+1}^{n+1}\frac{|Q_{j+1}^n|}{(\bar{K}_{j+1})^2}\right] + \frac{1-\theta}{2}\left[Q_j^n\frac{|Q_j^n|}{(K_j^n)^2} + Q_{j+1}^n\frac{|Q_{j+1}^n|}{(K_{j+1}^n)^2}\right] \tag{4.10}$$

4.3 DISCRETIZATION OF COEFFICIENTS

The substitution of all the abovementioned finite difference approximations into the flow equations leads to a pair of non-linear algebraic equations in terms of Q and Z, for every subsequent pair of points (j,j+1). For N computational points there will be a system of 2N-2 such equations for 2N unknowns. With the addition of the two boundary conditions the system has 2N equations and 2N unknowns. However the system of algebraic equations is non linear, due to the dependence of the coefficients on the flow variables (i.e. A(Z), B(Z), K(Z)).

There are various methods by which the coefficients of the flow equations can be discretized. The discretization of these terms must however, be done carefully, since the convergence and the accuracy of the scheme depends on it. In most cases, in order to solve the non-linear system, the system is first linearized i.e. the coefficients are evaluated on the basis of known values of flow variables at the time level $n\Delta t$. Then this linear system is solved, furnishing a first approximation to the flow variables at the time-level $(n+1)\Delta t$. The substitution of these approximations into the flow equations and a second resolution of the linear system (second iteration) leads to a new, second approximation for Z_j ,Q_j , for j=1,2,3...N and so on. In most cases the first approximation to the flow variables obtained from just one solution of the linear system is sufficient; when a second iteration is required, it furnishes an approximation which can be considered to be close enough to the exact solution of the non-linear system. In the basic Preismann formulation, the coefficients of the flow were represented as:

$$f(x,t) = \frac{\theta}{2}(f_{j+1}^{n+1} + f_j^{n+1}) + \frac{1-\theta'}{2}(f_{j+1}^{n} + f_j^{n}) \qquad (4.11)$$

In the Verwey's variant of the Preissman scheme the computation begins by assuming as a first approximation:

$$B_j = B_j^n \quad A_j = A_j^n$$

$$K_j = K_j^n \tag{4.12}$$

After solving the linearized system of equations a first set of coefficients ($K_j^{n+1/2}$, $B_j^{n+1/2}$, $A_j^{n+1/2}$) is calculated. In the second and subsequent approximations the coefficients are furnished by:

$$B_j = (B_j^n + B_j^{n+1/2})/2 \tag{4.13}$$

$$K_j = (K_j^n + K_j^{n+1/2})/2 \tag{4.14}$$

$$A_j = (A_j^n + A_j^{n+1/2})/2 \tag{4.15}$$

This formulation was adopted in many other schemes (Abbot and Ionescu, 1967; Vasilief, 1970). Schaffranek et al. (1981) modified the formulation such that a different time weighting factor, called χ, could be applied to the coefficients and functions other than the derivatives, in addition to using θ for difference terms. Thus quantities such as the cross-sectional area, top width, hydraulic radius, and the discharge in non derivative form in the equation of motion, represented by f(x,t), are approximated by:

$$f_j(x,t) = \chi f_j^{n+1/2} + (1-\chi)f_j^n$$

and

$$f(x,t) = \frac{\chi}{2}(f_{j+1}^{n+1/2} + f_j^{n+1/2}) + \frac{1-\chi}{2}(f_{j+1}^n + f_j^n) \tag{4.16}$$

The weighting factor χ is similarly taken to lie in the interval $0{,}50<\chi<1$. The Schaffranek modification will be adopted in the implicit formulation, as it gives greater flexibility and allows the programmer certain options.

4.4 FORMULATION OF DIFFERENCE EQUATIONS

Utilising all the abovementioned approximations and the notation f to signify function values furnished from the previous iteration according to equations (4.12) to (4.16), the flow equations are transformed into the following finite-difference expressions for the jth segment:

A. The continuity equation

$$\left[\theta\frac{Q_{j+1}^{n+1}-Q_j^{n+1}}{\Delta x}+(1-\theta)\frac{Q_{j+1}^{n}-Q_j^{n}}{\Delta x}\right]+$$

$$+\bar{B}\left[\psi\frac{Z_{j+1}^{n+1}-Z_{j+1}^{n}}{\Delta t}+(1-\psi)\frac{Z_j^{n+1}-Z_j^{n}}{\Delta t}\right]=0 \qquad (4.17)$$

Multiplying with $\Delta x\Delta t$ and rearranging:

$$Q_{j+1}^{n+1}[\theta\Delta t]+Q_j^{n+1}[-\theta\Delta t]+(1-\theta)(Q_{j+1}^{n}-Q_j^{n})\Delta t+$$

$$+Z_{j+1}^{n+1}[\bar{B}\psi\Delta x]+Z_j^{n+1}[(1-\psi)\bar{B}\Delta x]-$$

$$-[\bar{B}\psi\Delta x]Z_{j+1}^{n}-[\bar{B}(1-\psi)\Delta x]Z_j^{n}=0 \qquad (4.18)$$

Setting

$$C_1 = \bar{B}(1-\psi)\Delta x \tag{4.19}$$

$$C_2 = -\theta\Delta t \tag{4.20}$$

$$C_3 = \bar{B}\psi\Delta x \tag{4.21}$$

$$C_4 = \theta\Delta t \tag{4.22}$$

$$C_5 = -(1-\theta)(Q^n_{j+1}-Q^n_j)\Delta t + \bar{B}\psi\Delta x Z^n_{j+1} + \bar{B}(1-\psi)Z^n_j\Delta x \tag{4.23}$$

Equation (4.18) becomes:

$$(C_1)Z^{n+1}_j + (C_2)Q^{n+1}_j + (C_3)Z^{n+1}_{j+1} + (C_4)Q^{n+1}_{j+1} = (C_5) \tag{4.24}$$

B. The momentum equation

$$\left[\psi\frac{Q^{n+1}_{j+1}-Q^n_{j+1}}{\Delta t} + (1-\psi)\frac{Q^{n+1}_j-Q^n_j}{\Delta t}\right] +$$

$$+ \frac{2\beta\bar{Q}}{\bar{A}}\left[\theta\frac{Q^{n+1}_{j+1}-Q^{n+1}_j}{\Delta x} + (1-\theta)\frac{Q^n_{j+1}-Q^n_j}{\Delta x}\right] -$$

$$- \left[\frac{\theta}{2}\left[Q^{n+1}_j\frac{(Q^n_j)}{(\bar{A}_j)^2} + Q^{n+1}_{j+1}\frac{(Q^n_{j+1})}{(\bar{A}_{j+1})^2}\right] + \frac{1-\theta}{2}\left[\frac{(Q^n_j)^2}{(A^n_j)^2} + \frac{(Q^n_{j+1})^2}{(A^n_{j+1})^2}\right]\right]\beta$$

$$\left[\theta\frac{\bar{A}_{j+1}-\bar{A}_j}{\Delta x} + (1-\theta)\frac{A^n_{j+1}-A^n_j}{\Delta x}\right] +$$

$$+ g\bar{A}\left[\theta\frac{Z^{n+1}_{j+1}-Z^{n+1}_j}{\Delta x} + (1-\theta)\frac{Z^n_{j+1}-Z^n_j}{\Delta x}\right] +$$

$$+ g\bar{A} \quad \frac{\theta}{2}\left[Q_j^{n+1}\frac{|Q_j^n|}{(\bar{K}_j)^2} + Q_{j+1}^{n+1}\frac{|Q_{j+1}^n|}{(\bar{K}_{j+1})^2}\right] + \frac{1-\theta}{2}\left[Q_j^n\frac{|Q_j^n|}{(K_j^n)^2} + Q_{j+1}^n\frac{|Q_{j+1}^n|}{(K_{j+1}^n)^2}\right] +$$

$$- \frac{\xi\bar{B}}{g\bar{A}} V^2_w \cos(w) = 0 \qquad (4.25)$$

where

$$\bar{f} = \frac{f_j^n + f_{j+1}^n}{2} \quad \text{, for the first iteration}$$

and

$$\bar{f} = \chi\frac{f_{j+1}^{n+1/2} + f_j^{n+1/2}}{2} + (1-\chi)\frac{f_{j+1}^n + f_j^n}{2}, \text{ for any subsequent iteration}$$

and

f : the cross-sectional area A(Z), the width B(Z) or the flowrate Q(Z).
The superscript (n+1/2) shows that the function is evaluated within the time-step.

Similarly the A_j , K_j and Q_j are set:

$$\bar{f}_j = f_j^n \quad \text{, for the first iteration}$$

and

$$\bar{f}_j = \chi f_j^{n+1/2} + (1-\chi)f_j^n \quad \text{, for any subsequent iterations}$$

Setting

$$F_1 = \frac{2\beta\bar{Q}}{\bar{A}} \tag{4.26}$$

$$F_2 = \frac{1-\theta}{2}\left[\frac{(Q_j^n)^2}{(A_j^n)^2} + \frac{(Q_{j+1}^n)^2}{(A_{j+1}^n)^2}\right] \tag{4.27}$$

$$F_3 = \theta\frac{\bar{A}_{j+1}-\bar{A}_j}{\Delta x} + (1-\theta)\frac{A_{j+1}^n-A_j^n}{\Delta x} \tag{4.28}$$

$$F_4 = \frac{1-\theta}{2}\left[Q_j^n\frac{|Q_j^n|}{(K_j^n)^2} + Q_{j+1}^n\frac{|Q_{j+1}^n|}{(K_{j+1}^n)^2}\right] \tag{4.29}$$

$$F_5 = -\frac{\xi\bar{B}}{g\bar{A}}V^2_w\cos(w) \tag{4.30}$$

and multiplying by $\Delta x\Delta t$, equation (4.25) becomes:

$$Q_{j+1}^{n+1}[\psi\Delta x] + Q_{j+1}^n[-\psi\Delta x] + Q_j^{n+1}[(1-\psi)\Delta x] +$$

$$+ Q_j^n[-(1-\psi)\Delta x] + Q_{j+1}^{n+1}[F_1\theta\Delta t] +$$

$$+ Q_j^{n+1}[-F_1\theta\Delta t] + Q_{j+1}^n[F_1(1-\theta)\Delta t] + Q_j^n[-F_1(1-\theta)\Delta t] +$$

$$+ Q_j^{n+1}\left[-\beta\frac{\theta}{2}\frac{Q_j^n}{(\bar{A}_j)^2}F_3\Delta x\Delta t\right] + Q_{j+1}^{n+1}\left[-\beta\frac{\theta}{2}\frac{Q_{j+1}^n}{(\bar{A}_{j+1})^2}F_3\Delta x\Delta t\right] +$$

$$+ [-\beta F_2 F_3 \Delta x\Delta t] + Z_{j+1}^{n+1}\ [g\bar{A}\theta\Delta t] + Z_j^{n+1}[-g\bar{A}\theta\Delta t] +$$

$$+ Z_{j+1}^n[g\bar{A}(1-\theta)\Delta t] + Z_j^n[-(1-\theta)g\bar{A}\Delta t] +$$

$$+ Q_j^{n+1}\left[g\bar{A}\frac{\theta}{2}\frac{|Q_j^n|}{(\bar{K}_j)^2}\Delta x\Delta t\right] + Q_{j+1}^{n+1}\left[g\bar{A}\frac{\theta}{2}\frac{|Q_{j+1}^n|}{(\bar{K}_{j+1})^2}\Delta x\Delta t\right] +$$

$$+ g\bar{A}F_4\Delta x\Delta t + F_5\Delta x\Delta t = 0 \tag{4.31}$$

Setting

$$M_{1A} = \psi\Delta x \tag{4.32}$$

$$M_{2A} = -\psi\Delta x \tag{4.33}$$

$$M_{3A} = (1-\psi)\Delta x \tag{4.34}$$

$$M_{4A} = -(1-\psi)\Delta x \tag{4.35}$$

$$M_{5B} = F_1\theta\Delta t \tag{4.36}$$

$$M_{6B} = -F_1\theta\Delta t \tag{4.37}$$

$$M_{7B} = F_1(1-\theta)\Delta t \tag{4.38}$$

$$M_{8B} = -F_1(1-\theta)\Delta t \tag{4.39}$$

$$M_{9B} = -\beta\frac{\theta}{2}\frac{Q_j^n}{(\bar{A}_j)^2}F_3\Delta x\Delta t \tag{4.40}$$

$$M_{10B} = -\beta\frac{\theta}{2}\frac{Q^n_{j+1}}{(\bar{A}_{j+1})^2}F_3\Delta x\Delta t \tag{4.41}$$

$$M_{11B} = -\beta F_2 F_3 \Delta x\Delta t \tag{4.42}$$

$$M_{12C} = g\bar{A}\theta\Delta t \tag{4.43}$$

$$M_{13C} = -g\bar{A}\theta\Delta t \tag{4.44}$$

$$M_{14C} = g\bar{A}(1-\theta)\Delta t \tag{4.45}$$

$$M_{15C} = -(1-\theta)g\bar{A}\Delta t \tag{4.46}$$

$$M_{16D} = g\bar{A}\frac{\theta}{2}\frac{|Q^n_j|}{(\bar{K}_j)^2}\Delta x\Delta t \tag{4.47}$$

$$M_{17D} = g\bar{A}\frac{\theta}{2}\frac{|Q^n_{j+1}|}{(\bar{K}_{j+1})^2}\Delta x\Delta t \tag{4.48}$$

$$M_{18D} = g\bar{A}F_4\Delta x\Delta t \tag{4.49}$$

$$M_{19E} = F_5\Delta x\Delta t \tag{4.50}$$

Substituting equations (4.32) to (4.50) into equation (4.31)

$$Z^{n+1}_j[M_{13C}] + Q^{n+1}_j[M_{3B}+M_{6B}+M_{9B}+M_{16D}] + Z^{n+1}_{j+1}[M_{12C}] +$$
$$+ Q^{n+1}_{j+1}[M_{1A}+M_{5B}+M_{10B}+M_{17D}] + [M_{2A}Q^n_{j+1}+M_{4A}Q^n_j+M_{7B}Q^{n+1}_{j+1}+$$
$$+ M_{8B}Q^n_j+M_{11B}+M_{14C}Z^{n+1}_{j+1}+M_{15C}Z^n_j+M_{18D}+M_{19E}] = 0 \tag{4.51}$$

Setting

$$M1 = M_{13C} \tag{4.52}$$

$$M2 = M_{3A}+M_{6B}+M_{9B}+M_{16D} \tag{4.53}$$

$$M3 = M_{12C} \tag{4.54}$$

$$M4 = M_{1A}+M_{5B}+M_{10B}+M_{17D} \tag{4.55}$$

$$\begin{aligned} M5 = {} & Q^n_{j+1}(-M_{2A}-M_{7B}) + Q^n_j(-M_{4A}-M_{8B}) - M_{11B} \\ & - Z^n_{j+1}(M_{14C}) - Z^n_j(M_{15C}) - M_{18D} - M_{19E} \end{aligned} \tag{4.56}$$

Finally the momentum equation is written

$$(M1)Z^{n+1}_j + (M2)Q^{n+1}_j + (M3)Z^{n+1}_{j+1} + (M4)Q^{n+1}_{j+1} = (M5) \tag{4.57}$$

The general form in which equation (4.2) is expressed gives the modeller the flexibility to analyse the behaviour of the model for different weighting factors and to study the significance of each term of the momentum equation. Thus:

1. Equating coefficients M_{16D}, M_{17D}, M_{18D} with zero the model becomes the **gravity wave model** as the "friction term" is dropped.

2. Equating coefficients M_{1A}, M_{2A}, M_{3A}, M_{4A} with zero the term $\partial Q/\partial t$ is dropped and the model becomes the **quasi-steady dynamic wave model.**

3. Equating coefficients M_{1A}, M_{2A}, M_{3A}, M_{4A}, M_{5B}, M_{6B}, M_{7B}, M_{8B}, M_{9B}, M_{10B}, M_{11B} with zero the acceleration terms are removed and the model becomes the **diffusion wave model.**

Through this discretization method the implicit model becomes a powerful tool which can give insight into the significance of each term and helps in the identification of the appropriateness and range of application of each wave model. The modeller may also decide to evaluate different ways of centering the discretization of the dynamic equation, or to apply various models in order to understand the "physical behaviour" of the simulation program as opposed to using a black box approach. If the user is inexperienced, the program can be run using the default values which are developed in the applications mentioned in the following chapters.

4.5 BOUNDARY CONDITIONS

4.5.1 EXTERNAL BOUNDARY CONDITIONS

The boundary conditions should have the same numerical properties as the scheme used for the interior points. In other words, it is of no use to develop higher order of accuracy schemes when the boundary conditions approximate only to the first order.

Using explicit schemes or staggered implicit schemes (water stages and discharges are computed at different points) the determination of the boundary conditions requires special treatment. For the explicit schemes the method of characteristics is required to compute the second variable at the boundary, while for the implicit staggered schemes it is necessary to interpolate between the different points.

The Preismann class of schemes is not hampered by any of these difficulties. The user is required to specify the external boundary conditions by means of a hydrograph Q(t), or water-stages Z(t). The model uses these conditions directly in the formulation of the solution matrix at each time-step. The model accepts the following boundary conditions:

1. Flood hydrograph Q(t) from a catchment (for routing).

2. River terminates as a lake (steady water-stage or flowrate)

3. River terminates as a dead end (Q(t)=0).

4. Known stage-discharge relationship.

4.5.2 INTERNAL CONDITIONS

Internal boundary conditions may be conditions such as:

- River junctions.
- A relatively sudden (almost discontinuous) change in river cross-section.
- A storage basin not included in the flood plain schematization, etc.

All such points are considered as nodes of a network of river branches (Figure 13). Flow in the connecting branches is governed by the equations of motion and continuity, by the internal boundary conditions at the nodes, and by the relevant external boundary conditions.

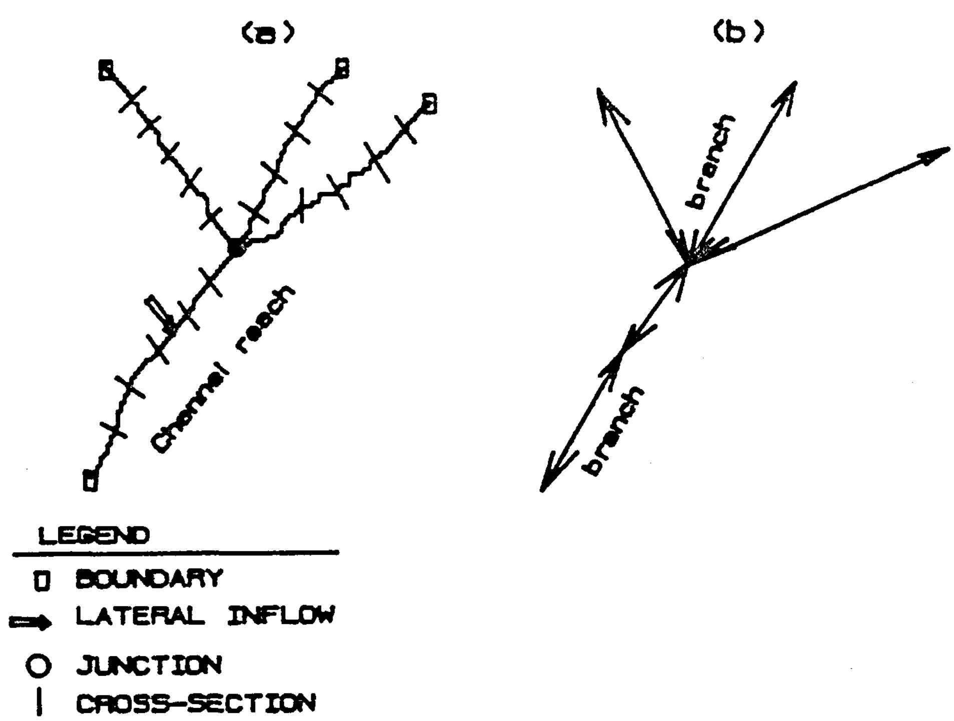

Figure 13. Example of (a) River Junction, and (b) model schematization

The junction hydraulic condition may be described by the continuity equation:

$$\Sigma Q_i - Q_o = \frac{ds}{dt} \tag{4.58}$$

and the dynamic equation:

$$Z_i + \frac{V_i^2}{2g} - h_i = Z_o + \frac{V_o^2}{2g} \tag{4.59}$$

in which

the subscript (i) represents any one of the inflow channels and (o) represents the outflow channel

s is the storage within the junction

h is the head loss through the junction

A river junction usually has a small storage volume in comparison to the volume of the flow, hence the term ds/dt in equation (4.58) is negligible. A fork type junction with three upstream branches flowing into one downstream branch (Figure 13), requires that equation (4.58) be rewritten as:

$$Q_1 + Q_2 + Q_3 = Q_o \qquad (4.60)$$

The head loss h in equation (4.59) depends on the characteristics of the flow in the junction and channel. It is not easily determined. In small mountain streams the flow is generally supercritical in at least one of the branches. However, for rivers the flow is usually subcritical in all the branches. For this case equation (4.59) can be approximated by the kinematic compatibility condition; i.e. at the junction the water surface is assumed to be continuous:

$$Z_1 = Z_2 = Z_3 = Z_o \qquad (4.61)$$

The river junctions considered in this study are those satisfying the conditions described by equation (4.60) and (4.61). These equations are used in conjunction with the transformation equations, developed in the next sections, in order to formulate a set of simultaneous equations with the unknowns, water level and flowrate at nodes in the looped or branched network.

4.6 CONTROL-WEIGHTING PARAMETERS

The discretization of the continuity and momentum parameters was based on three weighting factors:

- θ = the weighting factor determining the time between the two time-lines at which the spatial derivatives are evaluated.

- χ = the weighting factor (similar to θ) applied to the coefficients and functions other than the derivatives.

- ψ = the weighting function for the space derivatives.

A whole family of finite difference schemes may be obtained from the equations (4.3), (4.4) by varying the parameters θ and ψ. These range from fully implicit schemes when θ=1 to fully explicit schemes when θ=0 and fully backward when ψ=1 to forward schemes when ψ=0. Usually the space weighting factor ψ is set equal to 0,5. Values other than 0,5 result in instability. When ψ=0,5 the equations (4.3), (4.4) become the standard Preismann 4-point scheme. An additional reason for setting ψ=0,50 is that only in the special case when $\theta=\psi$=0,50, is the finite difference approximation of second order accuracy. Thus, the default value for ψ=0,50. However, a variable ψ was included as option in the program discretization, in order to provide greater flexibility for future program development. For instance, for the simulation of flood propagation on a dry bed, ψ can be set equal to 0 for the last section and fully implicit (use only the one point of the grid section). Using this method, numerical problems occurring when the water depth becomes very small, can be overcome.

The weighting factor θ transforms the finite difference equations from explicit schemes for θ=0 to fully implicit schemes for θ=1.

Varied values of θ in the range $0,50<\theta=<1$ have been tried by investigators. Fread (1974) referred to only the case of $\theta=0,50$ as a box scheme (classifying other cases as the four point schemes), while others (Basco, 1977; Abbot, 1974) adopted a broader definition for box schemes, including other values for θ. Lai (1965; 1967), Amein (1976), and Dronkers (1969) used $\theta=1$ for flows in tidal reaches. Amein and Fang (1970) used $\theta=0,50$ in their flood flow analysis, while Cunge et al. (1981) recommended $\theta=0,50$ for optimum accuracy and stability. Fread found $\theta=0,55$ to be the best value for slowly varied unsteady flow such as flood waves, while Chaudhry and Contractor (1973) recommended the use of $\theta=0,60$.

The selection of the appropriate values for θ is largely dependent on the particular flow conditions being simulated and the solution time-step. In order for the developed scheme to be unconditionally stable, θ must lie in the range $0,55<\theta=<1,0$. The default value for the implicit model is equal to 0,60. In Chapter 6, an example is given of the effect of θ on the stability and accuracy of the computations.

The weighting factor χ is similar to θ. Cunge et al. (1981) uses θ as the weighting factor for the terms Q^2/A^2 and the friction slope, while for all the other non derivative functions a value of 0,50 is used. However, the inclusion of the factor χ gives greater flexibility to the programmer. The χ value ranges between $0,50<\chi<1,0$. As suggested by Schaffranek et al. (1981) the weighting factor χ is set initially equal to θ and then it is adjusted as required during model calibration. As a default value for χ the same value as for θ is used.

4.7 MATRIX SOLUTION FOR SINGLE CHANNEL

For single channels with one boundary condition given at each end, the solution of the linearized matrix may be performed with any of the available methods for solving simultaneous equations. The most important methods are:

1. **Gauss elimination**

   Execution time is a third order function of the matrix size and there are many multiplication, division and subtraction operations, which contribute to loss of accuracy. Nevertheless, for less than 40 equations the technique is simple and useful.

2. **Gauss-Seidel method**

   This is used only for solving large numbers of linear equations, or for solving non-linear equations. It is an iterative matrix method. The number of iterations usually required is of the order of 5-10. In general, it is not easy to predict apriori the number of iterations needed by an iterative matrix method, it is therefore difficult to anticipate the computer effort.

3. **Double-Sweep method**

   This is the most frequently used method in industrial modelling and the principle of the sweep algorithm has also been used in this program. It utilises the banded matrix structure of the linear system of equations to compute the solution with a number of operations proportional to N. For a given number of points, the computer effort may be precisely estimated and, moreover, it increases from one model to another in proportion to the number of points N.

Major disadvantages of the sweep method is that it requires complex algorithms and considerable programming effort when applied to looped channel networks, or when supercritical flow is encountered. The mathematical formulation of the double sweep method will not be repeated since it can be found in most books on computational hydraulics. In physical terms this algorithm is a procedure in which the forward sweep transfers information given at one boundary to the other boundary where it is combined with the externally imposed condition. Since enough information is then available the solution is defined in a return sweep. As long as the flow is supercritical, the direction of the two sweeps with respect to that of the flow is of no importance; the method is symmetrical. However, as mentioned in the third chapter, the supercritical flow requires a change of the algorithmic structure and a different formulation of the matrix. If subcritical flow is transformed to supercritical flow then two or more algorithmic structures may have to be used in a single computation. For the abovementioned reasons, the sweep method becomes too cumbersome under supercritical flow conditions.

In the formulation of the implicit program, alternative algorithmic structures for supercritical flows were not constructed. However a "control" function checks the regime at each time-step and the user is notified of the change in the flow conditions and the source of instability.

An example of the formulation of the solution matrix for a single channel with 7 cross-sections is shown in Figure 14. The 6 reaches result in 12 equations [(n-1) reaches, therefore 2(n-1) equations]. However, from the 14 unknowns, two are given as boundary conditions, i.e. as a known water-level downstream in the last cross-section and as known discharge in the first

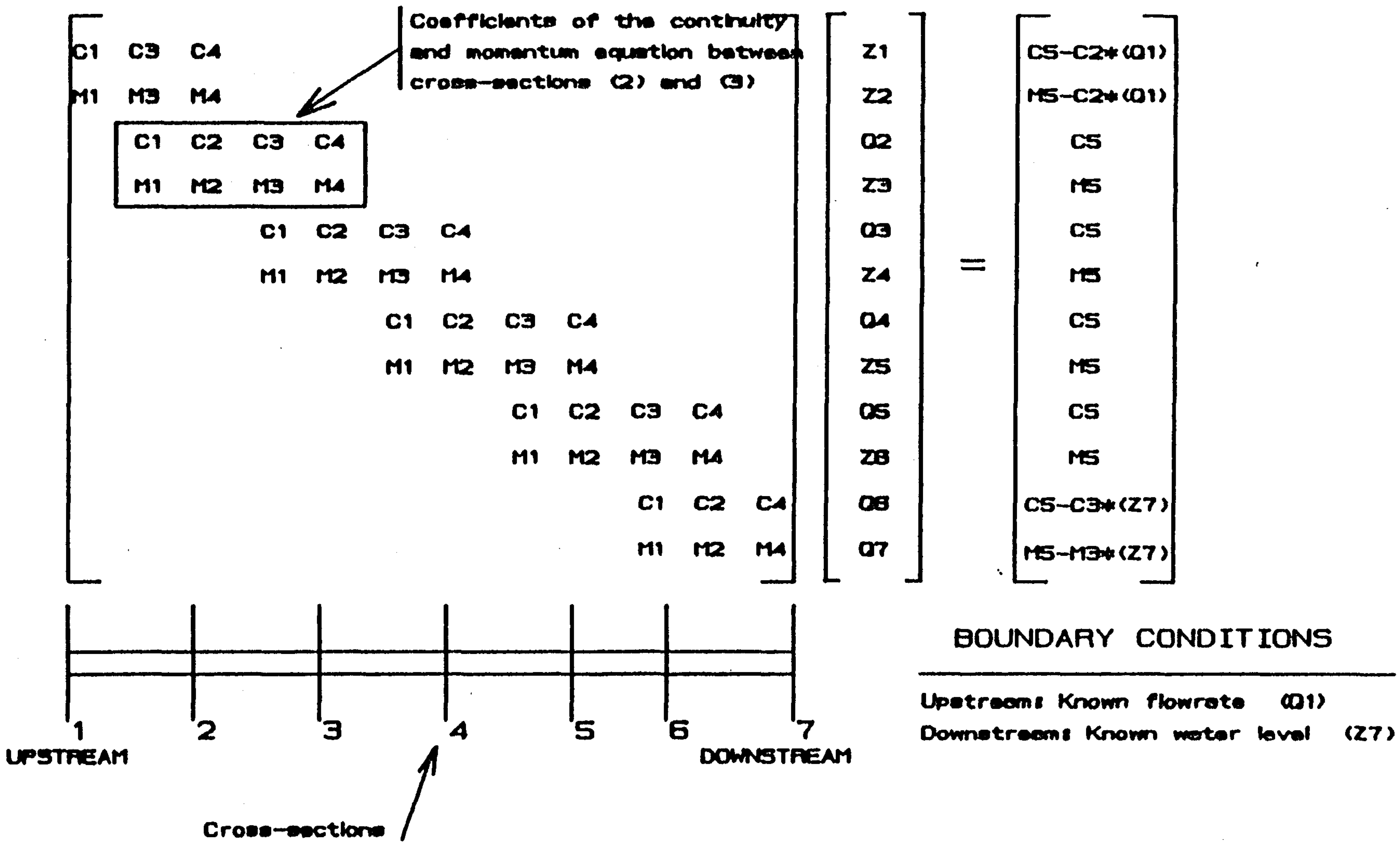

Figure 14. Example of formulation of the solution matrix for a single channel with 7 cross-sections

cross-section upstream. If the value of the discharge is substituted in the continuity and the momentum equations of the first estuary reach (i.e. 1st and 2nd equation), the number of unknowns is reduced by one to 2n-1. Similarly, substituting the value of the known water-level in the continuity and momentum equation of the last reach (i.e.11th and 12th equations) the number of unknowns is reduced to 2n-2. Thus the resultant system has 2n-2 unknowns which can be evaluated from the set of equations mentioned. At each time-step the water-levels and discharges are calculated at the end of the previous time-step and used as starting values.

Using the Preismann method the coefficient matrix that results is **banded pentadiagonal**. A banded matrix is one in which all the non-zeros lie in a relatively narrow region about the main diagonal. The bandwidth is derived from the maximum number of non-zero entries to any one side of the diagonal. If this number is M the bandwidth is 2M+1. Tridiagonal and pentadiagonal matrices, are two types of banded matrices for which special algorithms exist enabling solutions to be found efficiently. The procedure employed is called **LU decomposition** (Wilkinson and Reinsch, 1971). The whole process of LU decomposition is followed by forward and backward substitution from which the double sweep method originated. The efficiency of LU decomposition is illustrated in Table 1 . In order to compare the three methods a system of 1000 equations has been chosen.

Operations	Tridiagonal	Gauss elimination	Gauss-Seidel (1 iteration)
Multiplicat. & divisions	$5 \cdot 10^3$	$3 \cdot 10^8$	$3 \cdot 10^3$
Arithmetic Operations	$8 \cdot 10^3$	$6 \cdot 10^8$	$5 \cdot 10^3$

Table 1. Comparison of methods for the solution of banded matrix (Wilkinson and Reinsch, 1971)

From Table 1, it can be seen that LU decomposition is much more efficient than the Gauss elimination method, and comparable to the Gauss-Seidel method, only for the first iteration.

A pentadiagonal matrix has the general form:

$$\begin{vmatrix} c_1 & d_1 & e_1 & & & & & \\ b_2 & c_2 & d_2 & e_2 & & & & \\ a_3 & b_3 & c_3 & d_3 & e_3 & & & \\ & & a_4 & b_4 & c_4 & d_4 & e_4 & \\ & & & \cdots & \cdots & \cdots & \cdots & \\ & & & & a_{n-1} & b_{n-1} & c_{n-1} & d_{n-1} \\ & & & & & a_n & b_n & c_n \end{vmatrix} \begin{vmatrix} X_1 \\ X_2 \\ X_3 \\ X_4 \\ \cdots \\ X_{n-1} \\ X_n \end{vmatrix} = \begin{vmatrix} f_1 \\ f_2 \\ f_3 \\ f_4 \\ \cdots \\ f_{n-1} \\ f_n \end{vmatrix}$$

The algorithm for this system is as follows:

$$\delta_1 = d_1/c_1$$
$$\lambda_1 = e_1/c_1$$
$$\gamma_1 = f_1/c_1$$
$$\mu_2 = c_2 - b_2\delta_1$$

$$\delta_2 = (d_2 - b_2\lambda_1)/\mu_2$$
$$\lambda_2 = e_2/\mu_2$$
$$\gamma_2 = (f_2 - b_2\gamma_1)/\mu_2$$

$$\beta_i = b_i - a_i\delta_{i-2}$$
$$\mu_i = c_i - \beta_i\delta_{i-1} - a\lambda_{i-2}$$
$$\delta_i = (d_i - \beta_i\lambda_{i-1})/\mu_i$$
$$\lambda_i = e_i/\mu_i$$
$$\gamma_i = (f_i - \beta_i\gamma_{i-1} - a_i\gamma_{i-2})/\mu_i$$

$$\text{for} \quad i = 3,4,..,n-2$$

$$\beta_{n-1} = b_{n-1} - a_{n-1}\delta_{n-3}$$
$$\mu_{n-1} = c_{n-1} - \beta_{n-1}\delta_{n-2} - a_{n-1}\lambda_{n-3}$$
$$\delta_{n-1} = (d_{n-1} - \beta_{n-1}\lambda_{n-2})/\mu_{n-1}$$
$$\gamma_{n-1} = (f_{n-1} - \beta_{n-1}\gamma_{n-2} - a_{n-1}\gamma_{n-3})/\mu_{n-1}$$
$$\beta_n = b_n - a_n\delta_{n-2}$$
$$\mu_n = c_n - \beta_n\delta_{n-1} - a_n\lambda_{n-2}$$
$$\gamma_n = (f_n - \beta_n\gamma_{n-1} - a_n\gamma_{n-2})/\mu_n$$
$$x_n = \gamma_n$$
$$x_{n-1} = \gamma_{n-1} - \delta_{n-1}x_n$$

$$x_i = \gamma_i - \delta_i x_{i+1} - \lambda_i x_{i+2} \qquad i=n-2,n-3,.......,2,1 \tag{4.62}$$

The derivation of the abovementioned algorithm can be found through LU decomposition and has been published in many scientific papers (Wilkinson and Reinsch, 1971; Meis and Markowitz, 1981). The efficiency of the algorithm lies in the speed and the minimum storage requirements through realising that the arrays β_i and μ_i are used only to compute the arrays δ_i, λ_i and γ_i need not be stored once the latter group have been evaluated.

4.8 SOLUTION FOR LOOPED NETWORKS

4.8.1 DEVELOPING BRANCH-TRANSFORMATION EQUATIONS

The double-sweep method can be applied to branched channel systems, however with increased computational requirements. In looped channels the method is no longer applicable. The difference between branched and looped channels is shown in Figure 15.

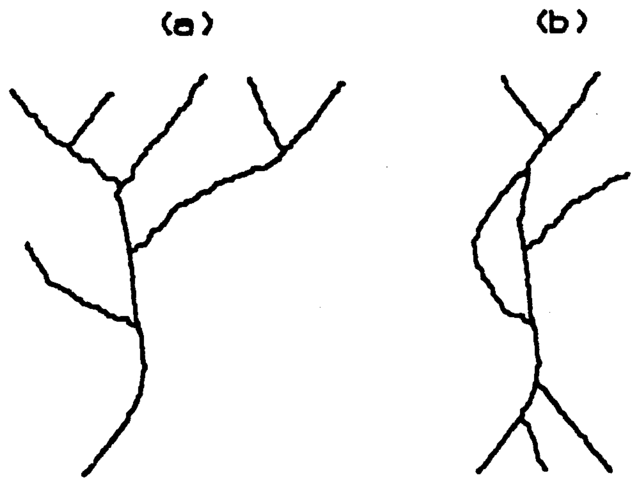

Figure 15. Branched and looped channels

If a program is to be of general use, it must be capable of simulating looped networks, since interconnected channels are a common feature in many rivers, especially where flood plains are involved. Therefore, a different solution algorithm must be considered. For subcritical flow in an open channel network, mutual backwater effects exist between the channel branches joining at a junction. Therefore, the branches cannot be treated individually when a dynamic wave model is adopted to route floods in an open channel network. Ideally, the entire network should be considered as a single unit and the flow in all the channels and junctions should be solved simultaneously.

The principles of the first looped algorithms were published by Friazinov (1970) who described and proved its numerical stability. The principle of the looped solution algorithms is based on the development of a system of simultaneous equations in which the only unknowns are the water-levels at the confluence of the branches. In this way the number of simultaneous linear algebraic equations to be solved by matrix inversion is limited to the number of nodes. Once the water-stages are known at the nodes, the water-stages and flowrates at intermediate points along each branch can be found by the double sweep method or any other technique.

The difficulty of the method is the formulation of the initial system of unknowns such as the water-stage and flowrates at each node, as it requires the development of equations relating the unknown water-levels and flowrates at the boundaries of each branch. This is obtained by formulating **branch transformation equations** which define the relationship between consecutive cross-sections (Schaffranek et al., 1981). The momentum (4.57) and the continuity (4.24) equations can be expressed in the following matrix form:

$$\begin{bmatrix} C1 & C2 \\ M1 & M2 \end{bmatrix} \begin{bmatrix} Z_j^{n+1} \\ Q_j^{n+1} \end{bmatrix} + \begin{bmatrix} C3 & C4 \\ M3 & M4 \end{bmatrix} \begin{bmatrix} Z_{j+1}^{n+1} \\ Q_{j+1}^{n+1} \end{bmatrix} = \begin{bmatrix} C5 \\ M5 \end{bmatrix} \tag{4.63}$$

Defining the following vectors:

$$L_j^{n+1} = \begin{bmatrix} Z_j^{\,n+1} \\ Q_j^{\,n+1} \end{bmatrix} \tag{4.64}$$

$$T_{(j)} = \begin{bmatrix} C3 & C4 \\ M3 & M4 \end{bmatrix}^{-1} \begin{bmatrix} -C1 & -C2 \\ -M1 & -M2 \end{bmatrix} \tag{4.65}$$

$$R_{(j)} = \begin{bmatrix} C3 & C4 \\ M3 & M4 \end{bmatrix}^{-1} \begin{bmatrix} C5 \\ M5 \end{bmatrix} \tag{4.66}$$

The Saint Venant equations for a reach j can be written in vector form:

$$L_{j+1}^{n+1} = T_{(j)}\, L_j^{n+1}\ R_{(j)} \tag{4.67}$$

Applying equation (4.67) successively to all the reaches of the branch the resulting equation relates the unknowns at the first and last (m) cross-section of each branch:

$$L_m^{n+1} = T L_1^{n+1}\ R \tag{4.68}$$

where T and R are obtained through successive substitutions of the transform equation from the (m-1) reach down to the first reach. The two matrices are:

$$T = T_{(m-1)}\ T_{(m-2)} \cdots\cdots\cdots T_{(1)} \tag{4.69}$$

and

$$R = R_{(m-1)}\ T_{(m-1)} (R_{(m-2)}\ T_{(m-2)}\ (\ R_{(m-3)} \cdots\cdots\cdots T_{(3)}\ (R_{(2)} T_{(2)}\ R_{(1)}) \cdots\cdots) \tag{4.70}$$

After the calculation of the vectors **T** and **R** for each branch equation (4.68) may be restated in matrix form as:

$$\begin{bmatrix} Z_m^{n+1} \\ Q_m^{n+1} \end{bmatrix} = \begin{bmatrix} T_{11} & T_{12} \\ T_{21} & T_{22} \end{bmatrix} \begin{bmatrix} Z_1^{n+1} \\ Q_1^{n+1} \end{bmatrix} + \begin{bmatrix} R_1 \\ R_2 \end{bmatrix} \tag{4.71}$$

or in equation form:

$$Z_m^{n+1} = T_{11}\, Z_1^{n+1} + T_{12}\, Q_1^{n+1} + R_1 \tag{4.72}$$

$$Q_m^{n+1} = T_{21} \cdot Z_1^{n+1} + T_{22}\, Q_1^{n+1} + R_2 \tag{4.73}$$

4.8.2 COEFFICIENT MATRIX FORMULATION AND SOLUTION

For each branch, using the abovementioned procedure, two branch transformation equations can be developed. Thus, for a network of N branches, 2N equations are developed relating the unknown water-levels and flowrates at the termini of each branch. The other necessary 2N equations are developed from the compatibility conditions at the nodes and the boundary conditions. For a network of N branches a linear system of 4N equations is formed with 4N unknowns. The system of equations may be expressed in matrix form as:

$$\mathbf{A} \cdot \mathbf{X} = \mathbf{B} \tag{4.74}$$

where

A : the coefficient matrix (4N·4N)

X : vector of 4N unknowns

B : right-hand column vector of 4N constants

N : number of branches

The formulation of the coefficient matrix of simultaneous equations, the unknowns being the water-levels and flowrates at the termini of the branches, will be shown by means of the example in Figure 16.

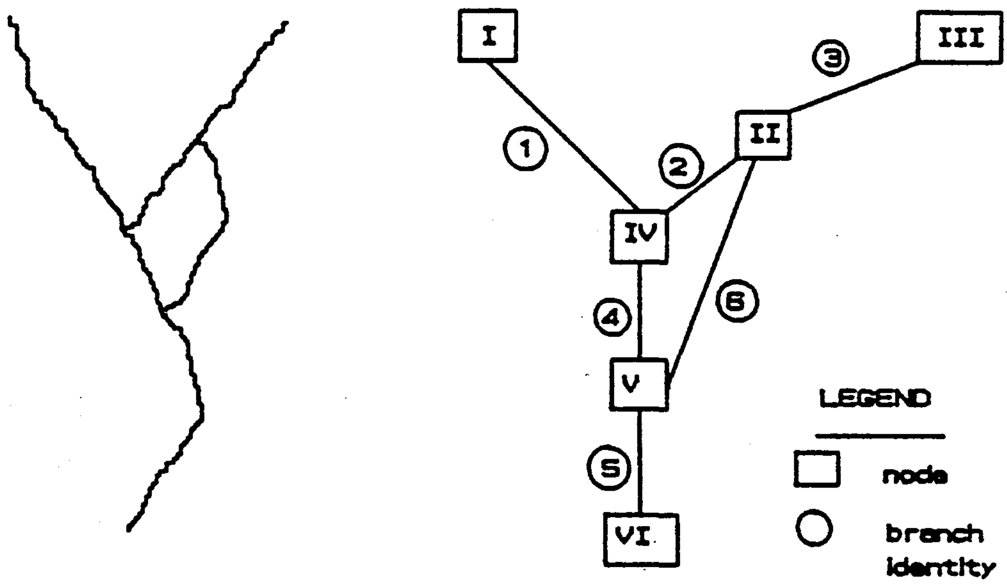

Figure 16. Hypothetical looped network and schematization for the looped model

The network has 6 branches numbered from 1 to 6 and 6 nodes numbered with Latin numbers I to VI. The compatibility conditions at the internal junctions II, IV, V are:

$$\text{Junction IV}: \quad Q^1{}_{IV} + Q^2{}_{IV} = Q^4{}_{IV}$$
$$Z^1{}_{IV} = Z^2{}_{IV} = Z^4{}_{IV} \qquad (4.75)$$

$$\text{Junction II}: \quad Q^3{}_{II} = Q^2{}_{II} + Q^6{}_{II}$$

$$Z^3_{II} = Z^2_{II} = Z^6_{II} \tag{4.76}$$

$$\text{Junction V} : Q^4_V + Q^6_V = Q^5_V$$
$$Z^4_V = Z^6_V = Z^5_V \tag{4.77}$$

where

the superscript refers to the branch identity and the subscript to the node.

The boundary conditions at the three external junctions consist of known stages as a function of time, thus:

$$\text{Junction I} : Z_I = Z_I(t) \tag{4.78}$$
$$\text{Junction III} : Z_{III} = Z_{III}(t) \tag{4.79}$$
$$\text{Junction VI} : Z_{VI} = Z_{VI}(t) \tag{4.80}$$

The coefficient matrix is formulated by the writing of the equations in the following order; firstly the branch-transformation equations for every branch, then the compatibility equations for each internal junction and finally the boundary conditions. The resulting system of simultaneous equations, written in matrix form, is shown in Figure 17. The resulting matrix is not banded and its dimension is limited to 4N where N is the number of branches. In this example the matrix dimension is 24. The simultaneous equations are solved using the Gauss-Jordan elimination method. This method is used as it is the most efficient for non-banded matrices and for less than 40 equations (Miller, 1981). In the Gauss-Jordan method, the elements of the major diagonal are converted to unity, and the elements both above and below the major diagonal are converted to zeros. Thus, the coefficient matrix is converted to a unit matrix. The resulting constant vector then becomes the solution vector. The solution of the matrix results in the determination of the water-levels and flowrates at the junctions for each time-step.

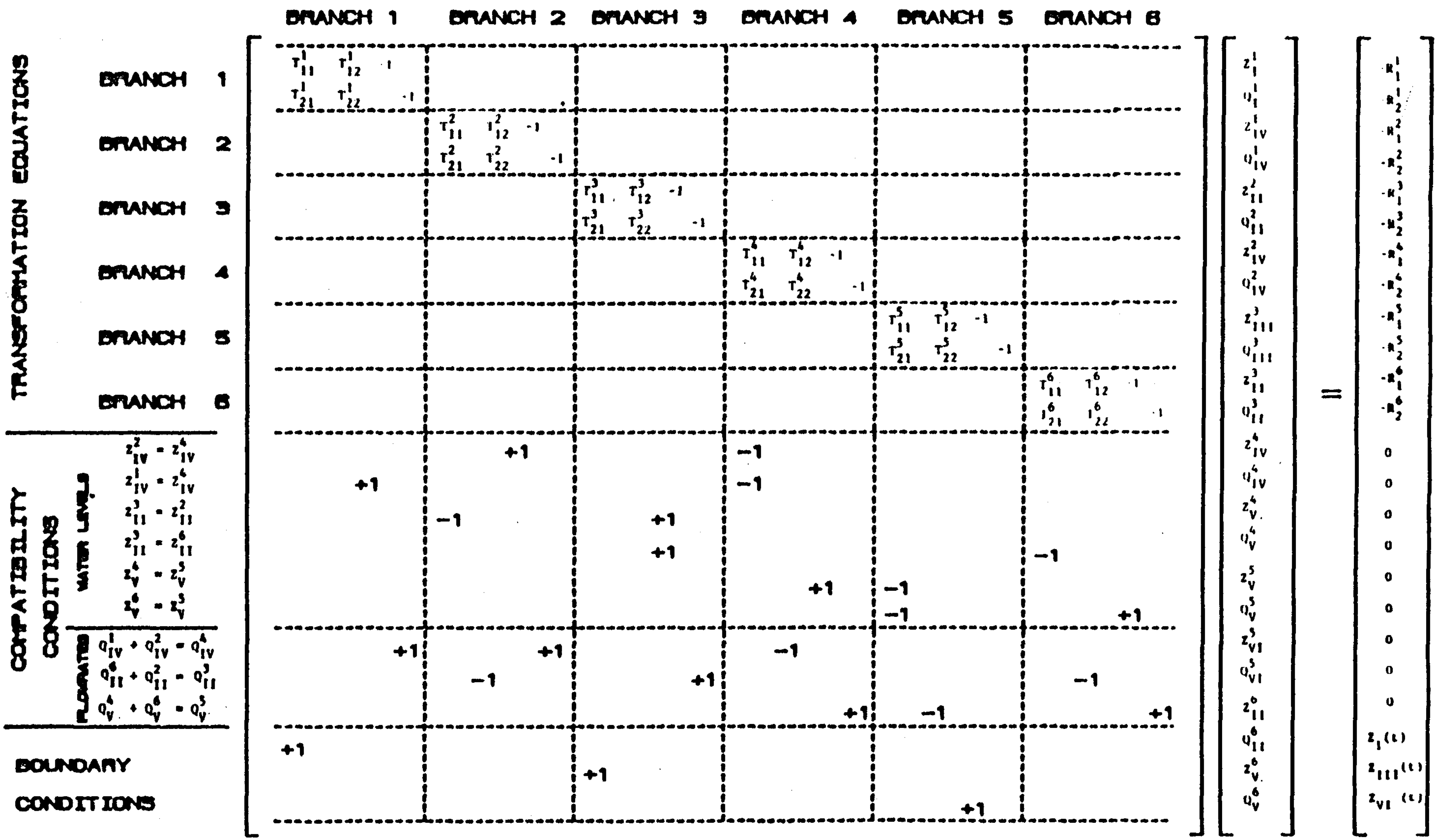

Figure 17. Formulation of the coefficient matrices for the hypothetical network shown in Figure 16.

4.8.3 SOLUTION ALGORITHM FOR THE IMPLICIT FLOW MODEL

The developed techniques for the solution of the looped network involve complicated procedures. However, it will be shown in Chapter 6 that the algorithm is efficient in terms of both speed and storage requirements. The model is designed so that each branch can accommodate up to 20 cross-sections. Thus, the complicated example in Figure 16, may correspond to a looped network of up to 120 cross-sections (6 branches x 20 cross-sections each). As can be seen in Figure 17, the resultant matrix is only 24x24, instead of 240x240 which other implicit methods would require (unknown water-levels and flowrates at each cross-section).

Once the water-levels and flowrates at the termini of the branches are determined, the storage and time requirements are a minimum, since the LU decomposition is very efficient. The steps of the implicit algorithm are shown in Figure 18. The solution is repeated at every time-step for the duration of the simulation. Depending on the accuracy requirements of the user the computations are repeated within the time-step. As the equations (4.24) and (4.57) are linearized the coefficients A(Z), K(Z) and B(Z) are evaluated, initially with values from the previous time-step. The solution of the algorithm results in a first approximation of the water-levels and flow-rates. The new values of the unknowns are substituted in the equations until the differences in the computed water-levels and flowrates of the last and previous iteration are less than a minimum, specified by the user. In most cases the algorithm converges to the exact solution after two or three iterations.

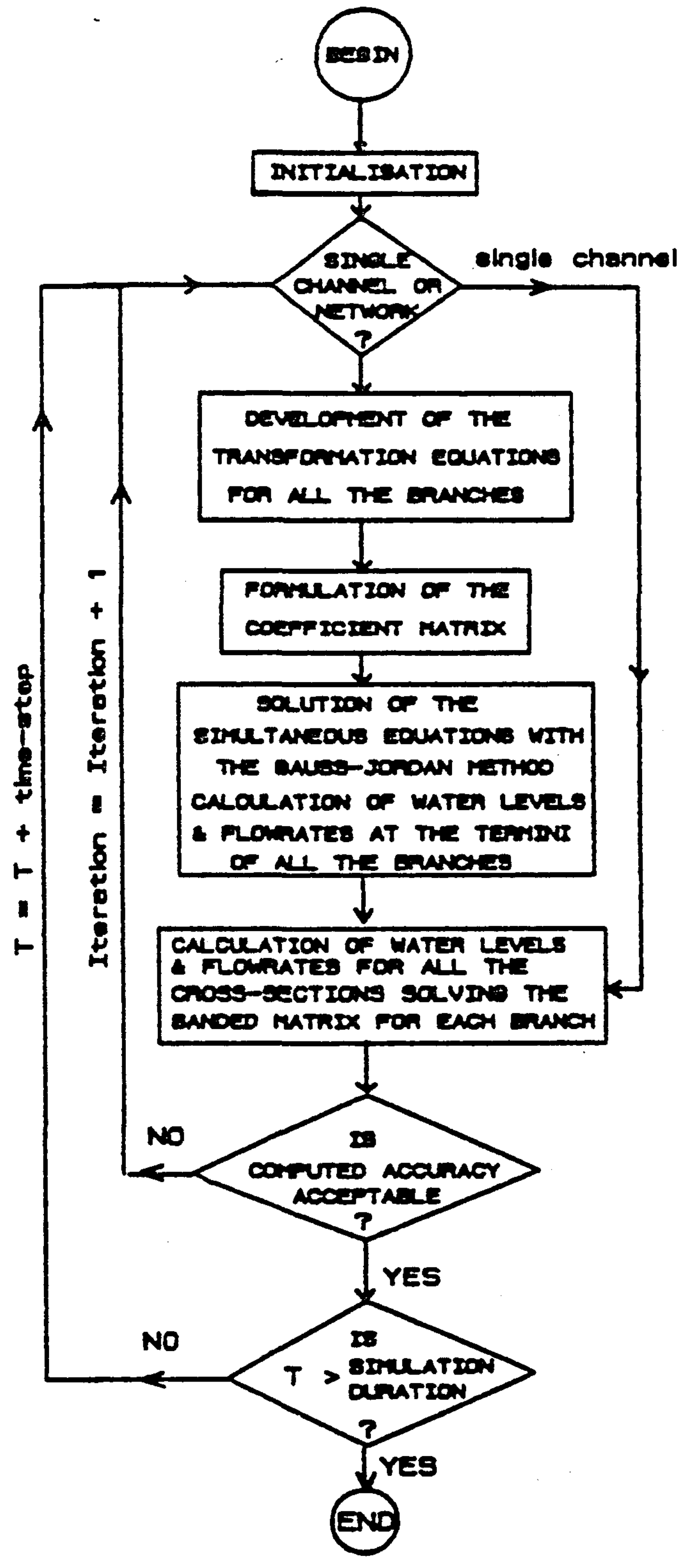

Figure 18. Implicit solution algorithm

4.9 MODEL STRUCTURE

In the past two decades a major research effort has been devoted to the development of various numerical simulation models. In contrast, only a minor effort has been directed to implementing and effectively using simulation modelling techniques (Lai, 1986). The use of unsteady flow simulation programs was limited to very specialised staff, and the handling of the data input and output for the simulation of complex river configurations could last for months.

According to the pre-development goals set up in Chapter 1, the developed suite of programs, called OSYRIS (Operational SYstem for RIver flow Simulation) should be accessible to practising engineers. However, such a goal in river flow simulation modelling involves two major tasks:

- The processing of the extensive prototype data with which to implement the model and by which to subsequently test, calibrate, and verify them.

- The model must provide the means by which the output may be made readily available in an efficient manner for analysing simulation results and for effectively portraying them in a visually comprehensible format.

4.9.1 HANDLING OF THE INPUT DATA

The OSYRIS suite of programs is supported by a powerful data input and editing pre-program. The pre-program can store and retrieve efficiently up to 400 cross-section data and up to 10 hydrographs as boundary conditions. The pre-program can be used to:

- Input the new data (cross-sections or boundary conditions).
- Edit the existing data.
- Call the main simulation program.

The cross-sectional data and the boundary data are stored in separate files. This set-up creates greater flexibility as the same cross-sectional data files can be combined with different boundary data files (different events for simulation). The data, once loaded from magnetic disc or input from the keyboard, are held in common storage for either direct access by the simulation programs or editing. The structure of this pre-program is discussed in Appendix (H), while guidelines as to its use are given in Appendix (B), which contains the User's manual.

4.9.2 HANDLING OF THE OUTPUT DATA

As a part of the operational system, a flexible output storage system has been developed. In this system, the output results generated from the numerical flow simulation are systematically stored. The basic output data to be stored, include water stages, velocities, flowrates and conveyances, at identified cross-sections.

These stored data are utilised by the modeller to perform meaningful analyses of flow simulation. For this purpose a series of supporting programs have been developed as graphic subroutines, plotting programs and a statistical package for model calibration and verification. Computer graphics are used extensively. The system supports:

- **Computer animation**: Water surface profiles are stored and the analyst can study the variations in water levels i.e as the flood increases and subsides.

- **Graph plots**: as computed discharge versus time, velocity versus time, mass curve plots, cross-section plotting etc.

4.9.3 COMPUTATION OF INITIAL CONDITIONS

At the start of the simulation, the implicit algorithm needs approximate water levels and flowrates at all the cross-sections. Therefore, a steady-state program called BACKWATER was developed to initialise the implicit algorithm. The program can handle bridges and the principles of its development can be found in Appendices (C) and (D). The BACKWATER program is chained from the pre-program and always precedes the simulation. If this option is selected by the analyst, the simulation can be performed only under steady state conditions. The operational arrangement of the suite of models is given in Figure 19.

Examples of the capabilities of the developed suite of models are presented in Chapters 5 and 6. In Chapter 5 the basic algorithms of the developed statistical package for model calibration and verification are outlined. Examples of screen graphics are shown in Appendix (E). The algorithms and the listing of all the programs are included in detail in Appendix (H).

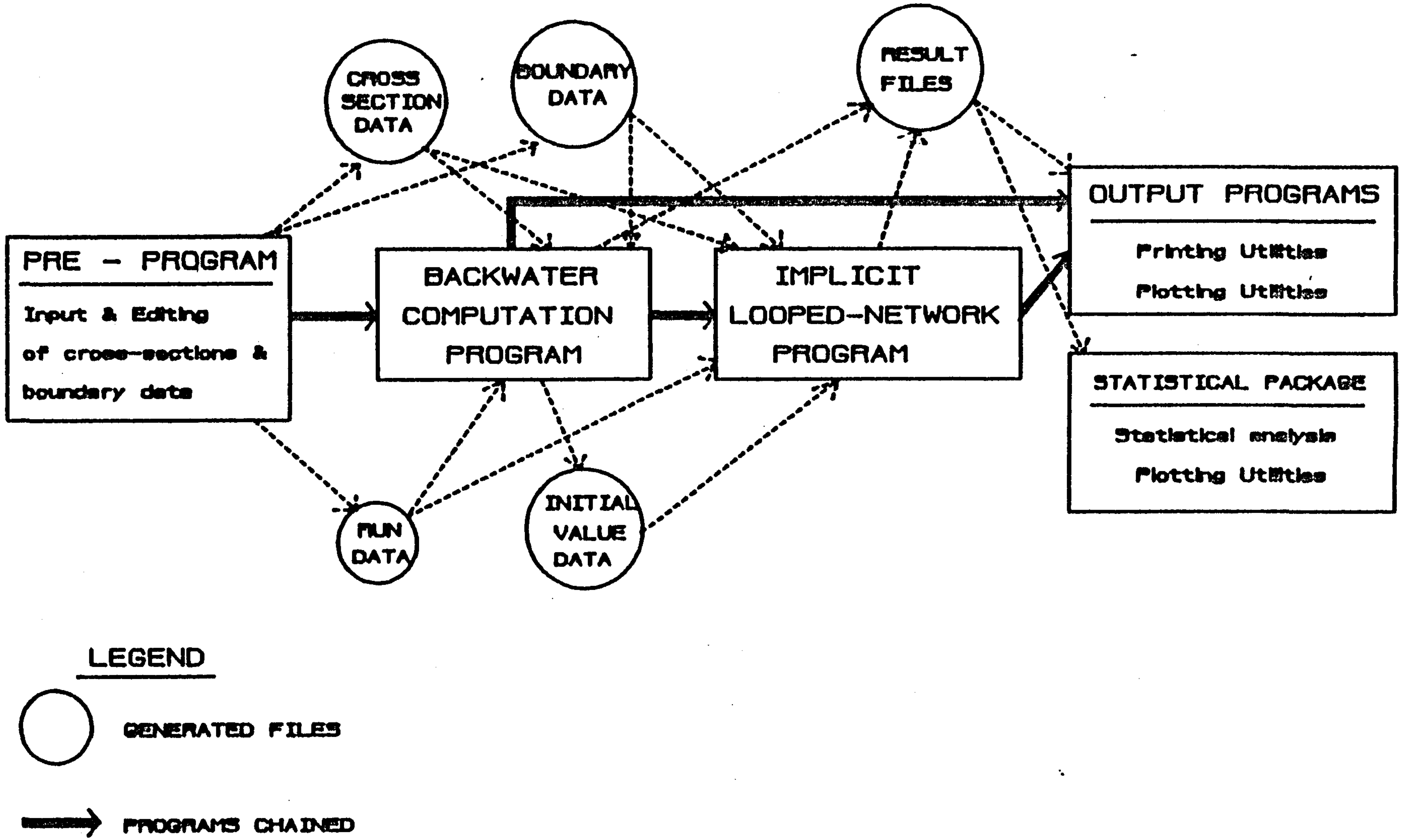

Figure 19. OSYRIS (Operational System for River flow Simulation)- Sequence of Operations

5.0 MODEL CALIBRATION AND VERIFICATION

5.1 INTRODUCTION

The possibility of errors in physical and numerical experiments is ever present. A model is an abstract idealisation of the system and contains approximations and simplifying assumptions. Therefore, in modelling the prototype situation, severe errors may be introduced depending on the applicability of the model used and the experience of the modeller. In a numerical simulation additional errors may be introduced by the finite difference approximations to differentials, the truncation errors, in the computation.

Hydrological simulation modelling involves the collection of survey data which can be expensive, depending upon the size and the accuracy required in the numerical river model. All field data are subject to a multitude of errors; instrument errors, insufficient measurements, neglect of meteorological effects, etc. The inaccuracies will be reproduced in the model so it is important that the field data match the detail and accuracy sought as output from the model.

Unsteady flow simulation in open channels poses another serious source of error. The inherent difficulty lies in the measuring of the parameters imbedded in the governing equation, particularly the "friction slope" parameters (Conveyance). Since these parameters are not physically measurable, they have to be evaluated using the governing equations as well as a set of concurrent input and output observations.

Once the model has been setup for flow simulation, it must be calibrated. The calibration process requires a procedure to evaluate the success of a given calibration and a further procedure to adjust the parameter estimates for the following calibration. Data for model calibration and verification consists of flow measured for continuous periods of time, together with recorded water-surface elevations.

In this chapter a rational calibration and adjustment strategy is developed. Thus:

- The criterion of the simulation success is defined as a set of goodness-of-fit techniques.

- The possible model parameters that have to be adjusted are identified and techniques for a sound model calibration are outlined.

- A statistical package of programs is developed to aid in model verification and the analysis of time-series.

5.2 PRINCIPLES OF UNSTEADY FLOW MODEL CALIBRATION AND ADJUSTMENT

Some model parameters are more appropriately obtained by direct measurement before beginning the calibration than by statistical criteria of goodness-of-fit. Channel properties such as the bottom slope, the reach length, and the cross-sectional geometry are specific examples. For each application, the modeller should give careful thought in deciding which parameters to estimate from available data on river and flow characteristics and which to estimate by adjusting values to minimise errors. The parameters to estimate from field information, are those which are tied to physical characteristics by the model structure for which reliable data records are available.

In computer simulation of open channel flow, three major factors relate to effective model adjustment:

- **Water-Surface Slope:** The most significant source of error arises in the measurement of the water-surface level. It has been estimated that surface waves lapping against the surveying staff result in the readings being up to ±5 mm in error at the calmer, slower flows and up to ±20 mm in error at very rough, fast flows (Bathhurst, 1986). Consequently, the mean water surface level and mean depth at a cross-section could be in error by up to ±5%, therefore by the theory of errors (Herschy, 1978), the water surface slopes could have errors of up to ±8%. Raising or lowering the stage reading (**datum correction**) at one end of a reach, with the other end fixed, automatically affects the surface slope.

- **Roughness-Resistance coefficient:** Model calibration is critically dependant on the use of proper values for the flow resistance coefficient. Correct adjustment requires repeated trials. The difficulty in evaluating the roughness-resistance coefficient for calibrating the flow model, stems principally from the fact that the energy-dissipation relationship is an approximation borrowed from the realm of steady, uniform flow. Often flow resistance varies under changing flow conditions. The applicable resistance coefficient could be a function of the following variables:

  - Flow depth
  - Turbulence
  - Water temperature
  - Bed regime of the channel bottom
  - Schematization of the prototype
  - Discharge

  Robbins (1976) performed studies on the hydraulic characteristics of the Lower Mississippi River which showed that at low discharges, values of the roughness varied by a factor of two and at high discharges the value varied by a factor of 1,3. For most river reaches the use of a constant roughness coefficient is adequate and the use of variable roughness coefficients should be considered only for secondary adjustments or for long simulation periods.

All of the above indicate that the roughness coefficient in unsteady flow simulation is not really a roughness at all, but a numerical coefficient which relates the overall section properties (hydraulic radius and cross-sectional area) to the discharge and the energy slope. Any procedure which attempts to use these conveyance coefficients as true roughnesses, for a typical composite natural channel section, is incorrect (Cunge et al., 1981). It is therefore necessary to adjust the model by trial and error in order to arrive at appropriate values for the different roughness-resistance coefficients which can be found. The initial estimates can be determined from the Manning equation or can be estimated.

- **Cross-sectional area:** It is possible, for the cross-sectional data to represent the schematized channel with an excessive cross-sectional area. This will result in a magnification of both negative and positive flows. A too small cross-sectional area, the result of entering a table of cross-section coordinates with too small a value of top width, produces the reverse effect (Lai, 1981). The error can be corrected by adjusting the boundary values. Thus, the stage values at the ends of the branch must be equally decreased or increased.

Even though the cross-sectional area adjustment has been widely recommended by many researchers (Lai, 1981; Schaffranek et al., 1981) it is the opinion of the author that the adjustment should be applied with caution. Data that can be measured, and thus determined with reasonable accuracy, should be less subject to adjustments than the data for which direct determination is impossible. Channel geometry data generally should not be altered during the calibration, as this data can be measured with reasonable accuracy. Parameter adjustments for the three key parameters is illustrated in Figure 20.

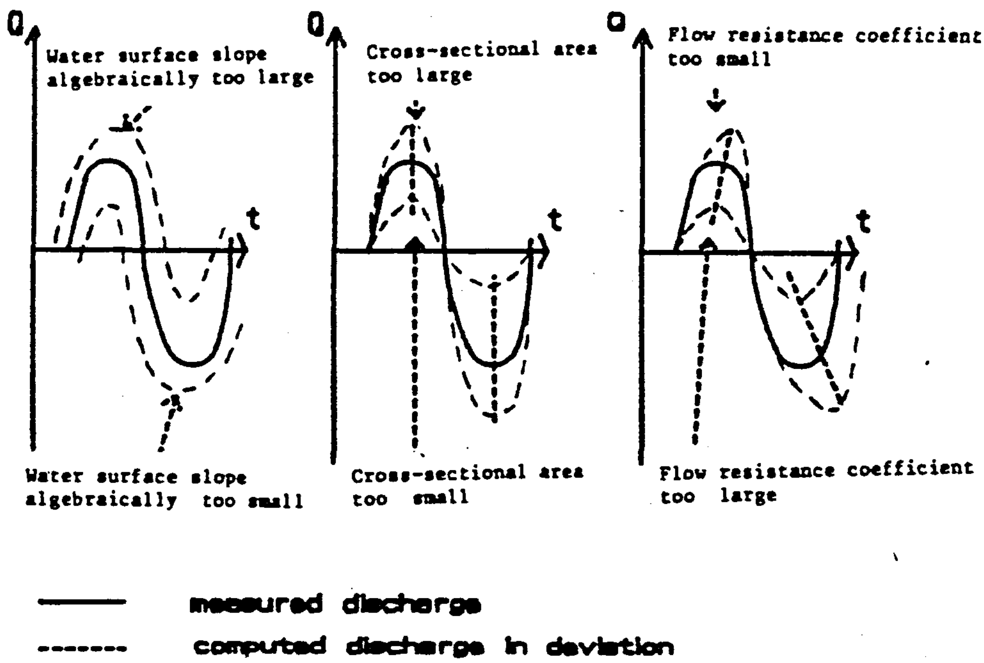

Figure 20. Basic principles of flow model adjustment (Lai, 1981)

In all the cases of parameter calibration and adjustment, **parameter values must remain rational and within reasonable limits.**

After the calibration of the key parameters there are many secondary parameters that may be adjusted, such as:

- **Variable roughness coefficient:** The use of a variable roughness coefficient is advocated only when the computation is extended to a wider range of discharges or a longer period and the flowrate with the constant roughness coefficient (originally satisfactory), begins to deviate from the average flowrate.

- **Wind stress term and lateral inflow/outflow:** If accurate data for the effect of the wind and the lateral inflow/outflow are not available, it is difficult to evaluate and calibrate these parameters. However, the effect of these terms on the simulation of flow in some waterways can be very important and could in fact overshadow major calibration parameters.
- **Weighting factors θ and χ:** The derivation of these factors was given in Chapter 4. Their values must be in the range $0{,}60 \leq \theta \leq 1$. For application purposes the optimal value of θ must be determined so as to minimise numerical damping of the computed flow while, at the same time, minimising the generated instability. The χ weighting factor was introduced by Schaffranek et al. (1981) during the development of their model. Typically, the weighting factor χ is initially set equal to θ and ultimately adjusted during the model calibration process. Discharge hydrographs computed using a χ value of 0,60 show a phase lag compared with those computed using values of χ equal to 1.

The input of the model is designed to assist the modeller in trial and error adjustments and the overall calibration process. A datum correction can be applied to each hydrograph and thus detected errors on the stage-elevation or the cross-sectional area can be easily corrected. Wind stress coefficients and the weighting factors θ and χ are treated as "**run parameters**" and can be altered during the simulation period. A separate analysis is given for the roughness-resistance coefficients, this provides the modeller with the necessary flexibility for optimum calibration of the parameter. Roughness-coefficients are entered initially for each cross-section and each segment therein (main channel and flood-plains). During the simulation process the roughnessess can be altered by a specified percentage (%), reset as steady, or set variable as a function of the flowrate. The roughness coefficient can be expressed in a quadratic form related to the discharge as:

$$n = n_o + a|Q| + bQ^2 \tag{5.1}$$

where

n_o : constant roughness coefficient
a, b : coefficients to be determined

The input of the model is designed to give the modeller the ability to calibrate efficiently and to adjust any of the key or secondary parameters easily. A sensitivity analysis of the important parameters is necessary prior to the calibration of the model in order for the user to gain experience as to the effect on the output of various parameter adjustments.

5.3 MODEL VERIFICATION

5.3.1 THE NEED FOR GOODNESS-OF-FIT CRITERIA

In unsteady flow simulation the distinction between calibration and verification of data is important. The model provides as output a continuous time-series of flows and water-levels for comparisons. Lai et al. (1978) argued that model verification using stages alone is insufficient to assure the validity of the results. Computed stages may be in close agreement with the prototype, whereas the computed and observed discharges may show considerable discrepancy. The most reliable approach would be for the model to be verified using discharges measured over continuous periods, together with concurrently recorded stage data. Measured discharges are however expensive to collect, inaccurate and impossible to obtain continuously during floods. Thus, the only continuous and reliable data available for most cases are recorded stage versus time along the river. The measured discharges can be used as a supplementary check of the calibration.

The verification process requires a procedure to evaluate the success of a given simulation. Exactly how closely the simulated and observed time-series correspond is measured by one or more statistical procedures or goodness-of-fit criteria. The procedure can range from being completely objective, using automatic optimisation routines to being pragmatically subjective - trial and error fitting by manual perturbation of model parameters and relying strongly on visual impressions of the correspondence between the simulated and observed time-series (Pitman, 1976).

As the calibration process for unsteady flow simulation can become very complex, optimisation procedures and automatic search techniques were not considered. Wormleaton and Karmegam (1984) applied an optimisation technique to optimise parameters in flood routing. The optimisation process involved minimising the errors in depth and discharge of the downstream routed hydrograph. The objective functions compared were the minimax and the least-squares.

Green (1985) outlined a number of goodness-of-fit criteria from which to choose in model performance studies. These criteria were used for the calibration of the model WITWAT, a single event kinematic stormwater model. A major conclusion of his study and that of previous researchers (A.S.A.C., 1982) is that there is no unique criterion defining a good calibration. Several statistics must be selected in order to measure goodness-of-fit.

The verification requirements of the unsteady flow simulation model developed are much more extensive than other hydrologic models as the model is able to simulate **single events** and **time-series**. Different statistics must be employed in each case. In single event modelling, the modeller might be interested primarily in the simulation of the peak flow rates, runoff volumes or/and hydrograph shapes. Thus, the selection of a fitting criterion, or a set of criteria, must take cognizance of the specific end result desired by the modeller.

The outputs of all the hydrologic models are subject to errors which may be **random** or **systematic**. Random errors occur when the model shows no tendency to over- or underestimate for a number of successive time intervals. Systematic errors occur when the sign of the error tends to persist over a series of time intervals. Both types of errors may be caused by imperfections in the structure of the model. Random errors in the data will undoubtedly produce random errors in the output. Systematic errors in the data on the other hand, will probably not be apparent as errors (differences between observed and estimated flows) in the output but will be reflected as incorrect values in the parameters of the model. If the model is used for continuous modelling, such as synthetic model generation over many days, systematic errors present in the model output could be of importance. In single event modelling, the concept of random and systematic errors is not as clear. The relatively smooth shapes of hydrographs ensure that runs of errors of the same sign must occur and it does not seem reasonable to classify the situation as one of systematic error. (Green and Stephenson, 1986). It is therefore doubtful whether systematic errors in single event modelling are of any real significance. The success of the calibration is evaluated by the modeller by a series of calculated statistics, and a series of graphical aids. In the following sections the adopted verification criteria are described.

5.3.2 GRAPHICAL DISPLAYS USED IN CALIBRATION

Computer graphics are used in all phases of the statistical comparisons and their utilisation for the model adjustment and calibration is considered essential. The following graphs are employed:

- **Continuous time-series plot of simulated flow superimposed on the recorded flow:** This plot provides a quick means of assessing the accuracy of the model output. Disagreements in peak flow rates or in total flow volumes, are immediately evident, and a qualitative assessment can be made.

- **A scattergram of recorded data (flowrates or water-levels) plotted against simulated flows:** This plot helps identify errors that cannot be detected easily from time-series plots. The plot reveals the presence of systematic errors in higher or lower magnitudes.

- **A scattergram of the % error in the simulated magnitude against the observed magnitude:** The plot is similar to the previous, but the relative error is emphasised.

- **Residual mass curve:** Plot of cumulative sum of departures from the mean for the simulated series superimposed on the cumulative sum of departures from the recorded flow. In both cases the recorded flow mean is used. The series of time-series values so obtained form a curve which commences and ends on the abscissa. The ordinate of the residual mass curve, at any point in time, depends on the history of preceding events. Comparison of the residual mass curves for observed and estimated flows may therefore reveal the existence of systematic errors in the estimated flows. As a simple direct test, the percentage error in the maximum range of the estimated residual mass curve can be used.

5.3.3 STATISTICS USED IN THE CALIBRATION PROCESS

For evaluating the results of hydrologic simulation, one would normally compare the time series. Errors in time-series data can be measured as absolute errors, relative errors with respect to the raw data origin or relative errors with respect to some other origin. In this study the absolute errors are used and are defined as:

$$e(i) = O(i) - C(i) \tag{5.2}$$

where

$O(i)$: ith observed value (water-level or flowrate)

$C(i)$: ith computed or simulated value

$e(i)$: residual or absolute error in the flow magnitude

For a continuous simulation the following statistics are employed:

- **Sum of squared residuals (SSR)**: The most commonly used objective function, defined as:

$$SSR = \sum_{i=1}^{n} [e(i)]^2 \tag{5.3}$$

where

SSR : sum of squared residuals

$e(i)$: residual

n : number of ordinates used in comparison

- **Sum of absolute residuals (SAR)**: This statistic was proposed by Stephenson (1979). It has the form:

$$SAR = \sum_{i=1}^{n} |e(i)| \tag{5.4}$$

Using an objective function of this form, the effect of large magnitude outlyers is reduced, while the effect of residuals with a value less than unity does not become less significant as would be the case if the values were squared (Green, 1985).

- **Sum of absolute area of divergence (SAAD)**: This statistic highlights the difference in the shape of two hydrographs. The statistic can be written:

$$\text{SAAD} = \Sigma \left| \frac{e(i) + e(i+1)}{2} \Delta t \right|_i \tag{5.5}$$

where

Δt : time-step

The effect of the number of ordinates can be removed by dividing the statistic by the number of ordinates. Thus:

$$\text{Absolute area/ordinate divergence} = \text{SAAD}/n \tag{5.6}$$

- **Reduced error of estimate (REE)**: The statistic was developed by Manley (1977) as:

$$\text{REE} = \left[\frac{\Sigma(O(i)-C(i))^2_i}{\Sigma(O(i)-\bar{O})^2_i} \right]^{1/2} \tag{5.7}$$

where

$\bar{O}$: the mean of the observed values

The objective function was chosen because it is at a minimum when the sum of the squares is at a minimum but also gives a dimensionless measure of the goodness-of-fit. It is in fact, equivalent to the standard error of estimate divided by the standard deviation of the flow record.

- **Proportional error of estimate (PEE):** The REE statistic gives equal weight to equal absolute errors. Thus, Manley (1978) developed a new statistic, PEE, which gives equal weight to equal proportional errors. It is given by:

$$PEE = \left[\frac{\Sigma(O(i)-C(i))_i^2}{\Sigma(\ \ O(i)\ \ )_i^2}\right]^{1/2} \tag{5.8}$$

  The REE will bias the optimisation to large flow events that will often have more effect than a sequence of errors at low flows, the converse is true of the PEE.

- **Mean and standard deviation of the residuals:** The mean is defined as the sum of the absolute residuals for an event, divided by the number of ordinates for that event. Thus:

$$M_e = (\sum_{i=1}^{n} |e(i)|_i)/n \tag{5.9}$$

  The variation or dispersion among the residuals is measured by the variance and the standard deviation. Variance is defined as the average, or mean, of the squared deviations of the residuals about the mean. The positive square root of the variance is the standard deviation:

$$S = \left[\frac{\Sigma(e(i)-M_e)^2}{n}\right]^{1/2} \tag{5.10}$$

  The mean deviation can be derived from the sum of absolute residuals by dividing by the number of ordinates of the event, thus removing the effect of the number of ordinates.

- **Standard error of estimate (SEE):** Jewell et al. (1978) introduced this statistic for the calibration of stormwater models. It is given by:

$$SEE = \left[\sum_{i=1}^{n} \frac{e(i)^2}{n-2} \right]^{1/2} \tag{5.11}$$

It is dimensional and independent of the number of points. The statistic may be seen as the sum of squared residuals by removing the effect of the ordinates and taking the positive square root.

- **Correlation coefficient (R_{so}):** This is the most important measure of the degree of correlation between two variables. The Pearson product-moment correlation coefficient, as it is called, is the most frequently used criterion for measuring the goodness-of-fit of two hydrographs (Sarma et al., 1969; Snyder et al., 1970). It is defined by:

$$R_{so} = \frac{1}{n} \sum_{i=1}^{n} \left[\frac{O(i)-\bar{O}}{S_o} \right] \left[\frac{C(i)-\bar{C}}{S_c} \right] \tag{5.12}$$

where

$\bar{O}$, $\bar{C}$: mean values of the observed and simulated time-series respectively.

S_o, S_c: standard deviations of the observed and simulated time-series respectively

Values of R_{so} vary between +1 and -1, zero being accepted as the null correlation value at which unity is approached with perfect agreement between O(i) and C(i).

- **Modified correlation coefficient (MR_{so}):** The correlation coefficient adequately measures the goodness-of-fit only when the two hydrographs being compared have nearly equal mathematical moments about a horizontal axis. MuCuen and Snyder (1975) proposed weighting the Pearson moment coefficient by the ratio of the standard deviations as a simple index for comparing hydrographs. Thus they proposed:

$$MR_{so} = (S_o/S_c)R_{so} \quad \text{if} \quad S_o<S_c$$

and

$$MR_{so} = (S_c/S_o)R_{so} \quad \text{if} \quad S_c<S_o \tag{5.13}$$

where

R_{so} : correlation coefficient

MR_{so} : modified correlation coefficient

S_c, S_o : standard deviations of the observed and simulated values.

The weighted moment is always smaller than the Pearson moment. The two coefficients will differ significantly in single event modelling.

- **Coefficient of determination (D):** This coefficient is very commonly used for measuring the degree of association between observed and estimated flows. It is defined as:

$$D = \frac{\Sigma(O(i)-\bar{O})^2 - \Sigma(O(i)-O_{est})^2}{\Sigma(O(i)-\bar{O})^2} \tag{5.14}$$

where

O_{est} is the simulated flow obtained form the regression line of O(i) on C(i)

The term $\Sigma(O(i)-\bar{O})^2$ is referred to as the initial variation and the term $\Sigma(O(i)-O_{est})^2$ is the residual variation, or unexplained variation. The coefficient of determination turns out to be the square of the correlation coefficient and therefore will always be less than unity (and less than the correlation coefficient). The three coefficients mentioned above, r_{so}, mr_{so}, and D, are all measures of the degree of association between the observed and estimated values. They do not, however, reveal systematic errors if they exist.

- **Serial correlation coefficient (SC_e):** This coefficient gives a measure of the impact that an error in previous time periods has on subsequent periods (systematic errors with respect to time). It gives an indication of the effect of error persistence as a low correlation means errors are damped out rapidly. It is expressed as:

$$SC_e = \frac{\Sigma(e(i)-M_e)(e(i-1)-M_e)}{(S_e)^2} \tag{5.15}$$

where

SC_e: serial correlation coefficient
S_e : standard deviation of residuals
M_e : mean of residuals

- **Coefficient of efficiency (E):** Nash and Sutcliffe (1970) proposed a criterion based on "least squares" fitting, expressing the proportion of the original sum of squares of the discharge which is accounted for by the model. If the residual sum of squares is defined as

$$F_1^2 = \Sigma[e(i)]^2 \tag{5.16}$$

which may be compared with the initial sum of squares:

$$F_o^2 = \Sigma(O(i)-\bar{O})^2 \tag{5.17}$$

where

$\bar{O}$ is the mean of the observed values

The term F_o^2 represents the initial variation and the term F_1^2 the residual or unexplained variation. The efficiency of the model is defined as:

$$E = \frac{F_o^2 - F_1^2}{F_o^2} \tag{5.18}$$

The criterion has been criticised (Garrick et al., 1978) on the grounds that even poor models may produce relatively high values, (80% or 90%) and the best models do not produce values which, on first examination, are significantly higher. The statistic is similar to the coefficient of determination, but not identical. The value of the statistic will always be less than unity. Aitken (1973) showed that if the results from a model are highly correlated but biased, that is, they do not plot randomly around the 45° line on the graph of observed versus estimated events, then the value of the coefficient of efficiency will be lower than the coefficient of determination. Thus, the two statistics can be combined to access systematic errors.

- **Residual mass curve coefficient (R_m):** Aitken (1973) proposed this statistic and it is defined as follows:

$$R_M = \frac{\Sigma(D_c-\bar{D}_c)^2 - \Sigma(D_c-D_e)^2}{\Sigma(D_c-\bar{D}_c)^2} \tag{5.19}$$

where

R_M : residual mass-curve coefficient

D_c : departure from the mean for the observed residual mass-curve

$\bar{D}_c$: mean of the departures from the mean for the observed residual mass-curve

D_e : departure from the mean for the estimated residual mass-curve

A value of R_M equal to unity indicates perfect agreement. The statistic is very important as it indicates whether the flow sequence contains systematic errors. The statistic is thought to have an important advantage over the coefficients of efficiency and determination in that it measures the relationship between the sequence of flows and not just the relationship between individual flow events.

- **Coefficient of persistence (CP):** Wallis and Todini (1975) suggested that if persistence in the residual fitting errors of the simulation is important, then the conventional tests of goodness-of-fit are inadequate. The residual mass-curve coefficient is a measure of persistence, but the statistic does not appear to be the most appropriate. They suggested the coefficient of persistence, CP, defined as:

$$CP = \Sigma A_i^2/F^2 \tag{5.20}$$

where

k : number of positive and negative runs

A : the individual area of each segment of deviation

F^2 : $\Sigma(O(i)-\bar{O})^2$

This statistic has dimensions of $(\text{time})^2$ so it is not strictly a coefficient.

For single event simulation the error in the simulated peak, volume and mean can be of importance. Aitken (1973) and Green (1985) point out that the model must be capable of reproducing the mean of the observed flowrates. Also for the comparisons of chapter 8, where different routing methods are compared, the error in the simulated peak flowrate is of importance. Thus, three additional parameters are used to compare the predicted with the recorded discharge hydrographs. These parameters are defined as follows:

$$\% \text{ error in the peak} = 100(C_p - O_p)/O_p \tag{5.21}$$

$$\% \text{ error in the Volume} = 100(C_V - O_V)/O_V \tag{5.22}$$

$$\% \text{ error in the mean} = 100(C_M - O_M)/O_M \tag{5.23}$$

where

O_p, C_p : observed and computed peak
O_V, C_V : observed and computed volume
O_M, C_M : observed and computed mean

A summary of the goodness-of-fit criteria is shown in Figure 21.

GOODNESS - OF - FIT CRITERIA

STATISTICS

Statistics dependent on the number of ordinates

- Sum of squared residuals
- Sum of absolute residuals
- Sum of absolute area of divergence

Statistics independent of the number of ordinates & dimensionless

- Correlation coefficient
- Modified correlation coef.
- Coefficient of efficiency
- Residual mass-curve coef.

Statistics independent of the number of ordinates

- Mean deviation
- Standard deviation
- Absolute area/ordinate of divergence
- Serial correlation coef.
- Standard error of estimate
- Reduced error of estimate
- Proportional error of estimate

Additional statistics for single events

- Ratio of Volumes, Peaks & Means (sim/obs)
- % error in Simulated Volume, Mean, Peak

GRAPHS

- Continuous time-series plots of simulated flow superimposed on the recorded flow
- Scattergram of recorded data plotted against sim. flows
- Scattergram of the % error or absolute errors of the simulated flows
- Residual mass-curves

TESTS WHICH REVEAL SYSTEMATIC ERROR

- Residual mass-curve coef.
- Maximum range of the residual mass-curve
- Comparison of the coef. of efficiency & determination

Figure 21. Summary of the goodness of fit criteria used for the unsteady flow simulation model verification

5.3.4 STATISTICAL PACKAGE DEVELOPED FOR THE EVALUATION OF THE CALIBRATION

The above statistical methods were assembled into two statistical analysis programs "GRSTAT" and "STATPL". The program "GRSTAT" reads the results output files generated by the unsteady flow simulation suite of programs and computes all the statistics as outlined in the previous section. The program "STATPL" plots the statistical graphs on the screen and sends them to the plotter should this be required. The algorithms of the programs "GRSTAT" and "STATPL" and the program listing are given in Appendix (H).

At this stage of program development the model is not used for prediction purposes. If the unsteady flow simulation model is to be used for medium- or long term hydrological forecasts, the statistical package must be coupled with stochastical evaluation methods such as spectral analyses, and so forth.

5.4 EXAMPLE OF MODEL CALIBRATION AND VERIFICATION

In this section an example calibration of the unsteady flow model is given for an ocean estuary situated at St.Lucia lake, with predominantly tidal flow. St.Lucia lake is a shallow water body situated on the subtropical east coast of Northern Natal. It is connected to the sea by a narrow estuary. The St.Lucia lake and the estuary were studied by Hutchison (1976) in an effort to simulate the water and salt circulation in the system.

Hutchison in his study used 11 water-level recorders and surveyed cross-sections from the estuary mouth at the ocean up to the St.Lucia lake. The simulation is repeated for only a part of the estuary, therefore only 11 cross-sections and three gauges were used. The location of the cross-sections is indicated on the plan of the estuary in Figure 22. The recorded water-levels at two gauges, namely, the Esengeni station upstream, and the Bridge station downstream were used as boundary conditions. The model was calibrated against measured water-levels in an intermediate gauge at Narrows station (Figure 22). Data were available for two periods:

- **First event : July 10-15, 1972**
- **Second event: December 23-30, 1972**

Water-levels were available for the two periods, for three recorders. In addition flowrates were measured at the Bridge station for the the first event. The discharge hydrographs are not considered very reliable as the charts are interrupted for short periods. Therefore, the measured discharges were used only as a supplementary check on the calibration.

Several calibration runs were performed in order to evaluate the optimum values of channel roughness. The final effective channel roughness chosen was n=0.023. Figures 23 and 24 illustrate the comparisons between model and natural system water-levels and discharges for the model run which yielded the best results. The simulation success is evaluated from the statistics in Figure 25 and from the graphical aids in Figures 26 to 28. The cumulative mass-curves shown in Figure 28 indicate that little systematic error remains, a fact supported by the mass-curve coefficient in Figure 25. The scattergrams indicate that the model simulated accurately both the high and the low flows. Inspection of the summary statistics for the first event, indicates that no further adjustment is necessary, as the values of most of the coefficients are very close to unity and the correlation is excellent. The calibration results can be further verified using the second event. The result of the simulation is shown in Figure 29. All the statistics had similar values to the first event.

The agreement of the simulated and measured discharges at the Bridge station is fairly good (Figure 24), however, it is very difficult to achieve the same degree of success as obtained for the water levels (Lai, 1981). As illustrated in Figure 24, the discharge in the estuary is tidal, with a period of 12,5 hours.

The runs were performed with a time-step of 30 minutes. The implicit variables were set equal to one (θ=1, χ=1, ψ=0,50). The model simulated accurately the prototype after very few runs. This can be attributed to the relatively simple configuration of the section of the estuary simulated. If the estuary mouth had to be simulated, then the calibration process would be more complicated as optimum values for the head losses in the mouth would have to be found. Wind shear stress was not considered as it is limited to the upper reaches of the estuary and the southern portion of the lake itself (Hutchison, 1976).

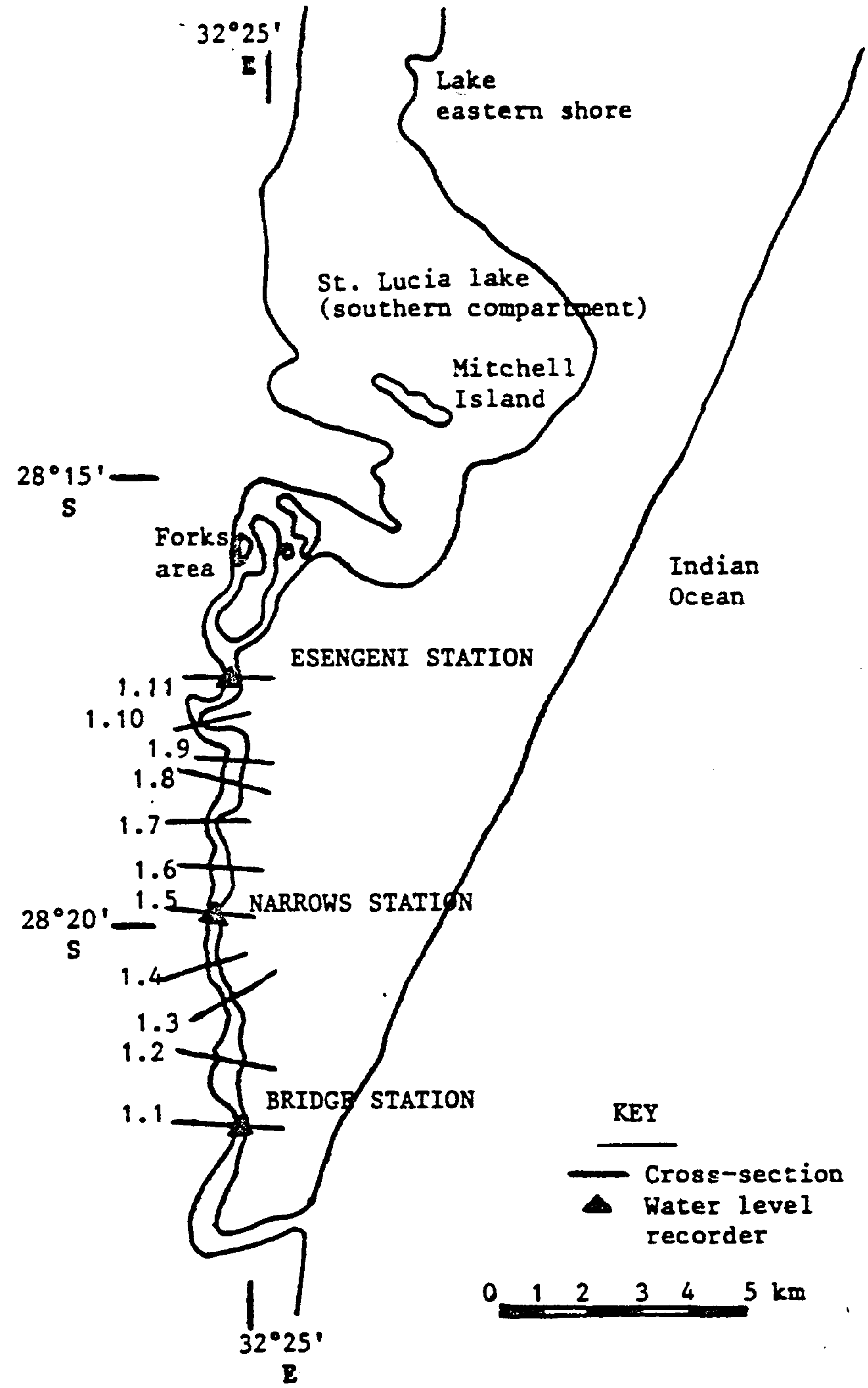

Figure 22. Plan view of St.Lucia lake estuary showing locations of cross-sections and water-level recorders

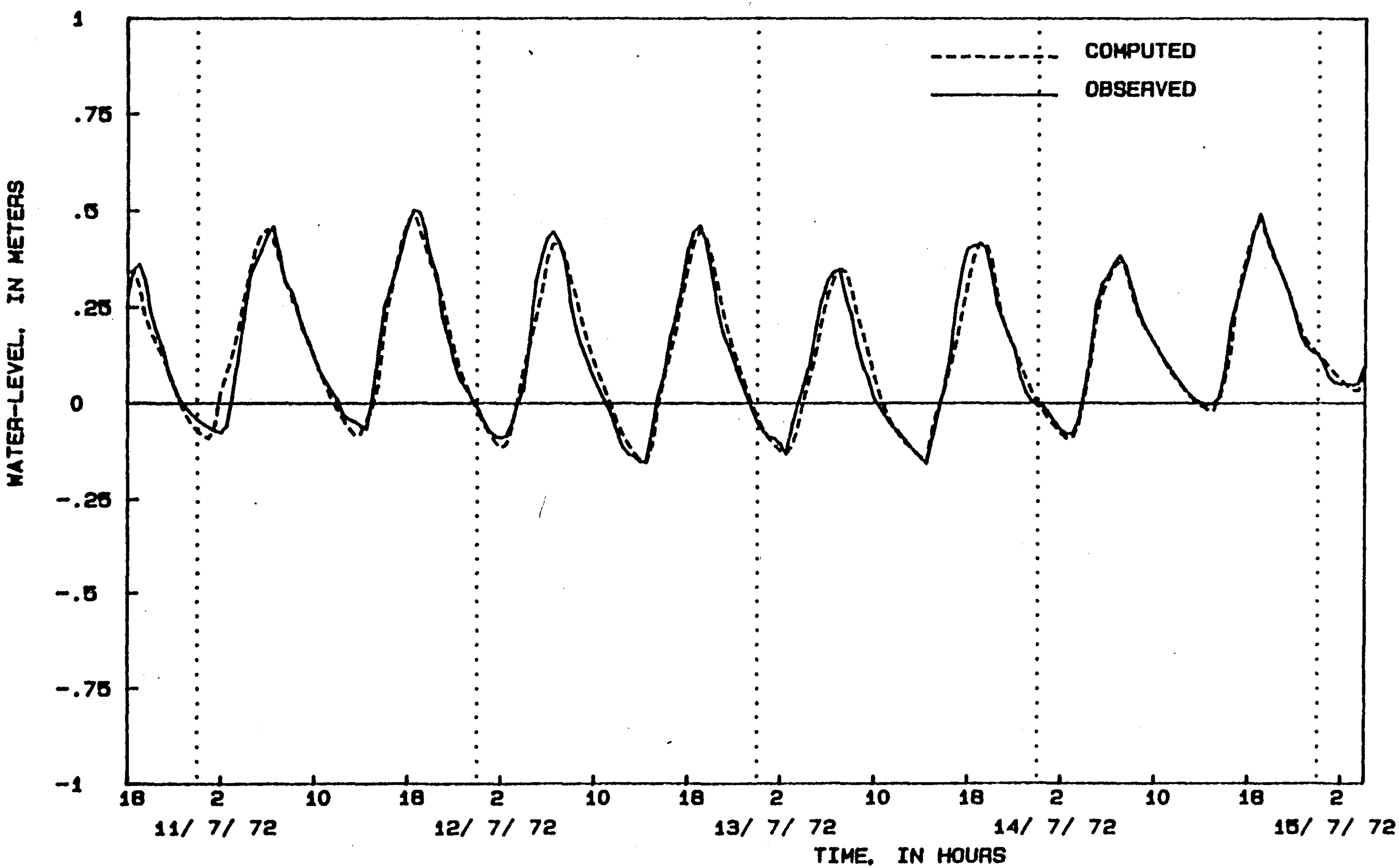

Figure 23 Observed and simulated water-levels from the St.lucia lake estuary - Narrows station - July 11-15, 1972.

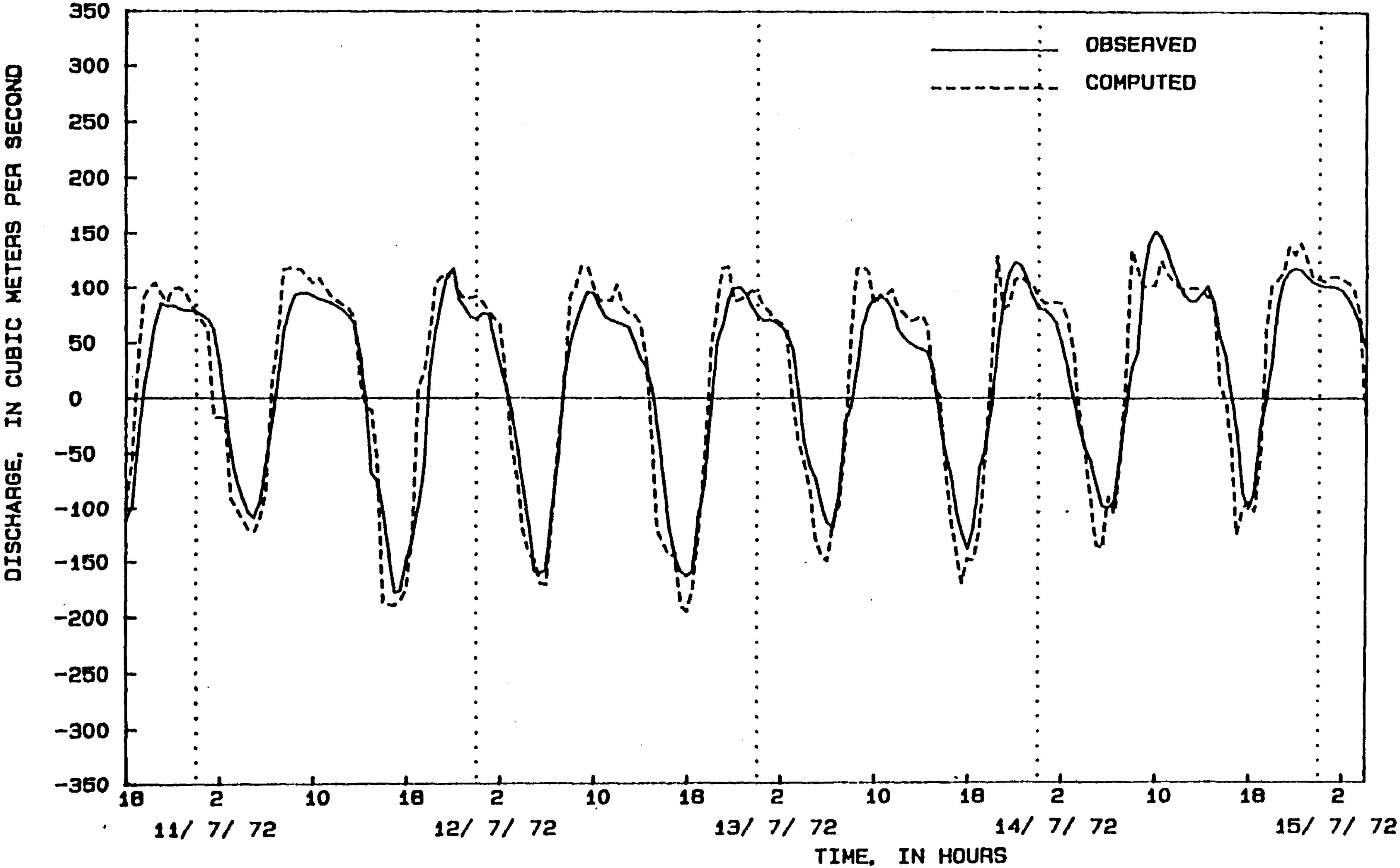

Figure 24. Observed and simulated flowrates from the St.Lucia lake estuary - Bridge station - July 11-15, 1972

```
UNSTEADY FLOW SIMULATION SUITE OF PROGRAMS
ONE DIMENSIONAL FLOW IN BRANCHED AND
LOOPED RIVER NETWORKS
STATISTICAL COMPARISONS
Developed by P.KOLOVOPOULOS

% error in the simulated maximum.......: -0.56
% error in the simulated mean..........: -0.04

Sum of squared-residuals (m)^2.........:  0.22
Sum of absolute residuals (m)..........:  6.01
Sum of absolute area of divergence(m*s): 223.8

Mean deviation.........................:  0.01
Standard deviation.....................:  0.03
Absolute area/ordin. divergence........:  0.84
Serial correlation coefficient.........:  0.73

Standard error of estimate.............:  0.03
Proportional error of estimate.........: 60.97
Reduced error of estimate..............:  0.20
Coefficient of persistence (hr^2)......: 60.82

Correlation coefficient................: 0.982
Modified correlation coefficient.......: 0.969
Coefficient of determination...........: 0.964
Coefficient of efficiency..............: 0.961
Residual mass curve coefficient........: 0.949
```

Figure 25. Statistical summary for calibrated model (simulated water-levels; St.Lucia lake estuary; Narrows station; July 11-15, 1972).

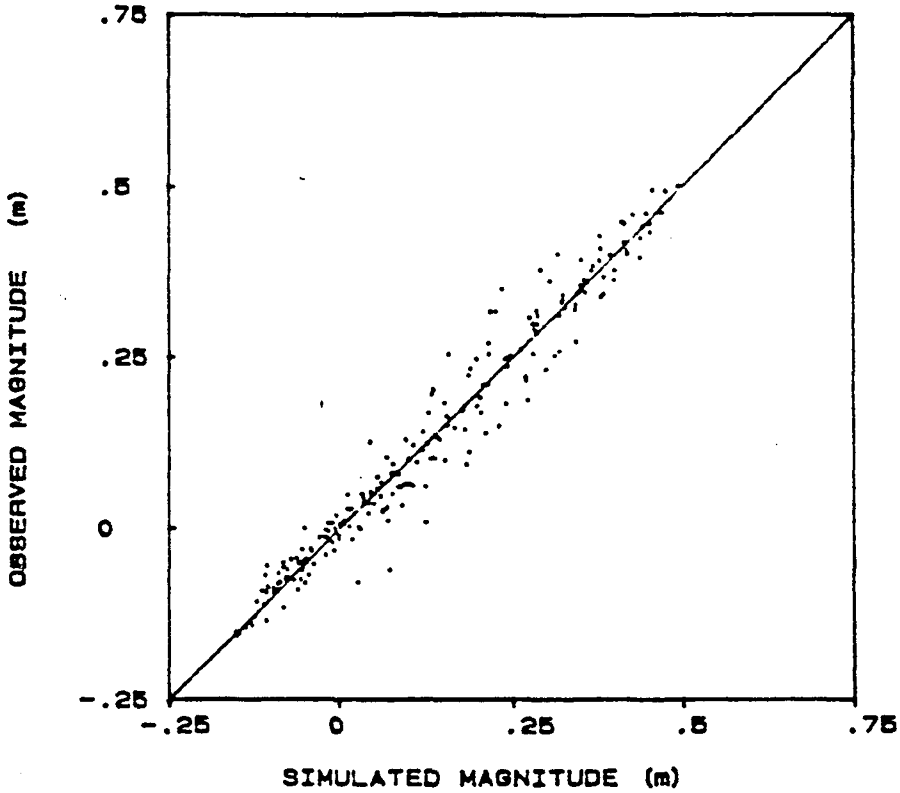

Figure 26. Scattergram of observed & simulated water-levels
(St.Lucia lake estuary; Narrows st.; July 11-15, 1972)

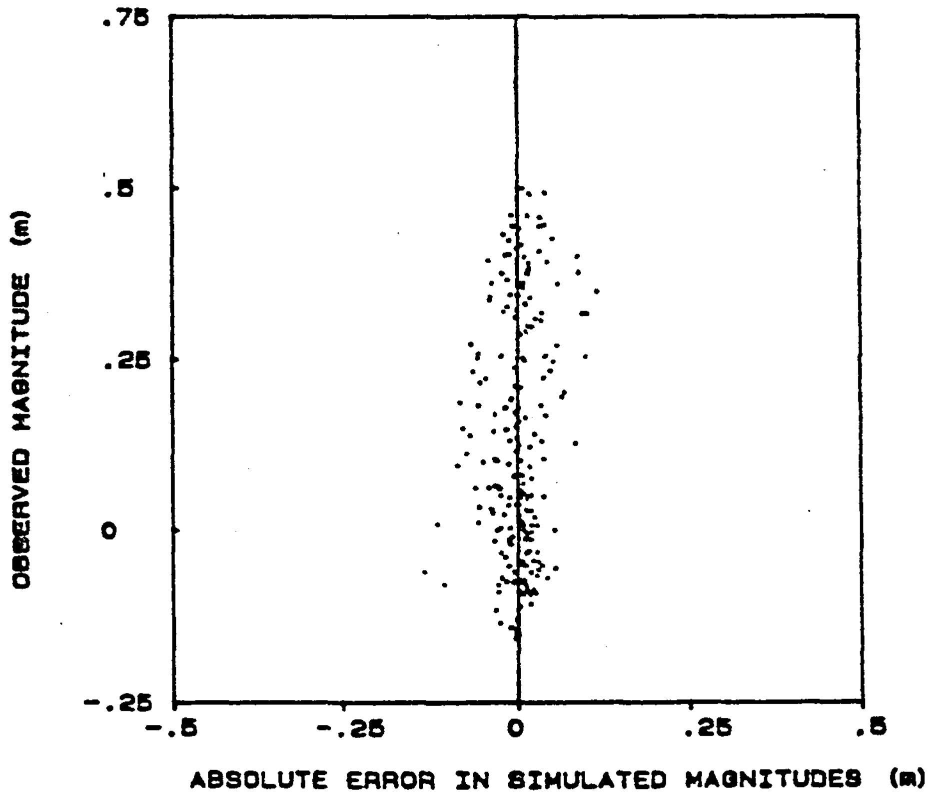

Figure 27. Absolute errors of simulated water-levels
(St.Lucia lake estuary; Narrows st.; July 11-15, 1972)

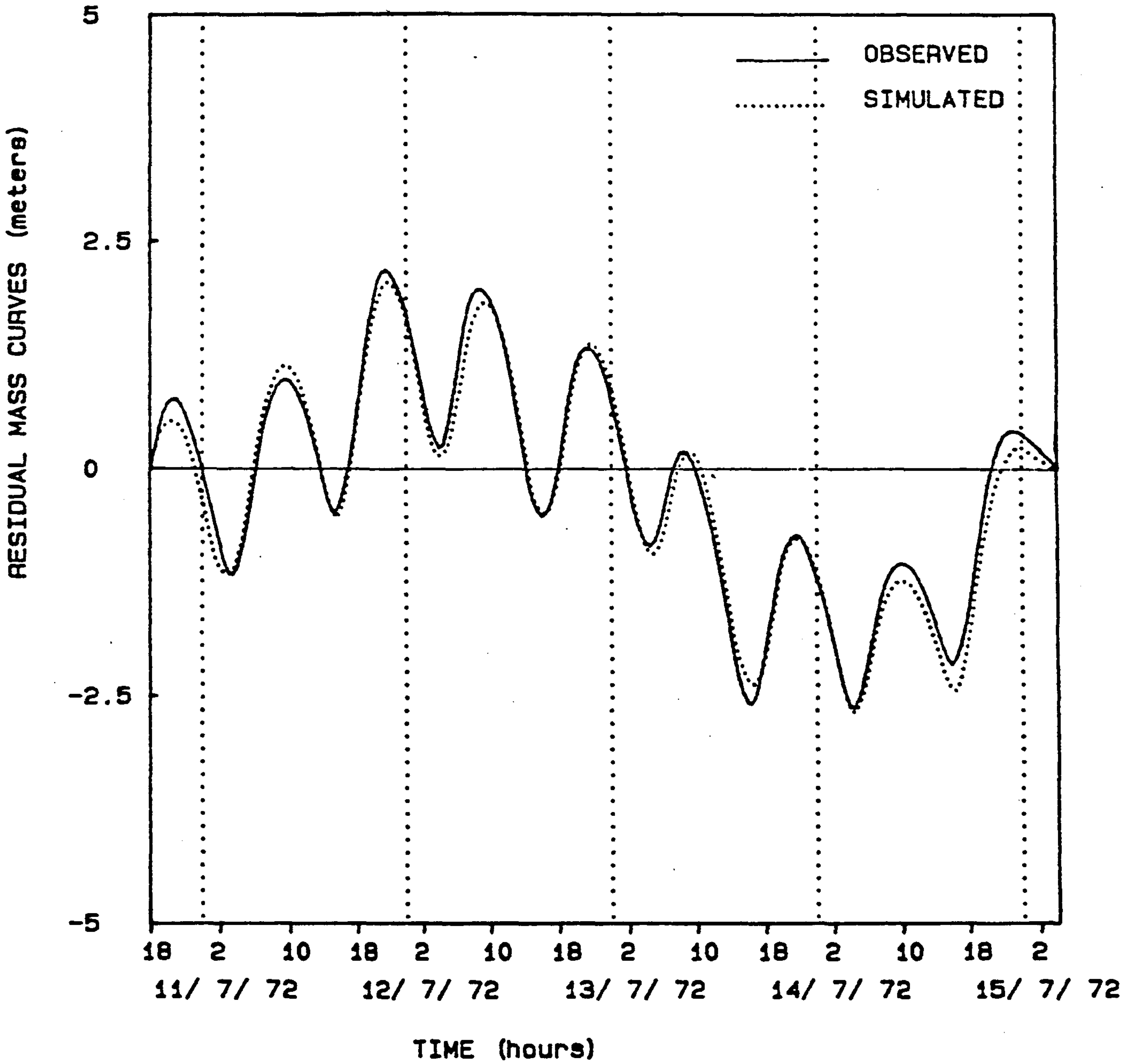

Figure 28. Residual mass-curves of observed and simulated water-levels (St.Lucia lake estuary; Narrows station; July 11-15, 1972)

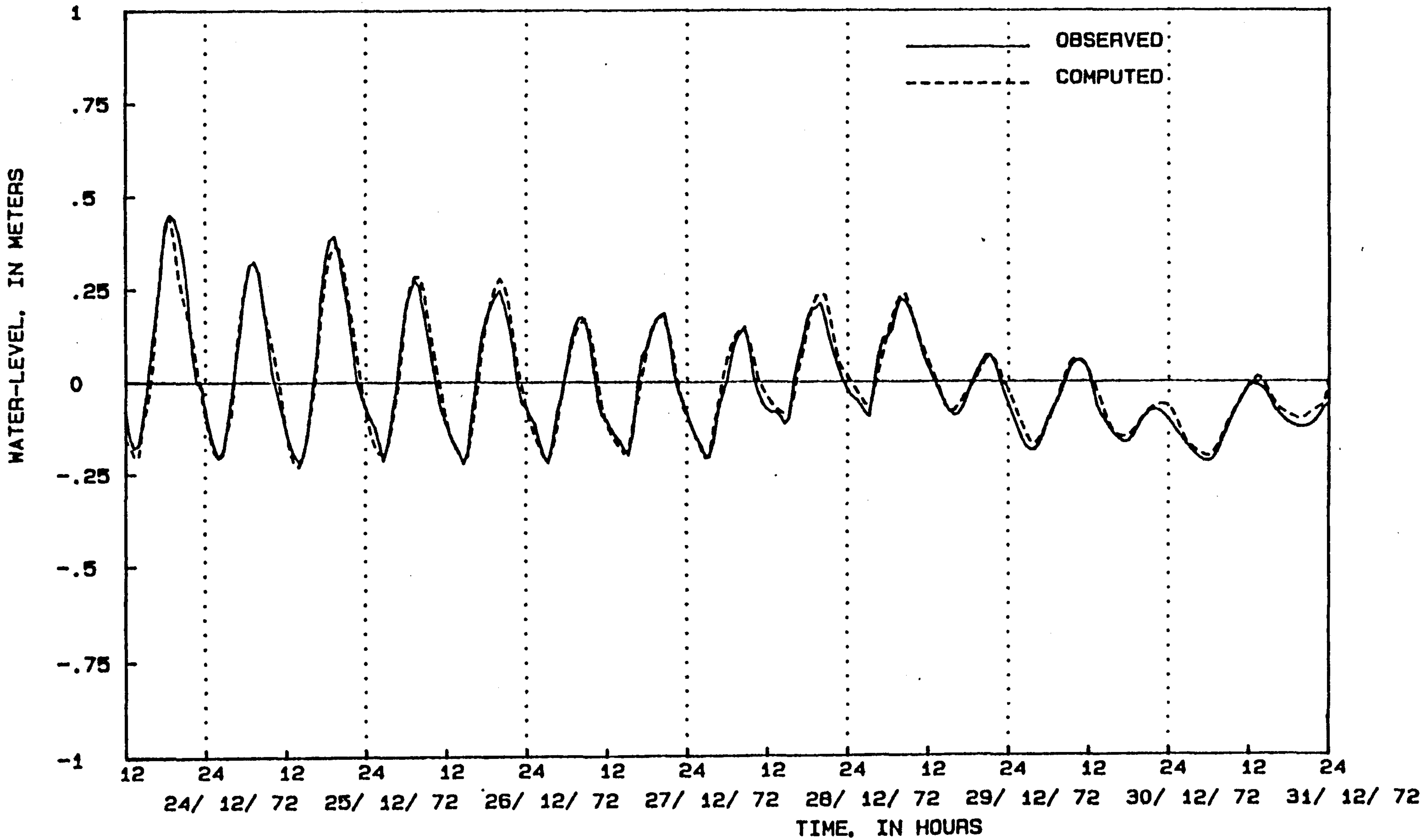

Figure 29. Observed and simulated water-levels from the St.-Lucia lake estuary - Narrows station - December 23-30, 1972.

5.5 CONCLUSIONS

The example shows the capabilities of the unsteady flow simulation model and the implementation of a successive calibration and verification. According to the analysis of sections (5.2) and (5.3), a systematic approach to model calibration and verification can be developed in three steps:

- **Preliminary calibration:** The data used as input to the model should be checked. Application of correlation techniques, and graphical techniques as mass curve plots can help to identify cases where normal relationships between data depart from an accepted pattern.

  The modeller must decide which parameters to estimate by adjusting values to minimise errors. Measured field data should generally not be altered during the calibration process. Data suspect to recorded water-surface elevation errors are corrected by applying datum correction to the boundary value data. Similar adjustments at all the boundary data points can correct errors due to excessive or too small cross-sectional areas. The preliminary model calibration involves successive adjustments of the roughness-resistance coefficients until reasonable agreement between the computed and measured flow data is achieved.

- **Refined calibration:** Once the preliminary calibration has developed compatible data series, the calibration needs to be refined to obtain the best possible matching of the time-series. The graphical aids give an immediate visual access to the quality of the calibration. The scattergrams and the residual mass curve plots reveal the systematic errors. The most important statistics for the success of the calibration are the coefficient of persistence, residual mass curve and efficiency which are checked as the acceptance criteria are made more demanding. The simulation is then repeated. Secondary parameter adjustments, as different weighting factors, variable roughness etc. are now included in the simulation.

- **Model evaluation and verification:** After the model has been calibrated, a different set of data is used to evaluate its performance. If the coefficient of efficiency and the residual mass curve coefficient and other statistics are satisfactory, then the model can be utilised to simulate flow conditions beyond the calibration range. Sufficient checks must be made to ensure the validity of the calibration for such extreme events.

Finally, applying a systematic calibration and verification process the following points must be taken into account:

- It is easier to obtain better agreement in stage or surface profile simulation than to achieve the same degree of success with discharge or velocity simulation.

- In order to avoid an unnecessary, complicated and prolonged model-calibration process, it is important to identify and correct errors in the directly measurable quantities as early in the calibration process as possible (Schaffranek et al. ,1981).

- It is unrealistic to expect the unsteady flow simulation model to generate output that is more accurate than the data input and the calibration data. Assuming the absence of systematic errors and blunders, it is generally agreed that stage measurements can be made to an accuracy of plus or minus 8% of the true value. These potential inaccuracies in the input should be considered during the calibration process.

- In all the phases of model calibration, the results and the parameter values must be checked for reasonableness. In other words, model calibration should not become the force-fitting of a physical situation to an inadequate model. If the reproducing of recorded floods is impossible or suspect to errors, the assumptions underlying the model may be incorrect or inadequate.

The methodology developed in this Chapter for the calibration and verification of the unsteady flow simulation model is applied to all the applications in the following Chapters.

6.0 MODEL IMPLEMENTATION

6.1 INTRODUCTION

Numerical simulation techniques based on the complete St. Venant equations for one-dimensional open channel flow have proved useful in the assessment of the extent of flooding and the design of flood control schemes. In the previous chapter techniques for model calibration and verification were outlined. In this chapter the ability of the model to simulate various river flow conditions is tested.

Seven examples were selected representing different practical application problems. Examples (6.2) and (6.3) display rapidly and highly varied unsteady flow over short reaches. The former uses hypothetical data (bore propagation caused by a turbine closure) and the latter is based on real data in an irrigation canal situated in France. Example (6.4) (Sabine river) is a simulation of a long reach (64 km) with limited data and over a long time period. Example (6.5) (Barkley-Kentucky canal) presents an interesting problem of reciprocating unsteady flow, where the flow pattern is controlled by the relative changes of water levels at both ends. Example (6.6) is an example of flood propagation caused by a partial dam failure. Example (6.7) (St-Lawrence river) was selected to demonstrate the ability of the developed model, to simulate the flow in interconnected channels, in a major navigation waterway 530 km long. Example (6.8) is the simulation of a South African river, the Vaal, and it's major tributary, the Klip river, with data from the recent floods of the summer of 1988.

These examples demonstrate the model's capability of handling different types of flow, and indicate the reliability and versatility of the numerical model.

6.2 BORE PROPAGATION EXAMPLE

Bores, or sharp-front surges occur frequently in canals and rivers. A sudden reduction in flow through a turbine can create a surge or bore that propagates upstream in the headrace. Failure of hydraulic structures can produce a huge wall of water which rushes downstream. Tidal bores are known to occur in estuaries throughout the world due to physical conditions and high local tide. Therefore the simulation of the propagation of a bore in a channel is of engineering significance.

The problem of propagation of a bore has been studied by a number of investigators interested in unsteady flow problems, for which sudden changes in either depth or flow, or both occur. Stoker (1948) used the method of characteristics for predicting the inception of a bore. Martin and DeFazio (1969) demonstrated that the simple finite-difference equation developed by Stoker could be adopted for open channel rapidly varied flow. In this example, the ability of the developed model to describe the bore propagation in open channels is demonstrated. At the same time, the model characteristics such as approximation, convergence, stability, and flexibility are analysed using θ and $\Delta t/\Delta x$ as variables.

The model was used to simulate a sudden turbine closure in a power canal. Similar numerical experiments were conducted at SOGREAH in 1964 (Cunge and Wegner, 1964), using a mathematical model of a trapezoidal channel having dimensions similar to the power canals in the Rhone River Valley (France). The invert width of the channel was 100 meters, Manning's coefficient 0,0125, channel slope 0,00002 and initial water depth approximately 14,0 meters. The side slopes used in this simulation were 1:3 and the channel was assumed to be 2000 meters long, conveying a steady discharge of 2500 m^3/s. The boundary conditions were:

- A constant water-level at the downstream boundary (reservoir).
- Variable discharge at the upstream boundary (power plant) as shown on Figure 30.

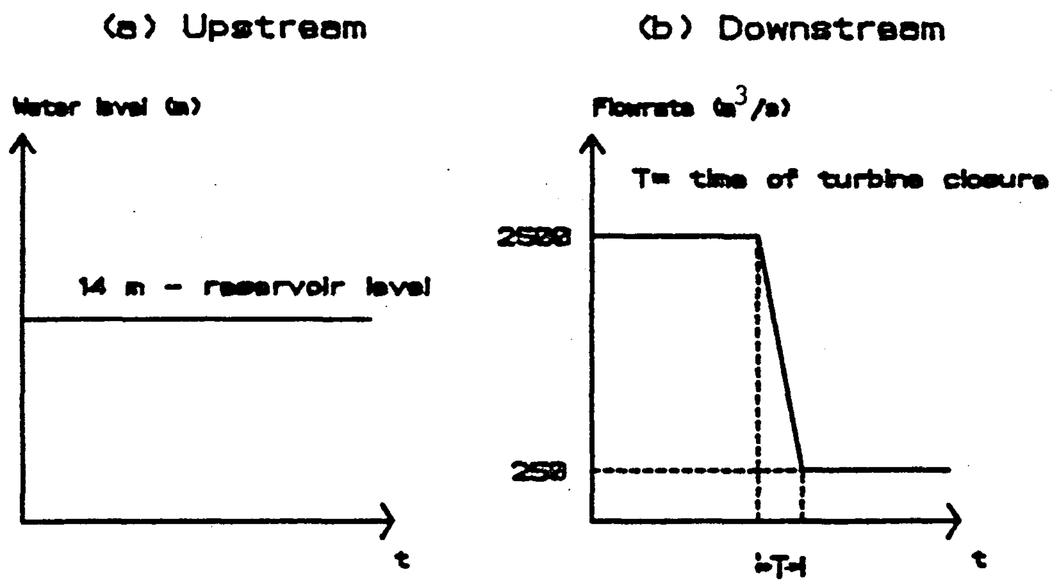

Figure 30. Boundary conditions

The initial height of the wave, due to the sudden turbine closure, can be calculated theoretically using Favre's formula (Favre, 1935):

$$\Delta Q/A = U_0 - \quad g(Ah'/\Delta A+J)(J+\Delta A/A) \qquad (6.1)$$

where

A, U_0 : the area and velocity of the steady initial flow respectively.

ΔQ : decrease in the discharge

h' : wave height due to ΔQ

ΔA : cross-sectional area increase corresponding to h'

J : distance from the centroid of ΔA to the free surface

Applying the formula to the example data, the h' is calculated iteratively to be $h'= 1,20$ meters. Approximately the same initial height was computed in the simulation, thus the model gives a good result for the initial wave height. The model output in graphical form provides the following information:

- Water levels along the channel at given times.
- Water-stage variation with time at given points.
- Discharge variation with time at given points.

Figures 31 and 32 show the water level and flowrate variation at the termini of the channel and at 700 meters distance from the power plant. In this example the turbine closure time from a flow of 2500 m^3/s to 250 m^3/s was 1 min. The weighting factor θ was maintained at a value of 2/3 for maximum accuracy.

It can be seen that a wave reflecting from the tunnel head keeps the same sign, while a wave reflecting from the reservoir will change its sign. The program computes the height of the main body of translatory waves and the variation in time following the two basic assumptions for the St. Venant equations. These are:

- pressure distribution in a given cross-section is hydrostatic,
- the vertical velocity components are negligible.

The program does not, however, evaluate the secondary Favre undulations which are apt to be superimposed upon the main wave body (Electricite de France, 1965). Although this exceeds the

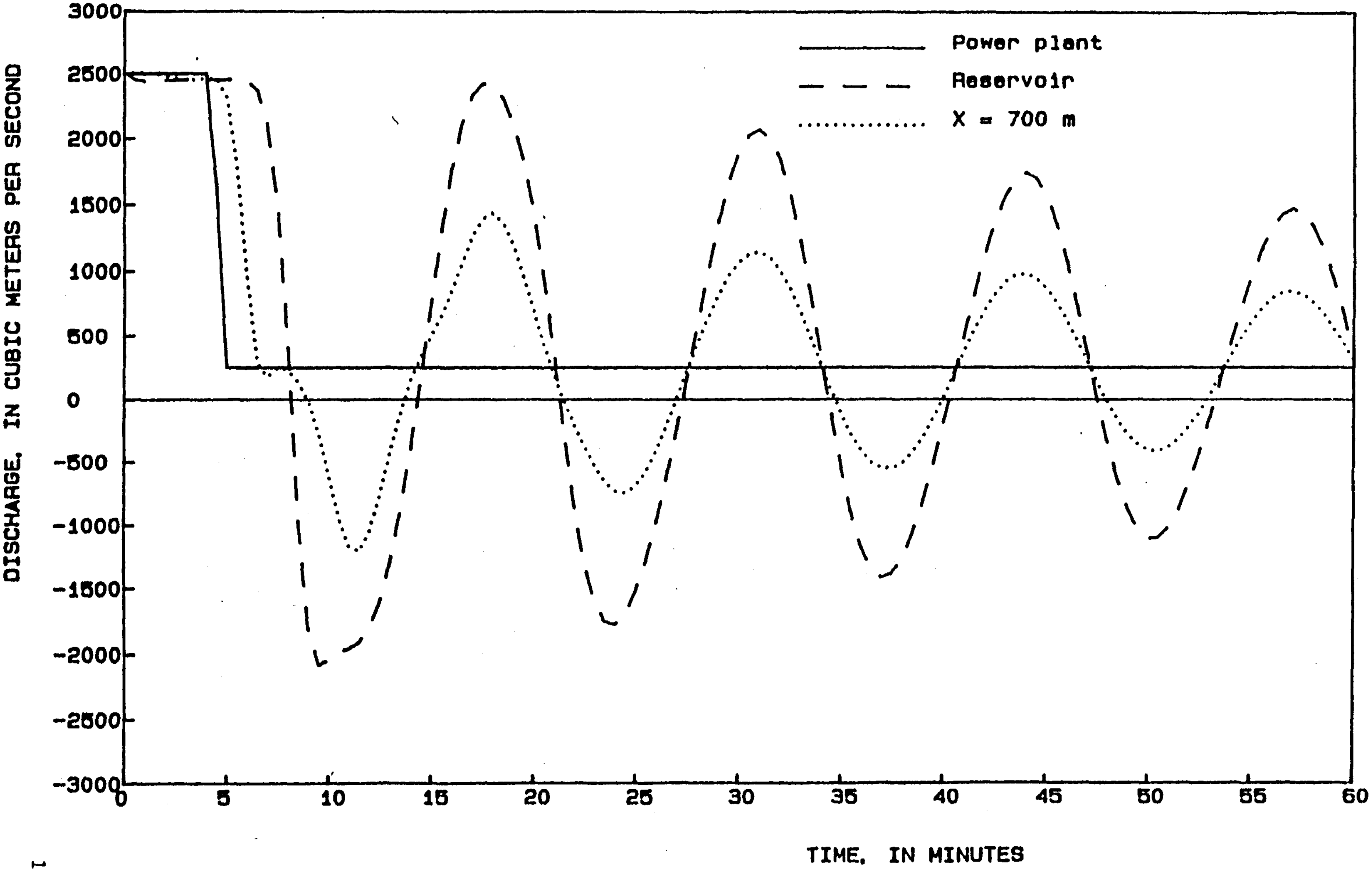

Figure 31. Simulated flowrates - turbine closure from 2500 m3/s to 250 m3/s in 1 min

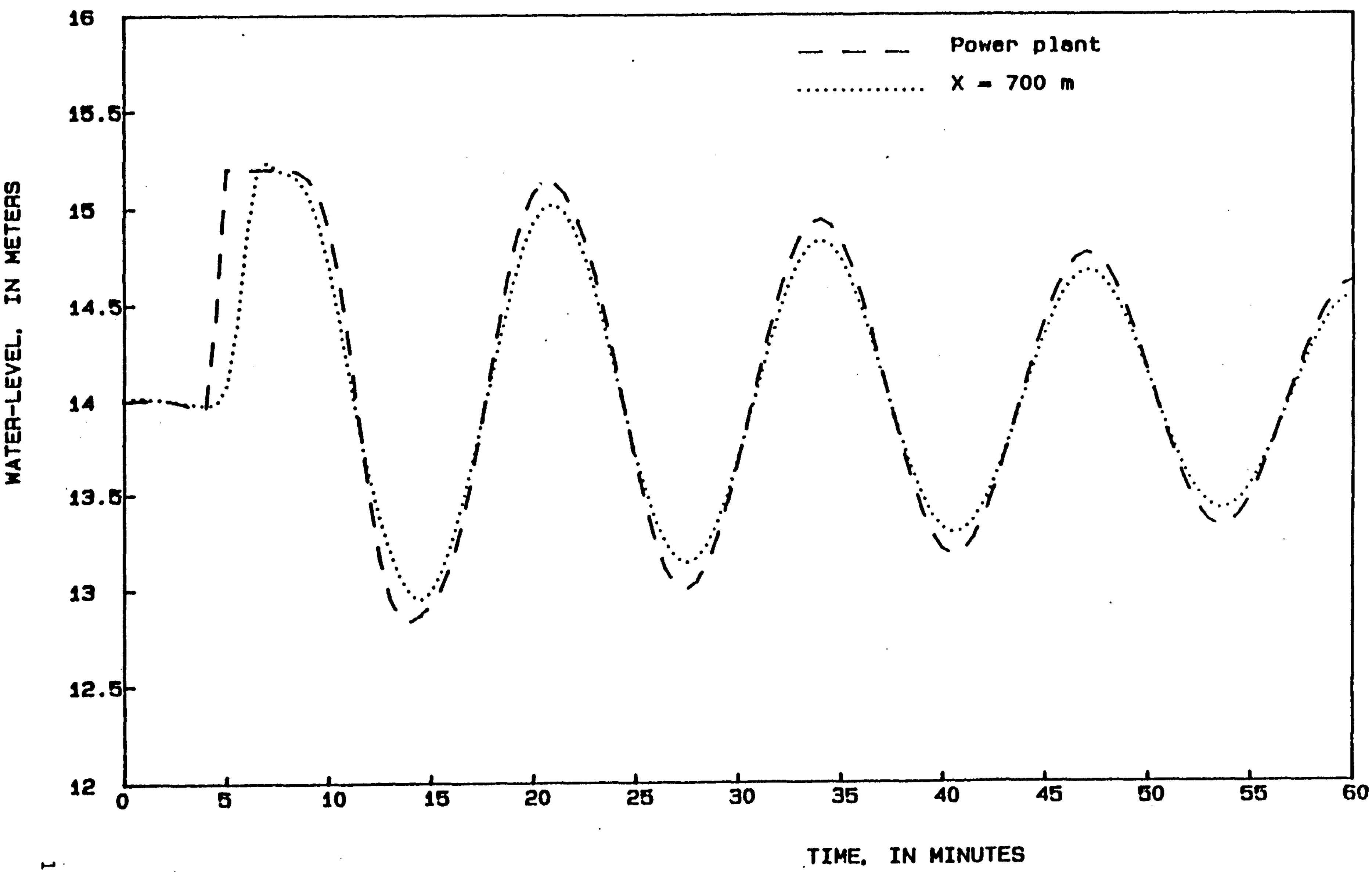

Figure 32. Simulated water levels - turbine closure from 2500 m3/s to 250 m3/s in 1 min

scope of the example, in practice, it is necessary to establish whether such secondary undulations exist and if so, determine their amplitude. This determination is based on experience gained through previous investigations of scale models and in the field. Secondary undulations are usually formed at Froude numbers between 1 and 1,3.

In Figure 33 the longitudinal profiles are shown for the same simulation, 60 sec and 180 sec after the turbine closure. Since the celerity of small waves computed by the formula $\sqrt{gA/B}$ is of the order of 9 m/s, the ratio of $\Delta t/\Delta x$ was kept in the same range. Two runs were performed initially, with different Δx and Δt values, while keeping the ratio $\Delta t/\Delta t = 8{,}33$ constant. From Figure 33 it can be concluded that the front is steeper when Δx is smaller.

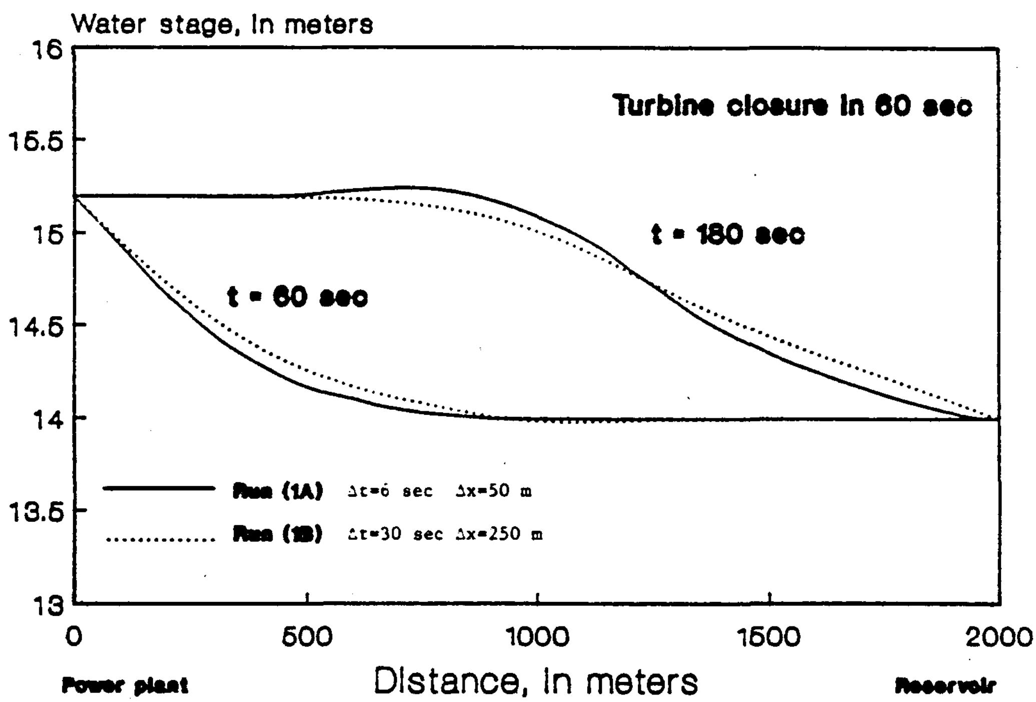

Figure 33. Longitudinal profiles - 60 sec and 180 sec after the turbine closure

The computations were repeated for a duration of turbine closure of 15 sec. Two sets of analysis were performed in order to investigate the effect of the variable ratio $\Delta t/\Delta x$ on the stability and accuracy of the computation. From Figure 34 it can be seen that when the ratio $\Delta t/\Delta x$ becomes smaller (Run 2B), the wave front becomes more diffused. If this ratio is very small, long artificial waves appear, without endangering numerical stability. The results are similar to the results of the SOGREAH's experiments. In Figure 35 the effect of θ on the stability and accuracy of the results are shown. A value of θ less than 0,66 (Run 3A) creates oscillations in the solution. The most stable occurred with θ=1 (Run 3C). However the final results are less accurate and the wave front is smeared, for the same Δx in all runs.

The above runs illustrate a rapidly varied unsteady flow simulation and the effect of the model variables on the stability and accuracy of the computations.

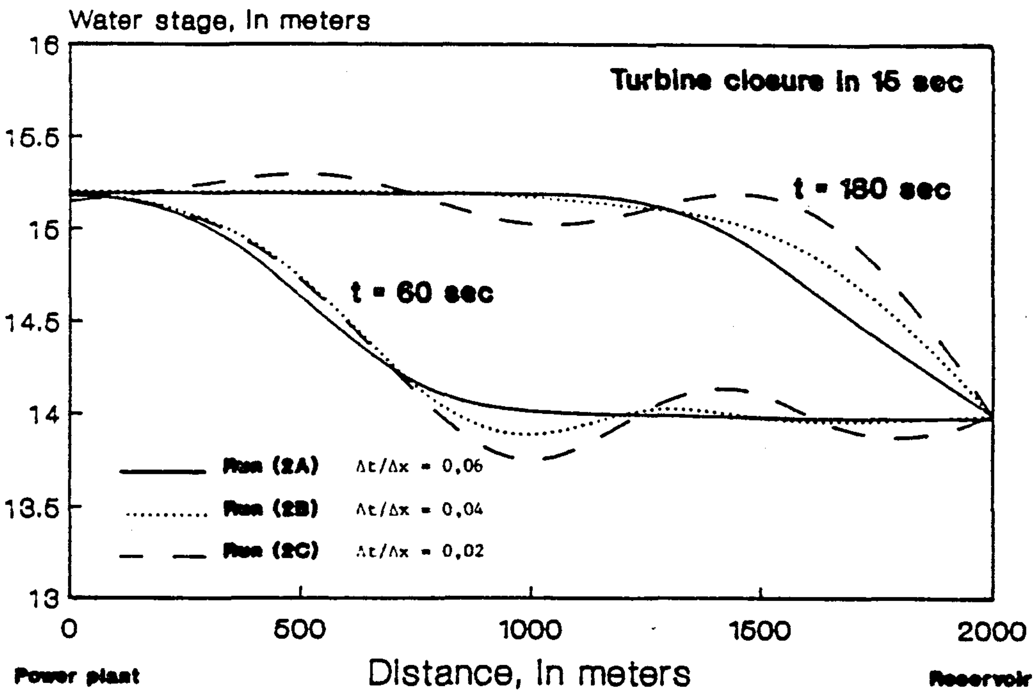

Figure 34. Effect of variable $\Delta t/\Delta x$

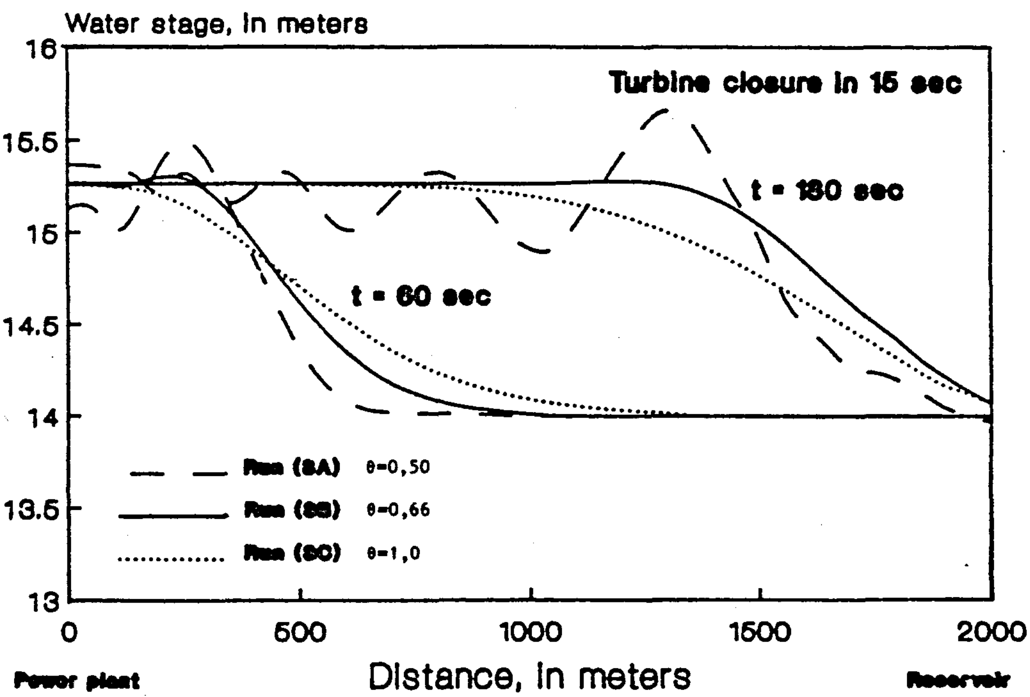

Figure 35. Effect of variable θ

6.3 CANAL DE PIGOUDET

The ability of the model to describe bore propagation was further tested by simulating a real life problem of an irrigation canal in France. Canal of Pigoudet, is a part of a system of irrigation canals of total length 25 km. The system of canals is described in an internal report of La Societe du Canal de Provence (1984). It consists of open conduits, galleries, automatic level regulation gates, manually operated gates and surge tanks.

The canal is concrete and has a trapezoidal cross-section uniform along the length of the channel, with 2,7 meters of bottom width and side slopes of 3:2. It has a maximum carrying capacity of 10 m^3/s. The longitudinal profile and the canal cross-section are shown in Figure 36.

Wignyosukarto (1983) discretised the canal into 23 cross-sections in order to simulate a bore propagation using the model CARIBA (SOGREAH, 1978). The simulation was repeated using the OSYRIS model. The original cross-sectional data were arranged in three branches. In Figure 37 the adopted schematization of the canal is shown. Sections (2.5)-(2.6) represent an automatic gate (Vanne de Pigoudet). The gate is of the radial type and is shown in Figure 38. The control structure is a source of instability if partially closed. However, in this simulation the gate is open.

Upstream (section 3.8) the flow is controlled by a gate and is steady at $Q=3,65\ m^3/s$. Downstream (section 1.1) the channel ends in a gallerie and the flow at the outlet is assumed to be critical. Therefore a relation of Q(Z) will be used as the downstream boundary condition. (Figure 39). Sections (3.6), (2.8), (2.1) and (1.4) are the points where the observations were taken. Five different roughness coefficients ranging from 0,0164 to 0,0189, were used for the sections (3.8-3.6), (3.6-2.8), (2.8-2.2), (2.2-1.6), and (1.6-1.1).

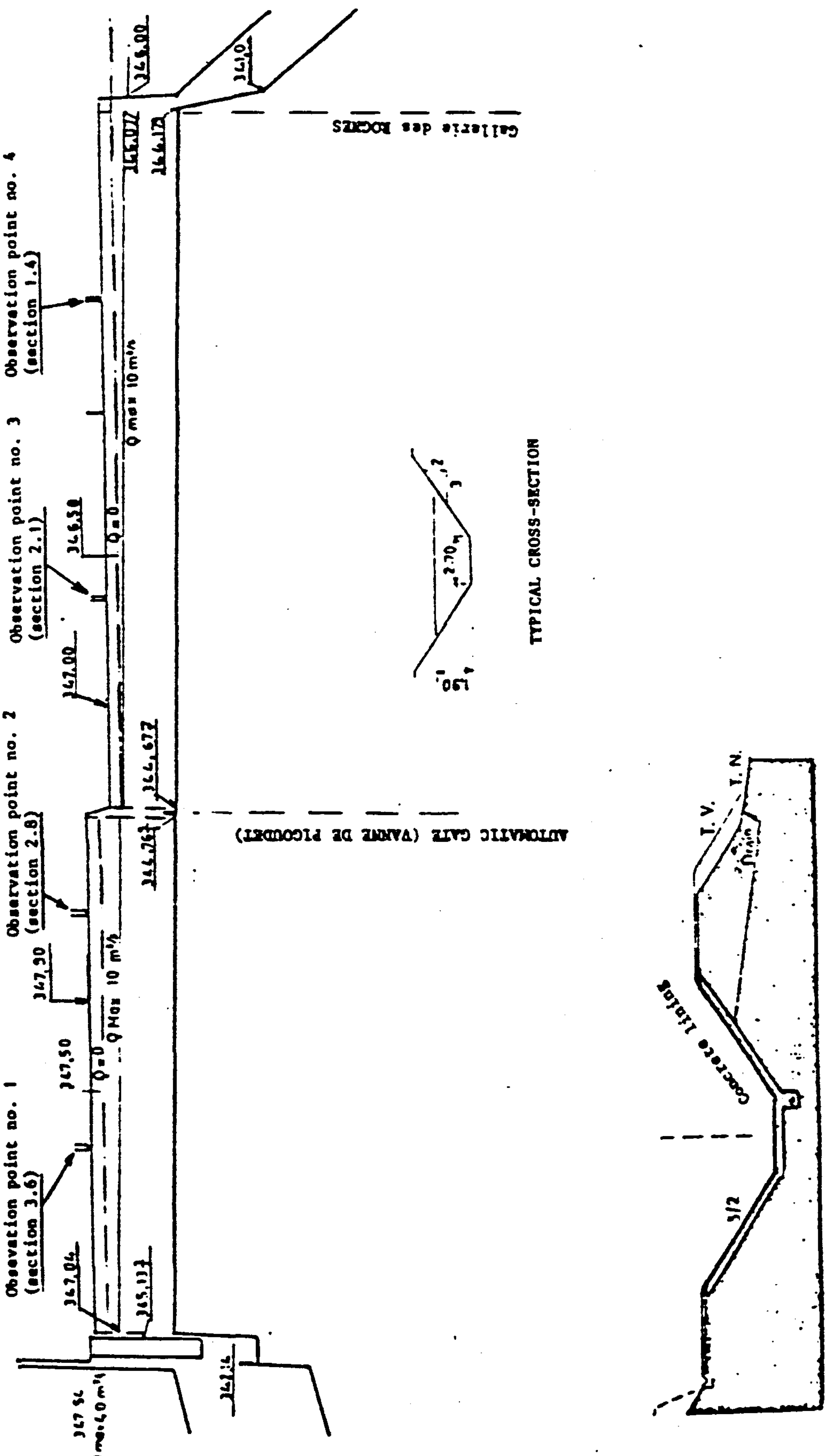

Figure 36. Canal de Pigoudet - Longitudinal profile & typical cross-section (Wignyosukarto, 1983)

To simulate the bore a sudden increase of discharge equal to $Q=2,65\ m^3/s$ was added to a steady flow with $Q=3,65\ m^3/s$. In his thesis, Tinguasangy (1983) compares the experimental results with the results of the CARIBA model. The simulation was repeated using the OSYRIS model and the results were compared. A time step of 2,5 min was used for the simulation. The computed water levels and flowrates at the observation points are shown in Figures 40 to 44. It is worthwhile noticing that the results are very similar to the experimental work and were obtained without any calibration using the roughness coefficients from the abovementioned thesis.

The results fitted well with CARIBA's model simulation results. This may be attributed to the similar numerical structure of the two models. The CARIBA model is a Preismann type implicit model. In this simulation, the weighting factor θ was maintained at a constant value of 1 for maximum stability. The slightly steeper front computed by the CARIBA model (Figures 40, 41) may be attributed to the lower θ value which was probably used. This is also indicated by the instability generated at the beginning of the simulation.

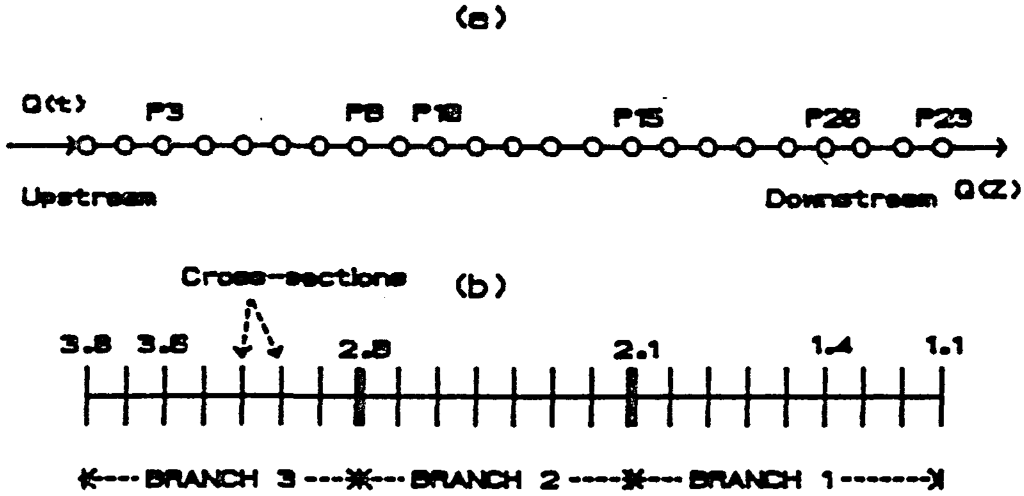

Figure 37. Canal de Pigoudet - Discretization used in the CARIBA model (a) and in the OSYRIS model (b)

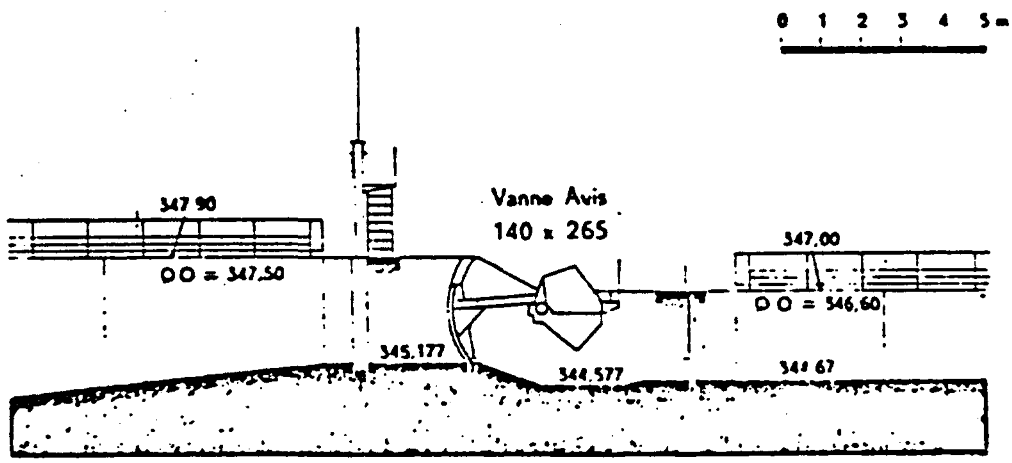

Figure 38. Automatic gate (Vanne) de Pigoudet (Wignyosukarto, 1983)

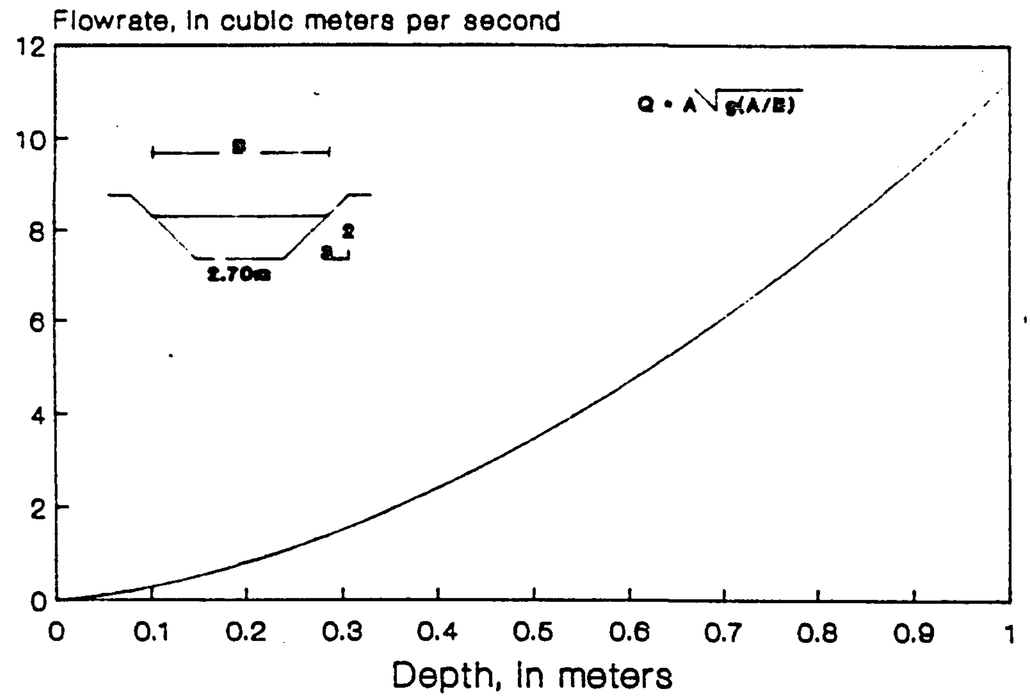

Figure 39. Canal de Pigoudet - Downstream boundary condition

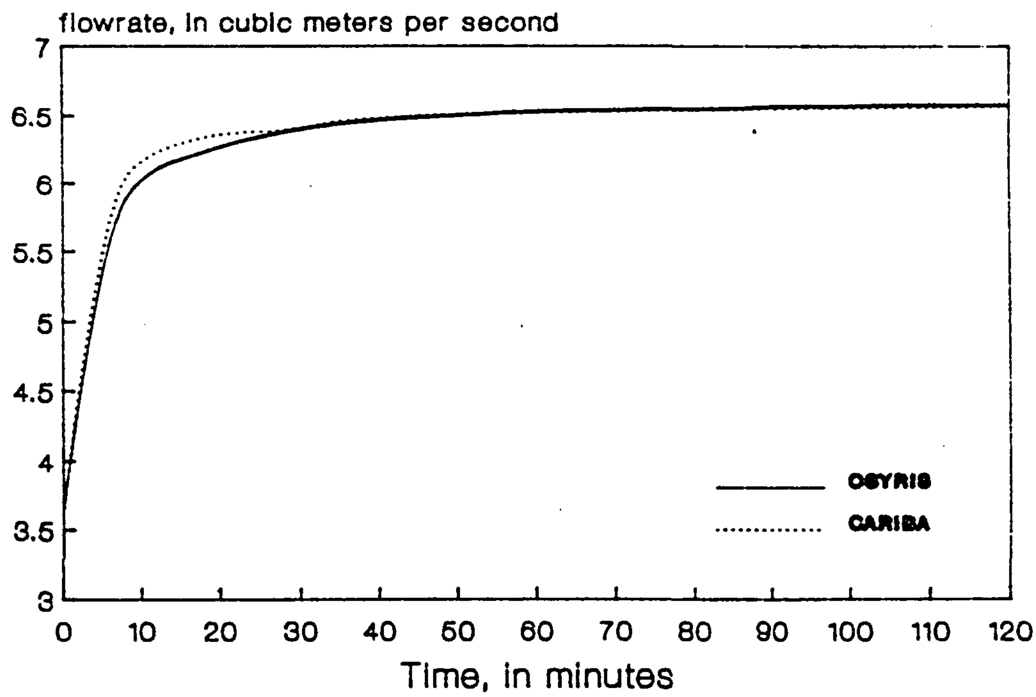

Figure 40. Canal de Pigoudet - Comparison of simulated flowrate hydrographs at section (3.6) - Observation point no. 1

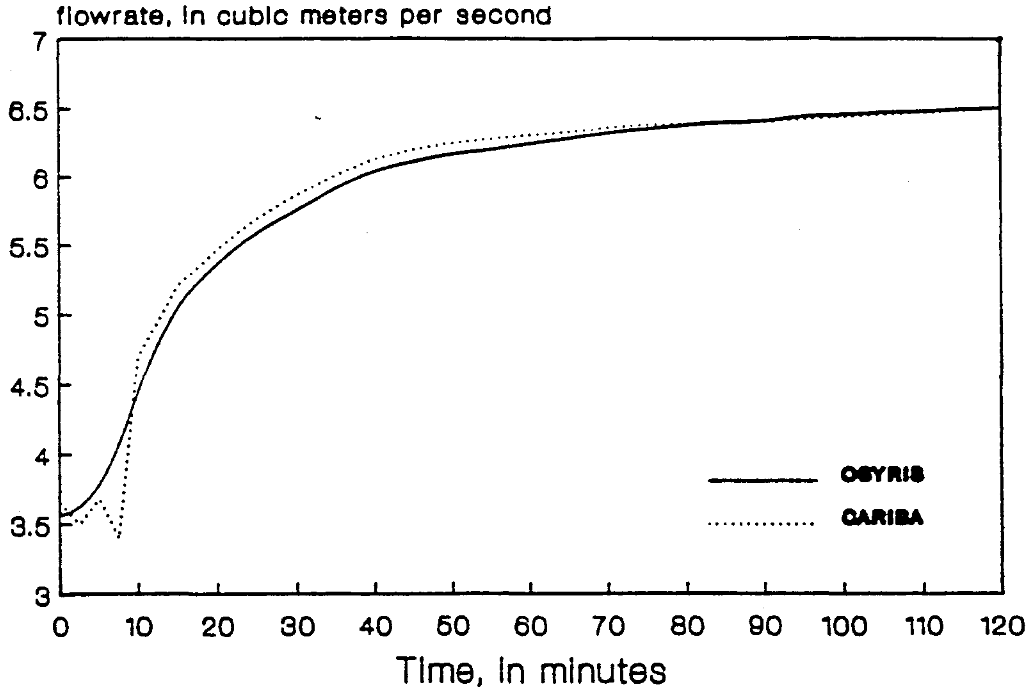

Figure 41. Canal de Pigoudet - Comparison of simulated flowrate hydrographs at section (3.1) - Observation point no. 2

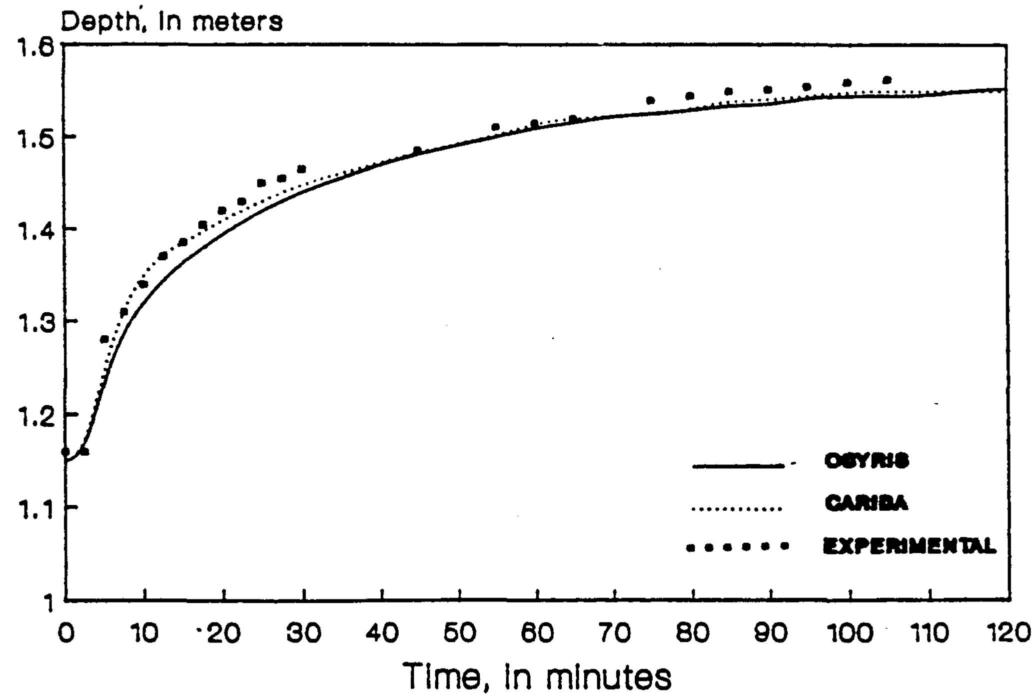

Figure 42. Canal de Pigoudet - Comparison of observed and simulated water levels at section (3.1) - Observation point no. 1

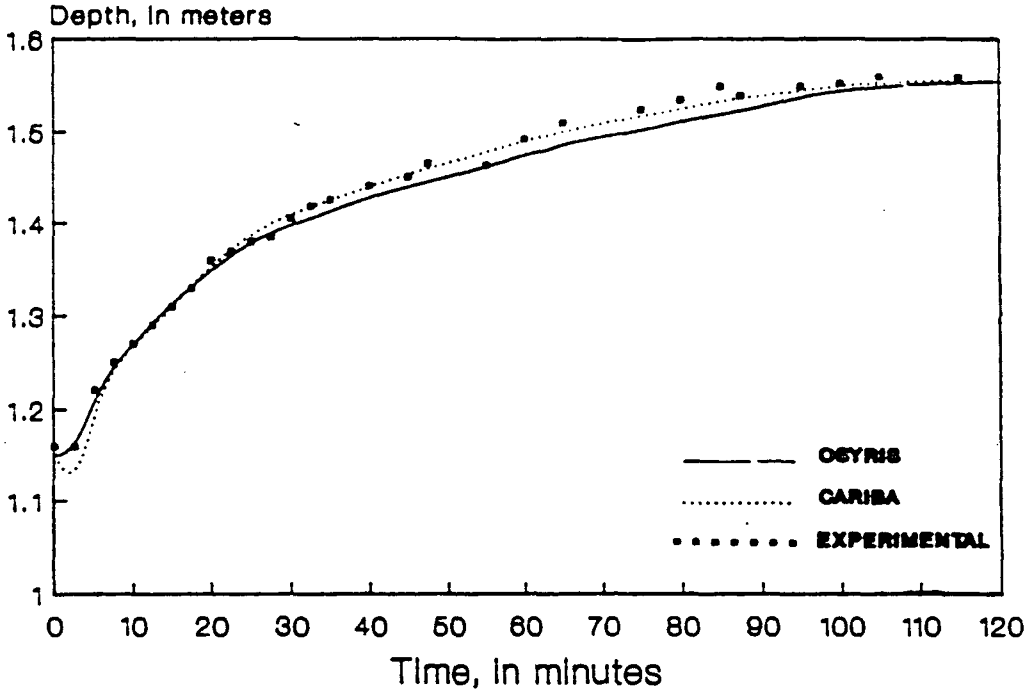

Figure 43. Canal de Pigoudet - Comparison of observed and simulated water levels at section (2.8) - Observation point no. 2

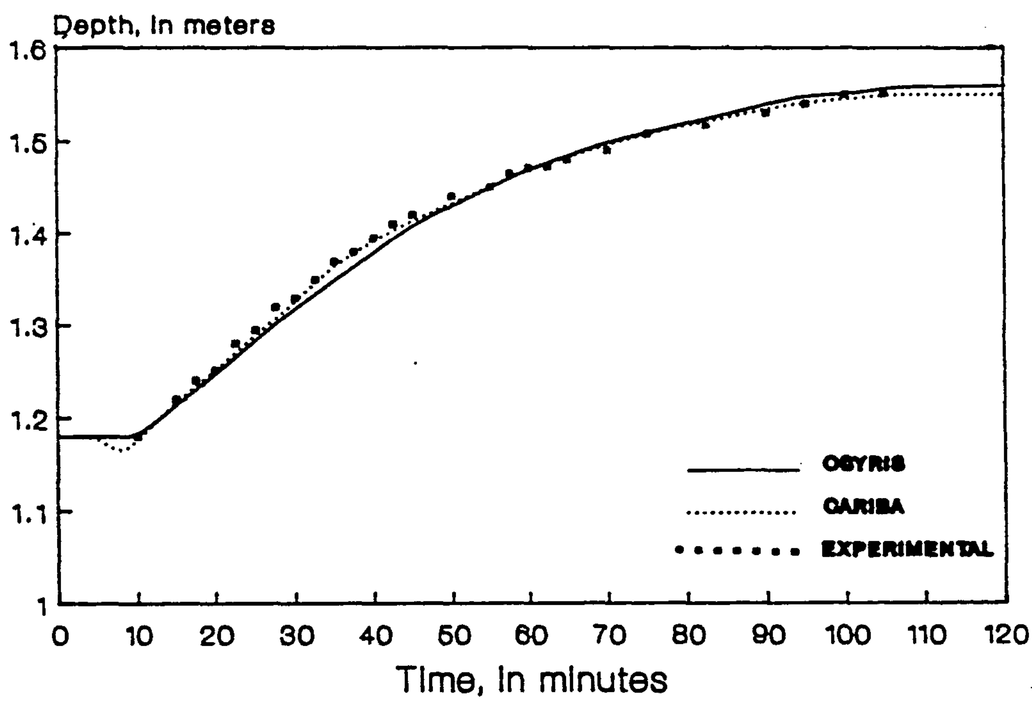

Figure 44. Canal de Pigoudet - Comparison of observed and simulated water levels at section (2.1) - Observation point no. 3

6.4 SABINE RIVER

The numerical model was applied to a 63 km stretch of the Sabine river (along the border of Texas and Louisiana) between Barkeville (upstream end) and Bon Weir (downstream end). The channel bottom slope over this reach of the Sabine river is approximately 0,13 m/km. The boundary data include:

- Observed upstream stage hydrograph from a gauging station near Barkeville (Figure 45).

- Observed downstream stage hydrograph from a gauging station at Bon weir.

- A calibrated downstream rating curve at Bon weir controlled by:

$$Q_R = 4,256 + 28,247\ y^{1,735} \tag{6.2}$$

where

Q_R the discharge in m^3/s
y the depth in m

Only four equally spaced sections were available, therefore the channel reach was divided into four sections 21 km apart. Channel cross-sectional width (B) is expressed as a function of the channel depth, y. The equation obtained from curve fitting is of the form (Amein and Chu, 1975):

$$B = a_0\ y^{a_1} \tag{6.3}$$

The coefficients, a_0 and a_1, for the situation in which y is shown in meters are given in Table 2.

Stationing kilometres	a_0	a_1
0	64,117	0,366
21	46,914	0,536
42	26,850	0,865
63	79,815	0,434

Table 2 : Sabine river - Cross-sectional data

Amein and Chu (1975) used the same cross-sectional data in order to demonstrate the capability of their four point implicit scheme. They estimated the Manning's roughness coefficient at n=0,027. The initial time t = 0 hr, corresponds to October 3, 1968. The initial upstream discharge was approximately 32,76 m^3/s, with an initial depth of 1,855 m. Downstream discharge was approximately 40,04 m^3/s with a depth of 1,22 m. The channel bottom elevation is 21,4 m upstream and 13,4 m downstream.

The observed upstream stage hydrograph and the downstream rating curve were used as boundary conditions. The computed downstream water stage hydrograph is compared to the observed hydrograph. In all the computations a time step of six hours was chosen. The computed downstream hydrograph from the application is shown in Figure 46 and is found to be in good agreement with the observed hydrograph.

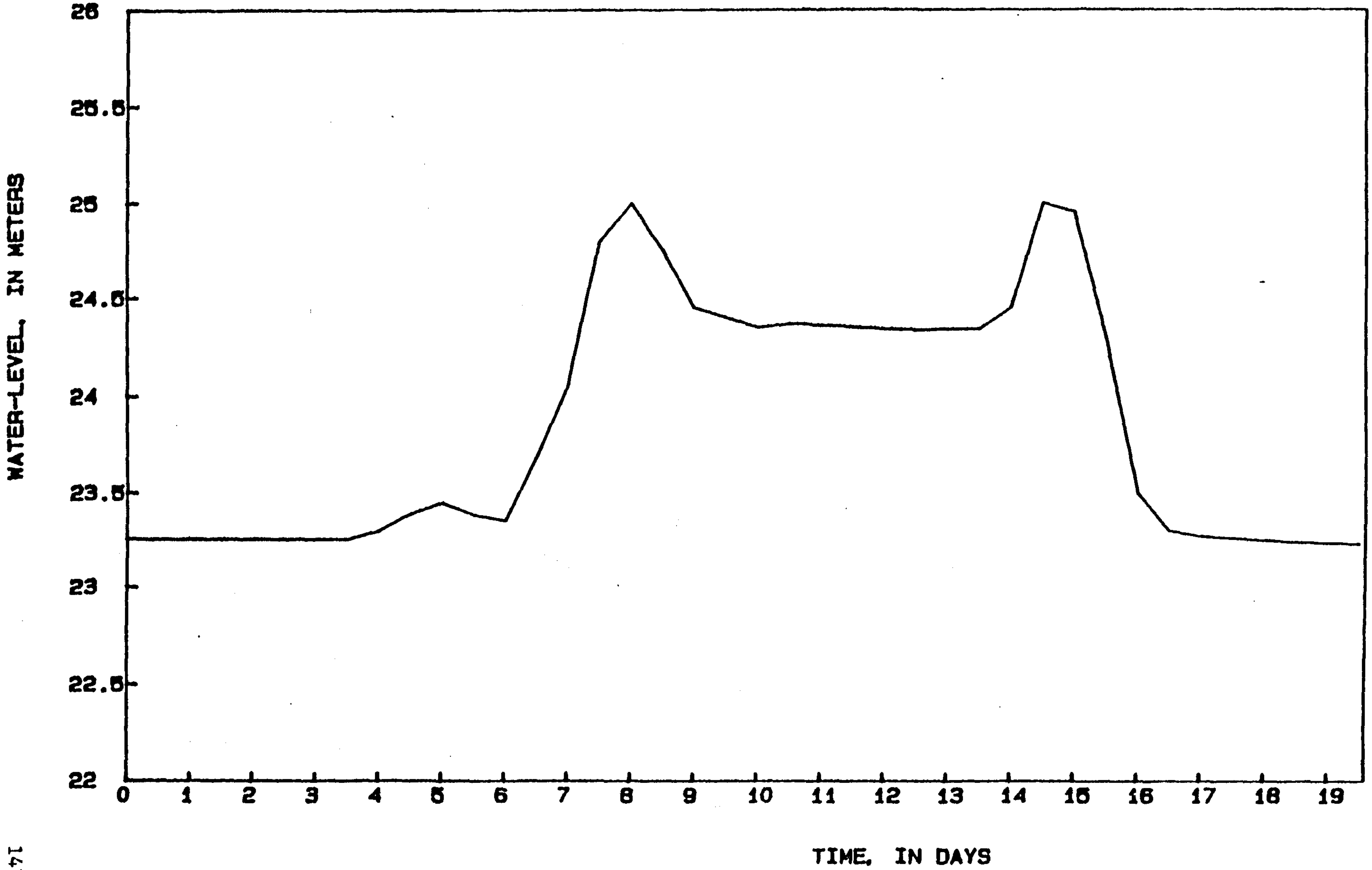

Figure 45. Upstream inflow stage hydrograph for Sabine river

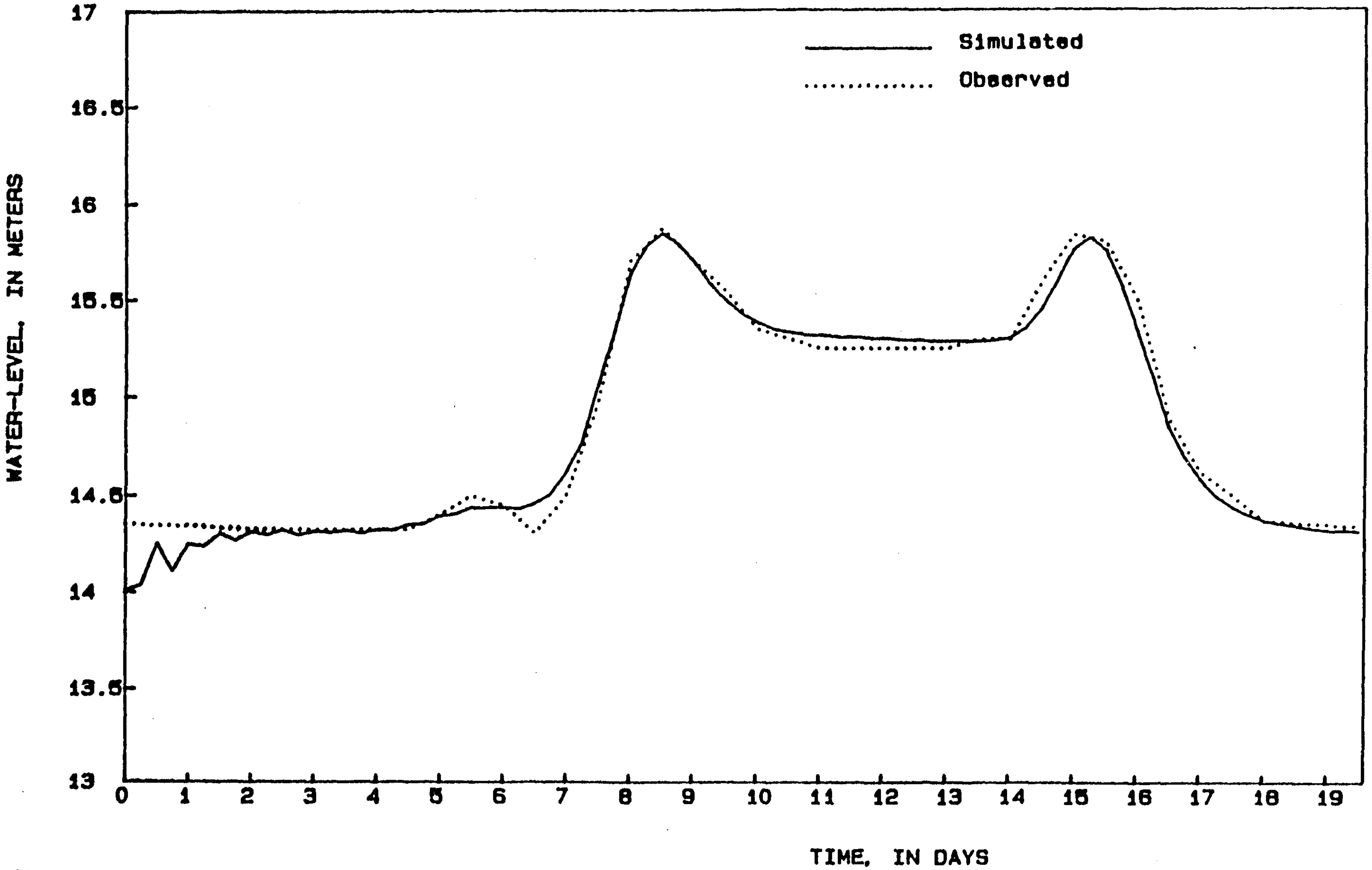

Figure 46. Comparison of observed and simulated downstream stage hydrographs for Sabine river

6.5 BARKLEY - KENTUCKY CANAL

Barkley-Kentucky canal is a man-made trapezoidal channel 1,9 km long, which joins Barkley reservoir on the Cumberland river to the Kentucky reservoir on the Tennessee river, in the USA. The general plan and a typical cross-section are shown in Figure 47.

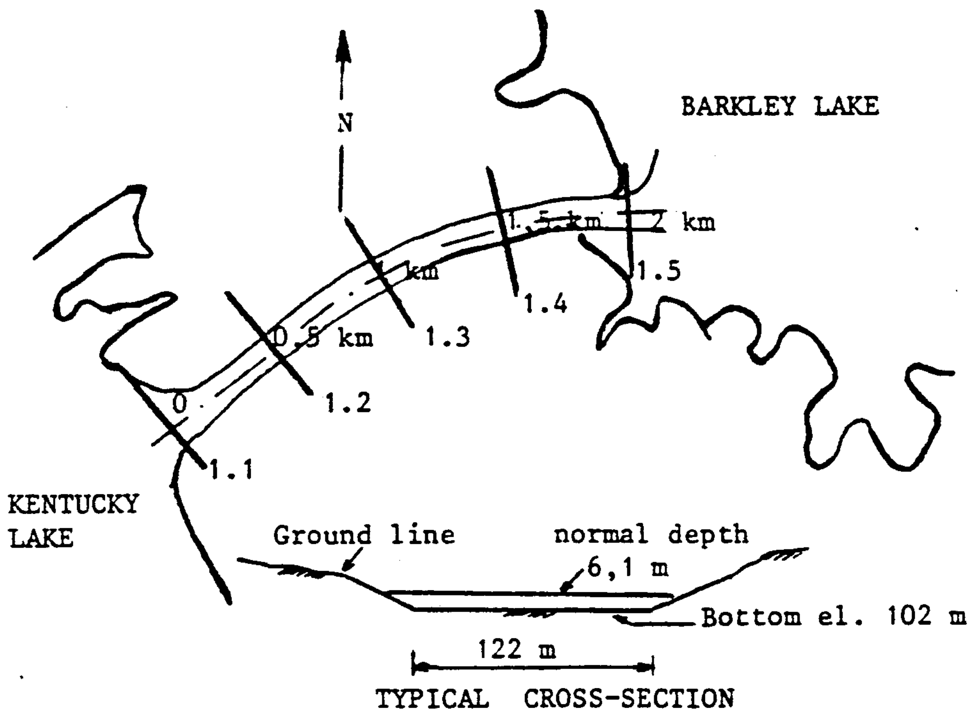

Figure 47. General plan and typical cross-section of the Kentucky-Barkley canal

The channel is 122 meters wide at the bottom with side slopes of 2 horizontal to 1 vertical. The channel bottom slope is almost horizontal. Flow is uncontrolled in the canal. The magnitude and direction of the flow is determined by the head difference which exists between the ends of the canal (maximum about 0,3 m, with a range of 0,03 - 0,15 m normally) (Garrison et al., 1969). As both reservoirs are influenced by intermittent power operations, the head difference, though small, is continuously changing and there is a continuous interchange of flow between the two bodies of water. Small fluctuations in stage at either end of the canal will force the flow to oscillate back and forth causing large fluctuations in discharge. As a result, the concept of defining the upstream or the downstream end of the canal cannot be adopted.

These characteristics make the Kentucky-Barkley canal a very interesting unsteady flow problem. The objective of this study is to determine the feasibility of simulating the oscillating flow conditions at either end of the canal. The canal is designed for navigation and the depth is normally 6,1 m, but ranges from 3,4 - 12,2 m. There is little variation in flowrate along the canal and no significant lateral inflows occur.

The observed stage hydrographs at both ends, shown in Figure 48, were adopted by Garisson et al. (1969) using an explicit scheme and by Amein and Chu (1975) using a direct rule scheme, to simulate discharge hydrographs in the canal. The channel reach was divided into five equal spaced sub reaches 0,5 km long. Manning's roughness coefficient for the canal was estimated to be 0,0275 by Garrison, et al. (1969). Bottom elevation is 102 m; the initial discharge of 1100 m^3/s from Barkley into Kentucky lake, was assumed constant through the reach. Initial time t=0 corresponds to 11.54 p.m. on the 8/8/66 and the initial water stage was 108,58 m at Barkley lake.

A time step of 1 hour was used and Kentucky lake was taken as the downstream boundary. The computed values of discharge at Kentucky lake are shown in Figure 49. The results of the model simulation were not compared to field measurements although they were available. The reason for this was the poor quality of the measured discharge data. The inaccuracy of the field measurements was as a result of the flow changing faster than the measuring time period of about 2 hours. The simulation results were compared with the computed results of Garrison, et al. (1969). The OSYRIS model gives very similar results to these obtained using the explicit method. This is in spite of using a time-step of one hour, as compared to the 15 sec time-step necessary in the explicit model in order to ensure the stability of the computations.

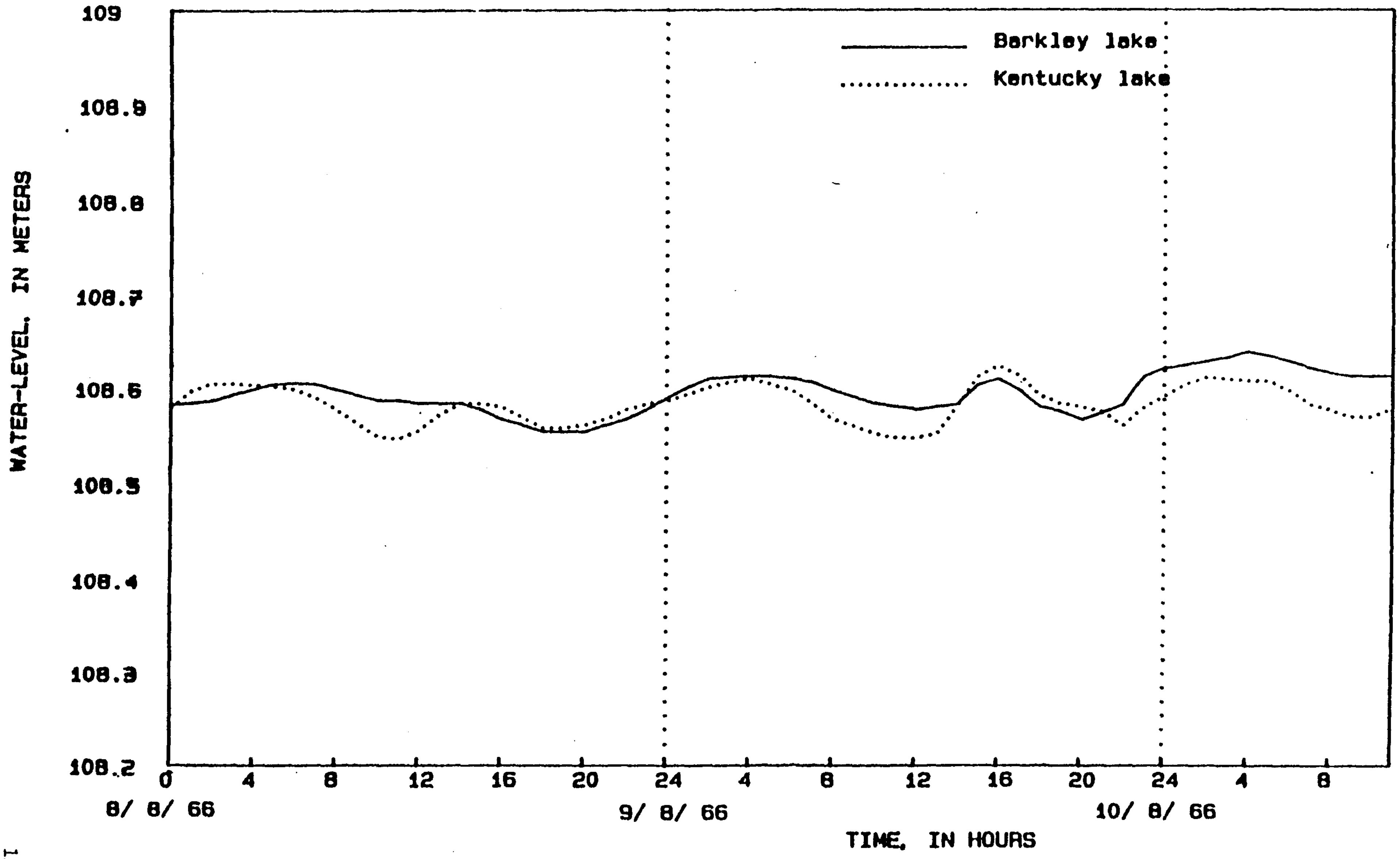

Figure 48. Observed stage hydrographs at Barkley and Kentucky lakes - ends of canal

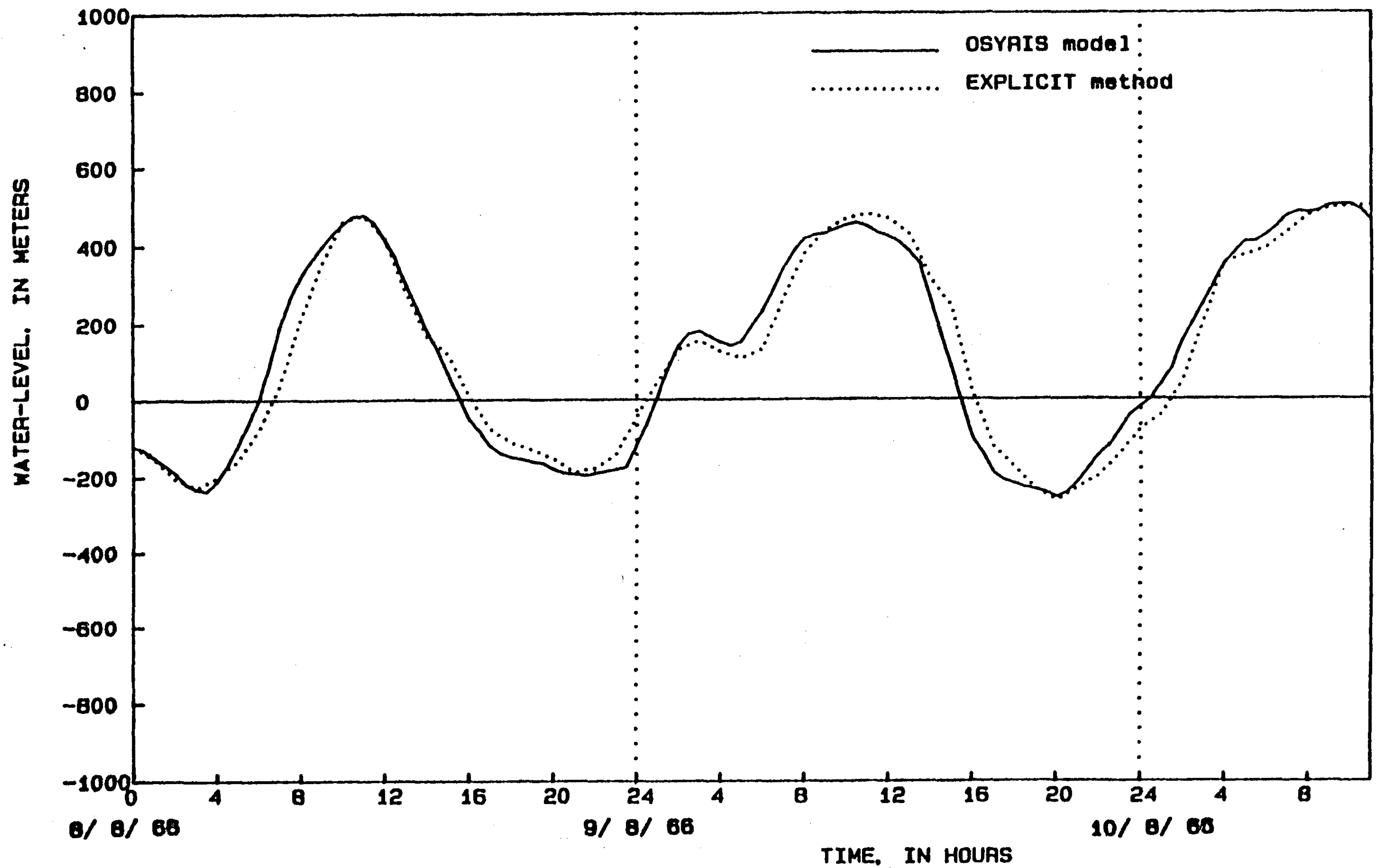

Figure 49. Comparison of computed discharge hydrographs at Kentucky Lake - end of the canal

6.6 GRADUAL DAM COLLAPSE

The problem of evaluating the effects caused by the breaking of a dam has attracted considerable attention in recent years. Dam failures are often caused by overtopping of the dam wall due to inadequate spillway capacity during large runoff inflows. Dam failure may also be caused by seepage or piping through the dam wall or along internal conduits, or due to earthquake damage.

Most investigators of dam-break flood waves have assumed that the breach formed in a failing dam encompassed the entire dam and occurred instantaneously. While this assumption may be valid for concrete dams, it is not valid for the large number of earth dams. The following example involves the routing of a flood from the hypothetical failure of an existing earth dam, the Bou Regreg Dam in Morocco.

The dam is located up river from the city of Rabat, and regulates the Bou Regreg and Grou rivers providing a dependable supply of potable water, for the demands of the coastal zone extending from Kenitra to Casablanca (Figure 50). This dam-break problem was first analysed by Ballofet et al. (1974), before the dam's construction. Safety considerations called for the design of a river diversion system during construction. The system included two cofferdams and a diversion channel. In order to provide data for a flood warning and evacuation plan, a hypothetical collapse of the upstream cofferdam was investigated. The upstream cofferdam was constructed of rockfill to a height of 28,5 m.

Dam break analysis involves two problems, i.e.;

- The computation of the outflow hydrograph from the reservoir.
- The routing of the flood wave downstream from the breached dam along the river channel and the flood plain.

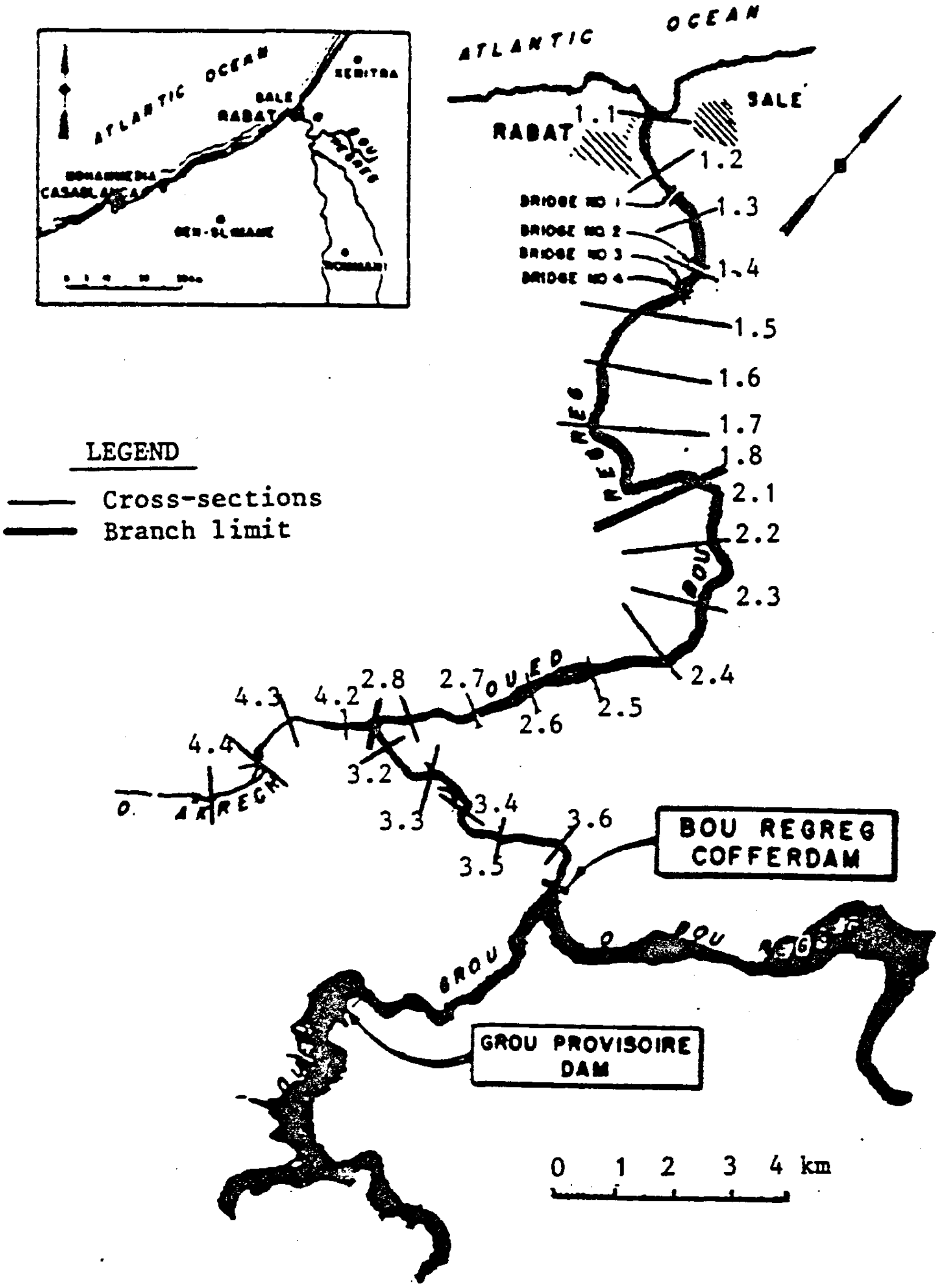

Figure 50. Map of Bou Regreg River

Sudden destruction of a dam results in a highly unsteady flow, with a forward wave (the 'positive' wave) advancing down the river, and a back disturbance (the 'negative' wave) propagating into the still water above the dam. The complexities of reservoirs geometry, dam-site cross-sections, and opening area complicate the computation of the outflow hydrograph from the reservoir. Therefore, a large degree of simplification of breach, reservoir and tailwater condition is required.

In this example, the outflow hydrographs for the reservoir were assumed to be the same as those computed by Ballofet et al. (1974) as no data about the dam site was available. Ballofet et al. (1974) expressed the outflow as a function of the reservoir level, with critical flow through a rectangular gap of a width which increased uniformly with time. They conducted many runs assuming different combinations of the initial reservoir level, duration of collapse, magnitude of hydrologic flood and state of blockage of the diversion channel. Four typical collapse hydrographs are shown in Figure 51 compared with the hydrograph of the attendant flood without collapse. The combination of the parameters , duration of collapse T_c, and reservoir level H_{res}, were:

- Run 1: T_c = 0,03 hrs H_{res} = 28,50 m
- Run 2: T_c = 3 hrs H_{res} = 28,50 m
- Run 3: T_c = 3 hrs H_{res} = 23,86 m
- Run 4: T_c = 9 hrs H_{res} = 23,86 m
- Run 5: no collapse

These computed hydrographs were inserted as upstream boundary conditions in the model. A two meter sinuisoidal tide was used as a downstream boundary condition. Cross-sections were taken every 1 km and were arranged in branches as shown in Figure 50. The simulation time step was 30 min and the θ value was set to 1 for maximum stability.

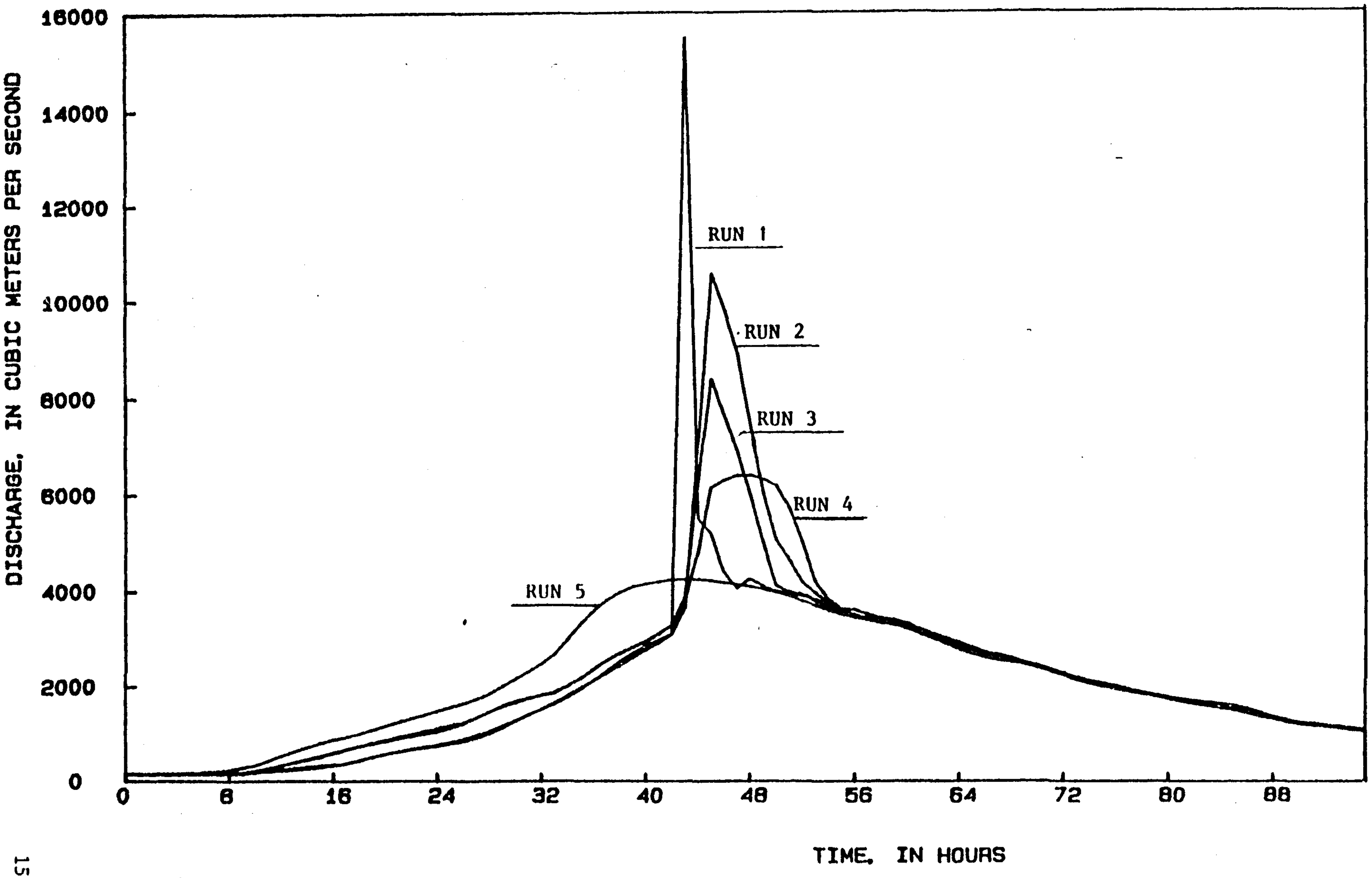

Figure 51. Outflow hydrographs from partial dam failure

The runs show the superiority of the implicit model when applied to real life problems compared to the explicit model LATIS, used by Ballofet et al. (1974), where a time step of 7 sec had to be adopted in order to ensure stability. Figure 53 depicts the simulated flowrates at cross-sections along the river for Run 2. The results are similar to those found by Ballofet (1970). The flood propagates rapidly in the confined reaches from (3.5) to (2.5). The flow further downstream expands into the flood plains and the peak is reduced drastically, while the propagation slows resulting in a time-lag of about 3 hours. Figure 52 shows the envelopes of maximum elevations for the five runs, related to the distance from the dam.

The example shows the applicability of the model in dam failure problems. It can be used for real time forecasting and disaster preparedness planning, by predicting dam-break flood wave peak stages, discharges and travel times. However, as the dam-break problem is complicated, further considerations must be taken into account. A one-dimensional schematization of the dam-break wave is generally assumed when the valley is long and narrow, as in this example. On the other hand, when the valley widens downstream of the dam, and conceptually large areas are flooded, a two dimensional schematization is called for. Even in the one-dimensional situation, additional problems require the building of specialised subroutines in order for the model to be generally applicable in dam-break problems, e.g.

- Computation of the travel of induced negative wave(s) until the impounded water is emptied and a new steady state flow is established through the body of water.

- Propagation of the dam-break wave in a dry bed, e.t.c.

However, these are out of the scope of the present example which merely shows the ability of the model to simulate such situations.

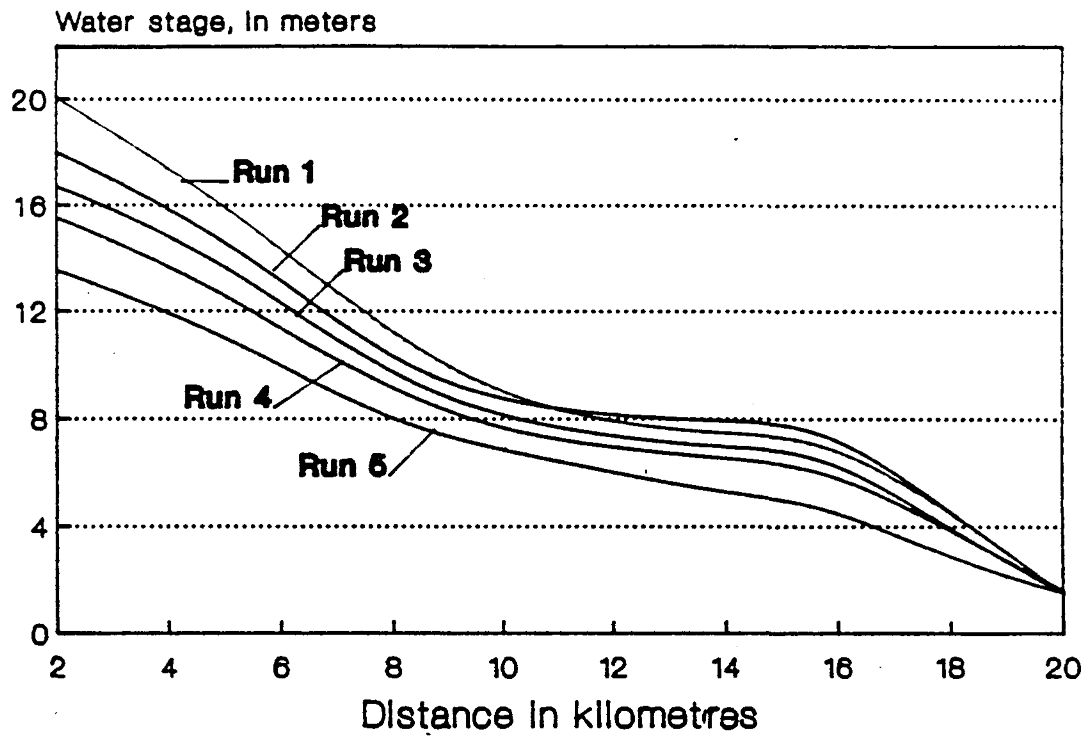

Figure 52. Maximum water stages for the Runs 1-5

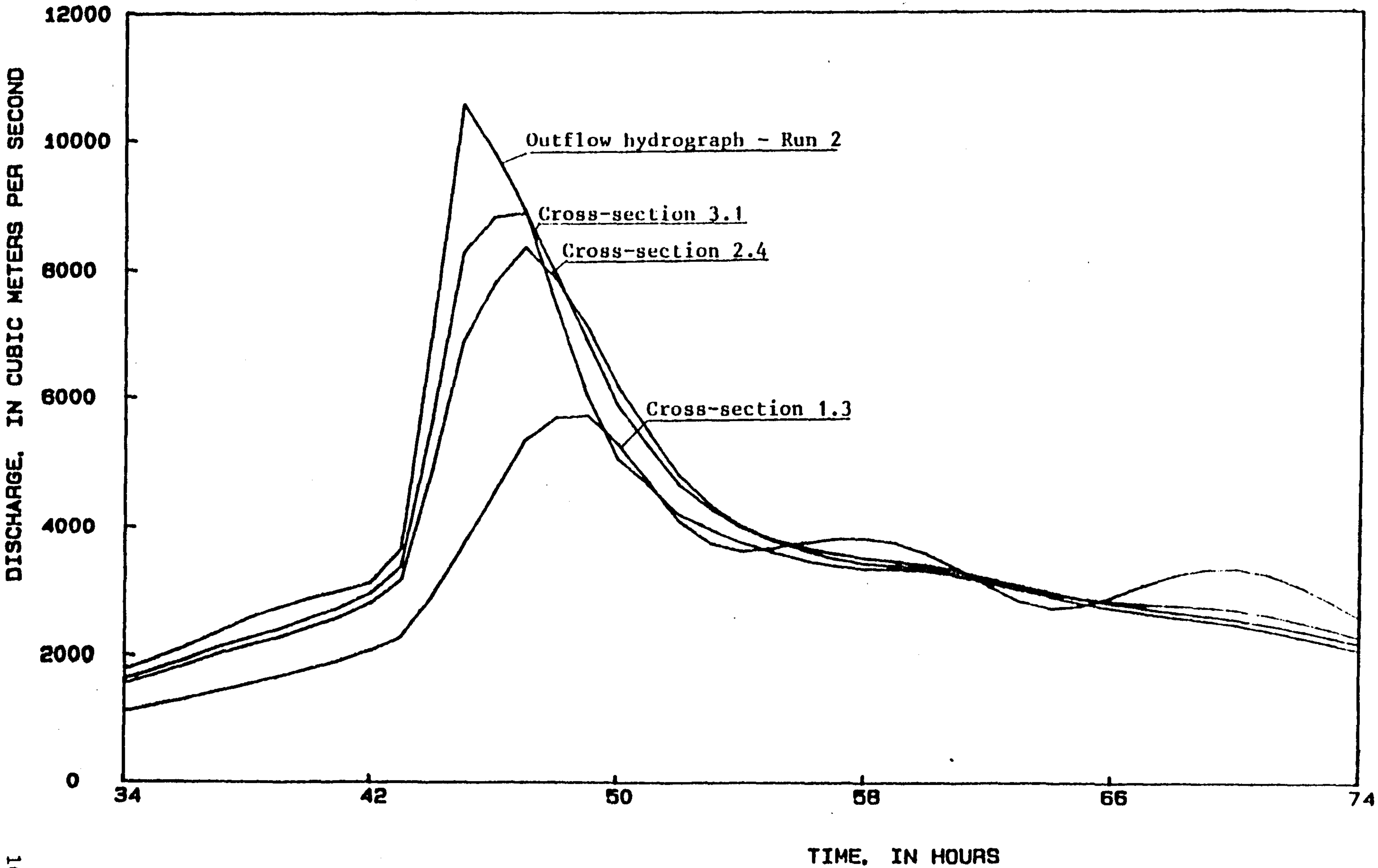

Figure 53. Computed flowrate hydrographs - Run 2

6.7 ST. LAWRENCE RIVER STUDY

6.7.1 INTRODUCTION

The St. Lawrence river is a vital navigation artery forming a navigable waterway from the Atlantic Ocean to the International Great Lakes and the Ports of Montreal and Quebec, in Canada. The river has been studied in the past using various numerical models. Two of the most well known studies are by Kamphuis (1970) and by Prandle and Crookshank (1974). In these studies, the simulation of the entire 528 km tidal reach was performed using one-dimensional models. Only detailed investigation of smaller sections of the river were conducted using two-dimensional models. The developed looped-network model was therefore considered sufficient for the simulation, being limited largely by the accuracy of the available data. The simulation of the St. Lawrence river exhibits the model's capability to simulate complicated river system configurations with extensive data input requirements.

6.7.2 ST. LAWRENCE RIVER DESCRIPTION

The boundaries of the simulation were taken at Father Point and Montreal (Figure 54). At Father Point, the seaward limit, the river is approximately 48 km wide and up to 330 meters deep. The tidal range varies from 1,5 to 4,5 meters. The tidal discharge at this section is so large that the tidal elevation could be considered independent of any likely changes in the upstream river.

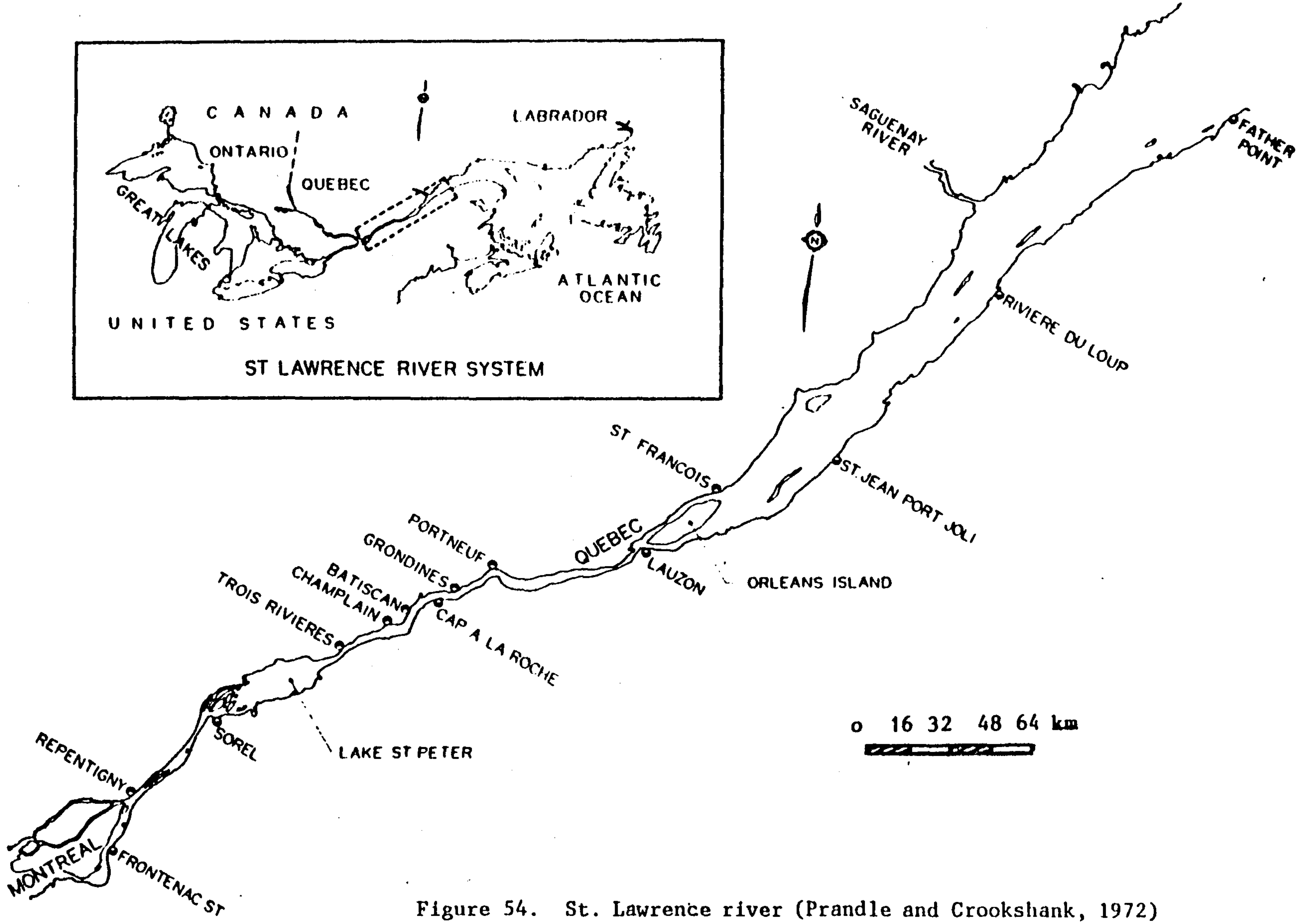

Figure 54. St. Lawrence river (Prandle and Crookshank, 1972)

The river geometry is quite varied from Father Point to Montreal. Midstream islands are present downstream of Quebec; Orleans Island is the only one that is large, compared with the other dimensions of the river, it is therefore the only one taken into account in the mathematical study. One of the important tributaries of the St. Lawrence river, with significant effect on the flow is the Sayuenay river. It enters the St. Lawrence river on the north shore 96 km upstream of Father Point. Upstream of the Saguenay the depth of the St. Lawrence decreases to an average of approximately 12 meters at Orleans Island, 240 km upstream of Father Point. At Orleans Island the river forms two distinct channels. At the upstream end of the island the river again converges to a single channel but with a breadth of less than 2 km at Quebec City. The narrow breadth is accompanied by an increase in depth to approximately 55 meters.

Upstream of Quebec the river broadens to an average of 3 km and the bed steepness increases causing rapid attenuation of the tidal amplitude. One hundred and forty km upstream of Quebec City the river again broadens into Lake St. Peter. Upstream of this point the river flow is undirectional for 48 km to the upstream limit at Montreal.

6.7.3 SCHEMATIZATION

In the schematization process the reach from Father Point to Montreal was divided into 204 sections. The sections were arranged into 20 branches for input to the looped-network model (Figure 55). From Father Point to Quebec the sections are 4,8 km long. At Orleans Island two separate channels are considered. From Quebec to Sovel 1,5 km sections are used, and from Sorel to Montreal the sections are again 4,8 km long.

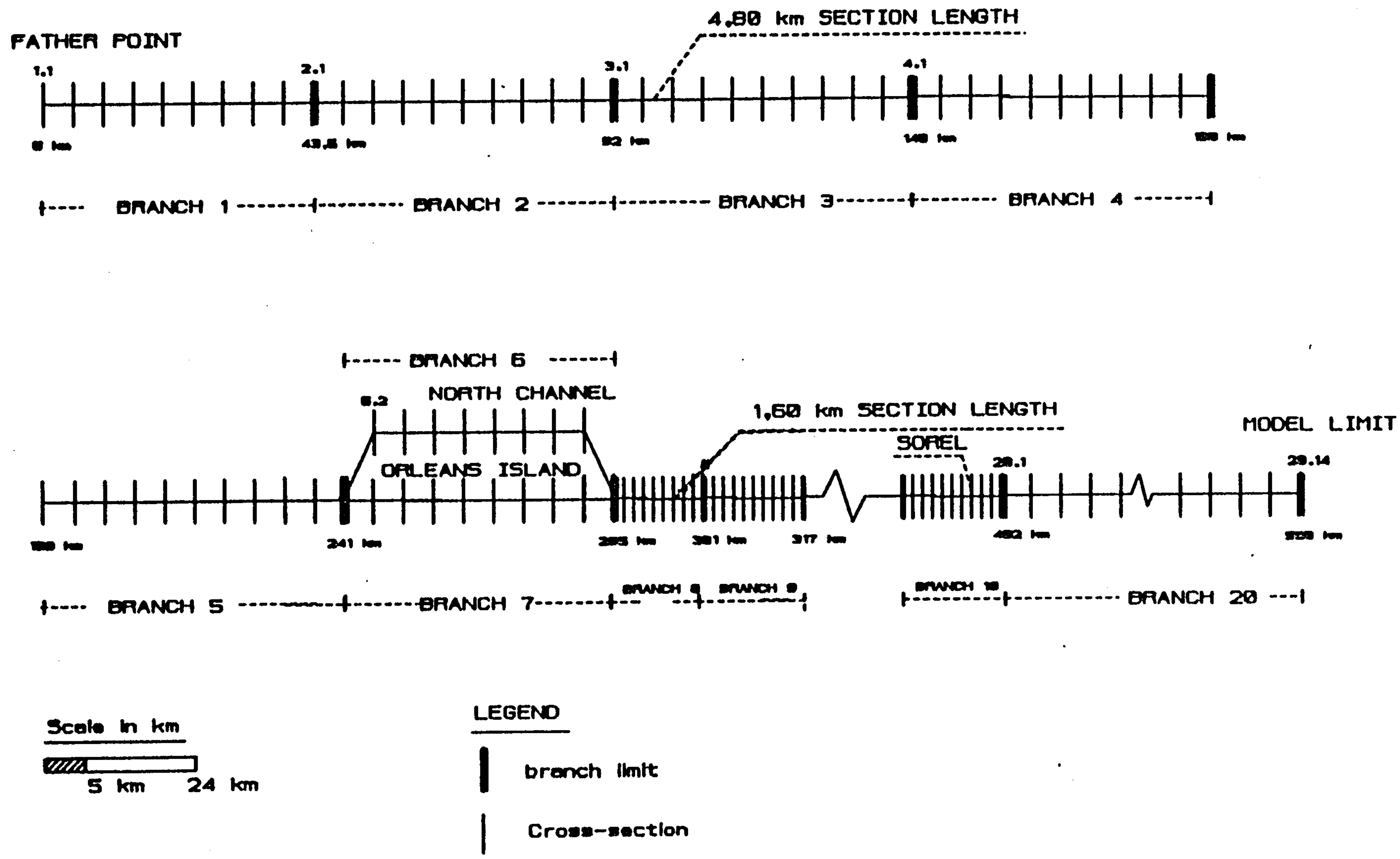

Figure 55. St. Lawrence river schematization and notation for input in the OSYRIS model

The section length is a function of the complexity of the river geometry and of the accuracies desired in the particular region. The data were derived from accurate surveys and hydrographic charts and are listed in the Kamphuis (1968) study. A summary of the characteristic dimensions for the 204 sections may be found in Appendix (F).

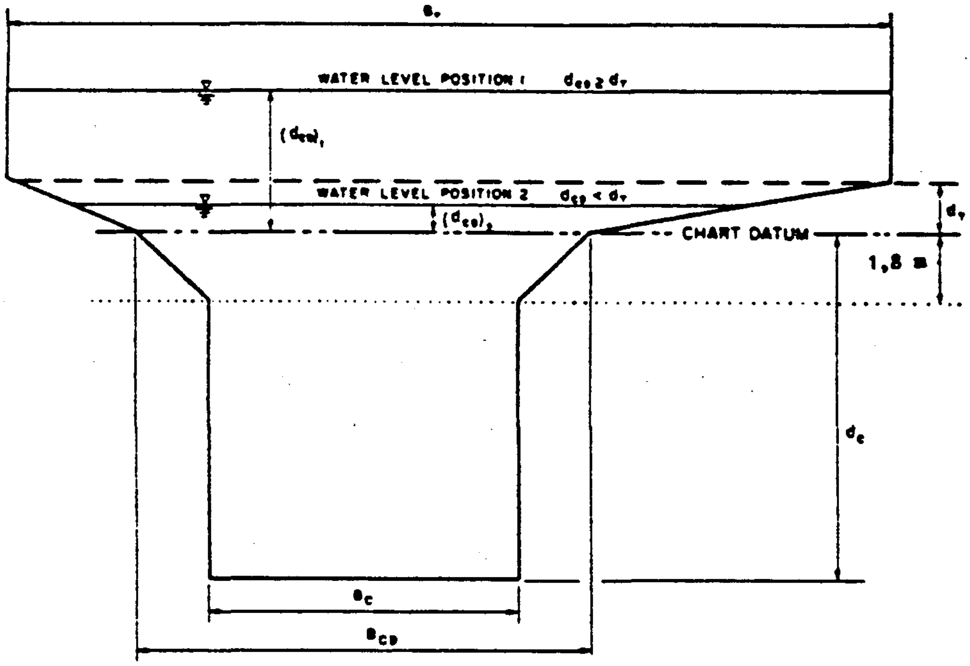

Figure 56. St. Lawrence river - Adopted schematization (Kamphuis, 1968)

The final river schematization is shown in Figure 56. The representative widths used are the total width B_T, the width at chart datum B_{CD}, and the width of the conveyance channel B_C. The three widths are assumed to occur at three distinct levels (-1,8 - 0 - d_T meters) with respect to chart datum. The critical points have been joined by straight lines.

The final schematized input is the tributary discharge, Q_T. The tributaries and their discharges, were collected into 12 groups,

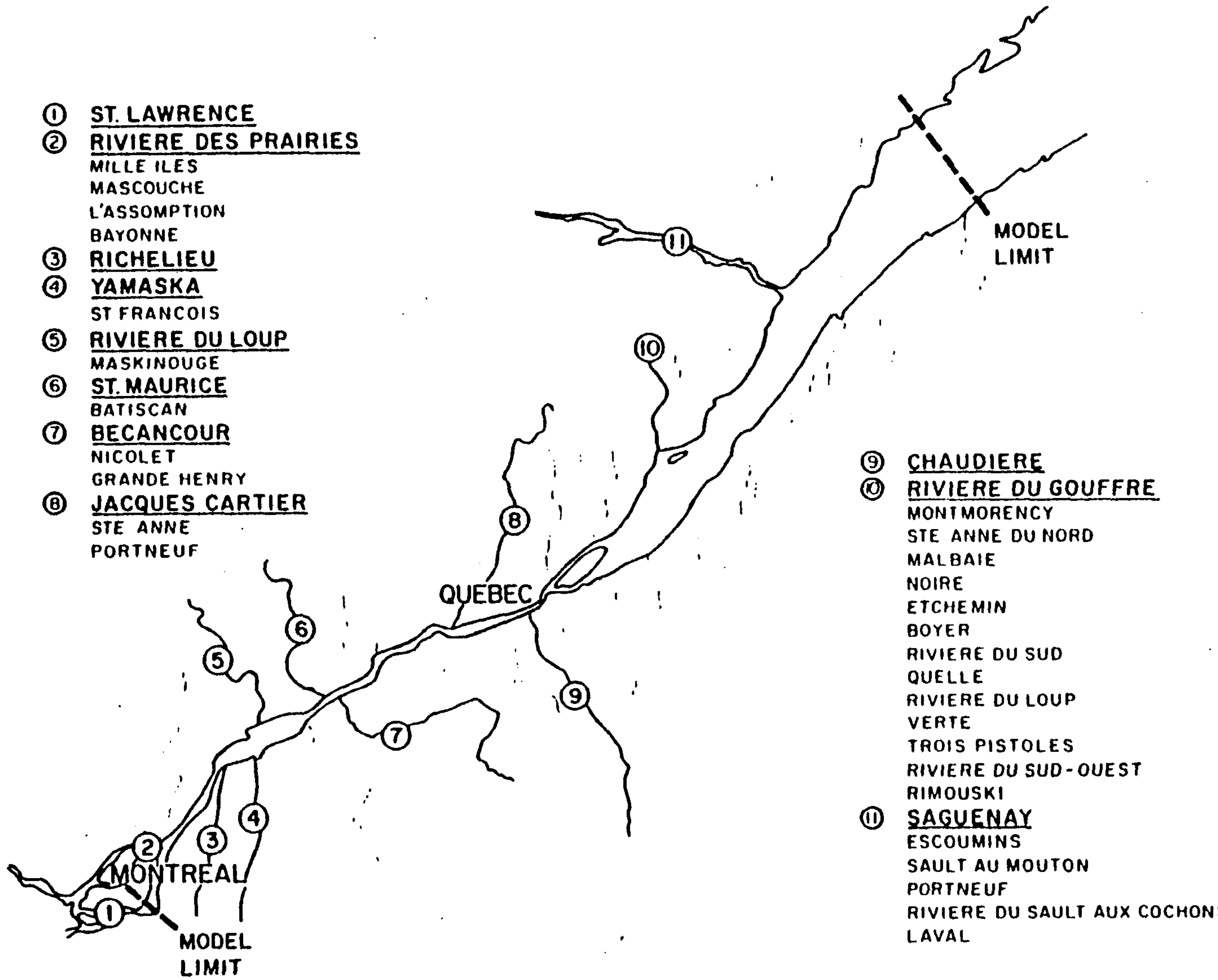

Figure 57. St. Lawrence river tributary grouping (Prandle and Crookshank, 1972).

entering at various points along the river (Figure 57). The discharges added into the system are the daily mean flows for the specified date. Since changes in the tributary inflow cause considerable changes in the results, the monthly mean discharges for the tributaries were not considered to be accurate enough for the calibration.

Kamphuis (1968) computed the discharge at the mouth of each tributary using a simple ratio of the total drainage area to the drainage area up to the gauging station, and multiplying this by the measured discharge at the station. This process is not entirely satisfactory. For rivers entering downstream of Portneuf the ratio of the tributary inflow to tidal discharge is so small as to render the problem negligible. Upstream of Portneuf the lack of accurate information on tributary inflows constitutes a limiting factor in the use of the model for reproduction or prediction of water levels in the river.

6.7.4 SIMULATION DETAILS

The boundary data input for the model are the initial conditions and the boundary conditions.. As initial conditions, estimated value of the downstream water stage and flowrate at time t=0 were inserted. These values were used by the developed steady state program to calculate initial conditions at all the cross-sections.

The downstream seaward boundary condition involved an expression for the tidal elevation at Father Point. The upstream condition at Montreal is the steady upland discharge recorded for the days of calibration. A time step increment value Δt, of 1 hour was used in the model simulation.

6.7.5 MODEL RESULTS

Having formulated the numerical model, the next step is the calibration as outlined in Chapter 5. In this example, the friction coefficients for each section were adjusted to force the model to reproduce, as closely as possible, a set of reliable recorded data. The data used for calibration consisted of hourly water-level recordings at 14 stations along the river. The sections between the water level gauges were assumed to have a constant friction coefficient. As Prandle and Crookshank (1974) recommended, no attempt was made to force the model to exactly reproduce any particular gauge since errors in the recorded data were always suspected. The initial friction coefficients used in the calibrated model were derived from the Kamphuis (1968) report. An actual bottom roughness value, a, was given for each cross-section, this value was converted into a Chezy friction factor using the relationship:

$$C = 32,7 \log(6y/a) \tag{6.4}$$

and in Manning's roughness by

$$n = R^{1/6}/C \tag{6.5}$$

where

a : is the bottom roughness

y : is the depth of flow

The values of the bottom roughness, a, is given for each cross-section in Appendix (F). Comparison of these values with those likely to be encountered in the actual river is a reflection of the limitation of the simulation.

In Figure 58 the computed water levels are shown at six cross-sections. It can be seen that in Sorel the tide has no influence as St. Peter's lake dampens any tidal component which propagates this far. In Figures 59 to 61 comparisons of the computed water levels with the available recordings are shown. An underestimation of the peak water levels of the tide in the Grondines station and the Lauson station may be due to the inadequate data regarding the tributary flows in the area.

A most important measure of the accuracy of simulation is obtained by comparison of velocities. Velocity recordings were available at St. Francois. The comparison with model results is shown in Figure 62.

The results of the simulation can be viewed as satisfactory, if the following considerations are taken into account:

- Variations in water levels across particular cross-sections can occur due to centrifugal forces, velocity variations, density variations and the Coriolis force.

- Some results indicate that the reference datum of certain gauges might be in error.

- The model predictions are limited by the accuracy of the boundary conditions. Of particular concern is the accuracy of the fresh water discharges used in the model.

- The model does not include wind forces or barometric pressure variations. In an estuary of this size this could cause substantial errors.

It can be concluded that the model is capable of simulating the tidal propagation in a major watercourse such as the St. Lawrence river. The accuracy is limited mainly by the accuracy of the available data used in the original calibration process, also in the specification of the boundary conditions.

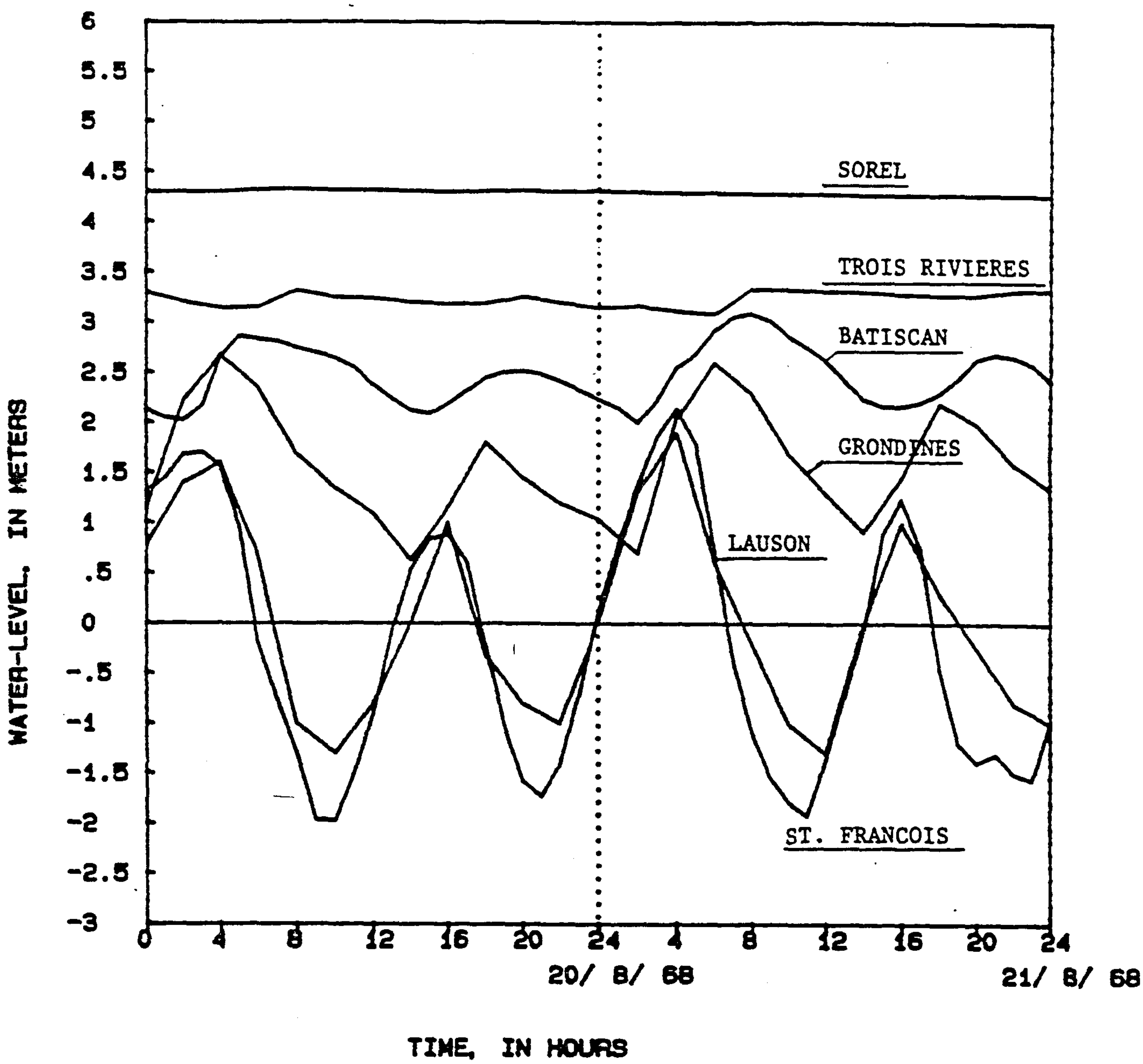

Figure 58. Computed water levels from the St. Lawrence river, August 19-20, 1968.

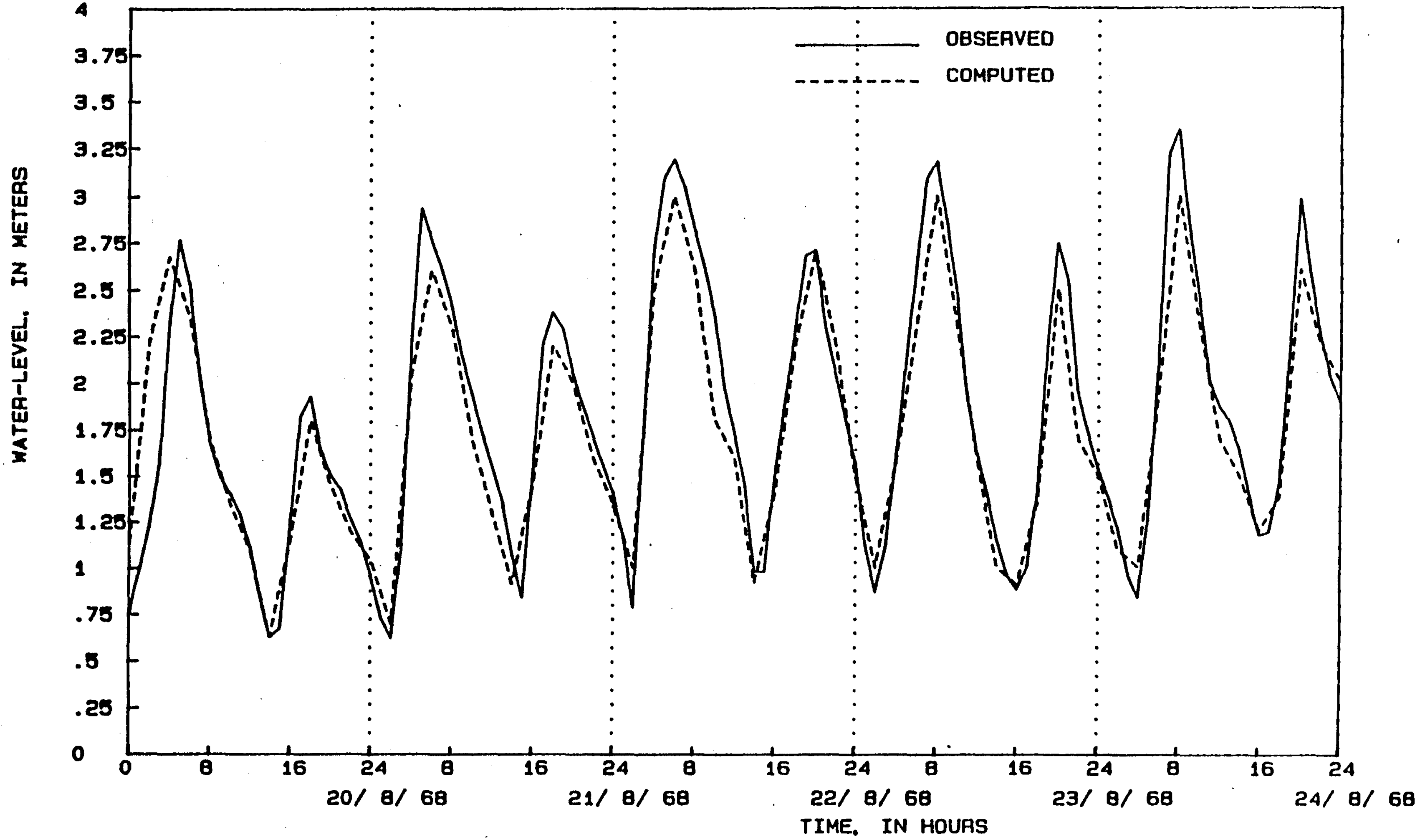

Figure 59. Observed and simulated water levels from the St.Lawrence river - Grondines station - August 19-23, 1968.

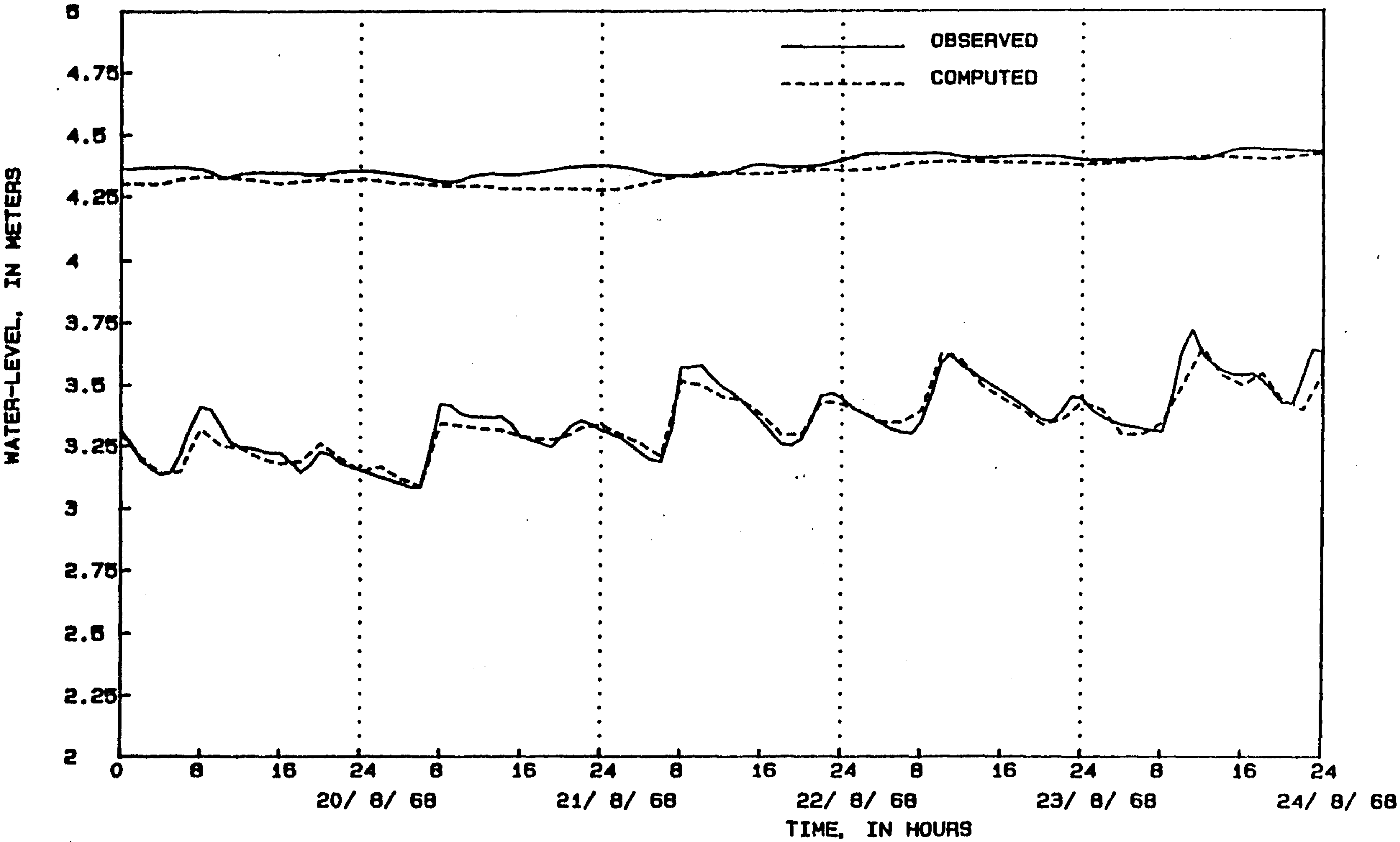

Figure 60. Observed and simulated water levels from the St.Lawrence river - Trois Rivieres and Sorel stations - 19/8/68.

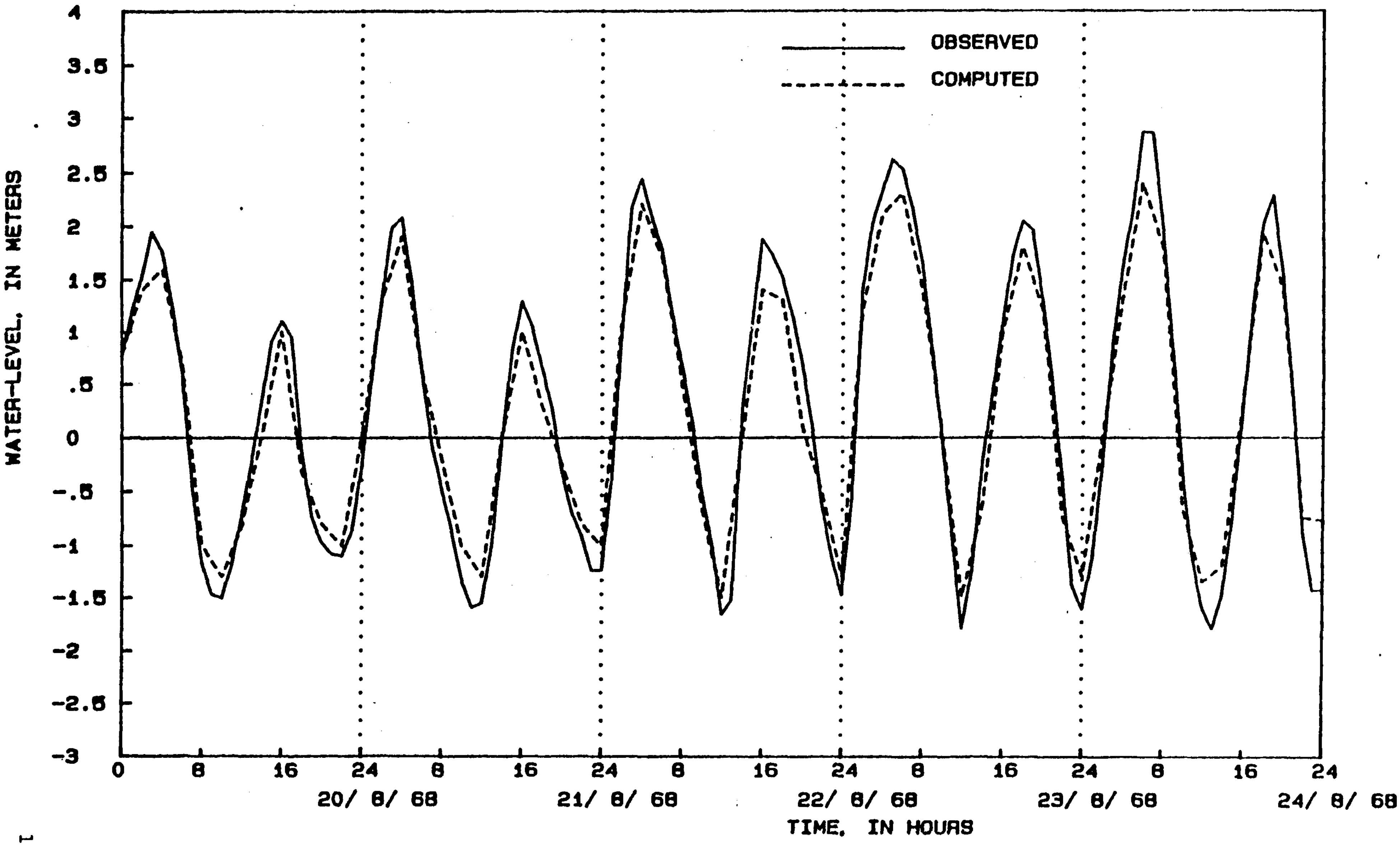

Figure 61. Observed and simulated water levels from the St.Lawrence river - Lauson station - August 19-23, 1968.

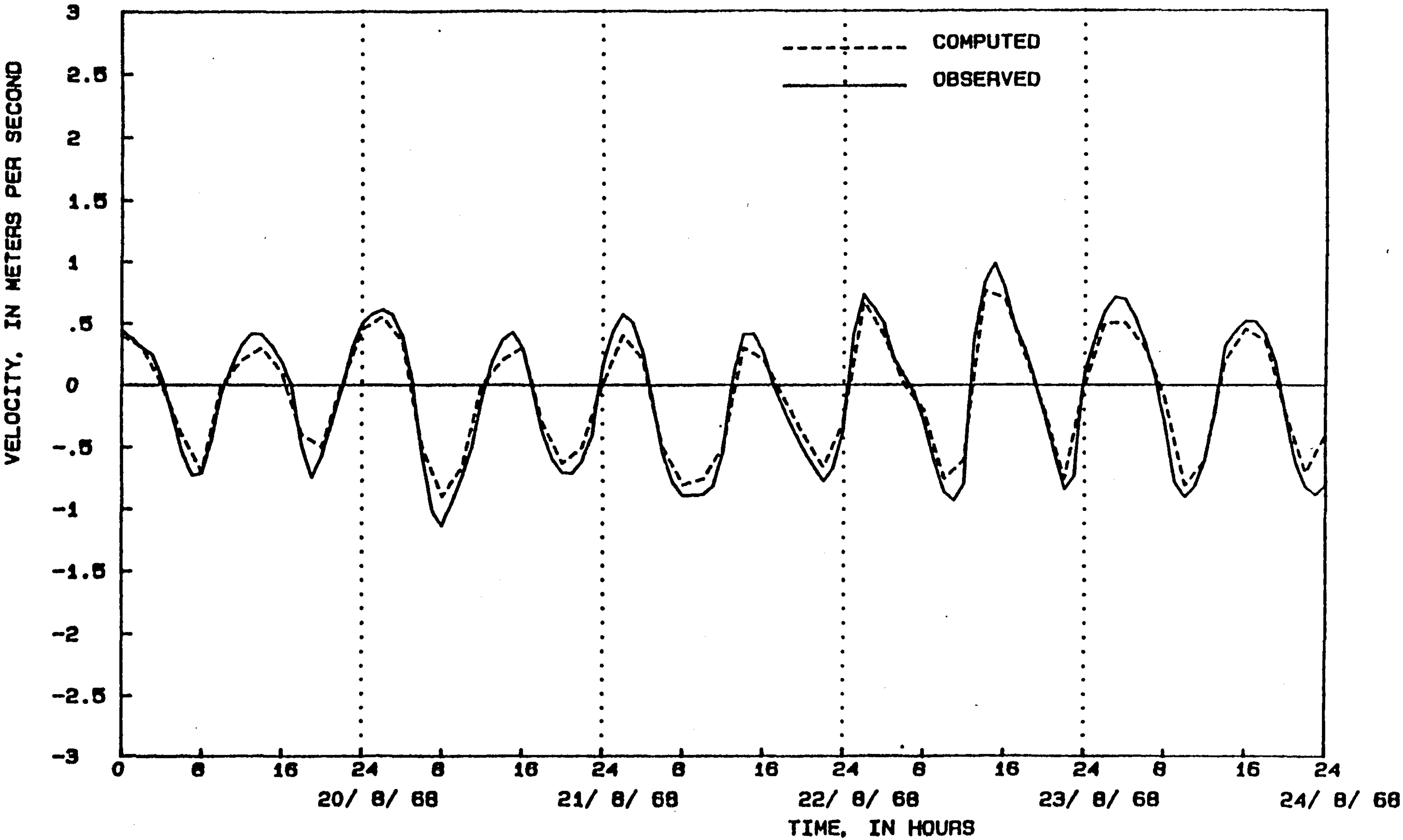

Figure 62. Observed and simulated velocities from the St.Lawrence river - St.Francois station - August 19-23, 1968

6.8 VAAL RIVER STUDY

6.8.1 INTRODUCTION

Rainfall over South Africa during the summer season of the year July 1987 to June 1988, was exceptionally high over a large area of the country, from Natal, westwards to South West Africa. The 'OSYRIS' model was used to simulate the floods of January 1988 in a major watercourse, the Vaal river, making use of unpublished recorded data from the Department of Water Affairs.

6.8.2 DESCRIPTION OF THE VAAL CATCHMENT AND THE VAAL RIVER

The Vaal dam is situated at the confluence of the Vaal and Wilge Rivers, approximately 75 km south of Johannesburg, South Africa and has a total catchment area of 38505 km^2 (Figure 63). The dam was constructed in the mid-1930s as a major storage unit of the Vaal River Development scheme - South Africa's first multi-purpose project.

The actual catchment area extends from the dam some 220 km inland and has a mean annual runoff (MAR) of approximately $2000x10^6$ m^3/yr. The catchment varies in elevation from about 3200 m above sea level at the south-eastern boundary in the Drakensberg mountains, where there are steep slopes, to 1450 m at the Vaal dam, where the land is relatively flat.

The section of the Vaal river analysed in this study extends between the Vaal dam upstream of the Watervaal river, and the

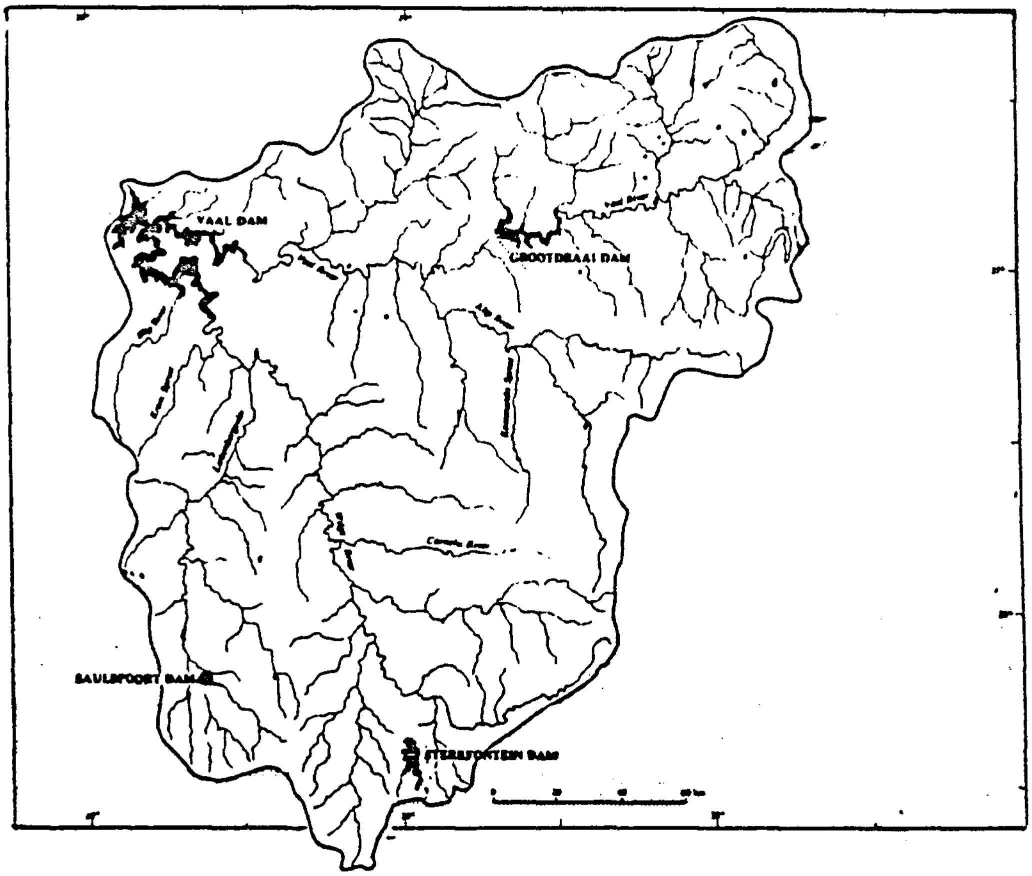

Figure 63. Vaal dam catchment (McKenzie, 1985)

Grootraai dam (Figure 64). The length of the watercourse simulated is approximately 100 km. The river meanders and in some parts has extensive flood plains of more than 1 km width. Various tributaries enter the system and are described in the following sections. The major tributary flowing into the Vaal river is the Klip river, with a drainage area of 4150 km^2. These two watercourses form a branched channel which was simulated using the unsteady flow model.

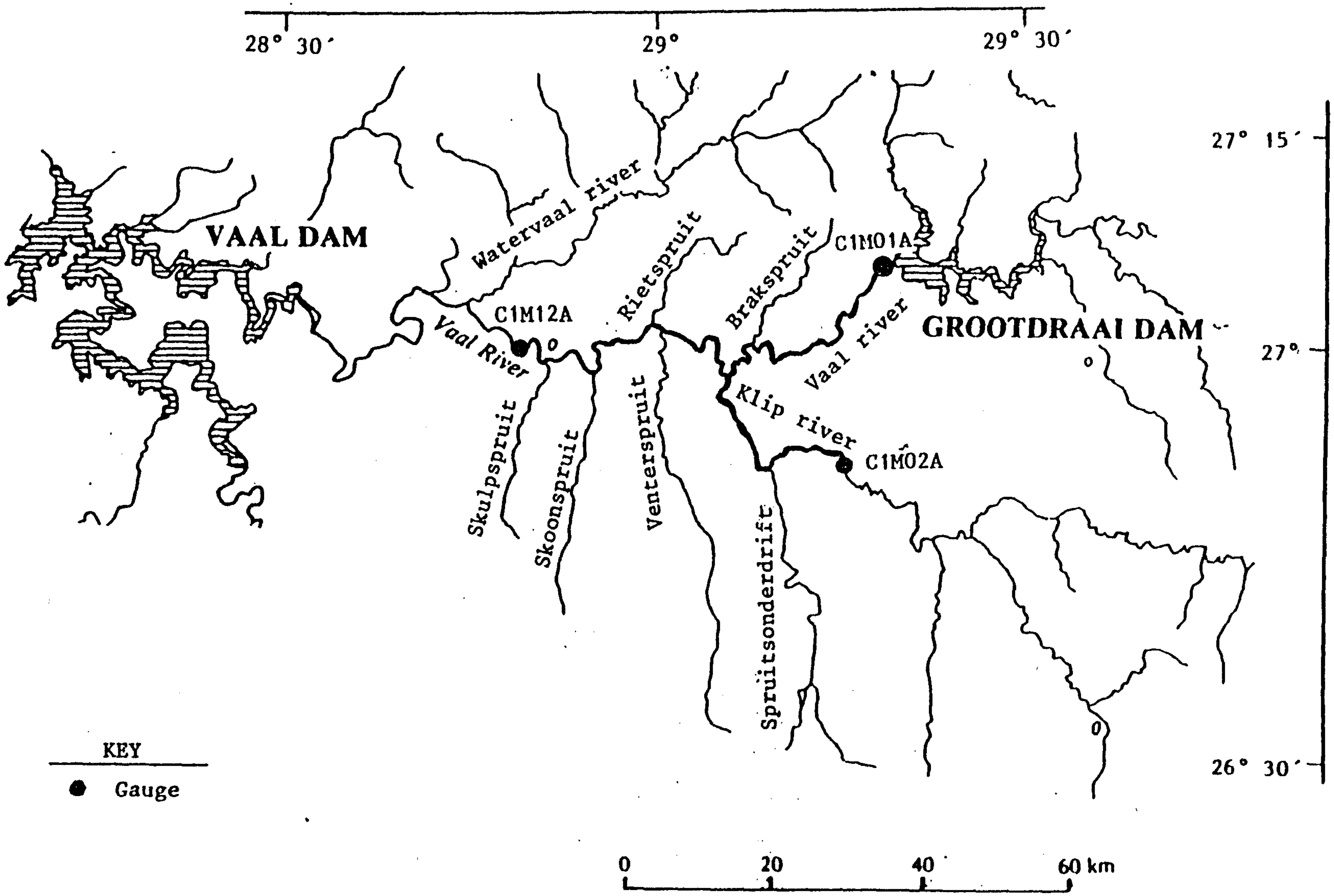

Figure 64. Vaal river (tributaries and gauge location)

6.8.3 DESCRIPTION OF BOUNDARY DATA AND STREAMFLOW GAUGES

There are several flow gauges within the Vaal dam catchment area. Unfortunately, the majority have very short records with many missing or unreliable (submerged weir) flow values. In order to simulate the floods, gauges had to be found which were reliable, operated simultaneously and have records available for more than one flood event. Three gauges met the prerequisites, namely the gauges at Standerton (C1M01A), Delangesdrift (C1M02A) and near Villiers (C1M12A) (Figure 64).

Gauge (C1M01A) is situated downstream of the Grootdraai dam. The flow passing through gauge (C1M01A) represents only the releases and spills from the Grootdraai dam, plus a small additional flow from the small catchment area downstream of the dam and upstream of the gauge. Gauge (C1M12A) was recently installed by the Department of Water Affairs (1985) and since then continuous records are available. Gauge (C1M02A) is situated near Delangesdrift on the Klip river and is a key gauge in the Vaal catchment as it is one of the gauges which forms the basis for flood warnings at the Vaal dam (McKenzie, 1985).

Three recorded flow events found to be suitable:

1. November 1985
2. January 1987
3. January 1988

The first two events were used for the calibration of the model and the third event for verification purposes. The flow records for these gauges are considered to be very reliable (McKenzie, 1985).

6.8.4 MODEL SCHEMATIZATION

The cross-sectional data were taken from field surveys conducted by the Department of Water Affairs. The distances between the cross-sections range from 500 m to 1200 m, depending on the river configuration. A total of 130 cross-sections, arranged in 12 branches, was available for input into the unsteady flow model.

The tributary discharges form an important schematized input. Various smaller tributaries contribute to the flow of the Vaal river and are entering the system between the three specified gauges. The most important of these shown in Figure 64, are:

- Skulpspruit river
- Skoonspruit river
- Venterspruit river
- Rietspruit river
- Spruitsonderdrift river
- Brakspruit river

Daily data for the discharges from the tributaries are in most cases not available. It was therefore assumed that the tributary discharges included in the numerical model, would represent the discharge for the associated drainage basin. The discharges added into the system are mean flows for the calibration dates. The determination of the tributary discharges remains somewhat subjective as the nearest gauging station is a long distance upstream of the mouth, for the majority of the tributaries. Similar to the St. Lawrence river simulation, this is a limiting factor on the accuracy of the calibration.

6.8.5 SIMULATION RESULTS AND DISCUSSION

The duration of the simulation period for the three events was taken as one month. This is the longest period over which the model has been applied. The time-step was kept to two hours throughout the simulation. Stability problems occurred for short periods of the simulation of the two first events as the flow in the branch downstream of the Grootdraai dam was very low. The boundary conditions were, therefore, slightly modified for very low depths, in order that the water level remain above a certain minimum value.

In Figure 65 the measured flowrates for gauge C1M01A are presented. It can be seen that the flow in most periods is very low and represents only the releases from the Grootdraai dam. For January 1987 the rainfall in the catchment was low. Only one release was made from the Grootdraai dam on the 11th of January 1987. On the contrary, in the Summer of 1988 it rained continuously and in January there were five releases from the dam with a total duration of seven days and a peak flow of 50 m^3/s. In addition, in January 1987 the contribution of the catchment upstream of the gauge C1M01A was negligible, while for January 1988 there is a continuous base flow of 5 to 8 m^3/s.

In Figure 66, the inflows from the Vaal and Klip rivers and the computed calibrated outflow downstream of the Vaal river for January 1987 are shown. The travel time of the peak flow is approximately 1,5 days and the peak attenuation is in the range of 8-10%, if one considers the contribution of the tributaries. In Figure 67, the comparison of the computed and measured water levels at gauge C1M12A is shown. For short periods in the middle of the month, the water levels were underestimated in spite of the good calibration of the model with respect to the previous events. This is attributed to the inaccuracies and underestimation involved in the establishment of the tributary

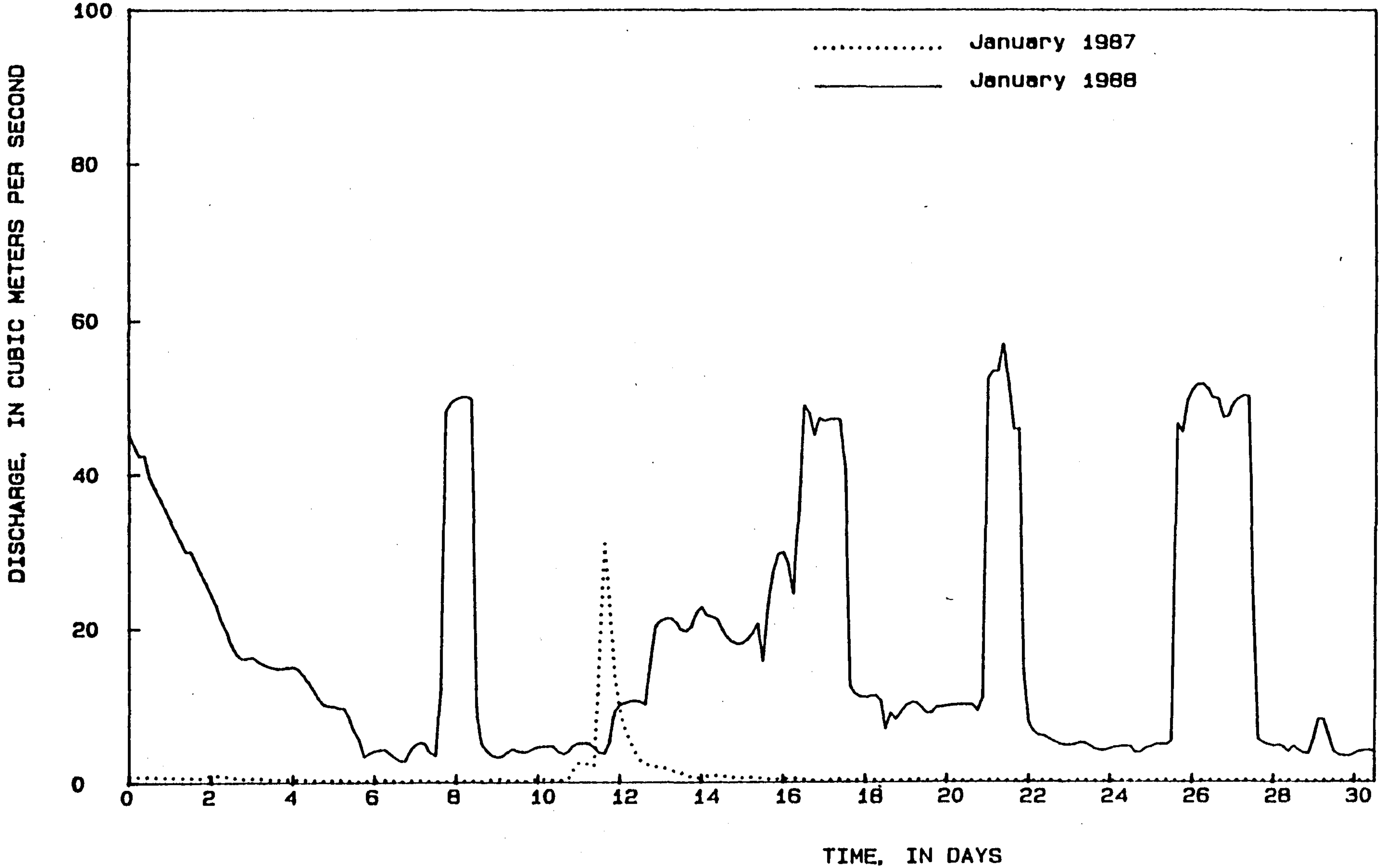

Figure 65. Measured inflows at gauge C1M01A for January 1987 and January 1988

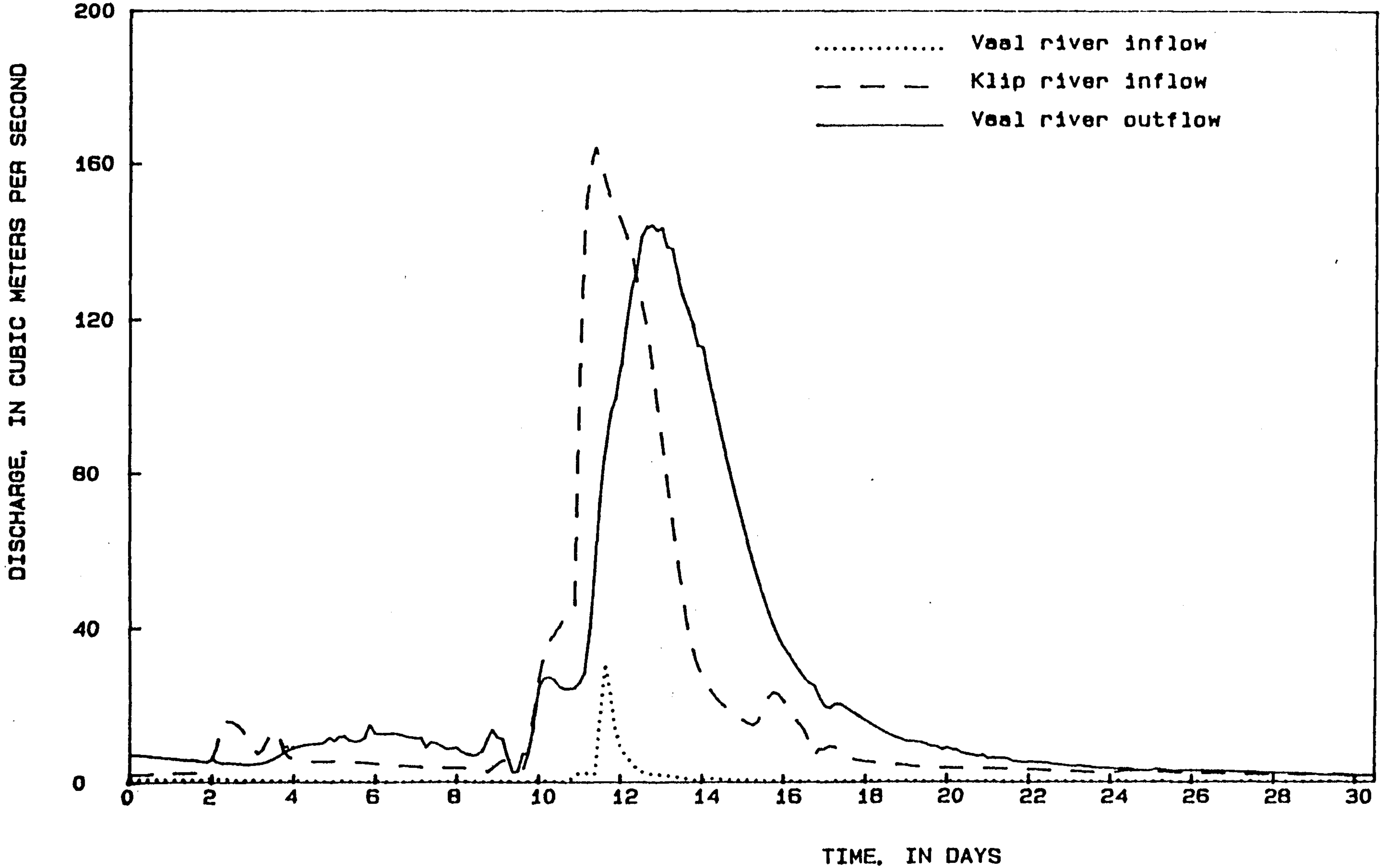

Figure 66. **Inflow hydrographs upstream of the Vaal and Klip rivers and computed outflow hydrograph for January 1987.**

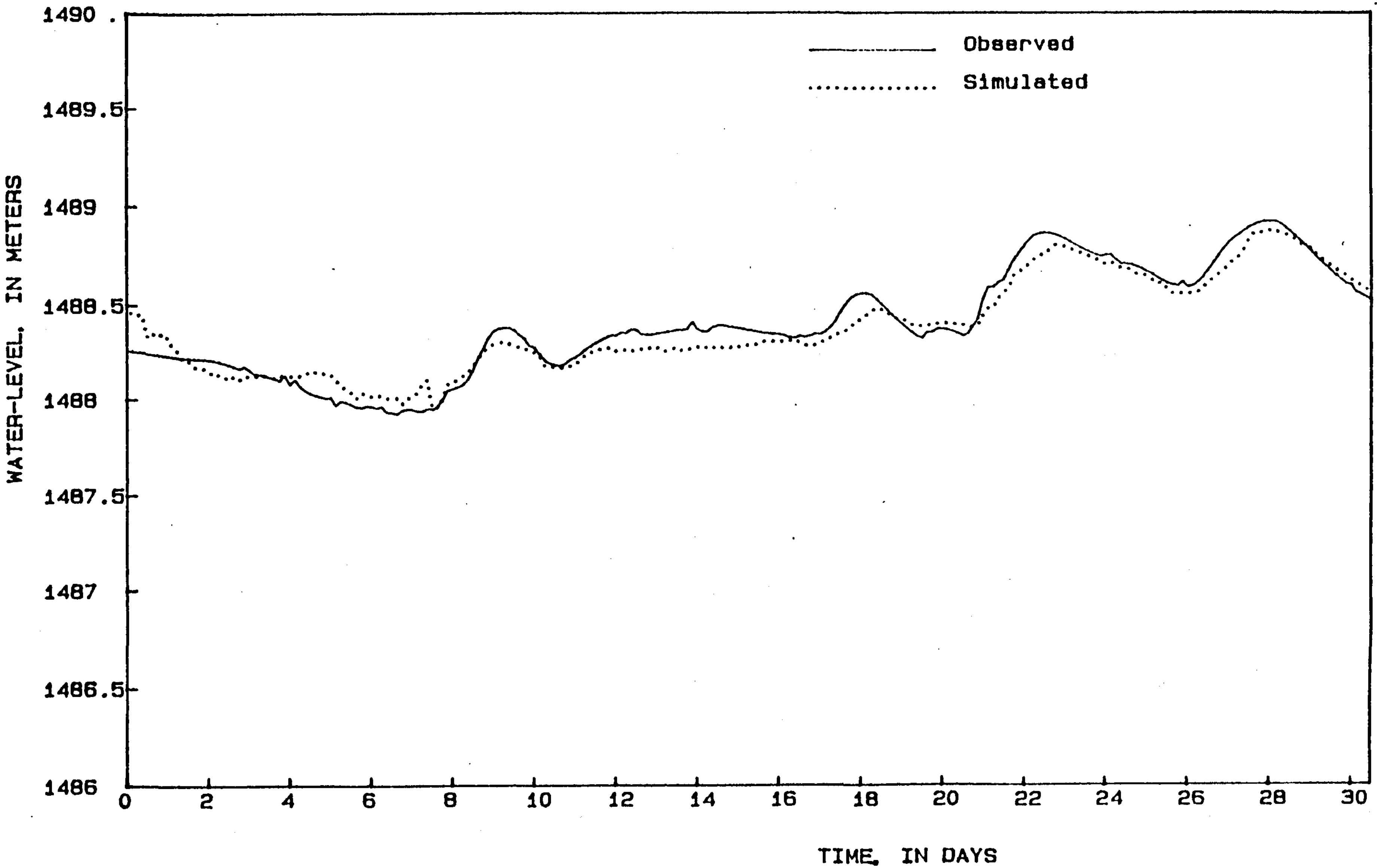

Figure 67. Comparison of observed and simulated water levels at gauge C1M12A for January 1988.

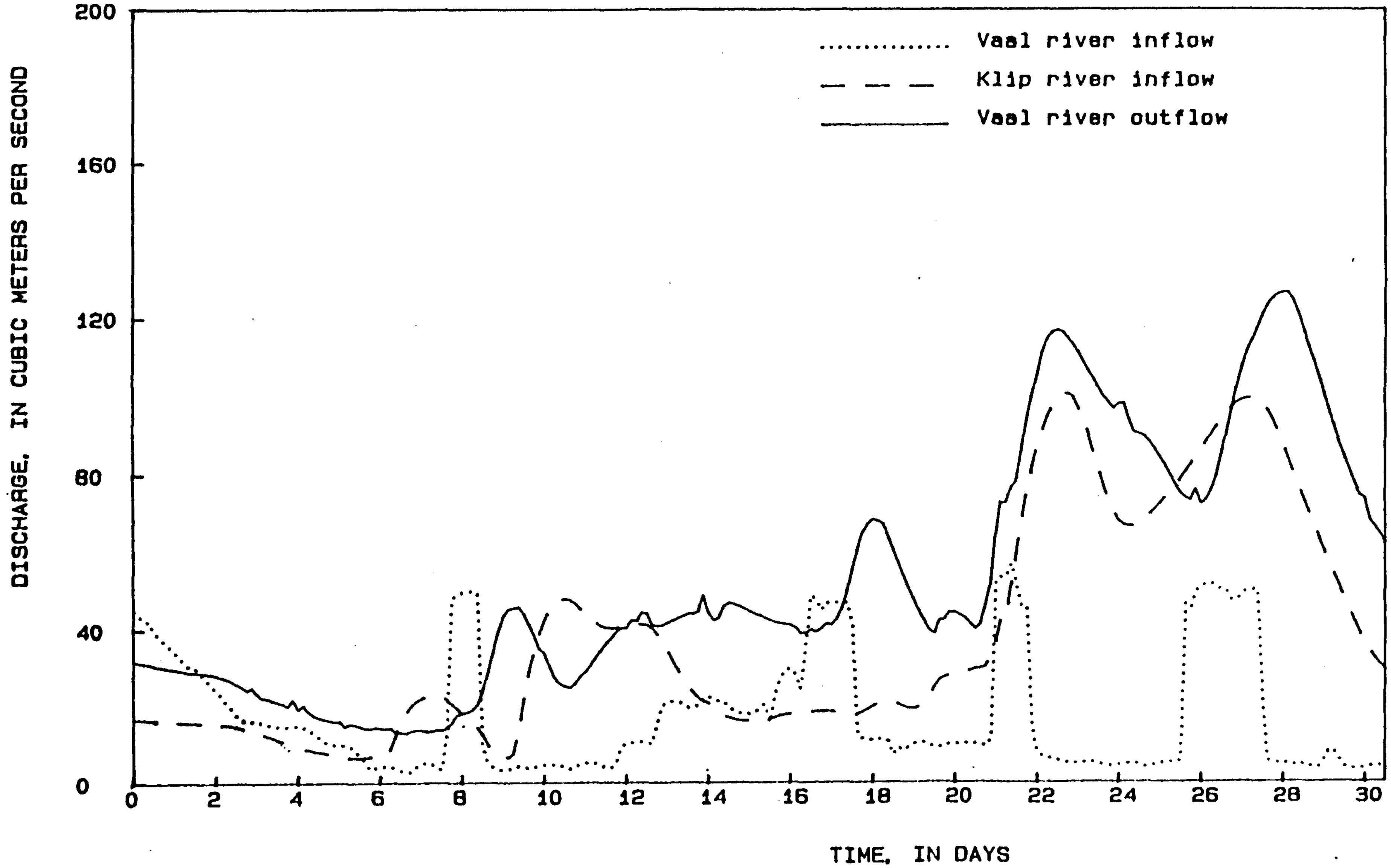

Figure 68. Inflow hydrographs upstream of the Vaal and Klip rivers and outflow hydrograph for January 1988.

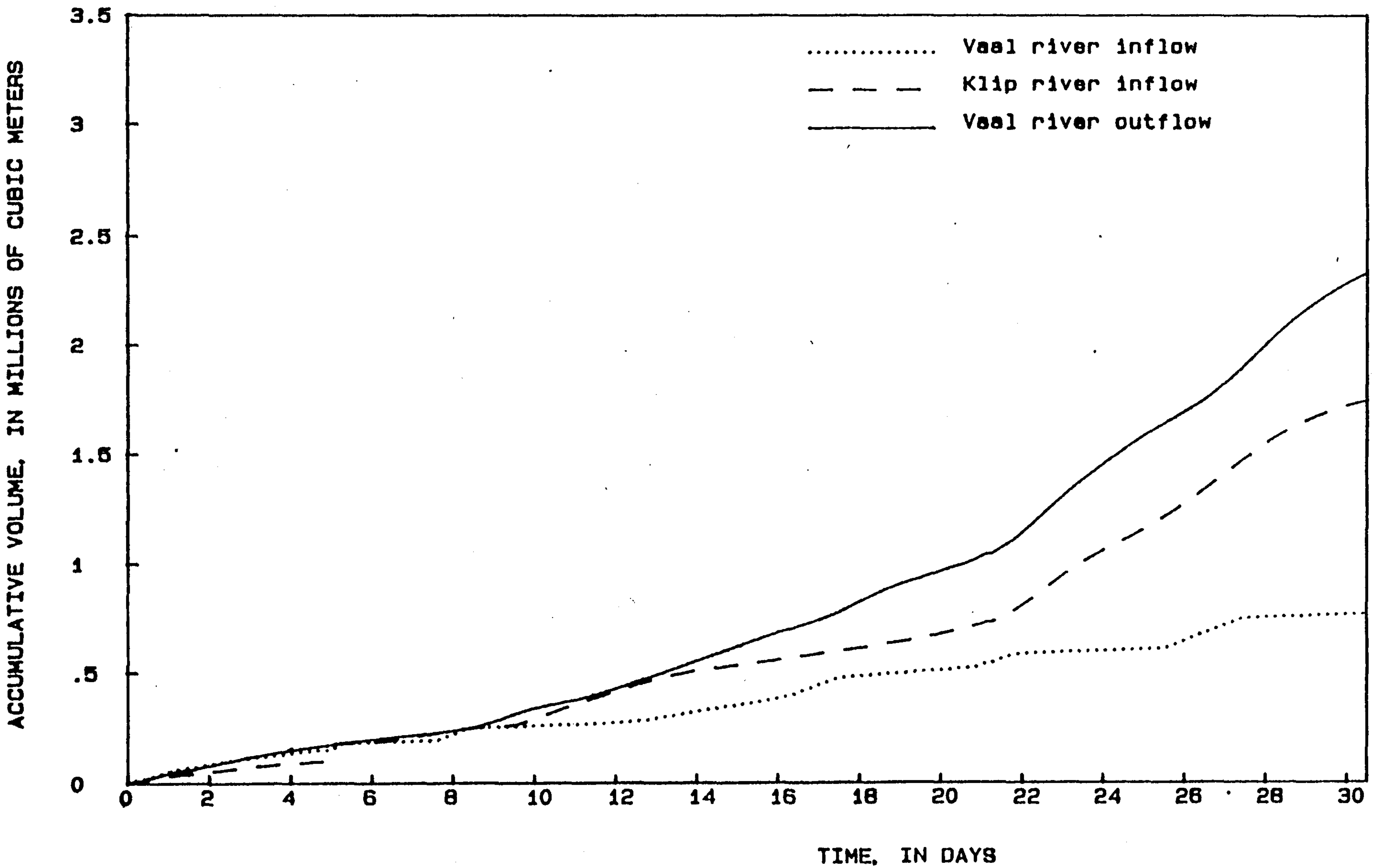

Figure 69. Mass curve plots for the Vaal and Klip rivers, January 1988.

inflows. The effect of the releases from the Grootdraai dam and the high contribution of the tributaries is also shown in Figure 68. The flows at the downstream end of the model are considerably higher than the upstream peaks of the flood from the Klip river in spite of the dispersion and attenuation of the flood.

Figure 69 illustrates the accumulated inflows and outflows from the Vaal and Klip rivers. The curves depict the net volume of water that has passed the given cross-sections up to that point in time. The steepness of the slope of the curves portrays the magnitude of the discharge at that instant. Therefore, the time at which the flood passes through each section can be deduced.

The application of the model in the Vaal river has shown that the model can be used for flood forecasting, flood warning and reservoir management. The long simulation period, however, increased the model execution time to almost 48 hours on an IBM-AT micro computer. This makes the calibration adjustments of the model a cumbersome exercise. For purposes of continuous simulation or flood forecasting the model would be better coupled to a simpler model (or a stochastic component), in order to describe the information contained in the forecast errors of the model. Cunge et al. (1981) recommends a three step strategy:

- The model is calibrated with all the available data.
- A simplified model is conceived for use in the forecasting itself. Its coefficients are calibrated by repeated use of the full model.
- The simplified model is implemented on a micro computer at the forecasting centre.

Application of such a system for longer time periods can lead to interesting conclusions regarding the relationship between the rainfall in the drainage basin and the flow in the river. For instance, it is a popular contention that short duration storms cause extreme flood peaks whilst storms of long duration result in large flood volumes. The continuation of the rainfall in February 1988 resulted in very high peaks in the Vaal river although the intensity was no higher than that for the flood of January 1987. The submerged weirs at the gauge stations during February 1988 are indicative of the above conclusion. Therefore data for February was either unreliable or no records were available at all. The high peaks could also be foreseen by the high flows (Figure 68) and outflow volume (Figure 69) computed at the downstream limit of the model at the end of January 1988. The above conclusion has been verified by the experience gained during recent major flood events, where, in general, high flood peaks were accompanied by large flood volumes (Pegram and Adamson, 1988; Kovacs, 1988).

6.9 RUN TIME REQUIREMENTS OF THE MODEL

The execution time of the model is a function of:

- The number of cross-sections.
- The number of branches.
- The number of boundary conditions.
- The number of internal nodes.
- The period simulated and the time-step.

Because of the many factors affecting the execution time of the model, it is difficult to give exact simulation durations. In addition, direct comparison with other models as regards execution times is not possible as most of the models were developed utilising different computer systems. From the previous applications and the the algorithm structure of the model the following points can however be noted:

- For a single branch the execution time of each iteration is limited mainly by the time required for the solution of the pentadiagonal matrix. The number of cross-sections is therefore the critical factor.

- For simulations with more than one branch, the execution time of each iteration increases considerably. This occurs as the matrix of unknown water levels and flowrates at the nodes in the river network, is not banded and is therefore solved by the Gauss-Seidel method. The execution time depends on the size of the formulated matrix, therefore on the number of branches, the number of boundary conditions and the internal nodes.

- In order to give a picture of the relative time requirements of the model, the following iteration times were recorded on an IBM-AT computer:

  - The St. Lucia lake estuary simulation (one branch, 11 cross-sections) : 10 sec/ iteration.
  - The Vaal river simulation (12 branches, 130 cross-sections) : 2,9 min / iteration.
  - The St. Lawrence river simulation (20 branches, 204 cross-sections) : 4,2 min / iteration.

  In general the model will converge very quickly in each time-step, within approximately two or three iterations. This does however, depend on the accuracy in flowrate and water level specified by the analyst.

- For simulation durations in the order of minutes or a few hours the model is comparable to the explicit models. For longer simulation durations (days), which are the more common durations for rivers, the implicit model is much faster. For example in the Sabine river simulation, Garrison et al. (1969) used a time-step of 15 sec, which corresponds to 17280 time-steps compared to the 72 time-steps used by the implicit model (one hour time-step).

- Most of the simulations performed lasted from a few minutes to a maximum of half an hour. The St. Lawrence simulation lasted for more than 20 hours on an IBM-AT micro computer. However, it must be remembered that the simulation was near the model's limits in terms of data capacity (20 branches, 204 cross-sections) and a total period of 5 days was simulated. Similarly, the simulation of the Vaal river lasted almost 48 hours. However, it was shown in the previous section that models based on the full Saint Venant equations are not normally used for continuous simulations.

The examples discussed above illustrate the ability of the model to describe various unsteady flow conditions and complicated river configurations. The simulations in the St. Lawrence and Vaal river show the applicability of the model to looped and branched channels, its limitations and some of the problems that the analyst confronts in practical applications.

7.0 FLOOD ROUTING IN PRISMATIC CHANNELS

7.1 INTRODUCTION

One of the most important flow phenomena in river hydraulics is the movement of flood waves in natural channels. A flood is most often the result of an excessive volume of runoff entering a channel over a restricted period of time, resulting in a translation wave which moves downstream.

The practical problems related to wave propagation along a channel are those of wave deformation or **wave subsidence**. More particularly the flood wave becomes longer (dispersion) and lower (attenuation) as it moves downstream.

This chapter deals with wave propagation in prismatic channels. The objectives are:

- The modification of the developed unsteady flow model to allow for the routing of hydrographs when the downstream boundary condition is unavailable.

- The developement of a nonlinear kinematic model for the routing of floods in natural rivers.

- The study of the spectrum of shallow water waves and the definition of the range of applicability of the approximation models.

- The study of the wave subsidence in prismatic channels and the identification of the pertinent parameters that affect it.

The abovementioned analysis will enable the modeller to identify, prior to the routing, the dominant mechanisms responsible for wave subsidence and to apply the appropriate approximation model, or to provide a qualitative knowledge of the amount of subsidence expected.

7.2 DOWNSTREAM BOUNDARY CONDITION FOR HYDROGRAPH ROUTING

It is always advantageous to have data at the downstream boundary. Water stage hydrographs may be available for some past flood, and can be used for model calibration. In general, they will not be known for the exploratory runs unless the downstream condition is a lake, reservoir, or tidal condition. If a river reach ends at any point other than a physical boundary it will not appropriate to introduce, for example, a fixed water level as a boundary condition as this will cause a reflection of the flood wave, thus obscuring the results.

In the literature, two of the most common methods used to account for the downstream boundary condition are:

- To use a steady-state rating curve as a condition downstream.
- To use the method of characteristics.

Both methods are examined, in terms of computational efficiency and accuracy.

- **Steady-state rating curve**

  These rating curves are always defined as single-valued relationships Q(Z), between discharge and water stage and they are either observed or computed at the downstream station (by a steady state computation model such as HEC-2). If a measured steady-state rating curve is not available at the downstream boundary a steady state relation, i.e. Manning equation, can be used as a condition. In this study the single value rating curve is assumed to be described by an exponential relationship between depth and flow, coupled by the Manning equation. Therefore, it is assumed that the single-valued rating curve, can be described by a function of the form:

$$Q = ay^m \tag{7.1}$$

where

a, m are constants

y is the depth of flow

Equation (7.1) is used as the last equation in the formulation of the simultaneous equations. The equation is nonlinear in water depth y, and must be linearized before it can be applied. A predictor-corrector technique similar to that used by Hornberger et al. (1970) is employed. For the first iteration, equation (7.1) is written for the last downstream cross-section using the Taylor series expansion (predictor) as:

$$Q^* = Q^n + \left.\frac{\partial Q}{\partial y}\right|^n (y^* - y^n) \tag{7.2}$$

and for the corrector it becomes:

$$Q_i = Q^* + \left.\frac{\partial Q}{\partial y}\right|^n (y_i - y^*) \tag{7.3}$$

where

n : denotes the previous time-step

* : the Q,y values from the predictor (first iteration)
i : subsequent iterations

and

$$dQ/dy = amy^{m-1} \tag{7.4}$$

The coefficients (a,m) are found at each time-step as follows:

- Water depths are assumed to be in the vicinity of the previous time-step's computed water level.

- The corresponding flowrates are calculated using Manning's relation.

- The values of (a,m) are computed using a spline function.

With the coefficients (a,m) known at each time-step for the last downstream cross-section, equations (7.2) and (7.3) are easily put into the form of equation (4.57) for application to the last node.

The assumption of a steady-state relation as downstream boundary, introduces an error in the computations in terms of a perturbation. The perturbation is a result of the unrealistic backward reflection of the waves which would otherwise propagate on downstream beyond the model limit, if no boundary condition were imposed by the model. If these waves are damped over a short distance, the false backwater influence is limited to a small distance upstream of the downstream boundary. Therefore, the model must be corrected for the effects of unsteady and nonuniform flow. The approach that was adopted is as follows: At the beginning of the computations, imaginary cross-sections are generated immediately downstream of the last downstream cross-section.

The cross-sections have the same slope and cross-sectional properties as the last downstream cross-sections entered by the modeller and are considered as a physical extension of the last downstream branch. Thus, the downstream boundary condition is sufficiently far downstream from the last cross-section in order that the perturbations do not reach the last station modelled.

- **Characteristic equation**

The use of the characteristic equations as boundary conditions allows discharge and depth to obey a combination of momentum and mass continuity relationships in the vicinity of the boundaries. The Saint Venant equations can be converted with some transformations into the following system of four ordinary differential equations (Evangelisti, 1966; Amein, 1966):

$$\frac{dx}{dt} = \frac{Q}{A} + c \tag{7.5}$$

$$-B\left(\frac{Q}{A} - c\right)\frac{dZ}{dt} + \frac{dQ}{dt} + gAS_f - \frac{Q^2}{A^2}\left.\frac{\partial A}{\partial x}\right|_{y=const.} = 0 \tag{7.6}$$

$$\frac{dx}{dt} = \frac{Q}{A} - c \tag{7.7}$$

$$-B\left(\frac{Q}{A} + c\right)\frac{dZ}{dt} + \frac{dQ}{dt} + gAS_f - \frac{Q^2}{A^2}\left.\frac{\partial A}{\partial x}\right|_{y=const.} = 0 \tag{7.8}$$

where

$y=A/B$ and $c=(gy)^{1/2}$ is the celerity of small disturbances

Equations (7.5) and (7.7) define, for each point of the (x,t) plane, the characteristic lines passing through it and along which equations (7.6) and (7.8) are satisfied.

Referring to Figure 70 and assuming that the dependent variables Q, Z have been evaluated along the $t=t^n$ line (say at point B, C), the solution proceeds as follows:

1. Initial trial values at point R are obtained by performing a linear approximation between points B and C. The linear solution method used, is the one developed by Wylie and Streeter (1978). Assuming that the characteristic $RP(c^+)$ is a straight line, two linear interpolation equations are solved, leading to:

$$c_R = \frac{c_B + r(c_C u_B - c_B u_C)}{1 + r[(\tau_+)_C - (\tau_+)_C]} \tag{7.9}$$

$$u_R = \frac{u_B - r(u_B - u_C)c_R}{1 + r(u_B - u_C)} \tag{7.10}$$

$$Z_R = Z_B - (Z_B - Z_C) r (\tau_+)_R \tag{7.11}$$

where

$$r = \Delta t/\Delta x \tag{7.12}$$

$$\tau_+ = u+c = Q/A + (gy)^{1/2} \tag{7.13}$$

2. The distance $\Delta x'$, of the point R from the downstream boundary is given approximately by:

$$\Delta x' = c_R(\Delta t) \tag{7.14}$$

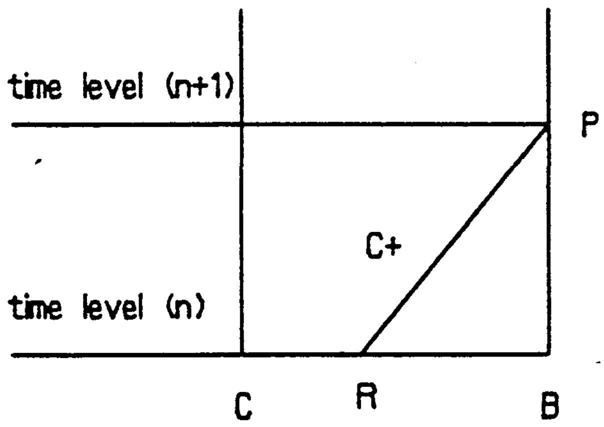

Figure 70. Characteristic solution for the downstream boundary

The flowrate at point R, Q_R, is then calculated using a quadratic spline through points Q_D, Q_C, Q_B using $\Delta x'$. As $\Delta x'$ is itself a function of Q_R, steps 1 and 2 are repeated until an accurate value for $\Delta x'$ is found.

3. Once Z_R, and Q_R are established, the relationship between Z_P and Q_P is found using the positive characteristic equation (7.8). Setting:

$$CF1 = B\frac{1}{2}\left[\left(\frac{Q}{A}\right)_P^{n+1} + (\sqrt{gy})_P^{n+1} + \left(\frac{Q}{A}\right)_R^{n+1} + (\sqrt{gy})_R^{n}\right] \quad (7.15)$$

$$CF2 = \frac{Q^2}{A^2}\;\frac{A_P^{n+1}-A_R^{n}}{x_B-x_R} \quad (7.16)$$

$$CF3 = gAS_f \text{ where } S_f=\frac{1}{2}\left[\left(\frac{Q^2}{K^2}\right)_R^{n}+\left(\frac{Q^2}{K^2}\right)_P^{n+1}\right] \quad (7.17)$$

and

$$B = \frac{B_R^n + B_P^{n+1}}{2}, \quad A = \frac{A_R^n + A_P^{n+1}}{2}, \quad Q = \frac{Q_R^n + Q_P^{n+1}}{2} \qquad (7.18)$$

the characteristic equation becomes:

$$Q_P^{n+1} - Q_R^n - (CF1)(Z_P^{n+1} - Z_R^n) = (CF2)\Delta t - (CF3)\Delta t \qquad (7.19)$$

The values at point P of the first iteration for the calculation of the coefficients (CF1), (CF2), (CF3), and (CF4) are approximated from the time-level (n) and for the subsequent iterations, by the computed forward values. Equation (7.19) relates the two unknowns at the downstream boundary (Q_P^{n+1}, Z_P^{n+1}) and can be used as the last equation for the formulation of the matrix of simultaneous equations.

The two methods were compared by routing different hydrographs, in prismatic channels of various shapes and comparing the computed hydrographs with published results. The characteristic method imposes a severe constraint on the time-step. The length of the characteristic used at the downstream boundary, between the old and new time levels, must be sufficiently small to enable the characteristic curve to be approximated by a straight line. Such a condition is given analytically by (NERC-Flood Studies Report, 1975):

$$\Delta t < \frac{c_{min}}{|dQ/dt|_{max} |dc/dQ|_{max}} \qquad (7.20)$$

where

$|dQ/dt|_{max}$ is the maximum gradient of the upstream hydrograph

c_{min}, $|dc/dQ|_{max}$ are the minimum and maximum values of c and $|dc/dQ|$ in the range of discharges anticipated at the downstream boundary

In addition, to ensure stability the Courant criterion must always be satisfied. Therefore, the characteristic through R and c^+, must not fall outside the line segment BC (Figure 70). In practice, it was found that in order for the characteristic method to be applicable, the time-step had to be of the order of a few seconds. This constraint, contrasts the whole concept of developing an implicit model applicable on micro-computers, where the duration of the simulation might be over an extended period e.g. days.

One of the test runs, taken from Viessman et al. (1972), involved the routing of a triangular discharge hydrograph down a rectangular channel. The channel is 6,1m wide and 3,2 km long carrying a steady uniform discharge of 23,34 m^3/sec at 1,83 m depth. The upstream flood wave has a peak of 56 m^3/s, increasing linearly over a period of 20 min. This upstream flow decreases linearly from its peak of 56 m^3/s to 23,34 m^3/s in 40 min. Additional properties given by Viessman et al. are S_o=0,0015 and n=0,020.

The explicit method employed by Viessman et al. utilised a 2 sec time-step and a 160 m distance-step size. A time-step of 2 min was used for this run. Distance steps of Viessman et al. were retained for all experiments. The results of the routing are shown in Figure 71. The hydrographs produced by both methods were so close to those of Viessman et al. that the curves could not be plotted separately in Figure 71. However, a time step of 5 sec had to be used with the characteristic method, since for larger time steps instabilities were generated in the solution. Figure 72 depicts the computed loop-rating curve at the downstream boundary. It can be clearly seen, that the effect of the steady-state relation used as downstream boundary, has been removed. In all the following comparisons, the steady-state relation is adopted as downstream boundary condition, corrected for unsteady effects.

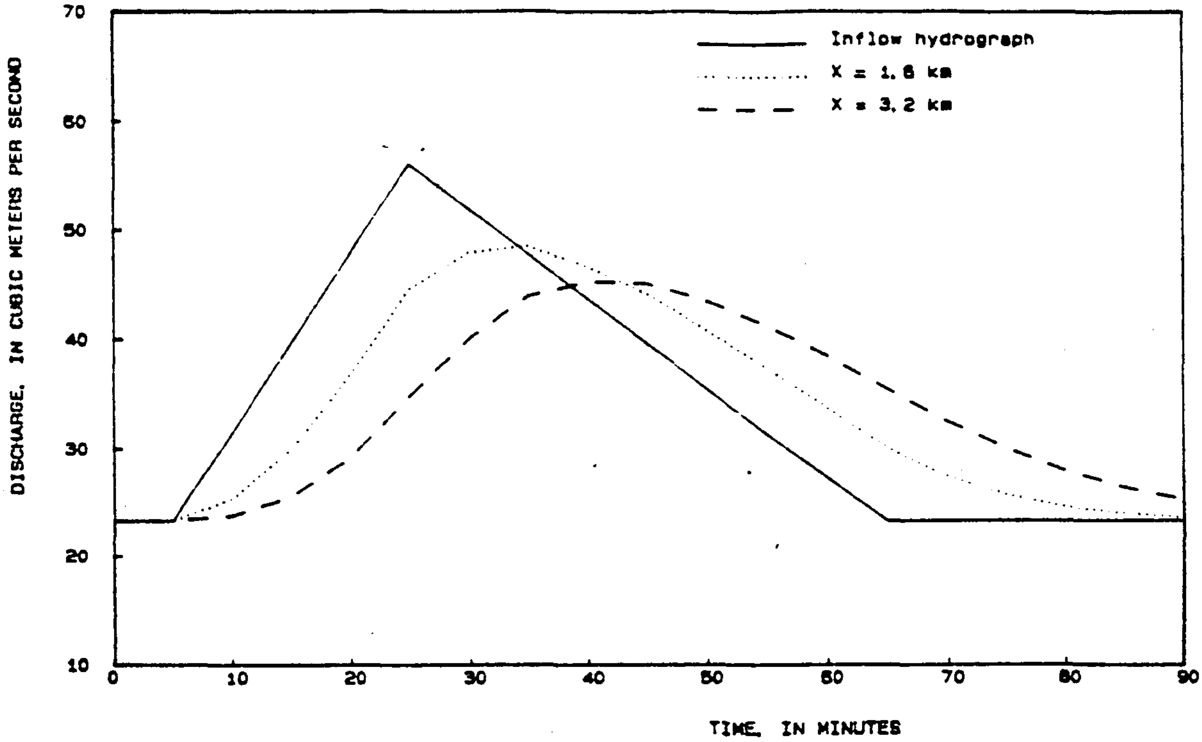

Figure 71. Hydrograph routing in prismatic channel

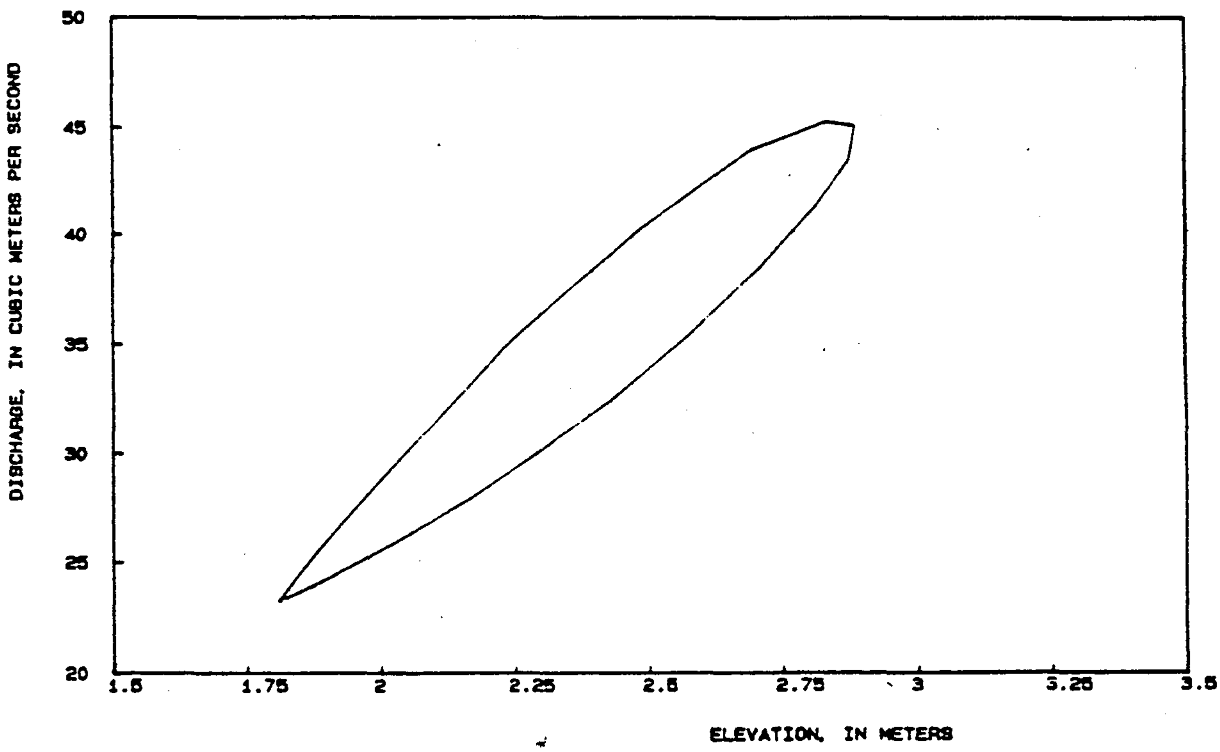

Figure 72. Loop-rating curve at the channel outlet

7.3 DEVELOPMENT OF A KINEMATIC MODEL FOR ROUTING IN NATURAL CHANNELS

In chapter 4 it was shown that by ignoring the acceleration terms in the momentum equation, the unsteady flow model becomes the "diffusion wave" model. In this chapter, a kinematic model is developed for the routing of floods in natural branched rivers. The development of the model is advantageous, as many flood routing problems can be solved quickly, simply and accurately, using a kinematic model without having to resort to the full dynamic equations.

In the kinematic-wave approximation, the inertia as well as the pressure terms of the momentum equation are neglected. The friction slope, S_f, is therefore approximated by the bottom slope, S_o, of the channel, as:

$$S_o = S_f \qquad \text{or} \qquad Q = Q_n \tag{7.21}$$

where

Q_n is the normal discharge described by any steady-state formula or by conveyance as $Q_n = K(Z)S_o^{1/2}$

In general, the momentum equation as used in kinematic flow can be written as an exponential relation between the depth of flow and the discharge, in the form of equation (7.1). The speed of a kinematic wave is that of a monoclinal wave:

$$c = \frac{dx}{dt} = \frac{dQ}{dA} = \frac{1}{B}\frac{dQ}{dy} = U + A\frac{dU}{dA} \tag{7.22}$$

Equation (7.22) describes the characteristic paths in the (x,t) plane. For most channels where the flow is in-bank;

$$dA/dy = B \tag{7.23}$$

where

B : is the channel width

Since Q is a unique function of depth (y) the kinematic wave speed is given as:

$$c = \frac{dx}{dt} = \frac{am}{B}\, y^{m-1} \tag{7.24}$$

Several conclusions can be drawn from equation (7.24) such as:

- Equal depths on both the leading and recession limbs of a hydrograph travel at the same speed.

- Since water at greater depths move at faster rates, it follows that the leading limb of the hydrograph will steepen and the recession limb will develop an elongated tail.

- Equation (7.24) is a forward characteristic, therefore kinematic waves are propagated downstream only.

The propagation of the kinematic wave does not depend on the downstream conditions. Therefore, the implicit algorithm developed cannot be applied to this model and a new algorithm was developed. Computations start from the most upstream channel for which upstream boundary conditions are specified and progress downstream, branch by branch, in a cascading manner, satisfying the flow continuity requirement at all junctions. Along each channel reach, (j,j+1), two equations are solved simultaneously at each time step (n+1):

- **The continuity equation :**

$$(C1)Z_j^{n+1} + (C2)Q_j^{n+1} + (C3)Z_{j+1}^{n+1} + (C4)Q_{j+1}^{n+1} = (C5) \tag{7.25}$$

o **A steady-state relation :**

$$Q_{j+1}^{n+1} = a \, (y_{j+1}^{n+1})^{m} \tag{7.26}$$

where

$$y_{j+1}^{n+1} = Z_{j+1}^{n+1} - BL_{j+1} \tag{7.27}$$

and $(BL)_{j+1}$ is the bed level of the cross-section (j+1)

For regular cross-sections the coefficients (a,m) are constants for all the depths and can be easily calculated. For a rectangular cross-section of width, B, and depth of water much smaller than B, the hydraulic radius becomes R=A/B. Substituting this radius into the Manning equation and comparing with equation (7.1) the coefficients are:

$$a = S_o/nB \tag{7.28}$$

$$m = 1{,}67 \tag{7.29}$$

For approximately rectangular channels, the width of channel, B, can be measured and the roughness coefficient, n, can be estimated. In this case the calculation of the value of (a) and (m) is easy. However, if the flow volume is large, the channel cross-sections may become irregular, and the coefficients (a,m) may only be valid over a limited range. The coefficients (a,m) are calculated in the vicinity of the previous time-step's computed water-level, in a similar manner as described for the downstream boundary condition. This imposes the following restriction on the kinematic model; for fast rising floods, the time-step used must not be very large, as the coefficients (a,m) will not be representative of the new cross-section's depth.

Once the relationship (7.26) for the cross-section (j+1) is defined, equations (7.25) and (7.26) are solved simultaneously for the unknowns (Q_{j+1}^{n+1}, Z_{j+1}^{n+1}). Setting:

$$T1 = (C1)Z_j^{n+1} + (C2)Q_j^{n+1} - (C5) \tag{7.30}$$

combining equations (7.26), (7.27), (7.30) and substituting into (7.25):

$$(C3)Z_{j+1}^{n+1} + (C4)a(Z_{j+1}^{n+1} - BL_{j+1})^m = (C5)-T1 \tag{7.31}$$

Equation (7.31) is nonlinear in Z_{j+1}^{n+1}. An approximate solution to this nonlinear equation is easily obtained by the following iterative solution:

Let

$$r = Z_{j+1}^{n+1}$$

and

$$f(r) = (C3)r + (C4)a(r-BL_{j+1})^m - (C5)+T1$$

then applying Newton's method:

$$r^{(k+1)} = r^{(k)} - \frac{f(r^{(k)})}{f'(r^{(k)})} \tag{7.32}$$

where

(k) is the kth approximation

and

$$f'(r^{(k)}) = (C3) + (C4)amr(r-BL_{j+1})^{m-1}$$

The validity and efficiency of the proposed model was tested against published results of flood routings with different wave models in a hypothetical network. Akan and Yen (1981), developed a diffusion wave flood routing model for channel networks using the overlapping segment technique. The resulting set of non-linear algebraic equations for each segment was solved using Newton's iterative method. They compared their model with the four point fully implicit model similar to that proposed by Baltzer and Lai (1968) and a non-linear kinematic wave model. The hypothetical network used, consists of two junctions and six branches as shown in Figure 73.

All branches are assumed to be rectangular in cross-section. The dimensions are listed in Table 3.

Chan. number	Length(m)	Slope	Width(m)	Manning (n)
1	600	0,0005	5	0,0138
2	600	0,0005	5	0,0207
3	600	0,0005	5	0,0207
4	600	0,0005	5	0,0138
5	600	0,0010	8	0,0141
6	600	0,0010	10	0,0125

Table 3. Channel data for the hypothetical network

Initially a steady flow condition is in operation corresponding to a discharge of 3 m^3/s in channels 1 and 4, 2 m^3/s in channels 2 and 3, 7 m^3/s in channel 5, and 10 m^3/s in channel 6. The inflow hydrographs at the upstream termini of the network are shown in Figure 74. A constant upstream inflow of 2 m^3/s, equal to the base flow rate, is adopted for channels 2 and 3. For channels 1 and 4, the inflow is a triangular hydrograph with duration of 18 min and peak flow of 12 m^3/s.

The computed hydrographs using the three models are shown in Figures 75 to 77 and are identical to the published results. The computed flowrates using the diffusion model were in good agreement with those of the dynamic wave model. In channels 2 and 3 a steady flow condition would prevail if the backwater effects of the other branches in the network did not exist. The kinematic model which ignores the backwater effects from

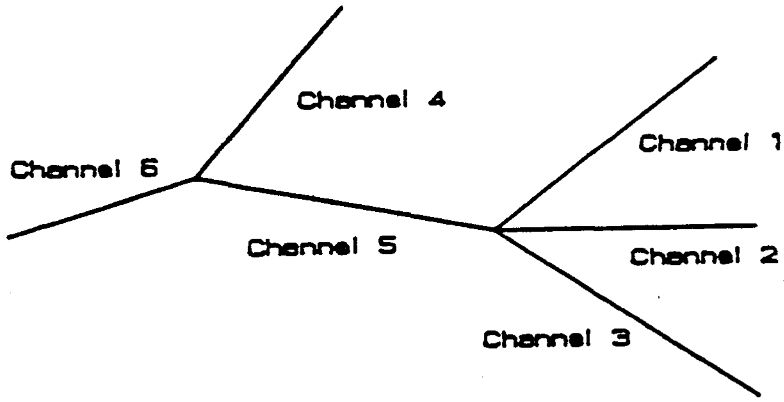

Figure 73. Hypothetical network

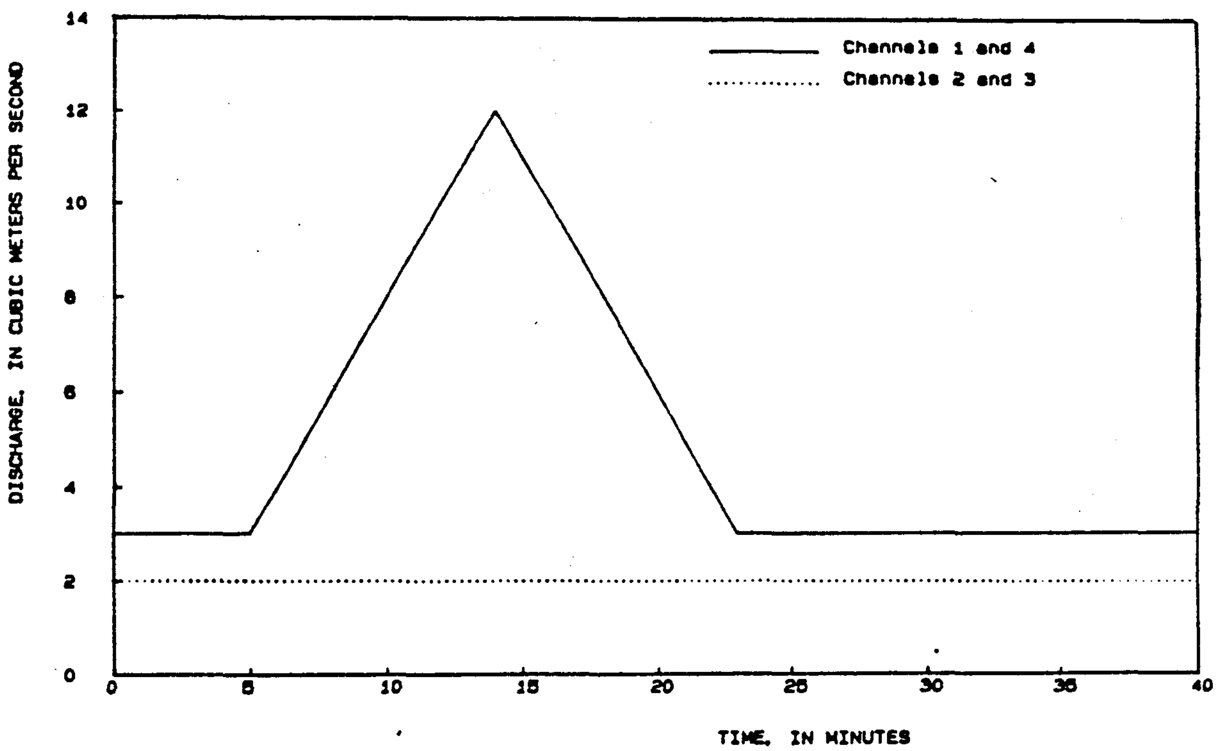

Figure 74. Upstream inflow hydrograph - Hypothetical network

downstream, predicts a steady flow in these two branches as shown in Figure 76. However, the flood wave travelling through channel 1 raises the water surface at the junction where branches 1, 2 and 3 join. This decreases the hydraulic gradient in channels 2 and 3 causing discharges lower than the constant upstream inflow and base flow rate. As the downstream backwater recedes with time, the excess water is released from the channel storage, and discharges higher than the constant inflow rate occur until steady state conditions are again reached.

The computed rating curves for the full dynamic and kinematic models at the outlet of channel 6 are shown in Figure 78. Comparison with the associated water level hydrographs (Figure 77) illustrates that as the flood hydrograph passes a point, the maximum discharge is first observed, then the maximum depth, and finally a point where the flow is uniform. Uniform flow occurs at the point of intersection of the steady-state rating curve with the loop-rating curve, close to the region of maximum depth.

The execution time for the developed nonlinear kinematic model was noticeably smaller than that of the full dynamic model (4 min against 15 min). The diffusion and dynamic models had similar execution times as the same algorithm is used in both models. The difference in the execution times for the kinematic and the dynamic wave models arises from the faster convergence of the former and the difference in the algorithmic structure (no simultaneous equations have to be solved for the kinematic model). This difference is expected to increase exponentially with increasing size of the network considered. Therefore, if the flood to be routed is of kinematic nature, and the backwater effects are not significant, it is much simpler and faster to use the developed kinematic model. The problem of identifying the flood wave type is addressed in the following sections.

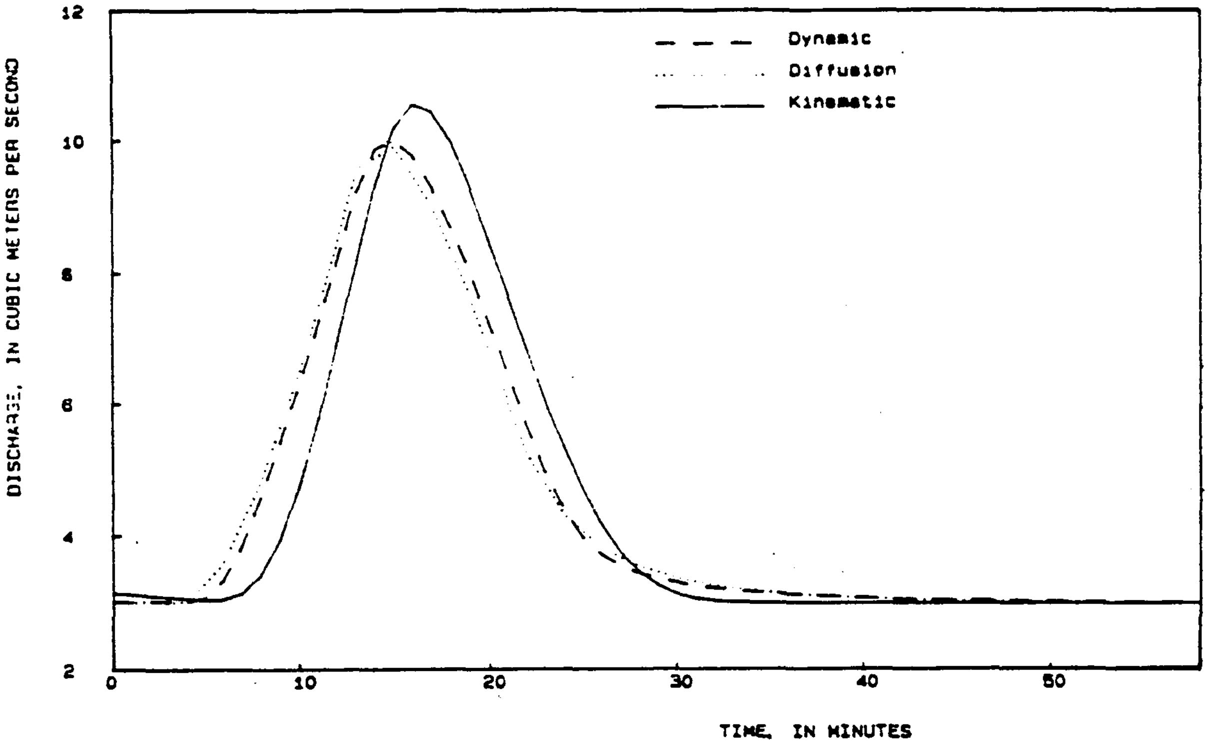

Figure 75. Simulated flowrates at the outlet of branch 1

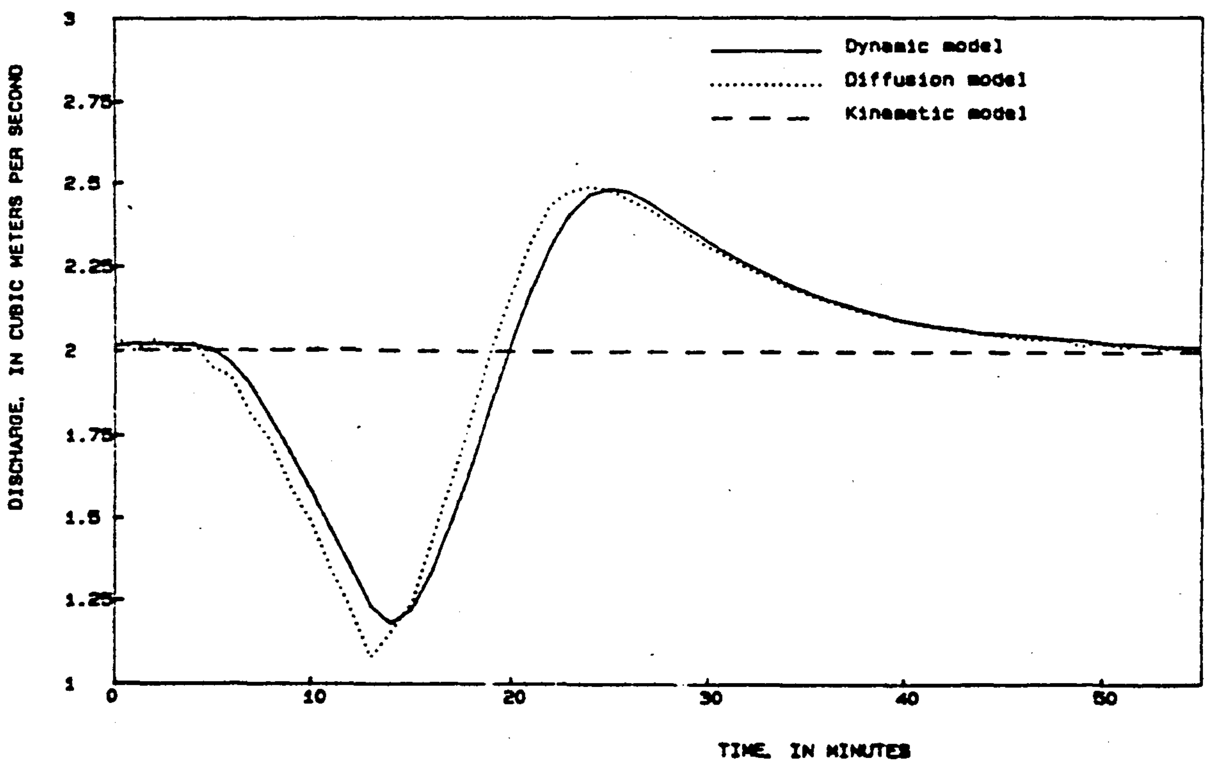

Figure 76. Simulated flowrates at the outlet of branch 2

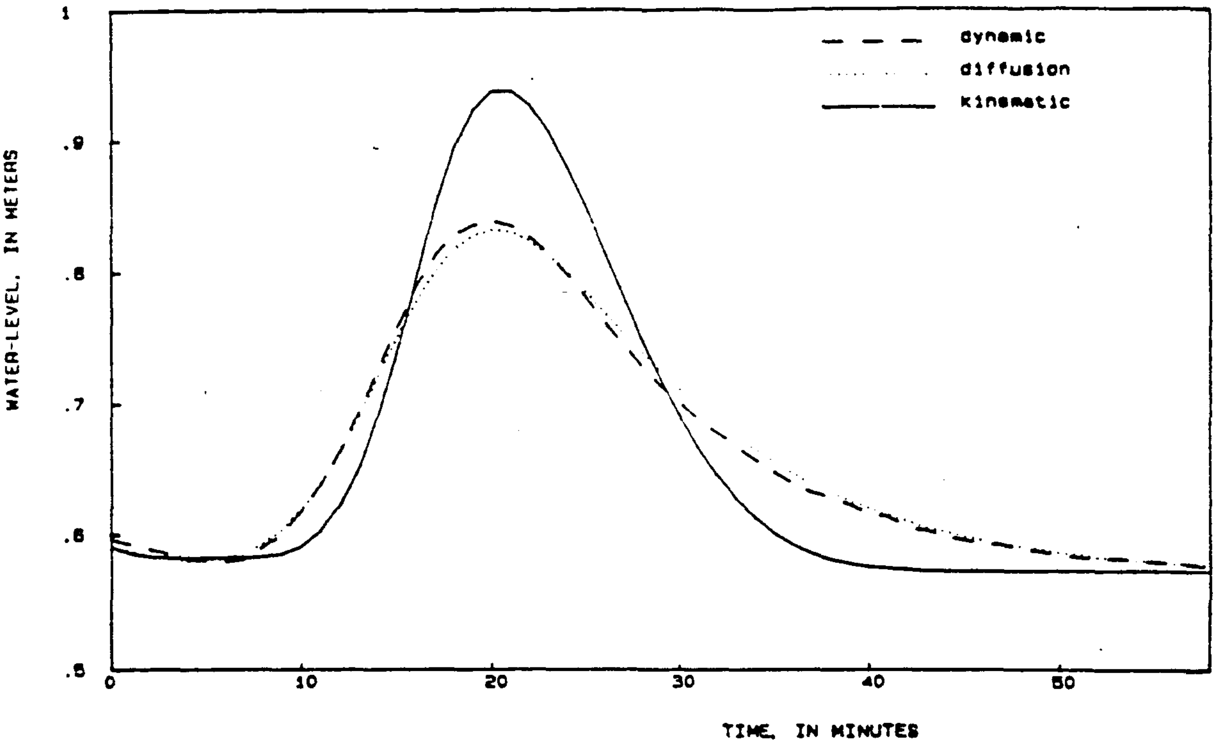

Figure 77. Simulated water levels at the outlet of branch 6

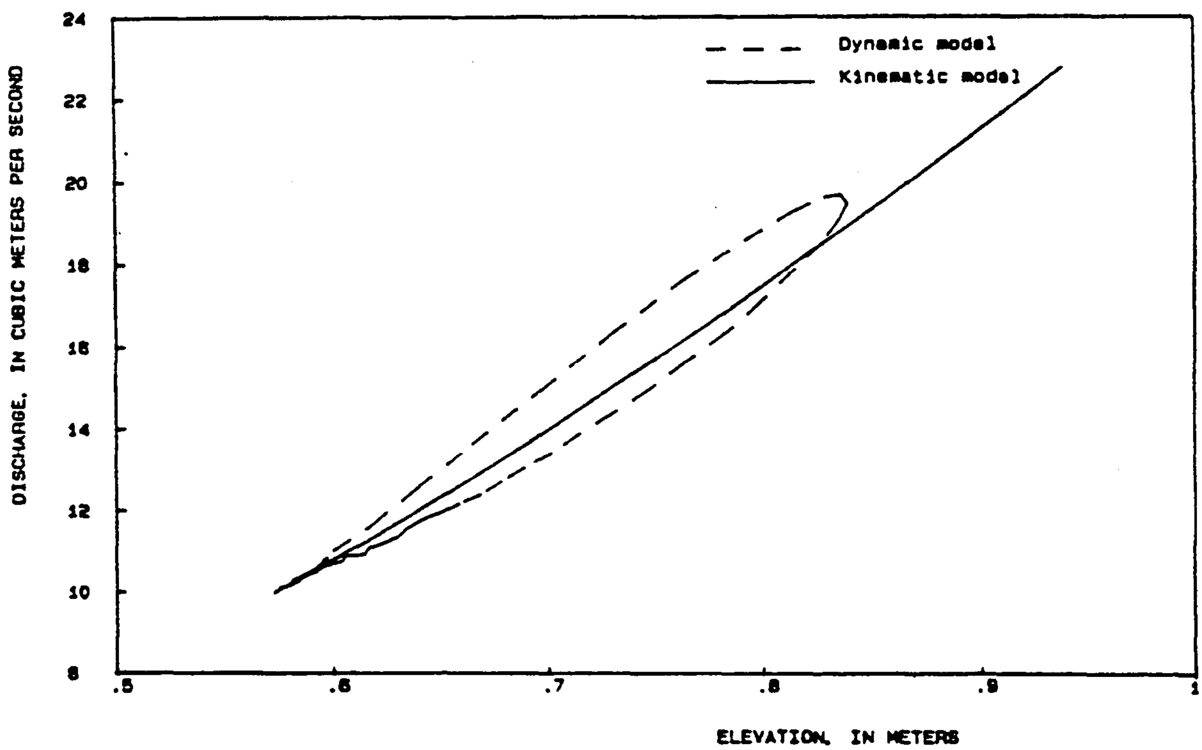

Figure 78. Loop-rating curve and rating curve at the outlet of branch 6

7.4 APPLICABILITY OF APPROXIMATION MODELS

In spite of progress in computational hydraulics, there is still considerable confusion among engineers as to where each approximation model should be applicable. This is attributed to the fact that a complete theory explaining the behaviour of waves of arbitrary shapes, does not exist. Over the years, several investigators have attempted to clarify the phenomenon of propagation of shallow waves in open channel flow. Most of the earlier studies on numerical solution of flood wave problems either dealt with the task of developing new numerical schemes, improving old schemes or applying these methods to specific field problems.

The first important contribution was made by Lighthill and Whitham (1955) who analysed in detail the concept of the kinematic wave and contrasted it to the dynamic wave. A qualitative study of subsidence in prismatic channels for small amplitude waves was made by Henderson (1966) and he concluded that there could be significant subsidence in prismatic channels.

Ponce and Simons (1977) applied linear stability analysis to determine the celerity and attenuation of shallow water waves through the wave number spectrum and within the practical range of mean flow Froude number. Ponce and Simons also proposed a division of the spectrum based on the wave celerity and distinguished gravity, kinematic and dynamic bands. This work was pursued further by Ponce et al. (1978) where criteria for determining the applicability of the kinematic and diffusive wave models were introduced.

Menedez and Norscini (1982) also applying linear stability analysis, made a general division of the spectrum of shallow water waves, taking into account the predominant physical mechanisms, and the attenuation and dispersive characteristics of the waves.

In this study, the findings of the researchers mentioned above are combined and tested in order to provide practical criteria for determining the applicability of each wave model. To obtain a generalised picture of the damping of flood waves in prismatic channels, a parametric study was made investigating the effects of wave parameters and arbitrary shapes, in conjunction with the defined practical criteria. The results provide an adequate qualitative picture and a quantitative first approximation for practical flow situations.

7.4.1 DEFINING THE SHALLOW WAVE SPECTRUM

All the theoretical models proposed by researchers for the study of the wave propagation problem were based on a small perturbation analysis. The following assumptions hold:

- The Saint-Venant equations are linearized by neglecting second order terms.
- The flow is initially in an undisturbed state characterised by a uniform flow with the following properties:

  u_o = steady flow mean velocity
  d_o = steady uniform flow depth
  and
  F_o = the Froude number of the uniform flow

$$F_o = u_o/(gd_o)^{1/2} \tag{7.33}$$

- A small sinuisoidal perturbation is introduced characterised by:

  L = the wave-length of the disturbance
  T_w = wave period of the perturbation
  $c = L/T_w$: wave celerity

The solution for a small perturbation in the depth of flow is postulated in the following exponential form:

$$d_1 = d_o d' \exp(i(\sigma x - \beta t)) \tag{7.34}$$

in which

d_1 = is a small perturbation to d_o

d' = is a dimensionless depth amplitude function

σ' = is a dimensionless wave number

β' = is a dimensionless complex propagation factor

x', t' = are dimensionless space and time coordinates such that

$$\beta' = (2\pi/T_w)L_o/u_o \tag{7.35}$$

$$\sigma' = (2\pi/L)L_o \tag{7.36}$$

$$x' = x/L_o \tag{7.37}$$

$$t' = tu_o/L_o \tag{7.38}$$

The value L_o is a reference channel length or, the horizontal length in which the steady uniform flow drops in head equal to its depth, and it is defined as:

$$L_o = d_o/S_o \tag{7.39}$$

When comparing wave amplitudes after one propagation period, the value of t' is symbolised as τ and given by:

$$\tau = T_w u_o/L_o \tag{7.40}$$

The propagation celerity c can be expressed in dimensionless form by dividing it by u_o, thus $c' = c/u_o$. Assuming that the wave attenuation follows an exponential curve the logarithmic decrement is defined as:

$$\delta = \ln(a_1) - \ln(a_0) \tag{7.41}$$

in which

a_1 and a_0 : are the wave amplitudes at the beginning and end of one wave period, respectively.

The value of δ is a measure of the rate at which the unsteady component of the motion changes upon propagation. For δ positive, amplification sets in; for δ negative the motion attenuates and dies away.

Ponce and Simons (1977) solved the linearized momentum equation and ignoring selected terms came to the following conclusions for each wave model:

- **Kinematic wave model (Inertia and pressure terms are neglected)**

  - The dimensionless celerity of the kinematic wave is:

    $$c'_k = \beta'_r/\sigma' = 1,5 \tag{7.42}$$

    Thus the celerity of a kinematic wave is independent of F_o and σ' and equal to 1,5 times the mean flow velocity.

  - The logarithmic decrement of a kinematic wave is zero, thus a kinematic wave propagates downstream without dissipation.

- **Diffusion wave model (Inertia terms are neglected)**

  - As with the kinematic model, diffusion waves propagate downstream only, and the diffusion wave celerity is independent of F_o and σ' and equal to 1,5 times the mean flow velocity.

  - The logarithmic decrement of the diffusion wave is:

$$\delta_d = -2\pi\ (\sigma'/3) \tag{7.43}$$

Diffusion waves attenuate as they propagate downstream, and the rate of attenuation is controlled by the dimensionless wave number σ'. The larger the dimensionless wave number, the larger the attenuation.

- **Gravity wave model (Friction and bed slope terms are ignored)**

  - Gravity waves propagate along two characteristic directions with celerities:

$$c_R = \beta'/\sigma' = 1 \pm F_o$$

or

$$c_R = u_o + (gd_o)^{1/2} \tag{7.44}$$

  - The logarithmic decrement δ_R is zero and gravity waves are not subject to attenuation.

  - The wave number, σ', tends to infinity (short waves relative to d_o)

- **Dynamic wave model (All terms in the momentum equation are considered)**

  - Dynamic waves propagate along two characteristic paths which can face either:

    - One upstream **(secondary wave)** and the other downstream **(primary wave)**.
    - Both downstream (Primary wave is the faster).

  - The propagation of a dynamic wave is a function of two dimensionless parameters, the wave number σ' and the Froude number F_o. The relative phase velocity c_r or

$(c-u_o)/u_o$, versus the dimensionless wave number, σ', for several values of F_o, is shown in Figure 79.

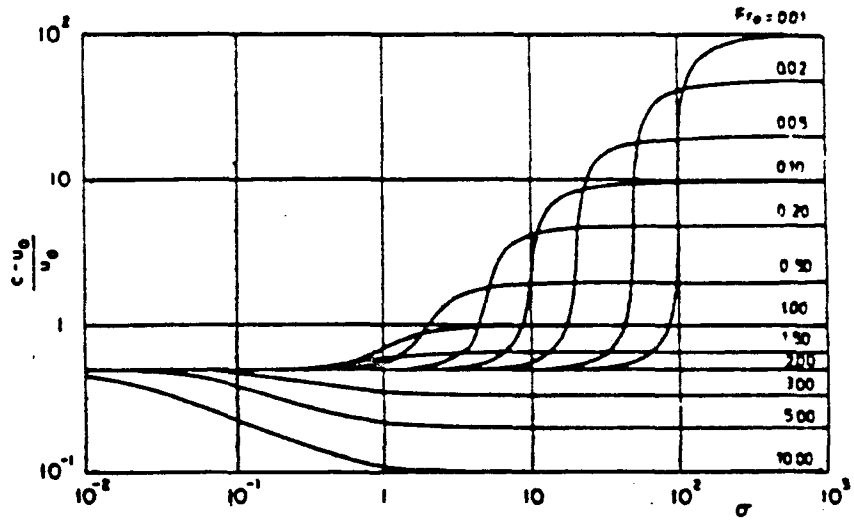

Figure 79. Dimensionless relative celerity, c_r, versus dimensionless wave number σ' (Ponce and Simons, 1977)

The following conclusions are derived from this Figure:

- There are three well-defined bands in the wave number spectrum.

  - A **kinematic band** corresponding to small values of the wave number σ', in which the relative celerity c_r is independent of both σ' and F_o.
  - A **gravity band** corresponding to large values of σ', in which c_r is independent of σ' and dependent only on F_o.

- **A dynamic band** corresponding to midspectrum values of the wave number in which c_r is a function of both σ' and F_o.

- In the kinematic band, c_r approaches asymptotically to a constant value of 0,50 which corresponds to that of a kinematic wave. In the gravity band, c_r approaches asymptotically the value $1/F_o$ which corresponds to that of a gravity wave. In the dynamic band, c_r lies between the kinematic and gravity wave celerity values.

Menendez and Norscini (1982) following the same reasoning of small perturbation analysis made a more complete and coherent formulation for defining different spectral shallow water wave bands, giving more emphasis on the dominant mechanisms in each band. Figure 80 shows that the wave length spectrum can be divided into 5 bands, depending on the Froude number:

- Two extreme bands ($\sigma'<<1$ and $\sigma>>1$) corresponding respectively to the kinematic and long gravity waves. They have in common the fact that they are both determined by the action of only two dynamic mechanisms: the former by gravity and resistance; the latter by inertia and pressure.

- Two intermediate bands that correspond to the diffusive waves. For the left lower intermediate band, $F_o<2$, pressure, gravity and resistance are of importance. For the right band, $F_o>2$, inertia instead of pressure becomes important. At the limit, $F_o<<2$, the intermediate band corresponds to non-neutral and nondispersive waves governed by the action of gravity, resistance and pressure.

- The central band where all the mechanisms are relevant. It corresponds typically to dynamic waves.

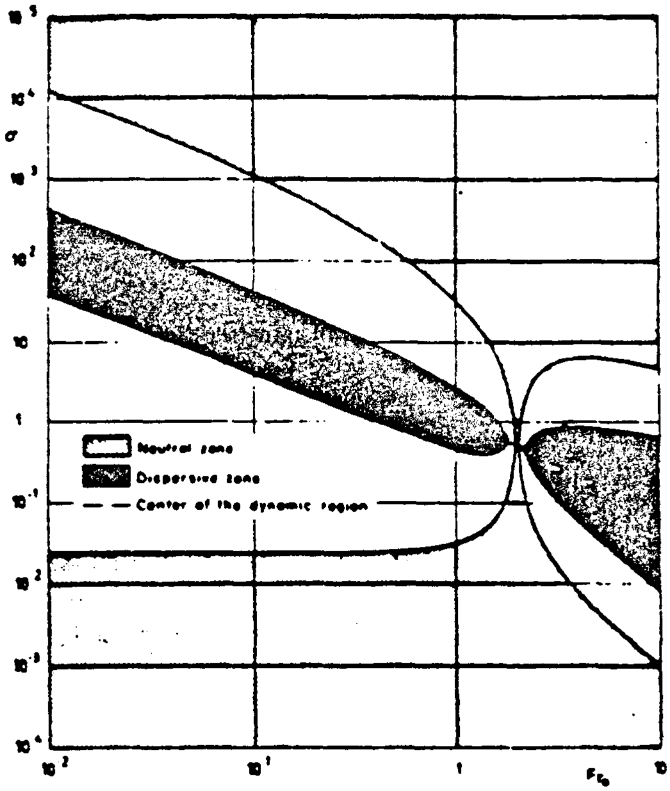

Figure 80. Spectrum of shallow water waves (Menedez and Norscini, 1982)

When F_o tends to 2, the central band initially disappears on both sides. Secondly the intermediate bands disappear. Therefore, the two extreme bands touch one another. There is therefore a region where kinematic and gravity waves coexist and are of similar importance. On the other hand, this transition is also a bridge between the two dynamic bands, characterising a region where all four dynamic mechanisms are relevant.

The Froude number spectrum clarifies the dynamic wave propagation and helps in a better understanding of the dynamic open channel flow phenomena. Thus, for primary waves (main body of flood wave), $F_o=2$ is the threshold dividing the attenuation and amplification. For $F_o<2$, primary waves propagate downstream and attenuate; for $F_o=2$, primary waves propagate downstream and neither amplify or attenuate; for $F_o>2$, primary waves propagate downstream and amplify.

For secondary waves, $F_o=1$ is the threshold dividing the propagation from upstream to downstream. For subcritical flow ($F_o<1$) secondary waves propagate upstream for $c_r>1$, or downstream for $c_r<1$. For supercritical flows ($F_o>1$) secondary waves propagate downstream. Secondary waves attenuate for all values of F_o and σ'.

7.4.2 PRACTICAL CRITERIA FOR APPROXIMATION MODEL APPLICABILITY

Henderson (1966) classified flood waves, into waves broadly characteristic of steep, mild and intermediate slopes, according to the magnitude of S_o. He did not offer specific guidelines to define any limiting points although he did conclude that the kinematic model is applicable in steep rivers; the diffusion model in mild and steep channels; and the dynamic model to all three.

Ponce et al. (1978) based on the analysis of Ponce and Simpson (1977) developed criteria for the applicability of the kinematic and diffusion model. The kinematic model will be valid when the attenuation factor of the diffusion model, e^{δ}, is close to 1. Thus, for at least 95% accuracy of the kinematic wave solution after one propagation period, τ has to be greater than 171. Combining the logarithmic decrement of the diffusion model with the celerity of the kinematic model $c_d=1,5$, the diffusion decrement comes to:

$$\delta_d = -8\pi^2/9\tau \qquad (7.45)$$

The criterion for the kinematic model to be applicable with 95% accuracy becomes:

$$T_w > \frac{\tau\, d_o}{S_o u_o} \qquad \text{or} \qquad T_w > \frac{171\, d_o}{S_o u_o} \tag{7.46}$$

For the diffusion model, combining equations (7.36) and (7.38) the dimensionless wave period can be expressed in terms of the dimensionless wave number, as:

$$\tau = 2\pi/c'\sigma' \tag{7.47}$$

and making use of equations (7.33) and (7.38):

$$\tau/F_o = T_w S_o (g/d_o)^{1/2} \tag{7.48}$$

The parameter τ/F_o for a wide range of F_o ($0{,}01<F_o<1{,}0$) is greater than 45 (Ponce et al., 1978). From a practical standpoint in order for the diffusion model to be applicable as opposed to the full dynamic equation, the ratio τ/F_o must be higher than 30. Therefore:

$$T_w S_o (g/d_o)^{1/2} > 30 \tag{7.49}$$

If inequality (7.49) is not satisfied, the diffusion model breaks down and the full dynamic model must be used.

Menendez and Norscini developed graphs as in Figure 80 for different maximum errors (ε) and combined them with the graph in Figure 79 to develop criteria for the model applicability. The methods were compared for a wide range of slopes and channels, and the criteria were found to give very similar wave period limits for the majority of cases. This result was also reported by Menendez and Norscini comparing their graphs with equations (7.49) and (7.46). However, because of the simplicity of the Simpsons et al. criteria they are preferred against the latter.

The diffusion model applicability criteria for different slopes (S_o) and initial depths (d_o) are plotted in Figure 81. The kinematic model applicability criteria for three different slopes are shown in Figures 82 to 84. The efficiency of these criteria in relation to the developed numerical models is evaluated in the next section.

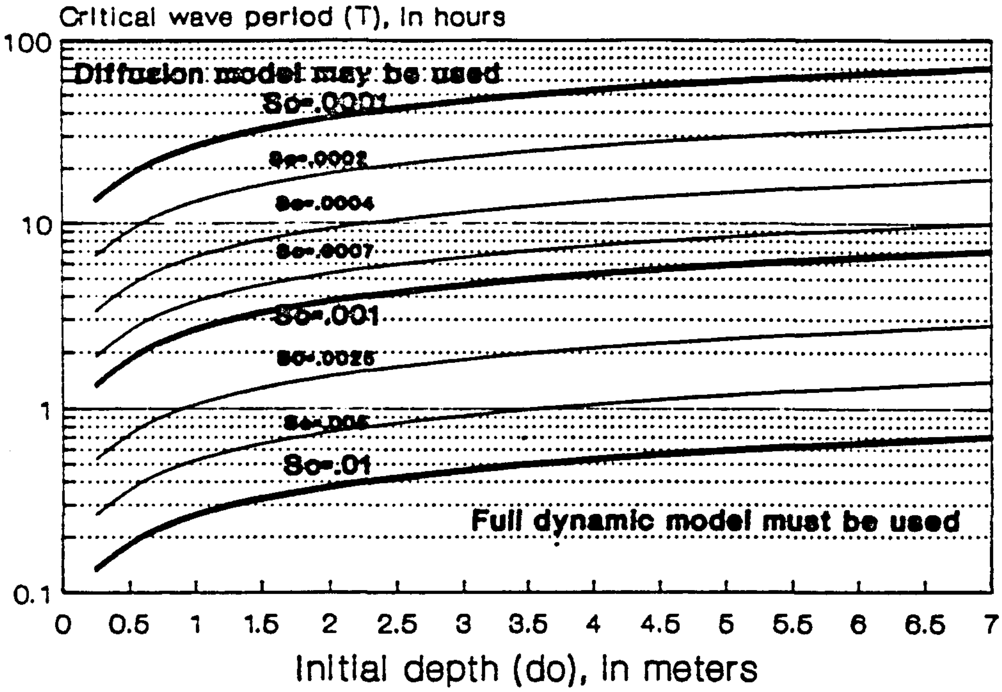

Figure 81. Diffusion model applicability criteria

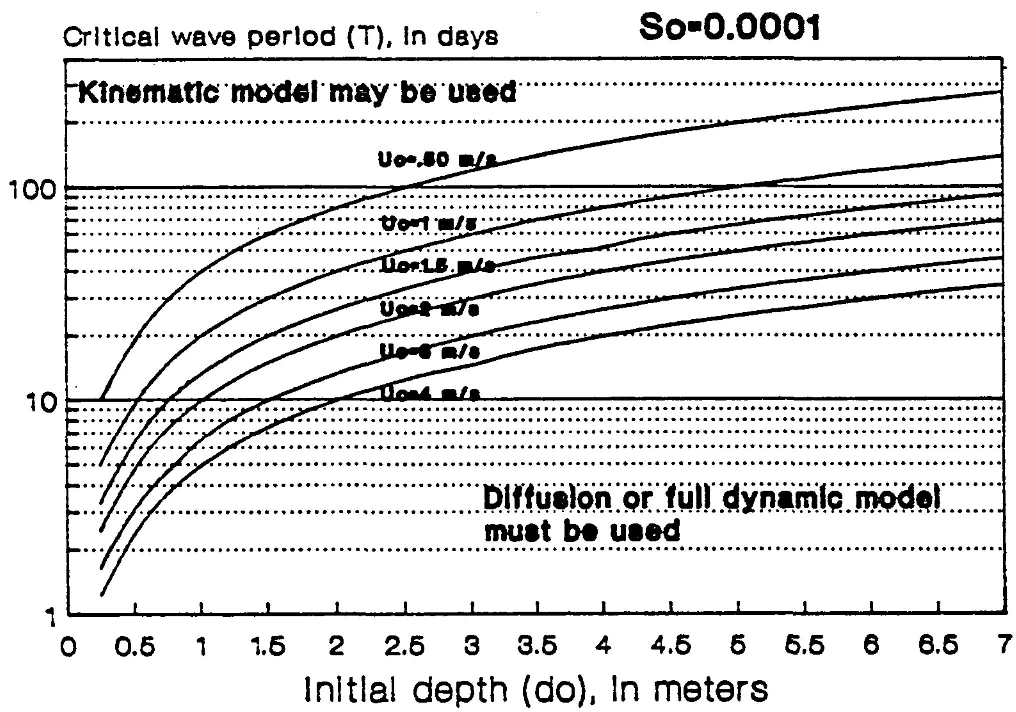

Figure 82. Kinematic model applicability criteria (S_o = 0,0001)

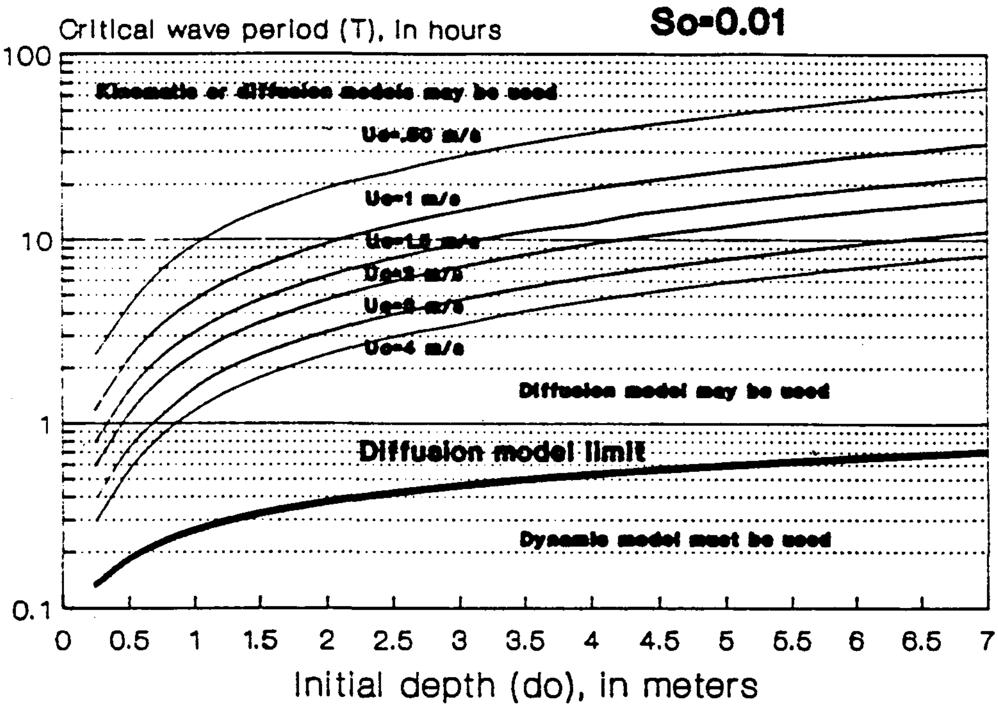

Figure 83. Applicability criteria (S_o = 0,01)

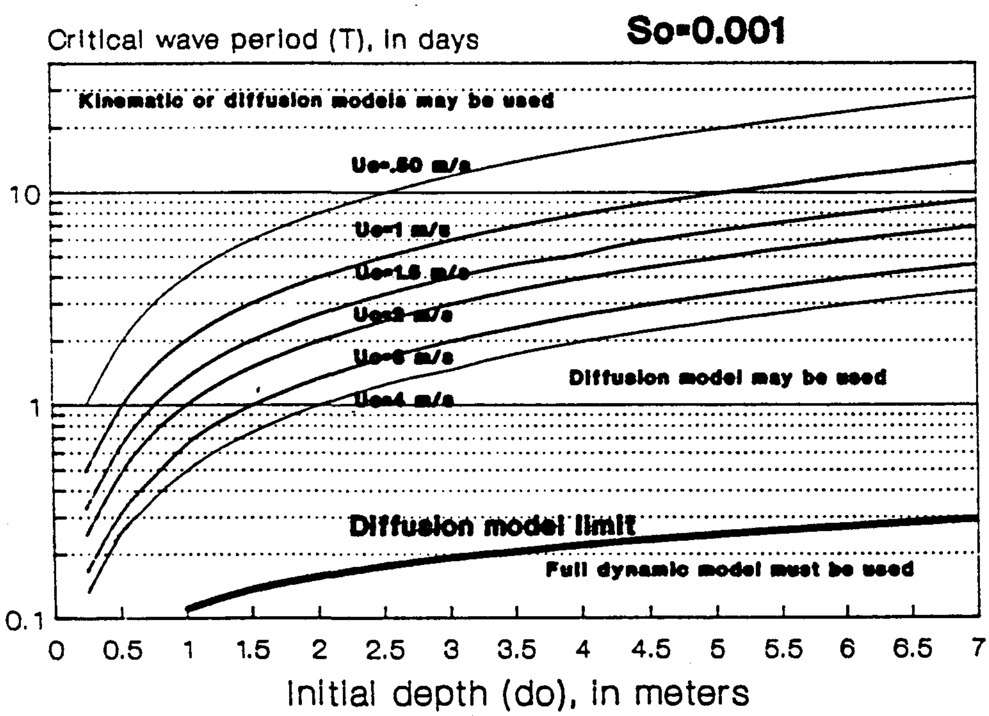

Figure 84. Applicability criteria (S_o = 0,001)

7.5 PARAMETRIC STUDY OF FLOOD-WAVE SUBSIDENCE

The validity of the developed applicability criteria is limited by the restrictive assumptions used in their formulation. For instance, the linearized equations have been derived by neglecting second order terms. In order to obtain a generalised picture of the damping of a flood wave in a prismatic channel and the applicability of equations (7.47) and (7.49) it would be better to investigate the subsidence of a range of waves, using the unsteady flow simulation model and to compare the results with the developed criteria.

Different flood hydrographs were routed in a prismatic channel with a slope of 0,001, width of 40 m and an initial depth of 2 m. From equations (7.47) and (7.49) the following criteria apply:

- The kinematic model is applicable for wave durations:

  $T_w > 2{,}52$ days.

- The diffusion model is applicable for wave durations:

  $T_w > 3{,}76$ hours.

Natural hydrographs cannot in most cases be represented by a small sinuisoidal perturbation. It is interesting to ascertain whether the criteria holds for hydrographs of different shapes and magnitudes. Referring to chapter 4, the solution of the difference equations will never be exactly the same as the full analytical solution of the differential equations. The truncations of the terms introduce an error, which will depend on the chosen time and length steps (Δx, Δt).

Bearing in mind that generally the smaller the time-step and point spacing chosen, the better the approximation to the correct solution of the differential equation and the more nearly correct the wave celerities produced will be, in all the simulations the spacing was kept small (100 m to 500 m) and the time-step in the order of minutes.

In practice, when a flood routing program is used for prediction purposes, or for the calculation of flood lines, the upstream hydrograph will probably be a synthetic flowrate hydrograph generated by an overland flow routing program such as WITWAT (Kolovopoulos, 1986); SWMM (Huber et al., 1982) etc. Synthetic flowrate hydrographs were generated using:

$$Q(t)= Q_b + Q_{amp}(t/T_p \exp(1-t/T_p))^{\beta} \tag{7.50}$$

where

β : is a constant taken as 16 (characteristics of of runoff hydrographs in the study region)

Q_b : is the base flow

Q_b+Q_{amp} : peak discharge for the flood

T_p : time to peak of the flood

For waves of a shape other than sinuisoidal, the wave period is approximated by the wave duration. For the given channel the importance of three wave parameters is investigated:

- Wave duration (T_w)
- Wave magnitude (Q_p)
- Time to peak (T_p)

The hydrographs were routed over a distance of 100 km. Different runs were performed depending on the distance in order to improve the accuracy. For routing over 2 km, Δx was taken as 200 m; over 20 km routing Δx was taken as 500 m; and for 100 km Δx=1km. Typical results of the modification of stage and discharge hydrographs are presented in Figures 85 and 86. The hydrographs are plotted for a duration of an inflow hydrograph of 4 hours.

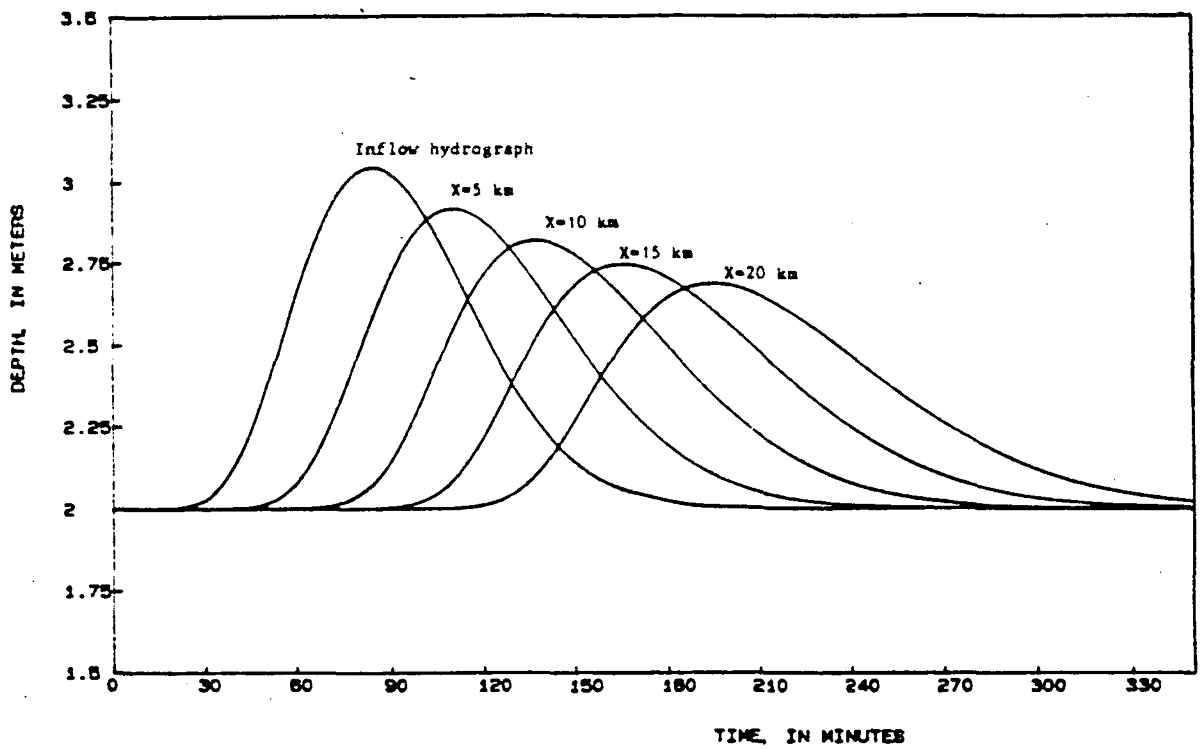

Figure 85. Subsidence of depth hydrograph with distance

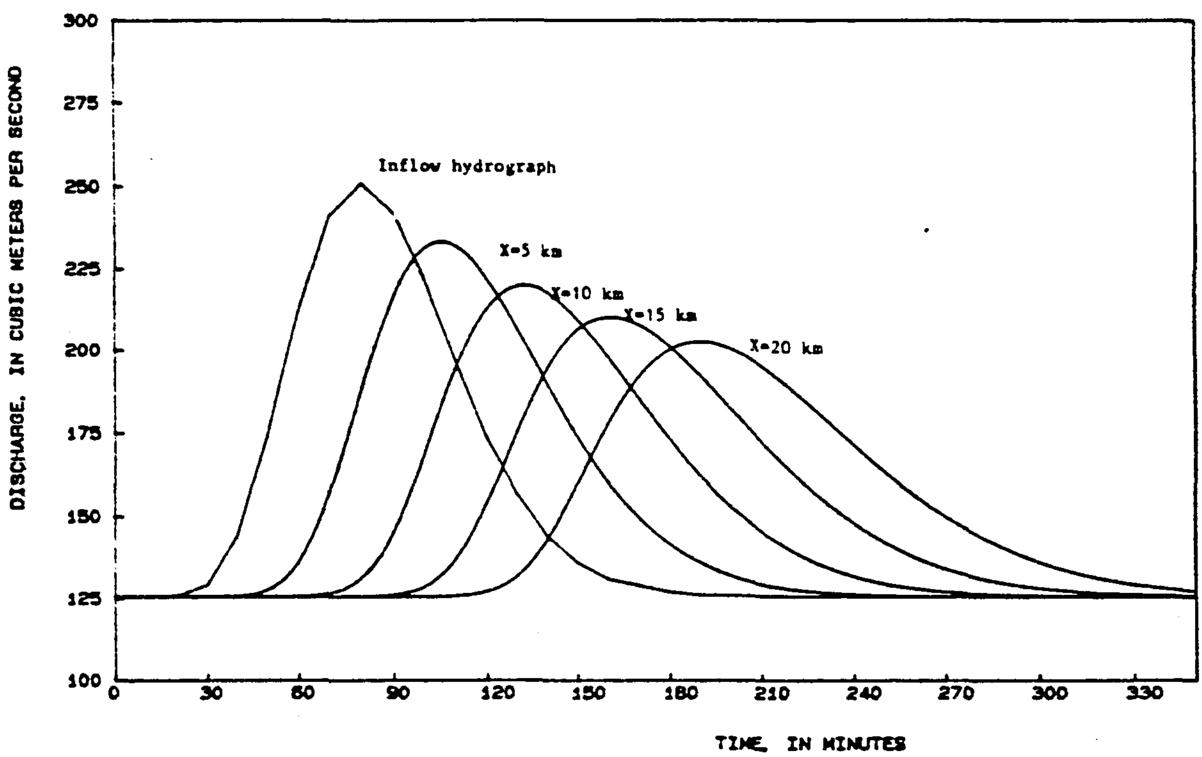

Figure 86. Subsidence of discharge hydrograph with distance

It is seen that there can be a significant subsidence of the wave with distance, which was observed in varying degrees for the majority of the cases.

7.5.1 EFFECT OF WAVE DURATION ON SUBSIDENCE

The variation of depth and flowrate with distance, for different T_w values, are presented in Figures 87 and 88 respectively. The results verify the small perturbation analysis, which states that the wave period has a pronounced effect on the subsidence rate. The wave amplitude subsides to 98% of the original amplitude at X=20km, for T_w=2 days, while the corresponding value is 62% for T_w= 2 hours. The rate of subsidence is very large in the initial reaches for low T_w values and the subsidence rate decreases only after the base hydrograph has spread significantly at a sufficiently remote downstream location thereby increasing the local wave duration.

Mozayeny and Song (1969) reported an exponential decay for the wave amplitude with distance. The present study shows that subsidence in the initial reaches is given by an exponential relationship such as:

$$Y = e^{-kx} \tag{7.51}$$

However, as the wave form is modified with distance, a constant exponent does not adequately describe the subsidence rate for the entire reach. The restrictive criteria of the small perturbation theory do not correspond exactly to the computed results. For the reference length L_o= 2 km, the error in the subsidence using the kinematic model was less than 5%, for a wave duration larger than 1 day. This difference cannot be entirely attributed to the very restrictive criteria but is also a result

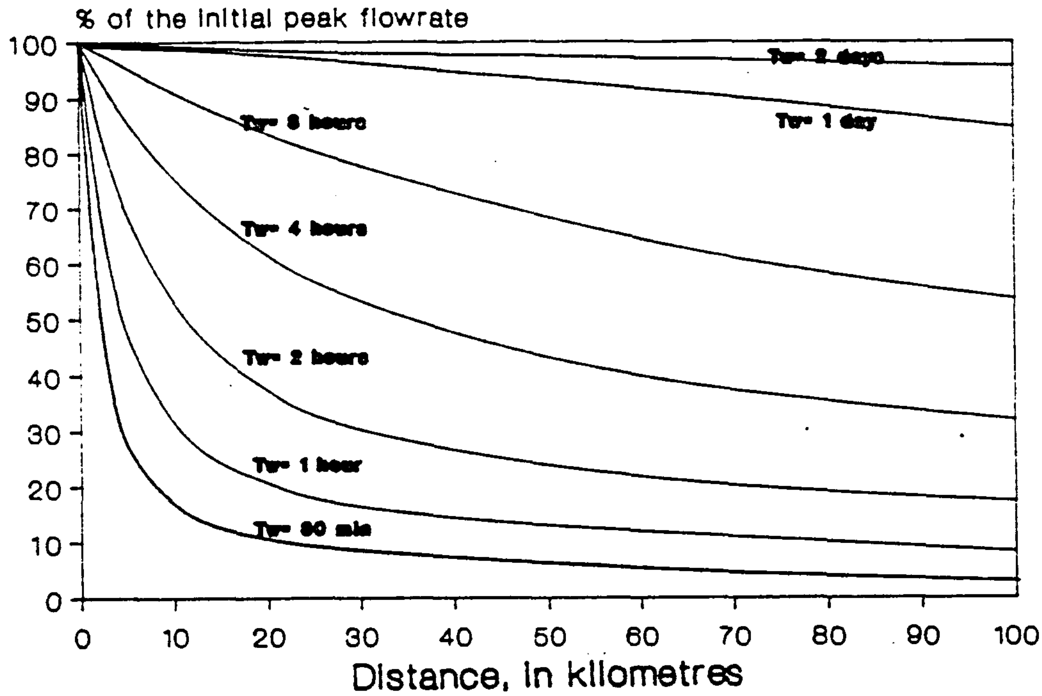

Figure 87. Effect of the wave duration on the peak flowrate subsidence

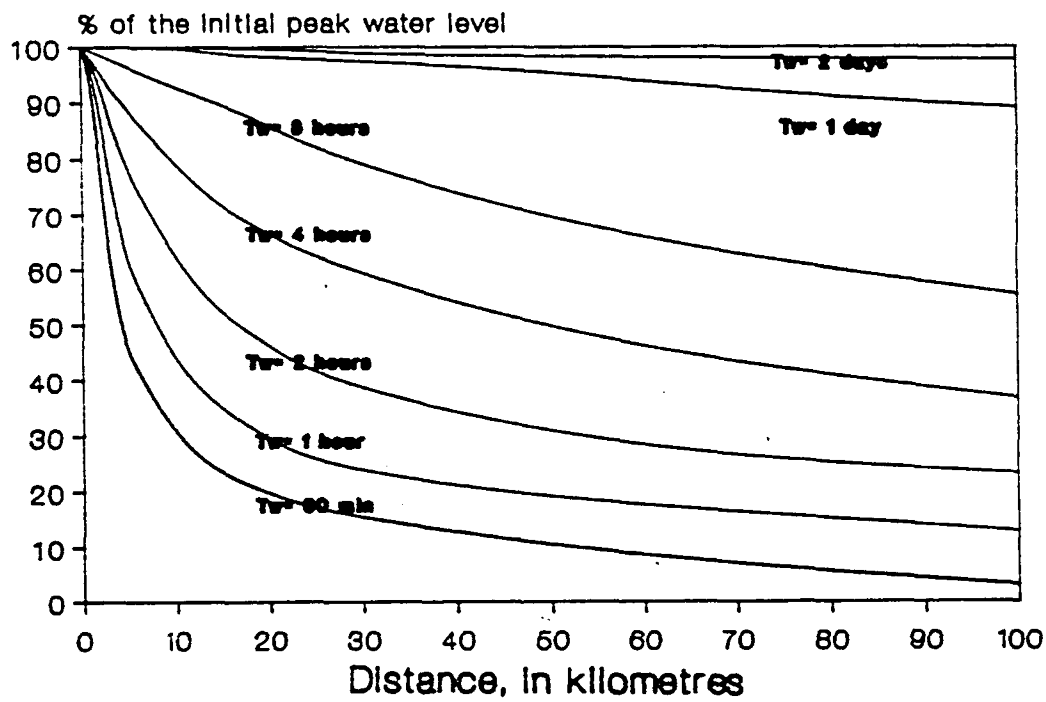

Figure 88. Effect of the wave duration on the peak water level subsidence

of the numerical solution. The truncation errors may mask the non-diffusive character of the analytical solution of the kinematic wave. The result is that the numerical solution of the kinematic wave may resemble the analytical solution of the full dynamic model, further complicating the modelling process (Ponce et al., 1978). The diffusive model gave an error of less than 5% compared to the full dynamic model for wave durations up to 2,5 hours. For durations less than 2,5 hours, instabilities appeared and the θ value was raised to 1 in order to dampen the instabilities. This suggests that, in practice, the diffusion model is applicable for a very wide range of wave durations, without loss of accuracy. When the diffusion model cannot be applied (acceleration terms become significant) the modeller is made aware of the instabilities in the solution.

7.5.2 EFFECT OF THE WAVE AMPLITUDE ON SUBSIDENCE

The subsidence of the water level peak is shown in Figure 89. The wave amplitude has only a minor effect on the wave subsidence when compared to the wave duration parameter. However, Figure 89 clearly indicates that subsidence is reduced for higher wave amplitudes. The wave amplitude at 20 km distance is 34 % and 30 % of the initial wave amplitude, for $Q_p = 2Q_o$ and $Q_p = 10Q_o$, respectively. This effect is not predicted by the small perturbation analysis because it is based on the linearized equations.

The effect of the wave amplitude on the flowrate peak is not plotted, as the difference in the reduction of the peak discharge for different wave amplitudes is very small, and the results after a distance are practically identical. The results confirm the nonlinearity of the subsidence phenomenon. This nonlinearity is more evident in the water level subsidence.

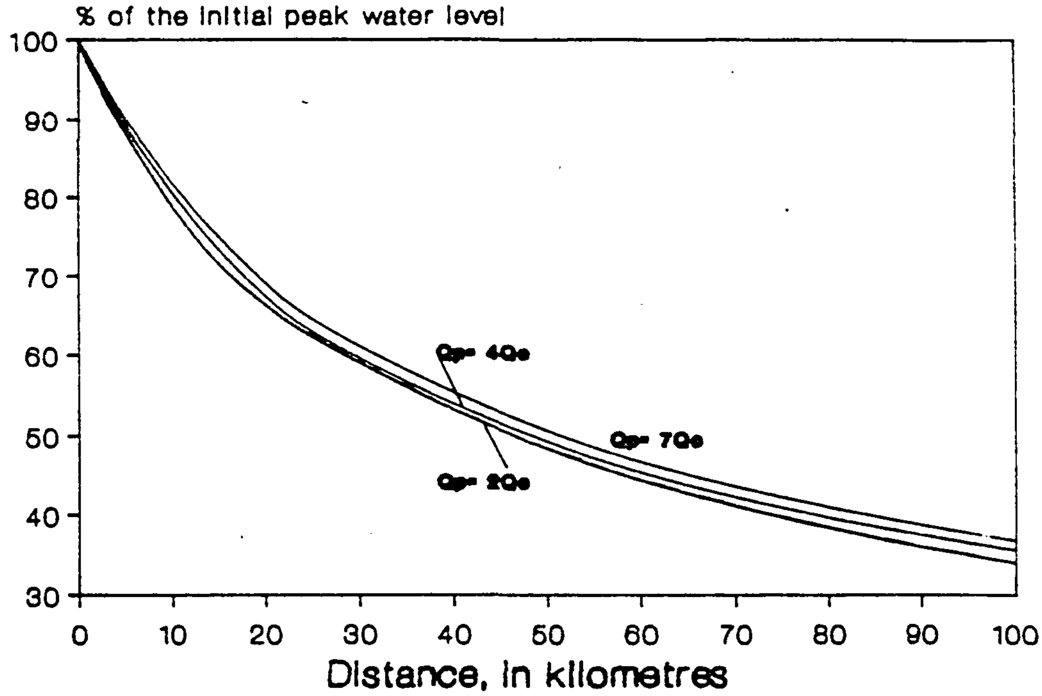

Figure 89. Effect of the wave amplitude on the peak water level subsidence

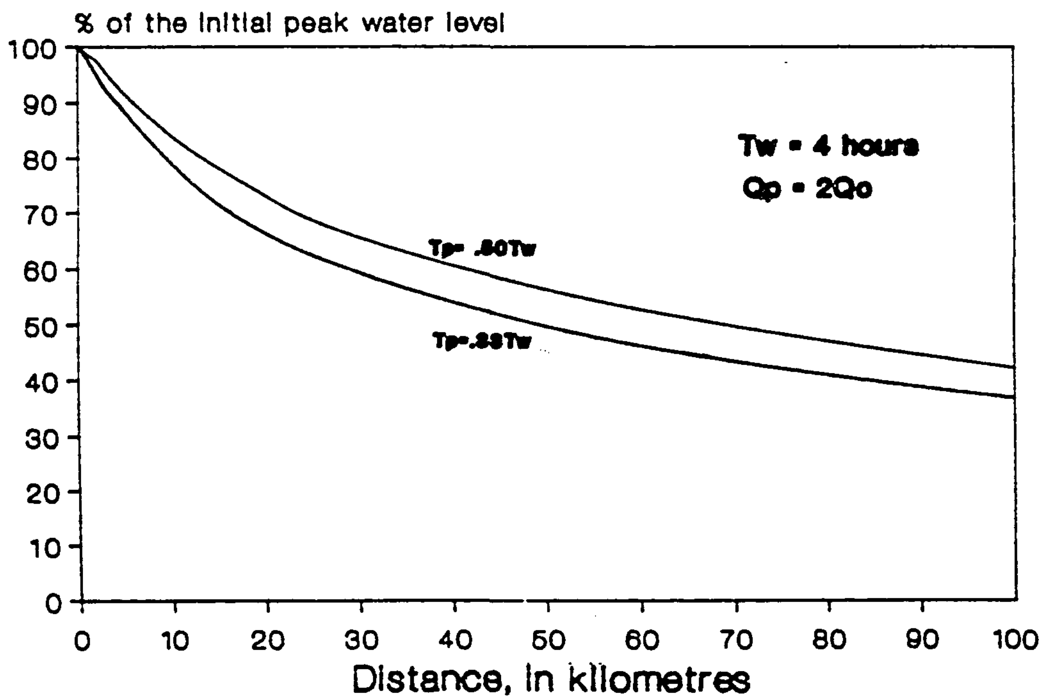

Figure 90. Effect of the time to peak on the peak water level subsidence

7.5.3 EFFECT OF THE TIME TO PEAK ON SUBSIDENCE

The graph in Figure 90 indicates that for the same wave duration and amplitude, slower rising waves have less subsidence than fast rising waves. Shorter time to peak is represented as an increase in the variation in intensity of the discharge on the rising limb of the hydrograph, as measured by the ratio $\Delta Q/\Delta t$. Numerical experiments using artificial upstream releases (Ivanova, 1967) have shown that the increase in the discharge variation intensity, tends to dampen the flood peak and increase the 'unsteadiness of the flow' as measured by the persistence and enlargement of the loop-rating curve.

7.5.4 EFFECT OF THE CHANNEL SLOPE ON SUBSIDENCE

All the developed theories identify the slope S_o as the critical channel parameter which effects flood subsidence. To verify this, floods were routed through a channel of changing slope. The results are shown in Figure 91. A flood with duration T_w of 1 day moves basically kinematically in a channel of slope S_o=0,001. After 20 km the reduction in the peak water level is less than 5%. The same flood, routed in a channel of slope S_o=0,0001 has a reduction of the peak water level of more than 40%.

Henderson (1966) states that the flood waves will be kinematic in rivers that are sufficiently steep. Steep slopes correspond also to overland flow, therefore most overland flow problems can be modelled as kinematic flow.

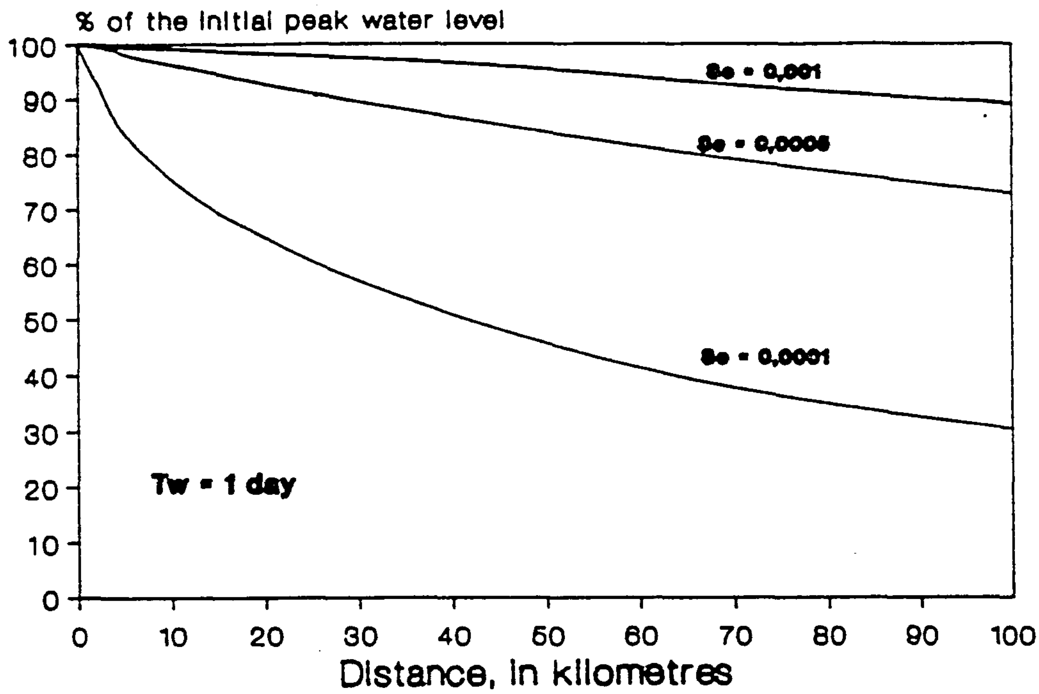

Figure 91. Effect of the channel slope on the peak water level subsidence

---

7.5.5 DISCUSSION OF RESULTS

The parametric study has shown the very strong dissipative characteristics of the dynamic waves. The dynamic waves are primarily manifested by the interrelation of the wave period and the bed slope. Thus, for mild channel slopes, the period has to be very long for the kinematic model to apply. The steeper the slope, the shorter the period required to satisfy the kinematic flow assumption.

Channel slopes of 0,001 and 0,0001 (which were used in the study of subsidence) produced theoretical wave duration limits of 2,52 and 80 days, respectively. In practice, the kinematic (and diffusive) models can be applied for a much wider spectrum of wave durations depending on the model used and the damping effect of the numerical solution.

The following conclusions are derived from the analysis:

- The approximation model applicability criteria, are a valuable indicator for the modeller to predict the wave subsidence in prismatic channels.

- The criteria should not be followed strictly, as, in modelling, the truncation errors mask the correct analytical solution and:

  - The kinematic model is applicable for a wider range of wave durations than suggested by equation (7.46).
  - The diffusion model is adequate for most practical applications and wave durations. In most cases the modeller is made aware of the inapplicability of the model by the instabilities in the generated solution.

- Wave duration is the critical parameter for the wave's subsidence.

- Inflow wave amplitude has a minor influence on subsidence, with lower amplitudes giving slightly higher subsidence. This is attributed to the nonlinearity of the subsidence phenomenon.

- The channel slope has a marked effect on subsidence with steeper slopes requiring shorter periods to satisfy the kinematic assumption.

- Slower rising hydrographs have less subsidence compared with rapidly rising hydrographs.

8.0 FLOOD ROUTING IN COMPOUND CHANNELS

8.1 INTRODUCTION

Flood routing in natural rivers is complicated by the large differences in geometric and hydraulic characteristics between the river channel and the flood plains. The flood plain is defined as the land area adjoining a river, stream, bay or lake, which is likely to be flooded during times of high water. The cross-section of a typical compound channel is formed by a deep water bed with natural levees usually on both sides (Figure 92).

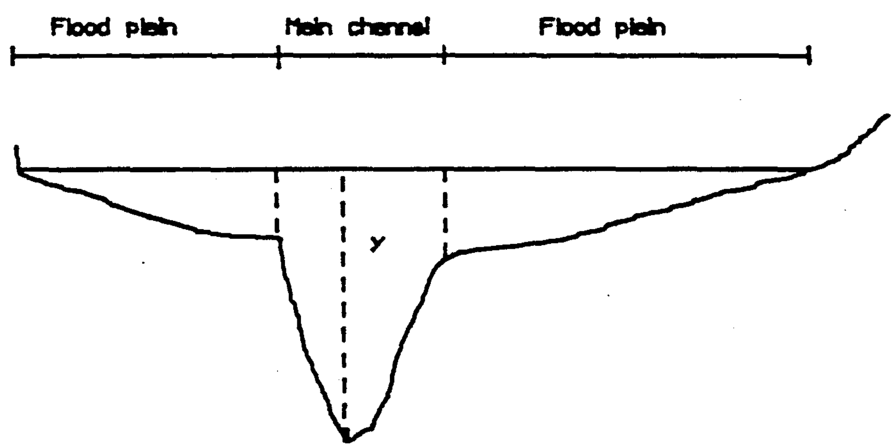

Figure 92. Typical compound channel

In the case of rivers with flood plains, when the depth of flow exceeds the depth of the main channel, the flood plains carry a proportion of the total discharge. In analysing the flow through open channels of regular sections, it is sufficient, in general, to calculate the total conveyance as outlined in chapter 2, and to use the overall hydraulic radius as the parameter which characterises the properties of the cross-section. However, flood routing in compound channels introduces many complications such as:

- The meandering of the main channel within the flood plain, which causes a portion of the total flow to "short-circuit" and proceed downstream along the more direct course afforded by the flood plain rather than along the more circuitous route of the meandering channel.

- Complexities are created by portions of the flood plain which act as dead storage areas, where the flow is usually negligible.

- Lateral flow can be appreciable.

- The interaction of the flows and the momentum transfer in the main channel and the flood plain.

Various techniques have been adopted by previous researchers to account for these complexities. However, in the literature it is evident that the one-dimensional models proposed, for the most part, allow poorly or inadequately for the majority of the complexities and ignore completely the momentum transfer mechanism. This is due to the lack of adequate experimental data in the seventies used to develop models able to describe such a complex process. As Knight and Demetriou (1983) stated: "the knowledge concerning the transfer of momentum is limited and the distribution of boundary shear stresses in complex cross-sections is poorly understood. This is surprising considering the many practical situations in which the natural cross-section is irregular in shape". As the literature survey in the next section shows, only during the last 5 years have researchers proposed equations based on flume data that account for the phenomenon under steady-state conditions.

The most flood-routing programs are based on the "off-channel storage" approach. This method assumes that the flood plain contributes only to storage, conveying virtually no discharge. The "off-channel storage" method is the most commonly used in unsteady flow modelling in rivers and channels, e.g. Ligget and Cunge, 1975; Baltzer and Lai, 1968; Cunge et al., 1981. If the velocity in the berms is relatively high, it is important to know the significance of the dynamic effect of the berm flow when modelling the river stage and discharge.

Another commonly used and expedient method of calculating the discharge in a compound channel is the "separate-channel" method, is based on splitting the cross-section into hydraulically homogeneous subdivisions. The conveyances for each subdivision are then calculated individually and summed to give the overall section discharge.

Both approaches can lead to considerable errors as none of these methods makes allowance for the interaction mechanism between a deep channel and its flood plain. As a result, no satisfactory rational basis is available for the analysis and design of complex channels, especially when shear distribution and flow resistance is considered. This is important since most natural channels and rivers are of complex cross-section rather than a simple one.

In this chapter the available techniques for the modelling of the unsteady flow in compound channels are examined, with emphasis on:

- The evaluation of the dynamic effect of the flood plain flow.
- The modelling of the momentum transferred between main channel and flood plain.

As a result of the analysis, the range of applicability of the existing flood routing models is defined and a new model for the accurate routing of floods in compound channels has been developed.

8.2 BACKGROUND

When the flow in a river channel is above the bank full stage mark and the adjacent flood plain areas are inundated, it is almost certain that the velocity on the flood plain will be considerably lower than that in the main channel. This is caused by the lower depth of flow on the flood plain and the often greater hydraulic roughness of the flood plain than of the channel. The velocity difference inevitably results in turbulence in the main channel/flood plain zone, which takes the form of a bank of vortices (Figure 93). This is referred to as the **turbulence phenomenon.**

The turbulence will cause the transport of the (longitudinal) momentum to the flood plain and the vertical plane between the main channel and flood plain will experience appreciable (turbulent) shear stress in the longitudinal (or flow) direction. These longitudinal shear stresses are referred to as **apparent shear stresses** (Figure 93). The shear stresses arising in the interface zone create energy losses which result in a net reduction of the discharge carrying capacity of a compound channel.

The momentum transfer mechanism was first examined by researchers over two decades ago but until recently no satisfactory models were proposed. Zheleznyakov (1966) was the first to be able to show that the flow in compound channels is mainly dominated by an intensive momentum exchange between the main channel and the

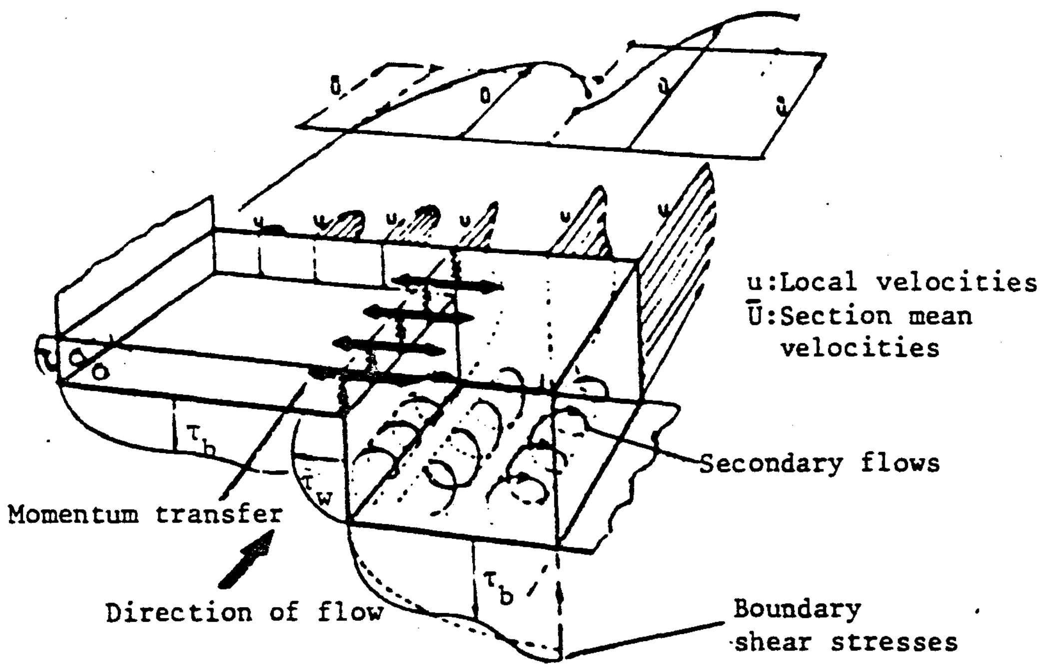

Figure 93. Momentum transfer mechanism in compound channels (Knight and Hamed, 1984)

adjoining shallow flood plain zones. He called the phenomenon the "**kinematic effect**", and demonstrated under laboratory conditions the effects of the mechanism in decreasing the overall rate of discharge for flood plain depths just above bank full. He showed that as the flood plain depth increased, the importance of the phenomenon diminished. Zheleznyakov also carried out field experiments which confirmed the significance of the momentum transfer phenomenon in the calculation of the overall discharge. Barishnikov and Ivanov (1971) reached similar conclusions and found a reduction in the section discharge capacity of up to 16%, due to the momentum transfer effect.

Sellin (1964) conducted flume experiments on a symmetrical compound section, and confirmed the presence of the "kinematic effect", photographing the vortices at the interface between the main channel and the flood plain. Sellin found that at the bank full stage a discontinuity exists on the rating-curve for a compound channel. He studied the transition region and concluded that a sharp increase in flow resistance occurs when the flood plain is inundated. He further found that for low flow depths on the flood plain (16% of the bank full channel depth), the discharge of the compound section can be appreciably less (30%) than the sum of the discharges obtained by introducing a smooth vertical wall at the interface.

Wright and Carstens (1970) analysed the case of a transversely horizontal flood plain, with flood plain depths 0,50 times the channel depth at bank full stage and larger. They found that the separate channel method gives results which compare favourably with the calculation of total discharge from their experiments, but gives segment discharges that are up to 10% in error. They suggested that an effective shear stress equivalent to the mean shear stress in the channel, be introduced over the entire vertical segment of fluid boundaries, to resist the flow in the channel and to propel the flow in the flood plain.

Yen and Overton (1973), plotted velocity distribution in an experimental compound channel and flood plain. Typical plots are shown in Figure 94, from which it may be seen that the interaction between channel and flood plain flows result in a distorted velocity pattern near the segment boundaries. They argued that there were planes of zero shear stress, represented by the dotted lines in Figure 94, rather than vertical segment boundaries, as suggested by Posey (1967).

Townsend (1968) performed his experiments in a channel with a single flood plain and studied the longitudinal and transverse characteristics of the flow. His results highlighted the tendency of the turbulence at the interface to disperse laterally across the flood plain. This illustrated the ability of the series of vortices present in the mixing zone to transport the finer

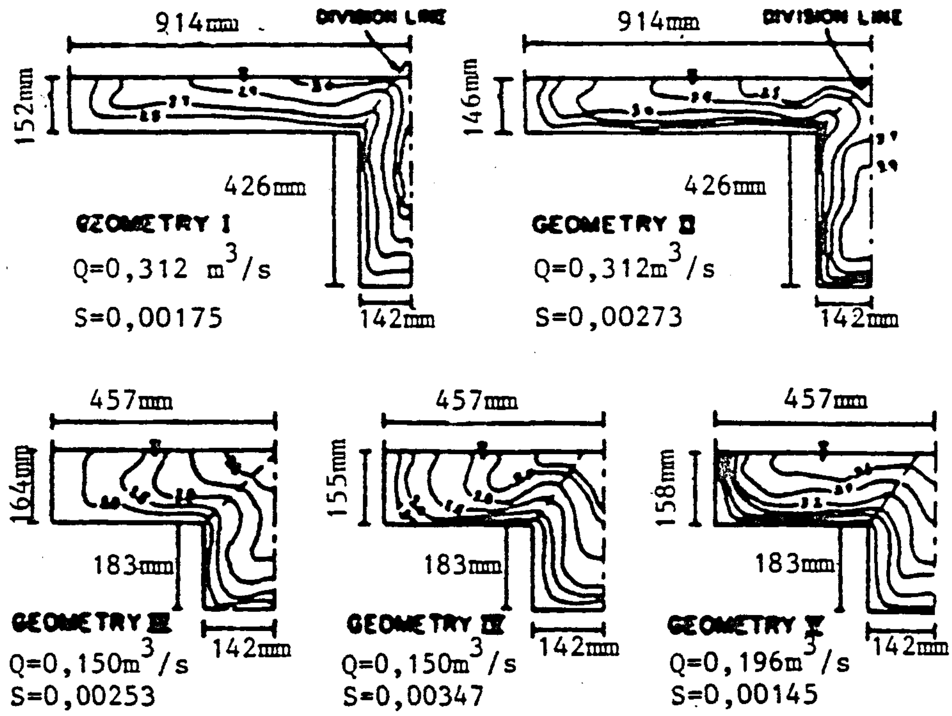

Figure 94. Velocity contours in compound channels (Yen et al., 1973)

sediment fractions from the fast flowing deep channel of the rivers on to the flood plains in times of flooding.

Ghosh and Jena (1971), measured boundary shear but they did not analyse the relative distribution of discharge. Myers (1973), also measured shear stresses in complex and simple channels. The results showed a decrease (up to 22%) in channel shear and an increase (by 260%), in flood plain shear. Their work was compared with that of Ghosh and Jena and a trend in shear stresses was detected.

Radojkovic (1976) described the turbulence phenomenon as a transfer of energy from the main channel, with a region of high velocity and hence high energy, to the flood plain, a region of low velocity and energy. In the process some of the energy taken from the main channel is dissipated through the turbulent eddies in the vicinity of the interface. The remaining energy is transferred to the flood plain. The energy lost from the main channel results in a reduction in the carrying capacity of the main channel; the energy transferred to the flood plain slightly increases its carrying capacity; the net effect is a reduction in the carrying capacity of the compound channel, due to the energy loss in the turbulent eddies.

As a result of work over the last decade, there is now an increased understanding of the physical processes dominating the flow in compound channels. Wormleaton et al. (1982) performed a series of laboratory tests in compound channels and used their data to derive a statistical relationship between the apparent shear stress on the vertical interface and several easily calculated parameters of the channel geometry and hydraulic characteristics. The accuracies of different methods of discharge were shown to be dependent upon the assumptions they make regarding the magnitude of the apparent shear stress on the particular interface chosen. Knight et al. (1983) after flume studies, presented equations giving the shear force of the flood plains as a percentage of the total shear force in terms of dimensionless parameters. They found that the division of flow based on linear proportions of the areas is shown to be inadequate on account of the interaction between the flood plain and main channel flows.

Prinos et al. (1985), examined in a laboratory study the turbulence for both "wide" and "narrow" channel conditions. They found that both longitudinal and vertical turbulence intensities were significantly higher in the mixing regions than their respective values in the central region of the main channel flow. In general, the mixing zone's longitudinal and vertical turbulence intensities were found to increase with an increase in the relative boundary roughness parameter for the compound section.

Myers (1987), based on theoretical considerations and flume experiments showed that the ratios of main channel velocity and discharge to flood plain values in a compound channel are independent of bed slope and are influenced only by depth and geometry. He also found that the ratios of channel velocity and discharge, to those of the flood plains follow straight line relationships with depth.

The following facts emerged from the investigation:

- There is an almost complete lack of field measurements with which to check scale effects in the model tests. Most of the model tests were associated with cross-sections for which the ratio of width to depth of channel was in the range 1:2 to 4:1; none could be located which were related to ratios larger than 4:1 whereas natural channels often display ratios of 10:1 or larger.

- Under certain conditions the conventional methods of discharge calculation in compound channels may underestimate or overestimate discharge capacity. This is largely due to conventional discharge estimation methods which do not account for the apparent shear stress occurring at the main channel flood plain interface. It has been shown convincingly that failure to allow for the existence of such mechanisms may result in erroneous channel analysis.

- Many different formulae and methods have been proposed but all of them have been developed and tested under steady state conditions. Therefore, the experiments mentioned, although leading to some highly interesting conclusions related to the problem of channel interaction, do not permit general conclusions to be drawn, especially for the much more complex conditions of unsteady flow.

8.3 APPARENT SHEAR STRESS

One of the broad objectives of research in channels of complex sections is to identify the factors or parameters influencing its resistance. Toebes and Sooky (1967), demonstrated that the overall friction factor in a channel with flood plains is higher than normal values. This difference in the friction factor, is caused by additional losses due to interaction of the main channel flow with that of the flood plain. It has been established that negligence of such a loss term, introduces considerable errors in the estimation of channel resistance.

Apart from relationships that Toebes and Sooky (1967) proposed, Ghosh (1973) showed that it is possible to compute the interaction loss parameter from the overall, flood plain and main channel mean shear values. This appears reasonable as shear drag and channel resistance are interrelated. In the analysis that follows, and in the assessment of the discharge computation methods, the geometric parameters that are used are defined as follows (Figure 95):

W_c = width of the main channel
W_f = width of the flood plain
A_c = area of the main channel
A_f = area of the flood plain
P_c = wetted perimeter of the main channel
$= W_c+h$
P_f = wetted perimeter of the flood plain
$= W_f+h$
A_T = the total cross-sectional area of flow
S_0 = the bed slope of the channel

For any regular prismatic channel under uniform flow conditions, the total retarding shear force acting upon the wetted perimeter is equal to the component of the gravity force in the direction

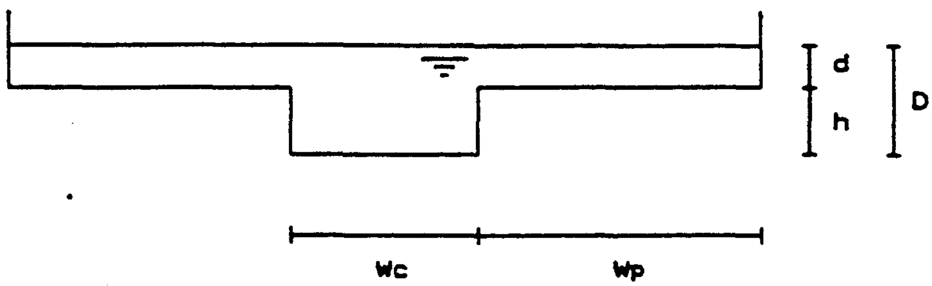

Figure 95. Definition sketch

of the flow. The gravity force component over a unit length of channel is given by (Figure 96):

$$F_g = W\sin\theta = \gamma A_T S_0 \tag{8.1}$$

in which

W = the weight of fluid per unit length of channel

γ = unit weight of water

For a typical compound channel, the boundary shear force per unit length is given by:

$$F_b = \tau_c P_c + \tau_f P_f \tag{8.2}$$

in which

τ_c & τ_f = the average boundary shear stresses for the channel and flood plain solid boundaries, respectively.

P_c & P_f = channel and flood plain wetted perimeters.

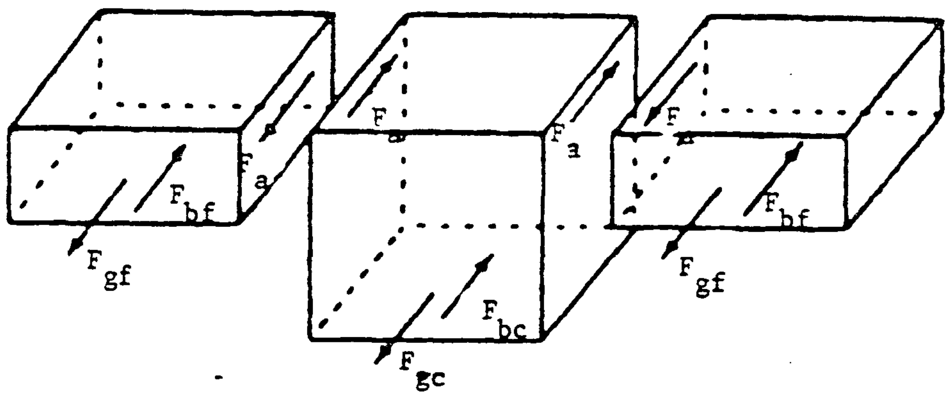

Figure 96. View of compound section showing forces acting on subdivisions

Equations (8.1) and (8.2) must be in overall equilibrium for any compound section. Moreover, the equilibrium between boundary shear and gravity forces must hold for any subdivision of the compound channel, as in Figure 96. In the case of these subdivisions, however, a part of the boundary shear force is provided by the force acting upon the interface between the adjacent subdivisions. This force, F_a, was termed the **apparent shear force** by Myers (1978) and Toebes and Sooky (1967). In the case of the main channel subdivision, the total retarding force per unit length may be written as:

$$F_{sc} = \tau_c P_c + \tau_{ai} P_{ai} = F_{bc} + 2F_a \tag{8.3}$$

where

τ_{ai} = the apparent shear stress acting upon the assumed interface(i)

P_{ai} = total length of the interface(i)

F_{bc} = the main channel solid boundary shear force.

The apparent shear stress on the interface between the main channel and the flood plain, τ_{ai}, is generally considered to be an indicator of the level of turbulence intensity. Equating the shear force F_{sc} given in equation (8.3) with the gravity force component in the main channel subdivision, F_{gc}, and rearranging, the following expression for the apparent shear stress is obtained (Wormleaton et al., 1982):

$$\tau_{ai} = \frac{1}{P_{ai}} (\gamma A_{ci} S_0 - \tau_c P_c) \tag{8.4}$$

The value of the average boundary shear stress in the channel, τ_c, must be obtained by measurement and integration of the boundary shear stresses at points around the channels wetted perimeter. Prinos et al. (1985) examined the structure of the turbulence in a laboratory study. They concluded that the apparent shear stress increases as the flood plain is approached. The mixing zone's longitudinal and vertical turbulence intensities were found to increase with an increase in the relative boundary roughness parameter for the compound section. The intensities were also found to increase with a decrease in the relative depth parameter. In both cases this was due to the higher cross-stream velocity gradients generated in the mixing zones.

The distribution of the shear stress is shown in Figure 97. In the main channel, shear stresses τ_0 decrease from a maximum value (τ_{om}) as the channel side wall and junction region are approached, and then increase in that part of the flood plain zone adjacent to the junction, as well as close to the bed of the flood plain. After reaching their maxima ($\tau_{oj}=\tau_{cj}$), the shear stresses continue to decrease with increasing distance into the flood plain zone from the junction, to approach an undisturbed value of $\tau_{0\infty}$.

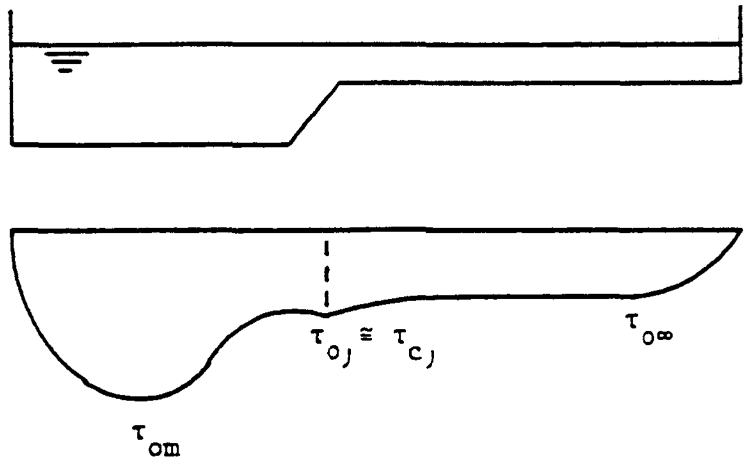

Figure 97. Cross-stream distribution of longitudinal shear stress

The ratio of the apparent shear stress (τ_a) and undisturbed value of flood plain stress ($\tau_{0\infty}$), namely $\tau_a/\tau_{0\infty}$ is referred to as the **relative apparent shear stress** and abbreviated to τ_r .

The relative apparent shear stress (τ_r) is a dimensionless form of the apparent shear stress and can be thought of as representing the intensity of vorticity in the mixing region. It normally ranges between 0 to 6, but it can reach values as high as 40 for very high levels of turbulence. Most of the methods of discharge computation examined in this chapter require the knowledge of the apparent shear stress (τ_a) or ratio (τ_r).

Many researchers have developed models for the prediction of the apparent shear stress. The first attempt was made by Rajaratnam et al. (1981) who proposed a very simplistic equation of the form:

$$\tau_r = 0,15(D/d - 1)^2 \qquad (8.5)$$

However, recent research has showed that the intensity of the turbulence is influenced by many factors, such as:

- **Flow depth:** represented by the ratio d/D

- **Bed roughness:** The rougher the flood plain bed is relative to the main channel, the lower is the average flood plain velocity relative to that in the main channel, and the higher is the turbulence intensity at a given flow depth.

- **Geometry:** This is described by the widths of the main channel and flood plains and the slope of the main channel bank.

Wormleaton et al. (1982) performed laboratory studies, carried out a statistical regression analysis on observed data and developed the following equation for the prediction of the apparent shear stress:

$$\tau_a = 13{,}84\ (\Delta V)^{0{,}882}\ (D/h)^{-3.123}\ (W_f/W_c)^{-0{,}77} \qquad (8.6)$$

where

ΔV = difference in average velocity between main channel and flood plain (m/s)

τ_a is in N/m2

Dividing equation (8.6) by γdS_0, the relative apparent shear stress is found to be:

$$\tau_r = (0{,}001412/dS_0)(\Delta V)^{0{,}882}(1-d/D)^{3{,}123}(W_f/W_c)^{-0{,}727} \qquad (8.7)$$

Prinos et al. (1985) following a similar procedure developed the following equation:

$$\tau_a = 0{,}874\ (\Delta V)^{0{,}92}\ (d/D)^{-1{,}129}\ (W_f/W_c)^{-0{,}514} \qquad (8.8)$$

where

τ_a is in N/m2

or in dimensionless form equation (8.8) may be rewritten as:

$$\tau_r = (1/11213dS_0)(\Delta V)^{0,92}(d/D)^{-1,129}(W_f/W_c)^{-0,514} \qquad (8.9)$$

Prinos et al. found this equation to give good results over a wide range of flow conditions. They used data with various geometries and roughnesses, some asymmetrical and some symmetrical, with both rectangular and trapezoidal main channel section.

Equations (8.6) and (8.8) were evaluated with the set of data of Wormleaton et al. (1982) and Knight et al. (1983). A major problem in assessing the two equations was the definition of ΔV. Wormleaton et al. found that there is a very strong correlation between τ_r and ΔV. They did not, however, indicate how ΔV is initially obtained for use in equation (8.9). The comparison of the two equations was made assuming that the difference in the velocity, ΔV, is calculated using the most common method, the vertical interface method, as outlined in this chapter. The results are shown in Figures 98 and 99.

The Prinos equation predicted τ_r in most cases with the smallest error. The performance of the Wormleaton equation was not adequate as in most cases the apparent shear stress was overestimated. Since τ_r is proportional to (ΔV) raised to the power of some constant, over-estimation of τ_r corresponds to values of ΔV that are too high, i.e. unrealistically high channel velocities or low flood plain velocities. Both equations performed better with the Wormleaton et al. (1982) set of data, than with the data of Knight et al. (1983). The equations performed very poorly and overestimated (by more than 100%) the apparent shear stress for the first 8 experiments of Knight et al. (1983). Thus for a width of flood plain smaller than the width of the main channel W_c/W_f=0,152/0,76. This indicates that for flood plain widths less than the width of the main channel, the proposed equations may not be valid. The results of the Prinos equations were very good particularly for values of measured apparent shear stress, in the range of 1 to 6. This suggests that for values out of this range a different approach might have to be adopted. The Prinos equation has the following additional advantages:

- It can account for main channels with sloping banks.

- It has been developed from more comprehensive data sets than the Wormleaton equation, incorporating roughened flood plains, and both symmetrical and asymmetrical sections.

Therefore, for the assessment of the discharge computation methods and the development of a flood routing model, the Prinos equation has been used. However, in order for the model to be applicable in all cases, it will be modified to account for values of τ_r larger than 6.

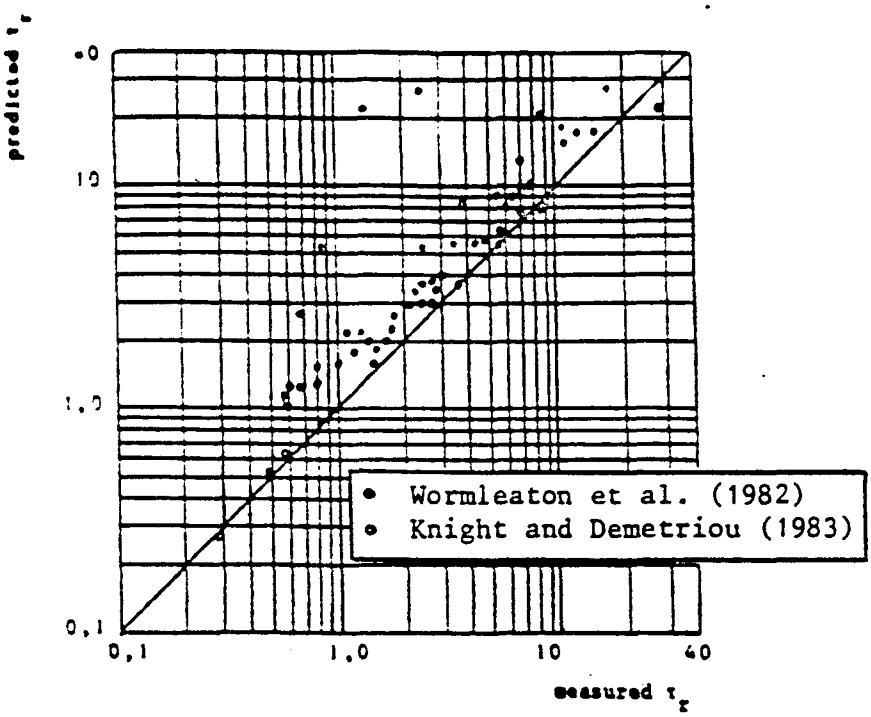

Figure 98. Error in the prediction of the apparent shear stress (Wormleaton equation)

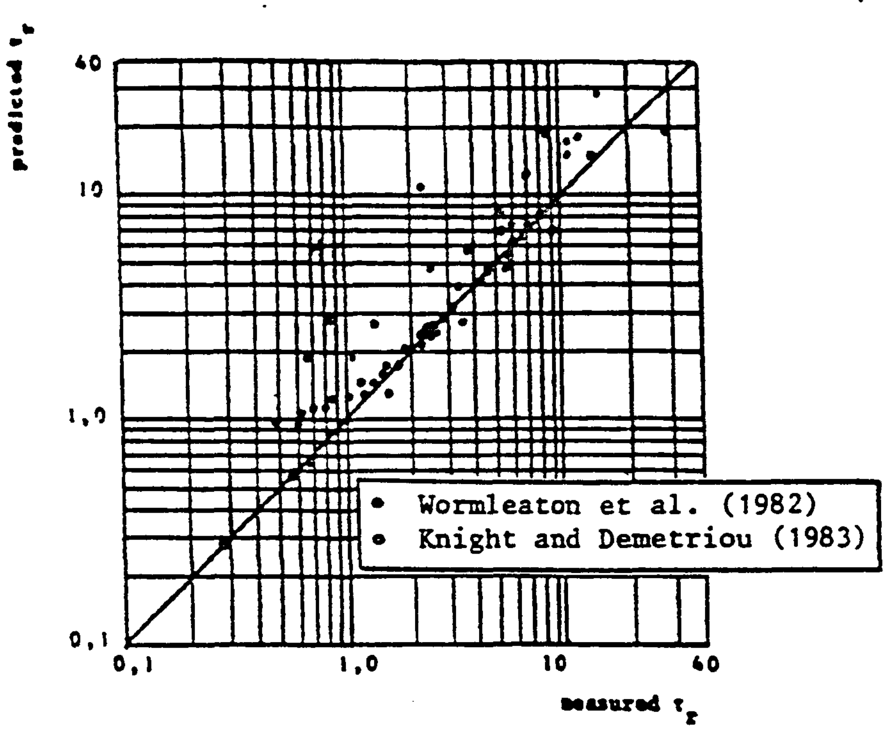

Figure 99. Error in the prediction of the apparent shear stress (Prinos equation)

8.4 DISCHARGE COMPUTATION METHODS - STEADY STATE CONDITIONS

It is very difficult to obtain field data with which overbank flow may be studied. This is mainly due to the fact that the stage of a river flooding its banks changes too quickly for all the necessary shear stress measurements to be taken (Myers and Elsawy, 1975; Bhowmik and Demissie, 1982). Because of the difficulty in obtaining sufficiently accurate and comprehensive field measurements of velocity and shear stress in compound channels under unsteady flow conditions, considerable reliance is still placed on well focused laboratory investigations under steady flow conditions to provide the information related to the details of the flow structure and the lateral momentum transfer. Such details are important in the application and development of numerical models aimed at solving practical open channel flow problems.

This chapter assesses 4 existing steady-state discharge computation methods and compares them based on published flume data, incorporating a fairly wide range of bed roughnesses and flood plain widths.

8.4.1 SEPARATE CHANNEL METHOD

The channel is divided into three homogeneous sections (main channel, left/right flood plains) and the discharge is calculated separately for each segment. It is assumed that the vertical fluid boundaries between the segments do not add to the wetted perimeter; in other words, these boundaries are taken to be planes of zero shear, and the method does not take into account the effect of the momentum transfer mechanism.

Discharge in each segment is calculated from an empirical relationship, i.e. Manning's equation. If "i" refers to the ith section, then the total discharge is given by:

$$Q = \sum_{i=1}^{m} Ki \; S_f^{\;1/2} \qquad (8.10)$$

where

$\sum_{i=1}^{m} Ki$ is the sum of the conveyances in the subsection as defined by relations (2.16, 2.17)

This method is included in the comparisons in order to identify the error in the discharge computation under steady state conditions when the momentum transfer mechanism is ignored.

8.4.2 VERTICAL INTERFACE METHOD

The most commonly used methods of calculating the discharge in a compound channel are based on splitting the cross-section into hydraulically homogeneous subdivisions. The methods differ however, in the assumptions they make regarding the location and nature of the imaginary interface plane between the main channel and the flood plain. A common feature of these methods is that the division lines start at the junction of the channel and the flood plain where the greatest disparities in roughness and flow depth occur.

The vertical interface method assumes that a vertical plane (interface) separates the main channel from the flood plains. It was originally assumed that there was no shear acting on these imaginary interface planes and they were therefore not included in the wetted perimeters of the adjacent subdivisions when calculating discharges. Subsequently, Wright and Carstens

(1970), proposed that the interface be included in the wetted perimeter for the main channel subdivision only, recognising that this channel would experience drag from the slower moving adjacent flood plain waters. Posey (1967) suggested that for d/D less than 0,30 the interfaces should be included in the wetted perimeter of the main channel, for d/D greater than 0,30 they should be excluded and they should be excluded from the flood plain wetted perimeter for all flow depths.

This method makes certain assumptions regarding the magnitude of the apparent shear stress. The interface is either ignored as wetted perimeter, implying zero apparent shear, or it is included in the main channel wetted perimeter only, implying that the boundary and apparent shear stresses are approximately equal in that subdivision. Wormleaton et al. (1982) tested the vertical interface method and found that at low flow depths the method overestimates the channel discharge capacity. The reason for this is that the average shear stress in the section is much larger than the apparent shear stress on the vertical interface. Thus the assumptions of apparent shear stress being equal to zero, or even equal to the average boundary shear stress, cease to be valid. At low flood plain depths, the momentum transfer effect is therefore far greater than allowed for in the method. In spite of the poor results the method is still used extensively, as is easy to implement.

8.4.3 INCLINED INTERFACE METHOD

Yen and Overton (1973) in trying to determine the lines of zero shear stress concluded that the lines start from the junction between flood plain and main channel, and are inclined towards the centre of the main channel with an angle of inclination to the horizontal ϕ (Figure 100).

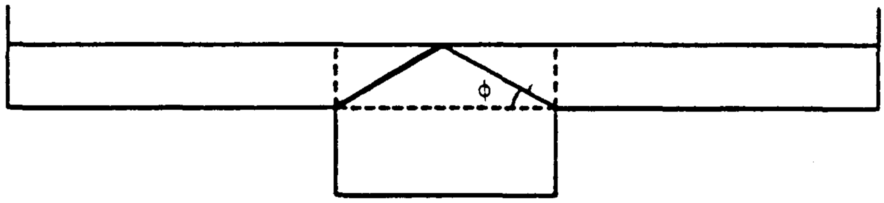

Figure 100. Vertical, horizontal and inclined division lines (Wormleaton et al., 1982)

The lines so determined need to be included as a section of the wetted perimeter in the flow computation when they are used as division lines.

The inclination of the division lines obtained from available data vary mainly with flood plain stage, although roughness distributions and other geometrical factors appear to have some influence. Yen et al. found that the division lines are generally slightly curved but can usually be approximated by straight lines. Knight and Lai (1985) showed that the angle of inclination, ϕ, ranges from 5° for very low depth ratios (d/D=0,13) to 50° (d/D=0,41) for higher ratios. Knight and Lai came to a conclusion similar to Yen et al., that the plane varies from an inclined one to a nearly horizontal plane as flow depth decreases. Moreover, the interface planes can be reasonably closely approximated by lines drawn from the main channel/flood plain junction to a point on the water surface at the centre of the main channel. These interfaces (Figure 100) are referred to as **diagonal interfaces**.

Wormleaton et al. (1982) performed a series of experiments in a laboratory compound channel, which enabled them to calculate the apparent shear stress that would occur across several different assumed interface planes. Comparing the results using horizontal and diagonal interfaces, they concluded that the apparent shear stresses across horizontal and diagonal interface planes were much smaller than those for the vertical planes. Neither exceeded the main channel boundary shear stresses, even at low flood plain depths. As the depth increased the shear stresses decreased and, particularly in the case of the horizontal interface plane, changed sign. This change of direction of the apparent shear stress indicates that at higher flood plain depths there is a transfer of momentum into the main channel, below bank full level, from the water directly above it. The smaller apparent shear stresses across these interface planes render them more suitable than the vertical planes for discharge calculation.

The most important contribution of Wormleaton et al. was the establishment of a criterion to determine whether the interface should be included in the main channel wetted perimeter or ignored. This criterion they defined as the **apparent shear stress ratio (ASSR)**- λ given by:

$$\lambda = \tau_{ai}/\tau_{ci} \qquad (8.4)$$

where

τ_{ci} = average shear stress in the main channel
τ_{ai} = apparent shear stress on the diagonal (d) horizontal (h) or vertical (v) interface

For a vertical interface the ratio ASSR (λ) ranges between zero, in the absence of apparent shear, and unity when apparent and average shear stresses are equal. For a diagonal interface the ASSR (λ) values lie within the range -1 to 1. ASSR values for the horizontal interface show a wider range of variation than those across the diagonal interfaces, becoming larger and negative at the higher depth ratios. As the depth ratio approaches 1, the horizontal and diagonal interfaces approach each other, their ASSR values therefore become equal. The experimental results indicated that for values of ASSR -(λ) up to 0,40 the diagonal interface plane should be excluded from the wetted perimeter of the main channel and for ASSR values greater than 0,40 it should be included in the wetted perimeter. The interface is always excluded from the flood plain wetted perimeter as it is assumed that wide flood plains will be considered therefore the propelling effect of the interface on the flood plain will be small.

Wormleaton et al. (1982) suggest that there is little to choose between the calculation methods using the diagonal or horizontal interface methods. James (1985) in his study of deposition of sediment in compound channels used the diagonal interface, as a horizontal interface creates an unrealistically small main channel. In this study diagonal interfaces were used to evaluate the ASSR method. The calculation of the apparent shear stress ratio (ASSR) is determined as follows:

The theoretical average shear stress, τ_{ai} around the total boundary of the main channel subdivision (including the interfaces) can be found by equating the total boundary shear force to the component of weight in the direction of flow. Thus:

$$\tau_{ci}(P_c+P_{ai})=\gamma A_{ci}S_0 \tag{8.12}$$

and so

$$\tau_{ci} = \frac{\gamma A_{ci}S_0}{P_c+P_{ai}} \tag{8.13}$$

where

P_{ai} is the length of the interface

and the apparent shear stress, τ_{ai}, on the interface can be calculated from the following equation, which is derived from equilibrium considerations:

$$\tau_{ai} = \frac{1}{P_{ai}}(\tau_{av}P_{av} - \gamma S_0(A_{cv}-A_{ci})) \qquad (8.14)$$

Referring to Figure 100 and rearranging the terms, equation (8.14) for diagonal interfaces (i=d) becomes:

$$\tau_{ad} = (\tau_{rd}-W_c/4)\gamma d S_0/P_{ad} \qquad (8.15)$$

Thus from equations (8.13) and (8.15), the values of $\lambda=\tau_{ai}/\tau_{ci}$ can be calculated for any interface in terms of τ_r and geometrical properties of the channel.

8.4.4 AREA METHOD/K METHOD

Holden (1986) in his thesis on discharge calculation in compound channels developed three new methods, namely the **area method**, the **k-method** and the **improved k-method**. The "improved k-method" is not included in the comparisons as it was found to be valid for only a limited range of channel geometries. The area method is a refinement of the diagonal interface method. It has the advantage that no knowledge is required of the shape of the interface, and it is not necessary to assume that the interface is a straight line (Figure 101). The main channel and flood plain are simply separated using a zero shear stress interface of unknown shape which is excluded from the wetted perimeter.

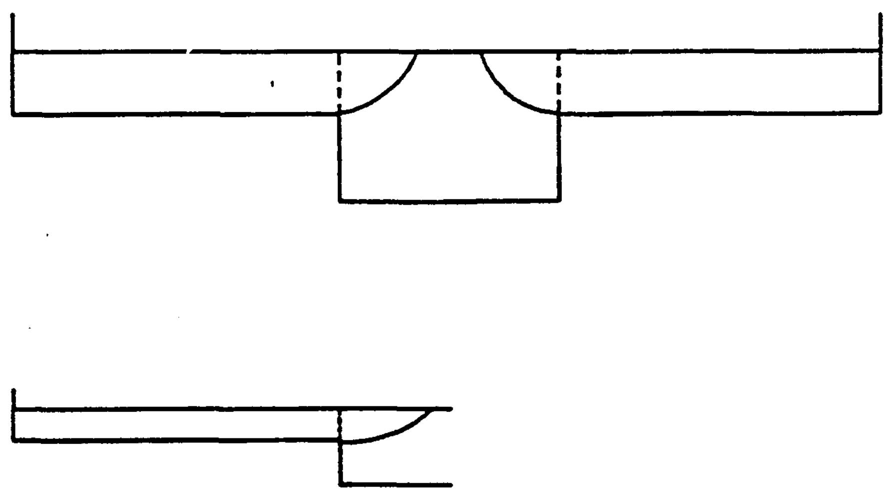

Figure 101. Probable shapes of interfaces used in the area method (Holden, 1986)

The area adjustment is made as follows:

$$A'_c = A_c - 2(\Delta A) \tag{8.16}$$

$$A'_p = A_p + 2(\Delta A) \tag{8.17}$$

$$\Delta A = \tau_r d^2 \tag{8.18}$$

where

A'_c = modified area of main channel
A'_p = modified area of flood plain

The area correction ΔA is derived theoretically as follows (Holden, 1986):

Consider the equilibrium of forces in the flood plain region, when a vertical interface divides the main channel from the flood plain:

$$\Sigma F_p - \tau_{av} d = \gamma A_p S_0 \tag{8.19}$$

where

ΣF_p is the shear force on the physical wetted perimeter of the flood plain P_f

Consider equilibrium when an inclined interface is used, such that there is zero shear on the interface:

$$\Sigma F_p = \gamma (A_p + \Delta A) S_0 \tag{8.20}$$

combining these two equations yields:

$$\gamma (A_p + \Delta A) S_0 - \tau_{av} d = \gamma A_p S_0$$

and simplifying

$$\Delta A = \tau_r d^2$$

The k method is an improvement of the vertical interface method. The wetted perimeter of the main channel is increased by $2k_c d$, therefore:

$$P'_c = P_c + 2k_c \tag{8.21}$$

where k_c caters for both the increase in resistance caused by the apparent shear stress on the interface, and for the reduction in average channel boundary shear. K_c is always positive because the increase in the interfacial shear stress is always greater than the decrease in boundary shear stress. Similarly the propelling effect of the interface and the distortion of the shear stresses on the bed of the flood plain are lumped into a single flood plain factor (k_p), which decreases the wetted perimeter as follows:

$$P'_p = P_p - k_p d \tag{8.22}$$

Considering the equilibrium of forces, the two coefficients k_c, k_p are given by the equations:

$$\frac{1}{k_c} = \frac{1}{\tau_r} \frac{A_c}{P_c} \frac{1}{d} - \frac{2d}{P_c} \tag{8.23}$$

$$\frac{1}{k_p} = \frac{1}{\tau_r} \frac{A_p}{P_p} \frac{1}{d} - \frac{d}{P_p} \tag{8.24}$$

Whichever method is adopted for the total discharge calculation it will be necessary to find the apparent shear stress (τ_r).

8.4.5 ASSESSMENT OF THE DISCHARGE COMPUTATION METHODS

Four discharge computation methods namely the separate channel method, the diagonal interface method, the area method and the k method were evaluated using published flume data. The separate channel method has been included in the comparisons in order to demonstrate the effect of ignoring the momentum transfer mechanism on discharge computation under steady state conditions. The vertical interface method was not included in the comparisons, as it's performance is poor when compared to the more reliable diagonal interface method.

The methods were tested with sets of flume data from Wormleaton et al. (1982) and Knight et al. (1983). Knight et al. , performed

3 sets of experiments with 6 data items each (Appendix G). They increased the main channel-flood plain ratio (W_c/W_p) from (2:1) for the experiments A1-A6, to (1:1,5) for the experiments A13-A18. For the first set of experiments (A1-A6) the area method did not perform as well as the k method and the diagonal interface method, but in all cases the error was less than 4%. For the other two sets of experiments, the area and the k method gave the best overall results (Figure 102). In Figure 102.a the discharge error for the diagonal interface method takes a sudden jump from a negative to a positive value at d/D approximately equal to 0,25. This corresponds to the point where λ exceeds 0,4 and the interface is no longer included in the wetted perimeter of the main channel.

Wormleaton et al. (1982) performed 5 set of experiments and the discharge error of the various discharge methods for the three sets of data (B-C-D) are plotted in Figure 103. The same flume dimensions (W_c/W_p=0,29/0,46) were kept for all the experiments, changing the roughness of the flood plains from 0,011 to 0,021. The area method and the diagonal interface method gave the best results. The separate channel method and the k-method over-estimated the discharge in all cases. The k-method performed significantly better than the separate channel method yet it still over-estimated discharges, especially at low flow depths.

The most consistent method was found to be the area method as it performed favourably compared with all the other methods and did not exhibit sudden jumps as did the diagonal interface method. James (1984) examined the diagonal interface method and found that it can lead to the main channel velocities being calculated to be smaller than the flood plain velocities. Furthermore, he concluded that the apparent shear stress criterion is vague and requires further experimental data as it was developed and tested from only a limited set of data.

In most of cases the error of the area method was within 5% of measured discharges, which is considered to be the range of possible error in the measurement of the flume discharges. In view of the good performance of the area method as well as its simplicity, it is considered to be a viable discharge computation method for application in real channels.

From the above assessment the following conclusions can be drawn:

- The separate channel method grossly overestimates the discharge and becomes highly inaccurate at low flow depths.

- The diagonal interface method is reasonably reliable but the λ criterion is vague and requires further research.

- The k-method is a refinement of the vertical interface method and performed better than the separate channel method, but the results are poor compared with the area method and the diagonal interface method.

- The area method is the most promising, as it is conceptually sound, and does not need any criteria in order to be applied.

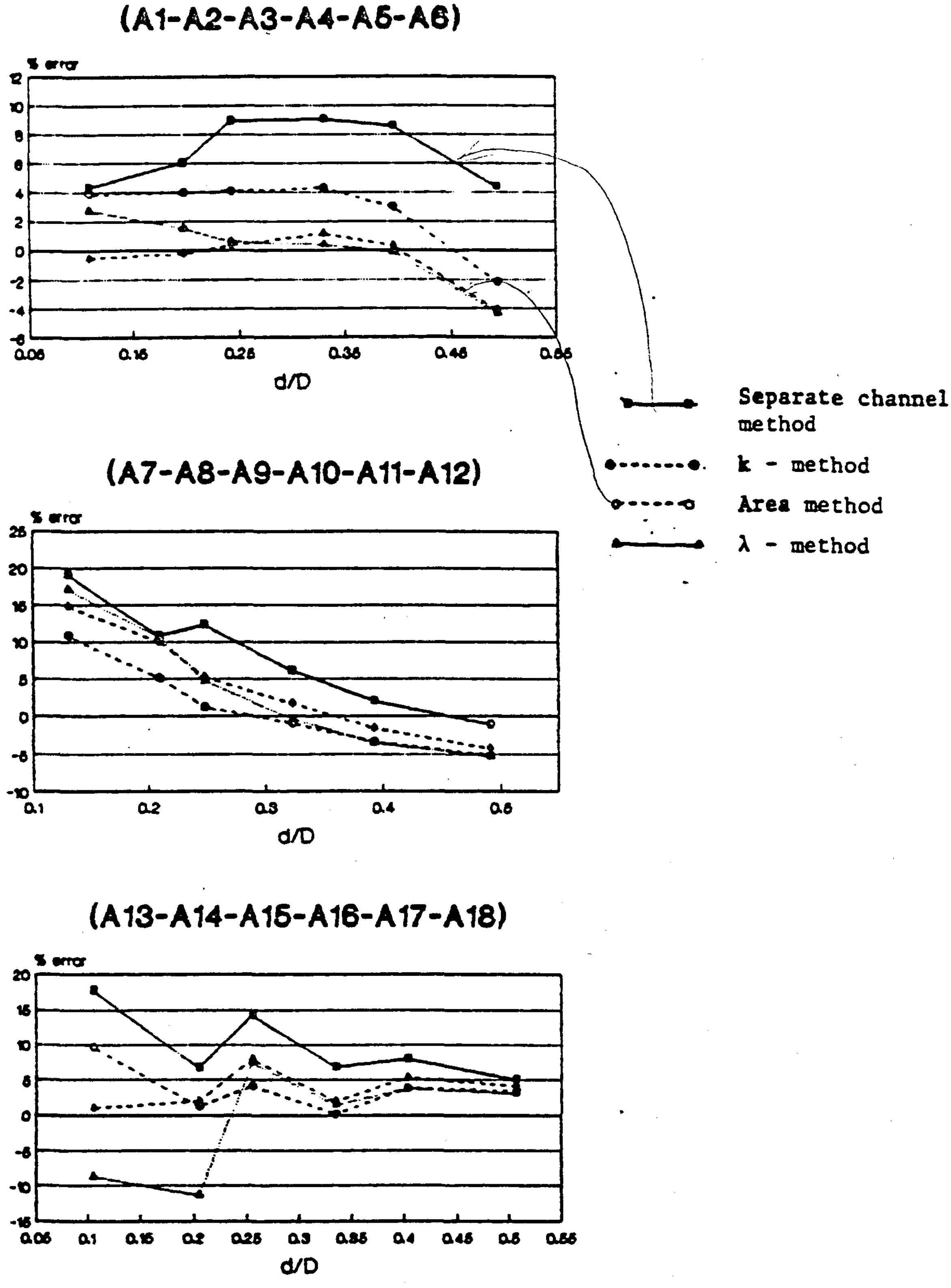

Figure 102. Assessment of discharge computation methods - Data of Knight et al. (1982)

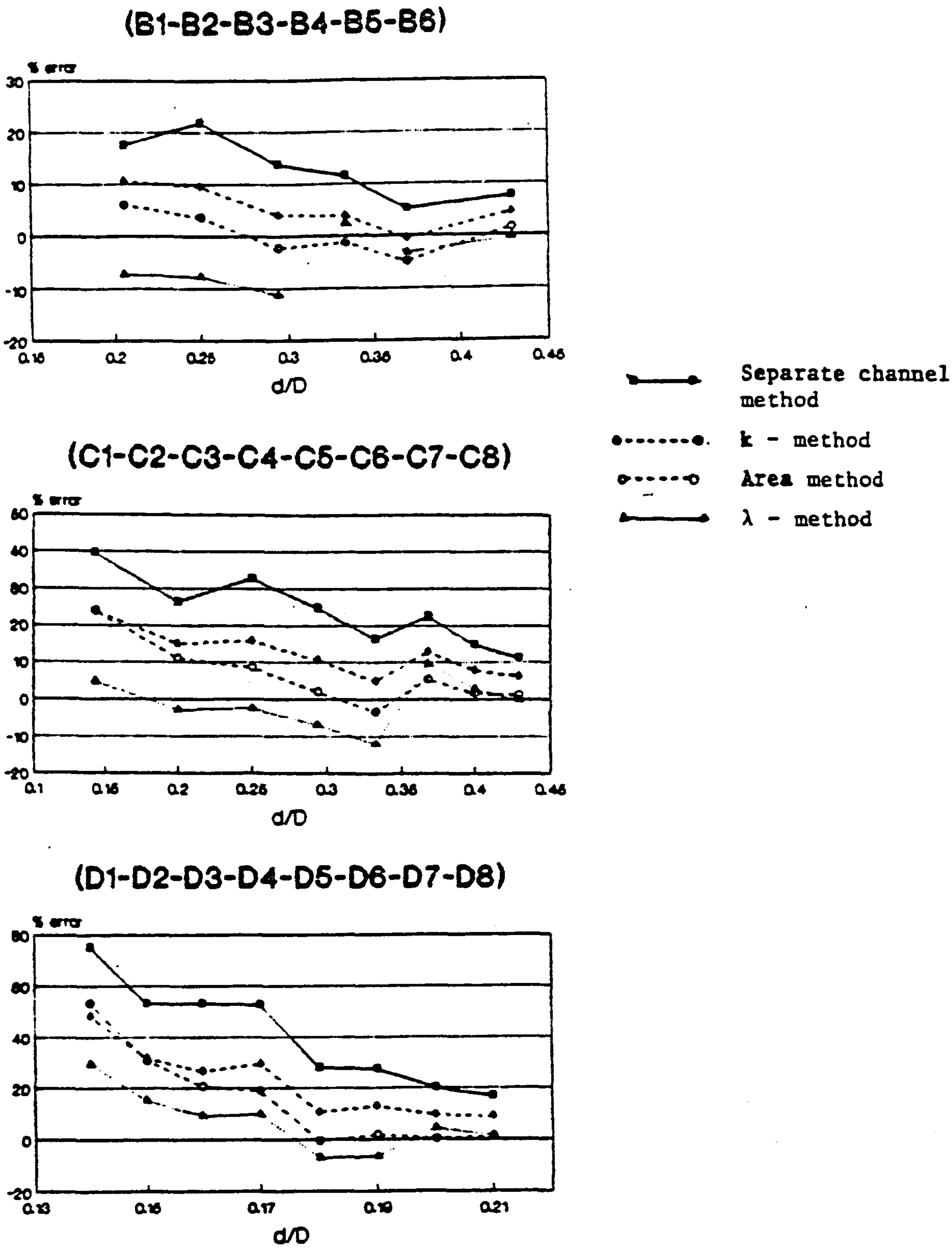

Figure 103. Assessment of discharge computation methods - Data of Wormleaton et al. (1982)

8.5 TECHNIQUES FOR FLOOD ROUTING IN RIVERS WITH FLOOD PLAINS

In the unsteady flow models, the hydraulic features of the river reach are generally lumped into the resistance term (S_f) as was described in Chapter 2. The resistance term is evaluated from a steady-state empirical resistance law of the general form:

$$Q = K(Z)\ S_f^{1/2} \tag{8.25}$$

where

K(Z) is the conveyance factor of the channel

Most of the developed unsteady flow models treat the flood plain as "off-channel" dead storage, conveying virtually no discharge, therefore the total conveyance of the compound channel K(Z) is merely the conveyance of the main channel. The method was first developed at the Delft Technological University by Abbot et al. (1967) and subsequently was adopted by most researchers. (Abbot, 1979; Ligget and Cunge, 1975; Miller and Cunge, 1975). In this case , the top width B(Z) in the continuity equation is replaced by the storage width $B_{st}(Z)$ and the area in the momentum equation, by the 'live' area A(Z). The terms are shown in Figure 104. The model will be referred to as the **"off-channel storage"** model.

The purpose of introducing the storage width $B_{st}(Z)$, is to take into account the fact that flooded zones often act only as storage areas. However, the introduction of a 'live' area A(Z) opens the door to arbitrary judgements and the model may not be representative of reality any more. Furthermore, it is not clear at what point the flood plain acts only as storage and no longer contributes to the momentum of the compound channel.

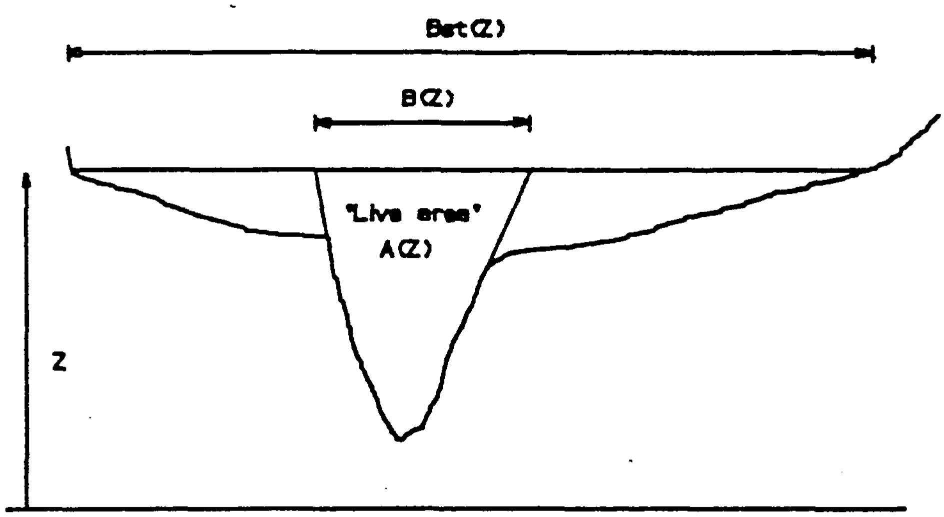

Figure 104. "Off-channel storage" model - Cross-section representation

A different approach is to treat the channel and flood plain as one continuous cross-sectional area. This is based on the assumption that the total force resisting the flow is equal to the sum of the forces resisting the flow in the channel and the flood plain. Usually an equivalent Manning roughness coefficient is used which is a weighted average of the roughness of the main channel and the flood plain. Alternatively, the total conveyance of the cross-section is calculated as the sum of the conveyances of the main channel and the flood plains. This model will be referred to as the "separate-channel" model.

Fread (1976) proposed a different approach for flood routing in meandering rivers. The basic concept of his model is to treat the flows in the river channel and the flood plain separately, from a one dimensional point of view. An approximate ratio of the flow in the flood plain to that in the river channel is found using Manning's equation, in which the friction slope is approximated by the slope of the river. Separate equations are written for the portion of flow in the flood plain and in the main channel. The equations are then combined, taking into account the computed ratio of flows. This approximation neglects the contribution of inertia effects in evaluating the friction loss, and is acceptable only in the case of very slowly varying transient flows. In addition, the separate channel and the off-channel storage models take into account the difference in velocities between the main channel and the flood plain using the momentum correction factor β in the momentum equation as defined in Chapter 2. When the flow is confined within the main channel the discharges in the flood plains are zero and the momentum correction factor is equal to unity. During flood periods, the flow overtops the flood plain, the discharge and the flow velocity in the flood plain are not equal to zero and the factor β is greater than unity.

Fread compared the performance of his model with the separate channel and the off-channel storage models, routing hydrographs in an idealised meandering river with a significant flood plain and a uniform cross-section (Figure 105). The discharge hydrographs were specified for the upstream end of a 150 km reach of meandering river with a bottom slope 0,0004. His results were almost identical with the results of the separate channel model.

Fread claimed that his method is computationally more stable compared to the other models. The separate-channel model was tested for a wide range of compound channels and in some cases instability was detected which could not be dampened. The reason lies in the functions A(Z) and B(Z) which are no longer continuous for a highly irregular cross-section. This feature causes computational complications, especially when the water-stage oscillates near the main channel/flood plain discontinuity. A procedure was developed which ensures that at the time-step the water-stage passes the discontinuity, the width that is used in the continuity equation is taken from the previous time-step. This introduces an error, and a very small oscillation at depths

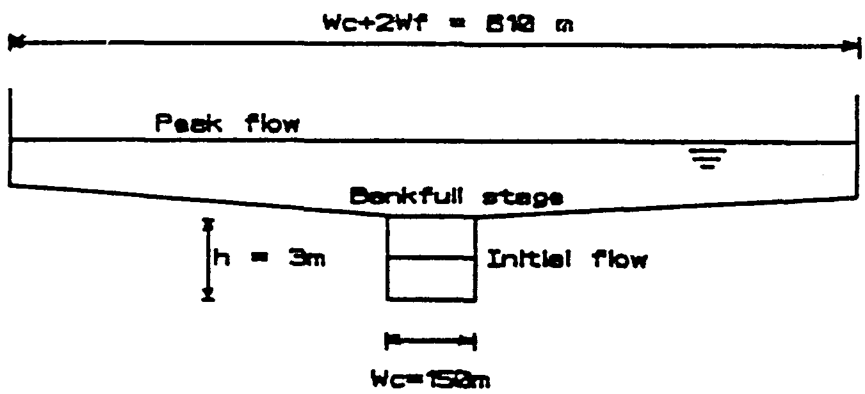

Figure 105. Typical cross-section used by Fread (1976).

near the cross-section discontinuity, which is damped out very quickly. In most cases the model was stable and the results are exactly the same as when the width discontinuity is taken as such in the computations.

The performance of the separate channel model was compared with that of the off-channel storage model using the same typical cross-section as Fread (1976). The pertinent characteristics of the channel and flood plain are: n_c=0,03; n_f=0,06; W_c=150; W_f=230; the flood plain slopes upward from the river to the valley buff line at a slope of 1m vertical per 1000m horizontal; and there is no lateral inflow. Hydrographs were routed for a distance of 50km and the discharge hydrographs were computed at the downstream end. The synthetic flood hydrographs at the upstream section of the reach were generated using the relationship:

$$Q(t)= Q_b+Q_{amp}((t/t_p)\exp(1-t/t_p))^{\beta} \tag{8.26}$$

in which

β = parameter

t_p = time to peak

Q_b = base flow

Q_b+Q_{amp} = peak discharge for the flood

The time for the floods to peak was taken as 0,40 of the total hydrograph duration and β was given a value of 10. In order to minimise numerical errors, 1-hour time-steps and 1 km cross-section spacing were used. The cross-sections were arranged in three branches with 16 cross-sections per branch. Typical routed hydrographs using the two models are shown in Figures 106 and 107. From the plotted hydrographs at the downstream end, it becomes evident that the storage method may significantly underestimate the peak flowrate, while the water levels are overestimated.

For a critical assessment of the differences between the two models, attention is focused on the attenuation and travel time of the hydrograph peaks. These are normalised to the peak attenuation ($A_{p.b}$) and travel time ($T_{p.b}$) associated with the flow condition when the channel flow is bank full. Bank full discharge is a useful reference point in any study of channels with flood plains. Normalization about the bank full condition focuses on the differences in the computed attenuation and travel time of each model due to the presence of the flood plain (Fread, 1976).

The attenuation characteristics of the two models are shown in Figure 108 to 111. In all the graphs the normalised peak flowrates ($Q_{p.i}/Q_{p.b}$) of the upstream hydrographs (i) are plotted on the horizontal axis. In other words, the horizontal axis of the graphs shows the ratio of the peaks of the different upstream

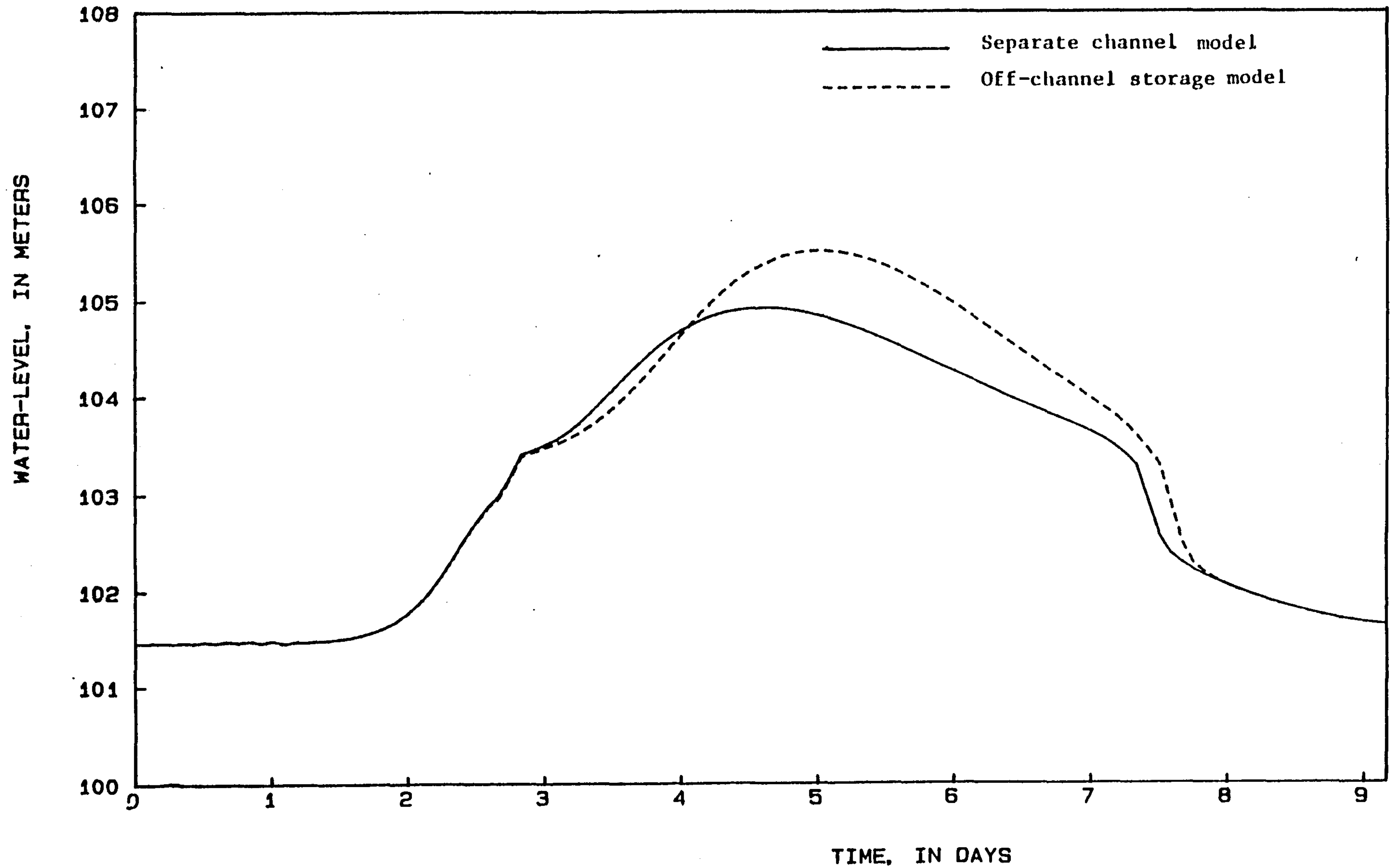

Figure 106. Typical water level hydrographs computed by the separate-channel and off-channel storage models

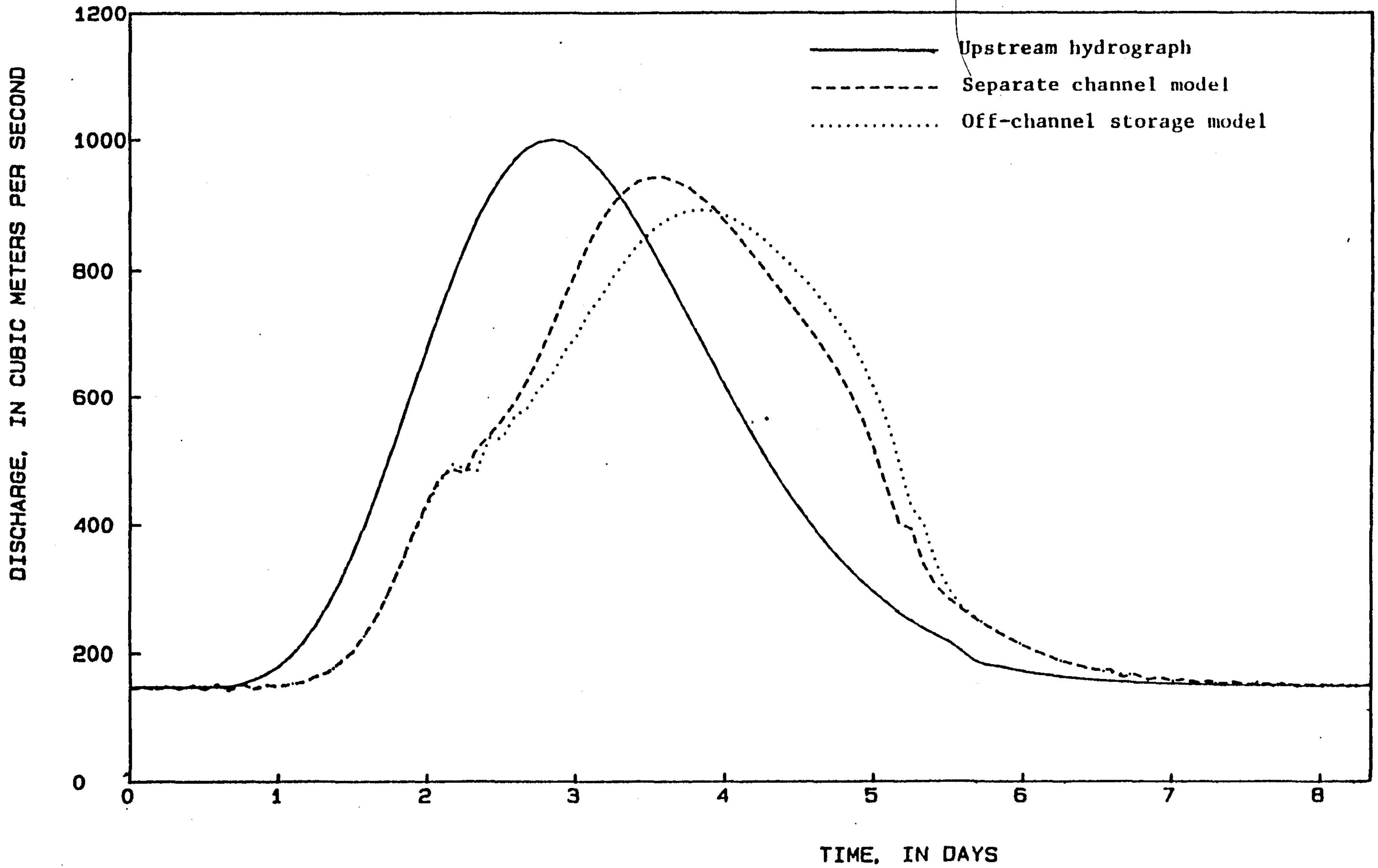

Figure 107. Typical hydrographs of separate-channel and off-channel storage models

hydrographs ($Q_{p.i}$) to the peak of the upstream hydrograph for bank full flow ($Q_{p.b}$). Graphs 108 and 109 focus on the characteristics of the computed downstream peak flowrates for the two models. For high flows ($Q_{p.i}>2Q_{p.b}$) the normalised attenuation of the peak flowrate ($A_{p.i}/A_{p.b}$) computed by the off-channel storage model, was twice as high as that computed by the separate-channel model (Figure 108). The computed normalised peak flowrate of the separate-channel model was delayed by a factor of more than 1,5 times when compared with the off-channel storage model (Figure 109).

Graphs 110 and 111 show the difference between the two models of the computed attenuation and the travel time of the peak water level. For high flows ($Q_{p.i}>2Q_{p.b}$) the storage model overestimates the water level by more than 0,50 meters and the peak water levels are retained for more than 10 hours longer than the travel time computed by the separate-channel model.

Figures 108 to 111 prove that the assumption of storage in the flood plain can lead to a significant error in flood routing computations. The flowrates are underestimated, the water levels are overestimated and a higher stage is estimated at the flood peak. Remembering that the computation of the water levels is of the utmost importance for the calculation of the flood lines, the off-storage model is seen to be a more conservative approach as opposed to separate channel model. Assuming negligible flow in the flood plains, may not however, provide an accurate representation of the actual flow conditions.

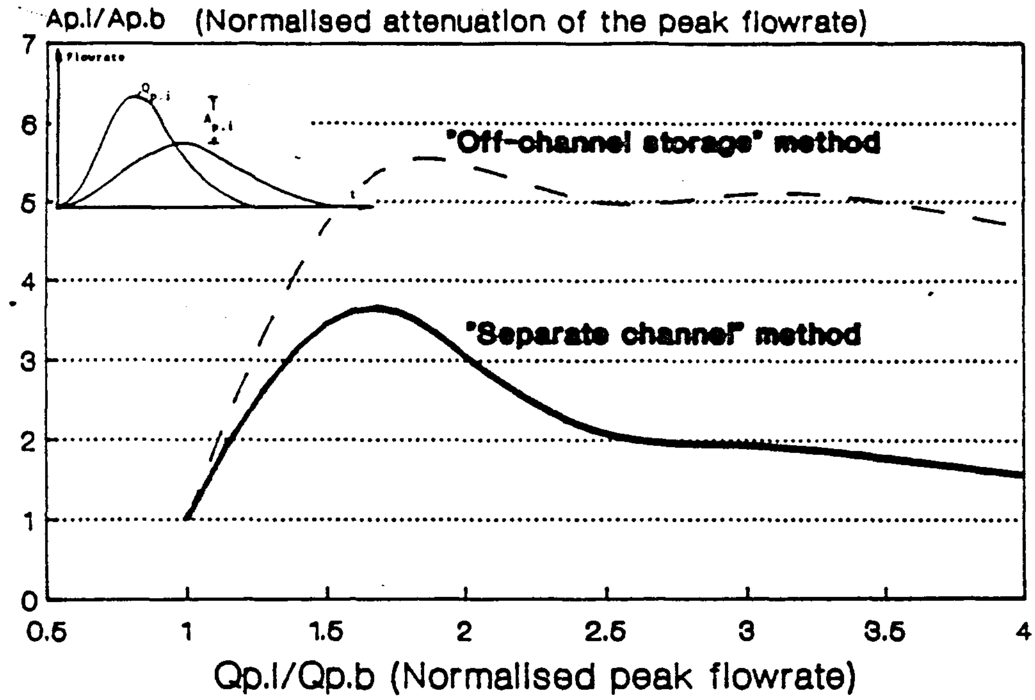

Figure 108. Peak flowrate attenuation characteristics of the "separate-channel and off-channel storage models

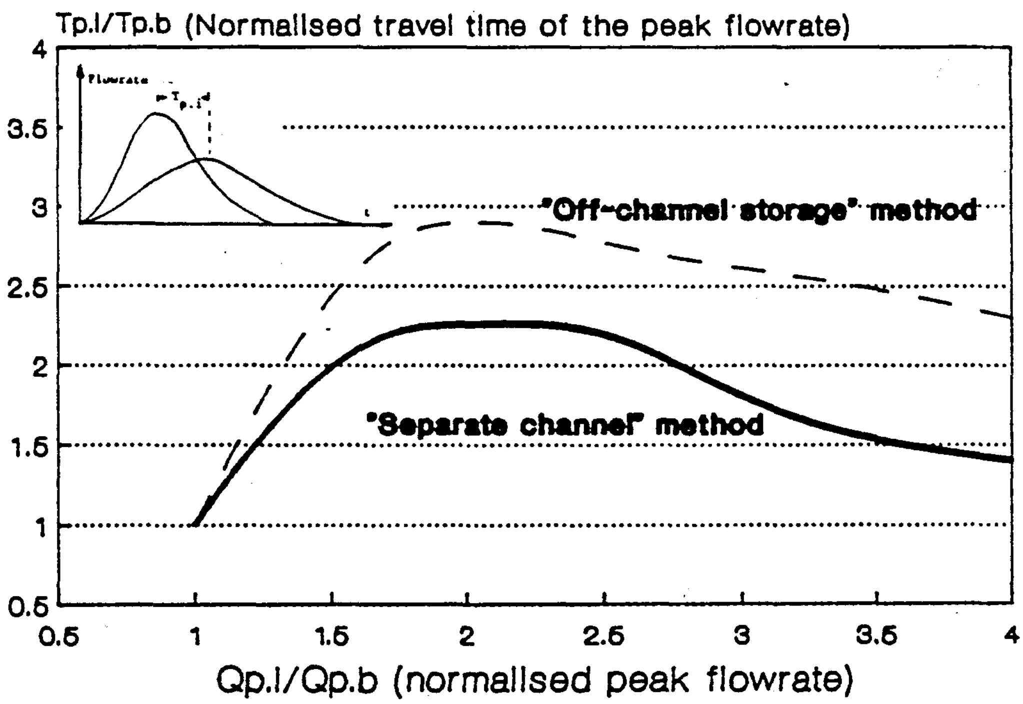

Figure 109. Peak flowrate travel-time characteristics of the "separate-channel and off-channel storage models

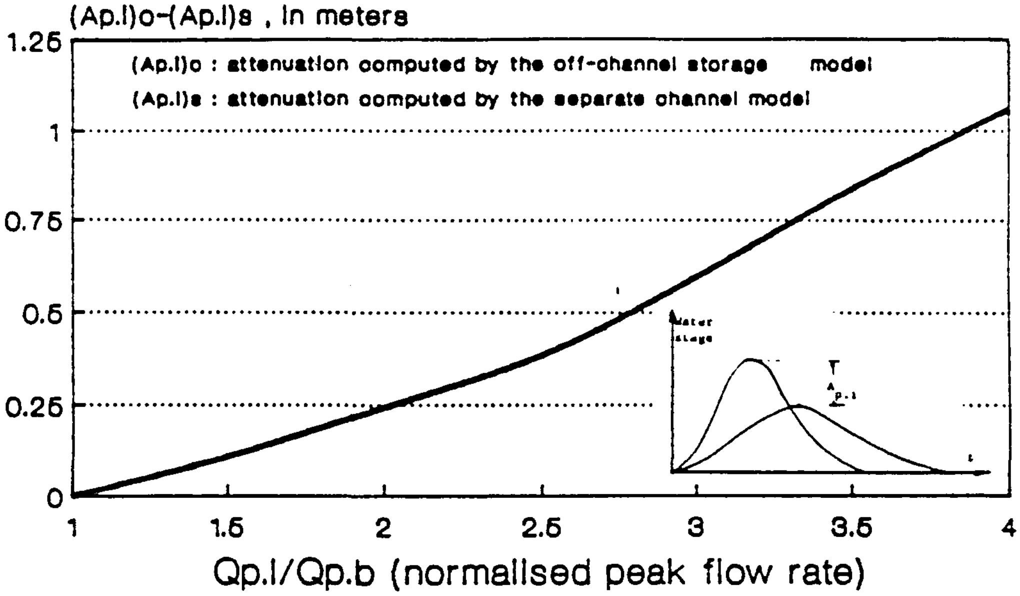

Figure 110. Difference in the peak water level attenuation using the "separate-channel and off-channel storage models

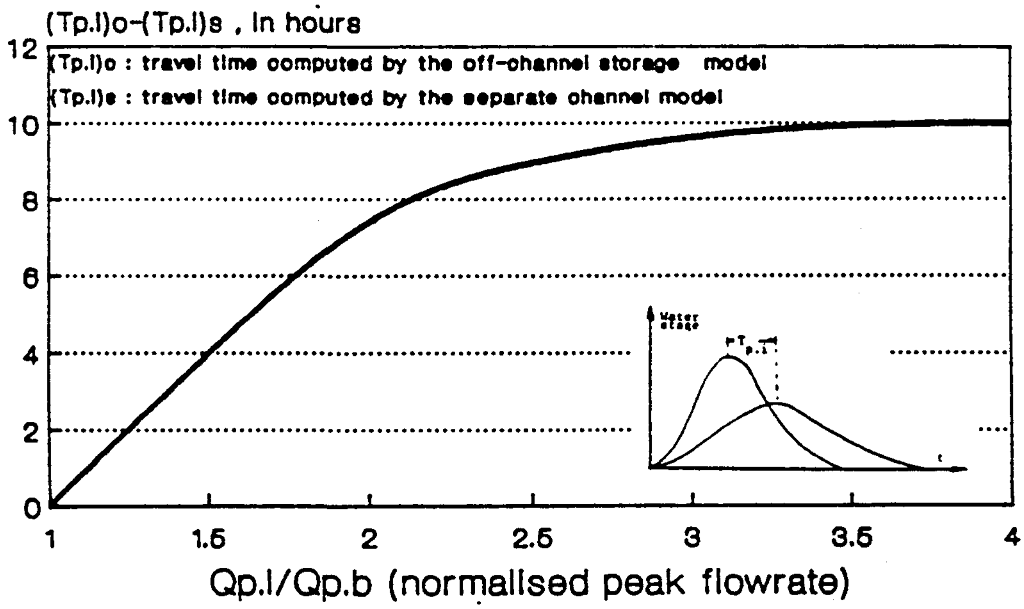

Figure 111. Difference in the peak water level travel-time using the "separate-channel and off-channel storage models

8.6 CHANNEL MEANDERING

Fread's model accounted for the extent of meander or sinuosity by introducing the flow path length ratio:

$$L_r = L_c/L_f \tag{8.27}$$

where

L_c = the length of the meandering channel

L_f = the length of the flood plain between the upstream and downstream boundaries

A different approach was adopted in the development of this model, which gives the user greater flexibility. The modeller specifies, for each reach, three lengths L_c, L_{fl}, L_{fr}, being the length of flow in the main channel, the left and the right flood plains respectively. The flow path length is adjusted linearly as the flood plain is inundated according to the relationship:

$$L = \frac{L_c Q_c + L_{fl} Q_{fl} + L_{fr} Q_{fr}}{Q_c + Q_{fl} + Q_{fr}} \tag{8.28}$$

In this way, the accuracy depends on the modeller's ability to correctly describe the meandering of the main channel within the flood plain and the short-circuiting of the main channel flow. A similar approach was suggested by Perkins (1970).

The problem of a meandering channel will not be pursued further as the meandering river is subjected to both lateral and longitudinal movement in reality caused by the formation and destruction of bends. In general bends are formed by the process of erosion and deposition. In such a case, the mathematical model should be coupled with an algorithm for the study of transient phenomena in natural alluvial channels.

8.7 DEVELOPMENT OF AN IMPROVED FLOOD-ROUTING MODEL

The only truly adjustable term during model calibration is the conveyance factor K(Z). Therefore K(Z) may absorb all kinds of head losses such as those due to sediments, unidentified singular losses etc. Cunge et al. (1981) emphasised the danger in this situation as modelling systems should always have the capability of representing the most important of these losses using special features. The model should not attempt to represent them by conveyances, as the predictive capability of the function K(Z) will be lost. Furthermore in many practical flood routing problems the field data may be limited and it might be impossible to calibrate the model. It is therefore important to identify and isolate the effect of the momentum transfer mechanism on flood routing problems in compound channels.

The effect of the main channel /flood plain interaction for an unsteady flow model will be reflected in the conveyance factor. Since in the unsteady flow, a steady-state empirical law for the calculation of friction slope is used, it is logical to extrapolate the procedures of the proposed steady-state computation methods to develop a more accurate flood routing model.

Based on the conclusions of the previous analysis, the model will:

- Incorporate the Prinos equation for the calculation of the apparent shear stress at the interfaces.

- Use the area method for the computation of the total conveyance.

In order that the model be applicable in all conditions, the Prinos equation must be corrected for values of apparent shear stress greater than 6. Since ΔV is a function of τ_r, an iterative procedure was adopted. For the first iteration, τ_r is calculated using the vertical interface method. If τ_r is greater than 6, the area method is used for the following iterations. The procedure converges within approximately five iterations. The results are shown in Figure 112. The scatter for τ_r values larger than 6 is much smaller than for the results when no iterative procedure is adopted. The Prinos equation tends to overestimate the apparent shear stress for values of τ_r less than 1. However the error is not significant in the discharge computations. In general, Figure 112 indicates a good overall performance by the Prinos equation although more testing is necessary.

The area method was found to be preferable to all other methods for the following reasons:

- It is computationally simple.
- It has a sound theoretical basis.
- It does not require previous knowledge of the shape or inclination of the zero shear stress interfaces.
- It is not based on any limit or ratio in order to be applicable.
- The error in the total discharge computation is in the same range or less when compared to the other methods.

By incorporating these features as options in the unsteady flow simulation model, the effect of the momentum transfer mechanism in flood routing can be analysed. The problems addressed are:

- The effect of the mechanism on flood routing.
- If the effect is significant, then how sensitive is it to the pertinent parameters ?

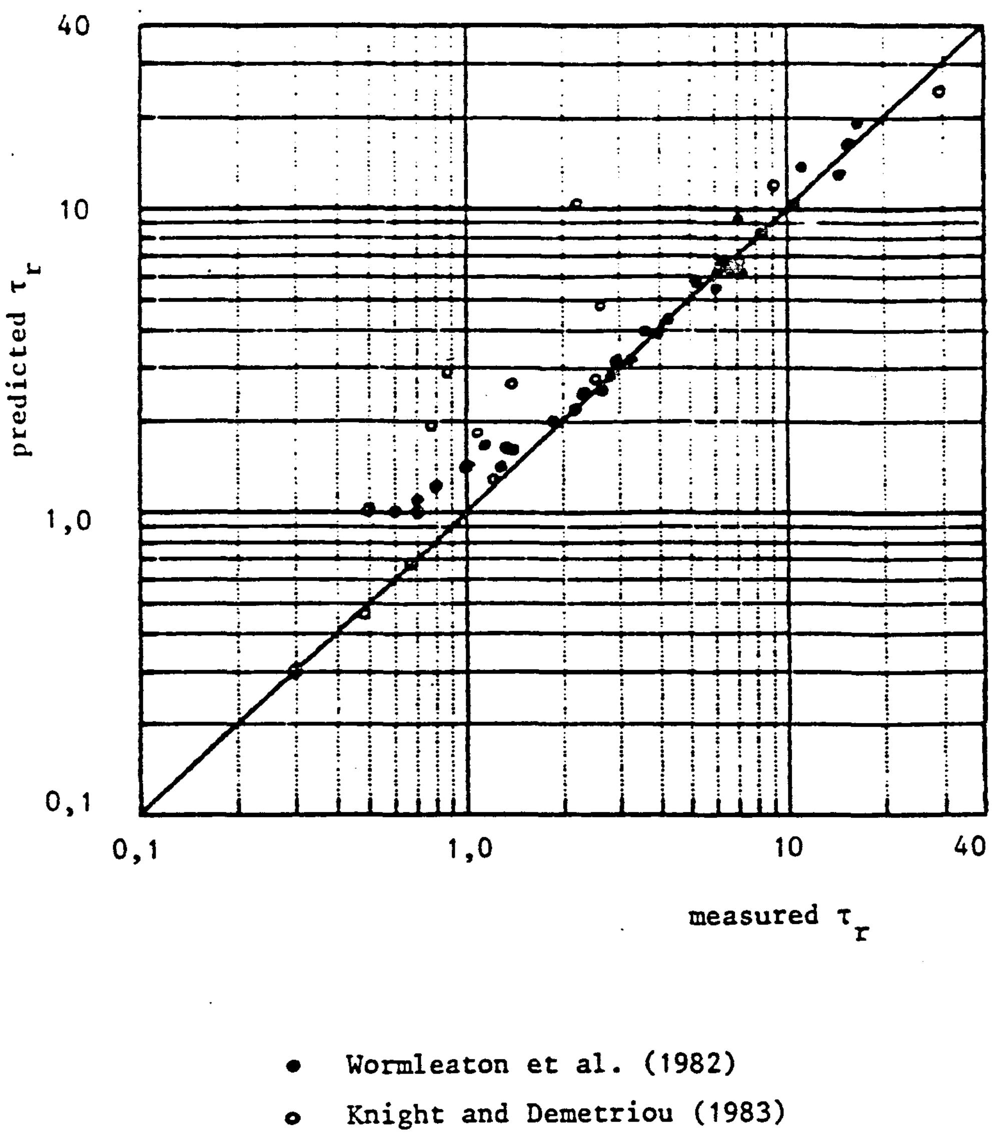

Figure 112. Assessment of the Prinos equation in conjunction with iterative procedure (area method)

- For which channel dimensions the phenomenon can safely be ignored and flood-routing can be simulated using the existing conventional models.

A range of hydrographs were routed through a compound channel with symmetrical flood plains and smooth boundaries. The length of the channel was 5 km and the slope S_0=0,0006. The other parameters were: W_c=3m; W_f=5m; n_c=0,018; n_f=0,036. The dimensions of the channel were kept in the same ratio but to a larger scale as those from the flume experiments performed by Wormleaton et al. (1982).

The separate-channel and area models were used for the simulations. The upstream hydrographs had durations of 6 hours and peaks ranging from 15 m^3/s to 30 m^3/s. Figures 113 and 114 depict the routed flow hydrographs for low and high flows, using the different models. For low flows (Figure 113), the momentum transfer mechanism leads to attenuation of the flowrate hydrograph and the results are similar to the off-channel storage model. The error in the calculated peak is 7% with the area method and more than 10% with the diagonal interface method.

For higher flows (Figure 114), the results of the separate channel and area models are identical. The off-channel storage model underestimated the peak flowrate by 25% while the effect of the momentum transfer mechanism in the calculated total flood discharge hydrograph was found to be minimal.

The effect of the main channel/flood plain interaction is more evident on the water level hydrograph (Figure 115). Even though the calculated peaks were approximately the same with all the methods, the momentum exchange mechanism delayed the falling limb of the water level hydrograph by more than half an hour. Turbulence reduced the flood plain velocities and the flood plains acted only as storage, conveying virtually no discharge.

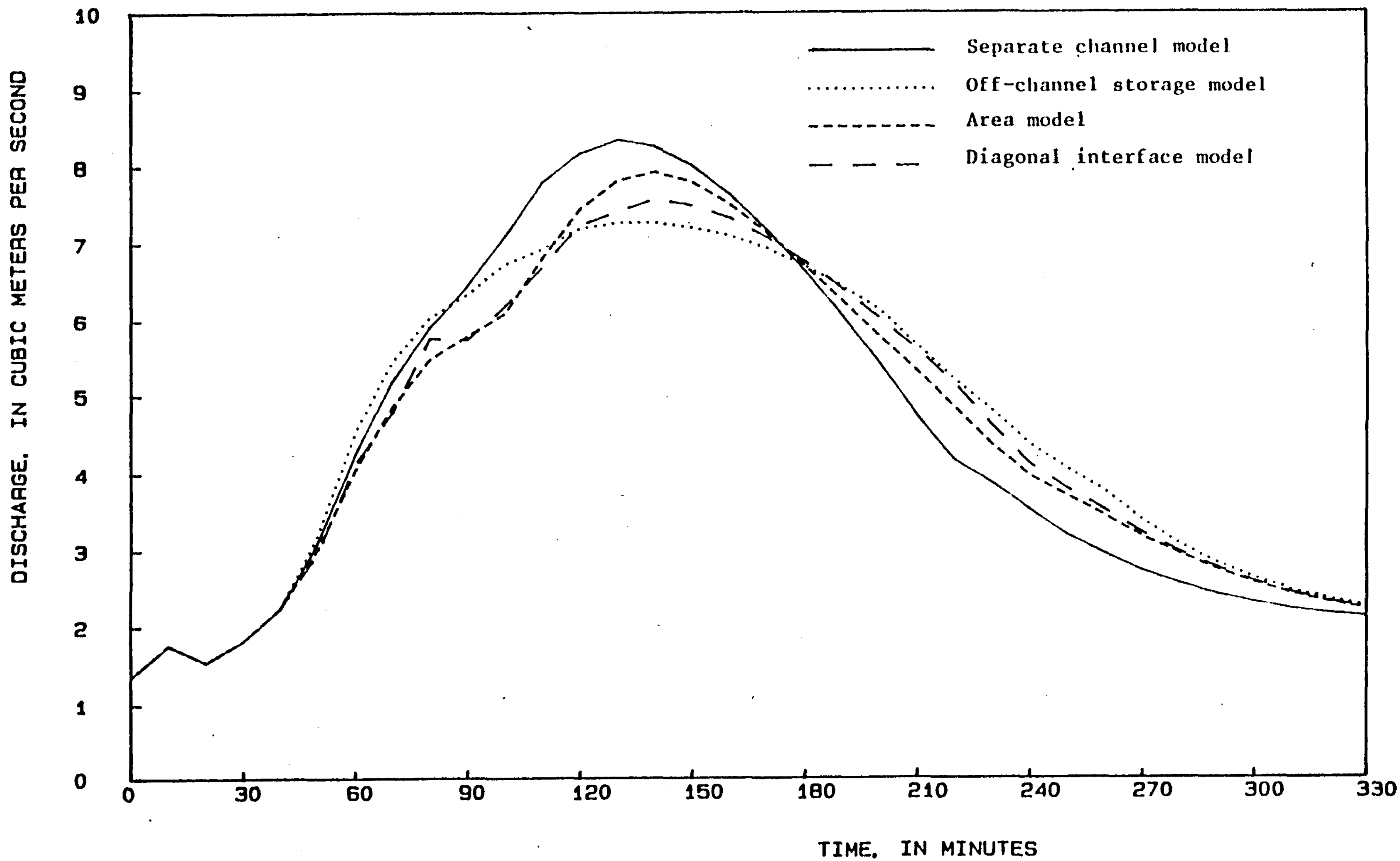

Figure 113. Calculated flood discharge hydrographs by four flood plain models - case study- outlet -(low flows)

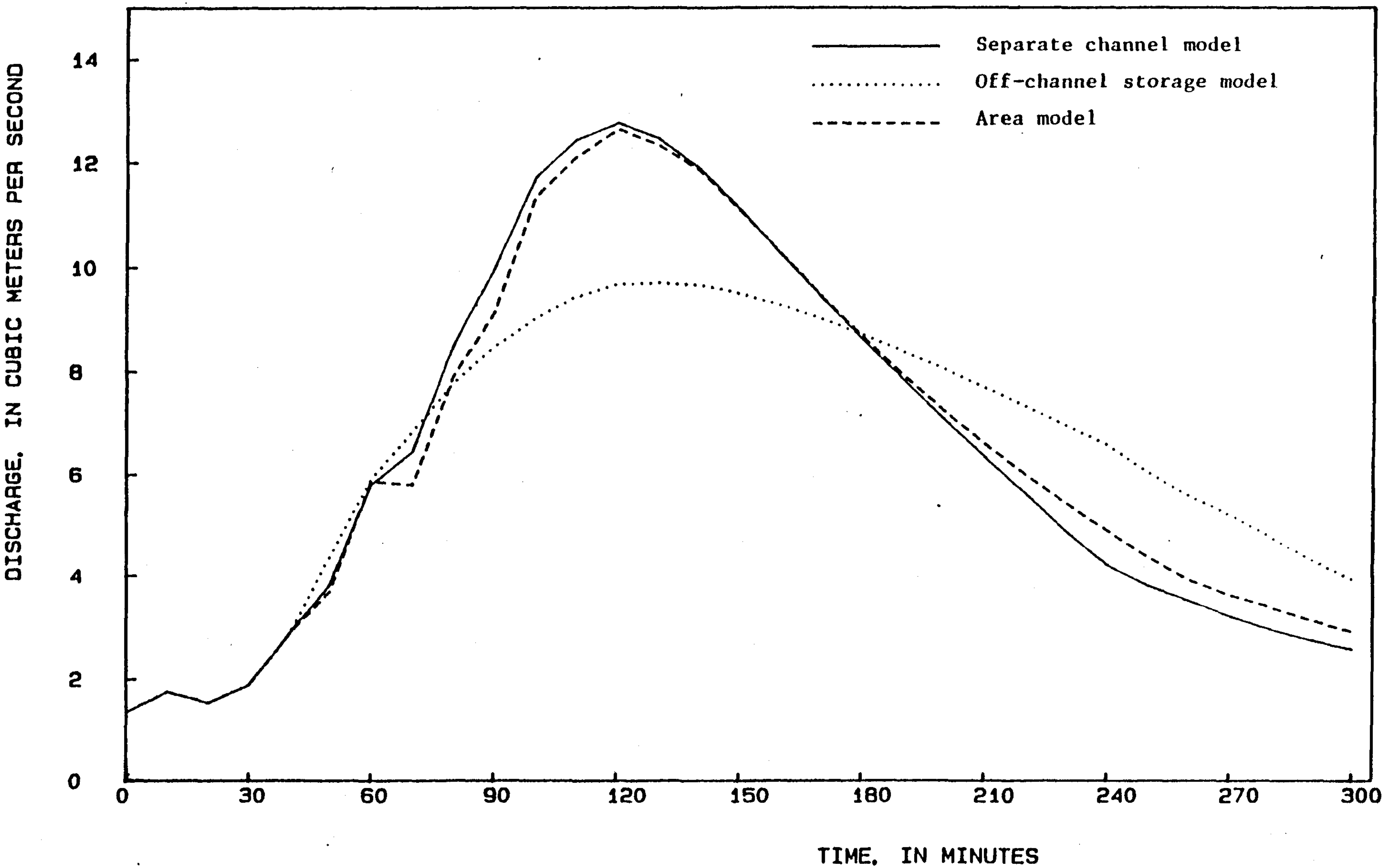

Figure 114. **Calculated flood discharge hydrographs by** three **flood plain models - case study - outlet** (high flows)

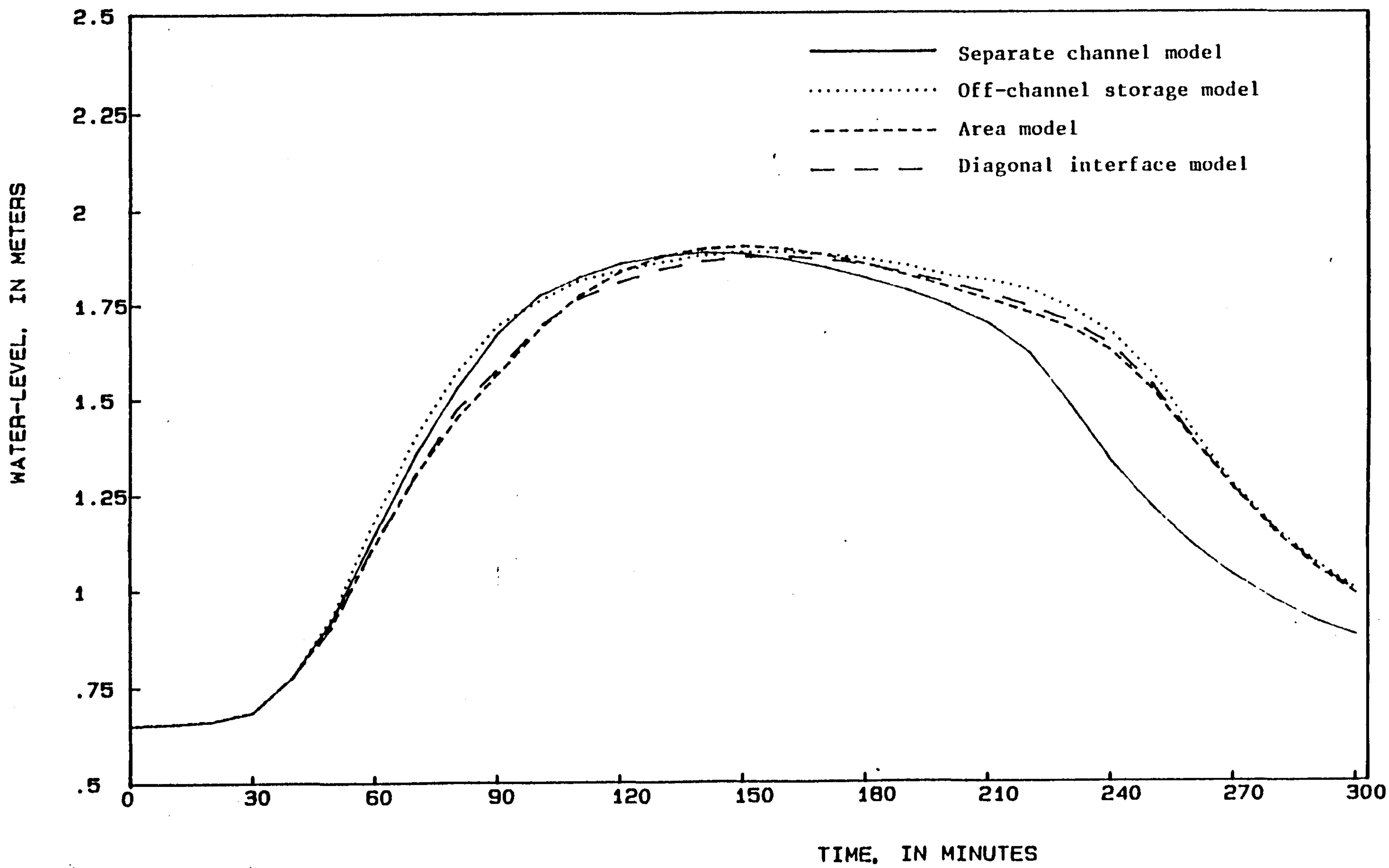

Figure 115. Calculated water-level hydrographs by four flood-plain models - case study - outlet

All the results are better illustrated in the loop-rating curves plotted in Figure 116. The momentum exchange creates a shift of the loop-rating curve downwards and to the right, and a modification of the rising and falling branches of the rating curve. The loop closes somewhat for depths near the junction of the main channel/flood plains and opens at other depths. It is interesting to note that the effect of the momentum mechanism on the loop-rating curve is not the same as the effect of an increase in the roughness of the channel, although both cases result in a decrease in the conveyance. In the latter case the loop-rating curve shifts downwards and to the left and the loop opens up.

Perhaps the most noticeable feature of the results is depicted in Figures 117 and 118. These figures show the distribution of discharge in the main channel and the flood plains, for low and high flows, allowing for the transfer mechanism (area method) and ignoring it (separate-channel method). In spite of the accurate prediction of the total discharge for high flows, if the momentum transfer mechanism is ignored, then the calculated discharges in the main channel and flood plain subdivisions exhibit a large error. The overestimation of the main channel capacity is compensated for by an underestimation of flood plain discharge. The error in each subdivision's flowrate is more than 10%. The results are in agreement with the findings of Wormleaton and Hatjipanos (1985) in their experimental analysis of the flow distribution in compound channels. It is obvious that the separate-channel method does not accurately model the proportions of flow in channel and flood plain at the lower depths. The discrepancy peaks at a depth of 0,40, where flood plain capacity is underestimated by around 27% by the conventional method.

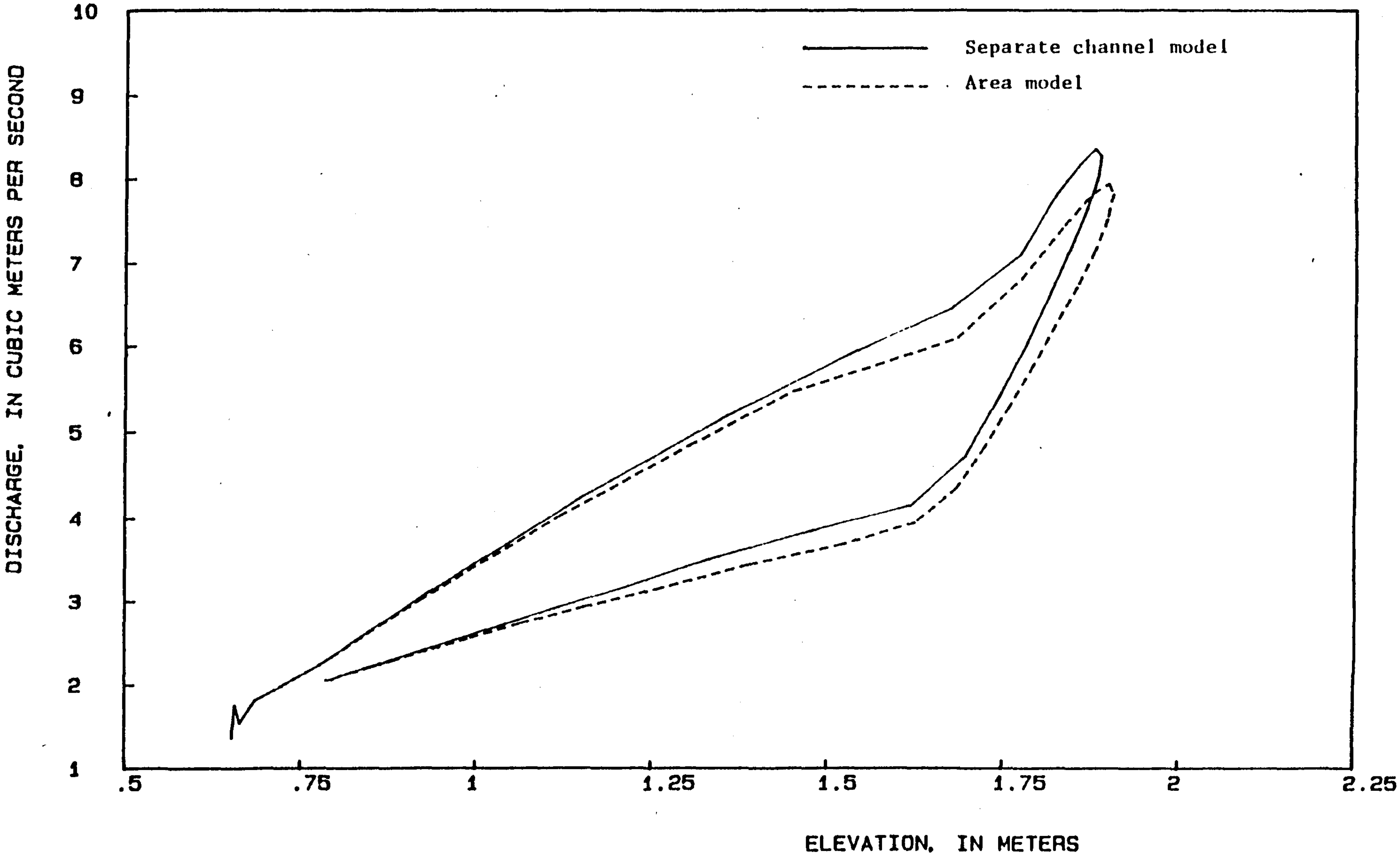

Figure 116. **Shift of the computed loop-rating curve, caused by the momentum transfer mechanism**

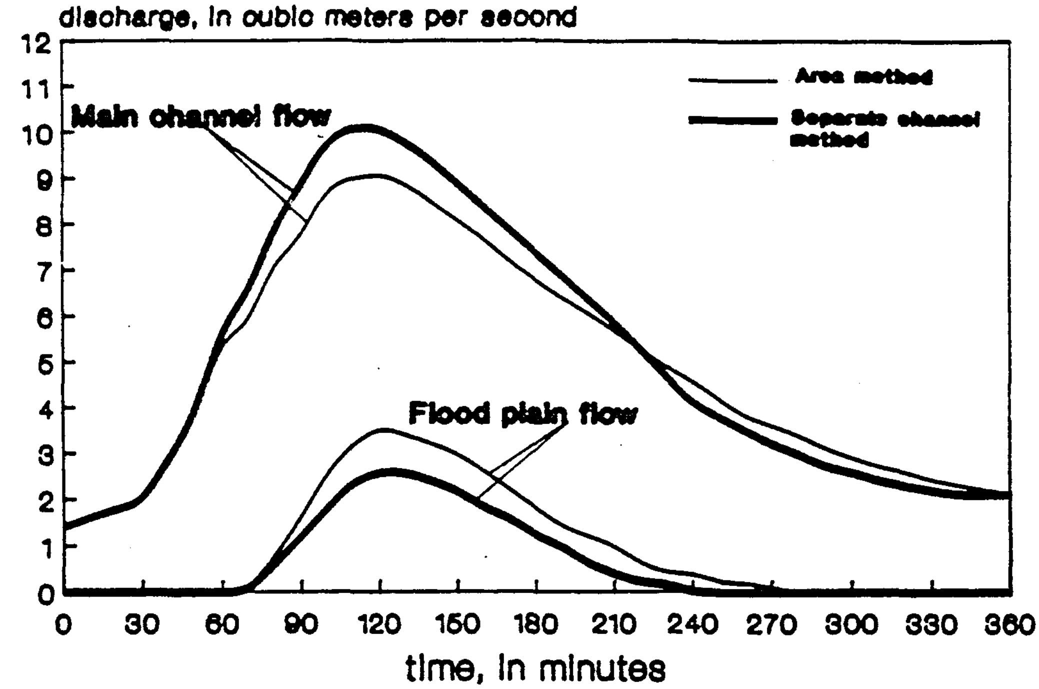

Figure 117. Error in the flow distribution in the main channel and flood plains - case study (high flows)

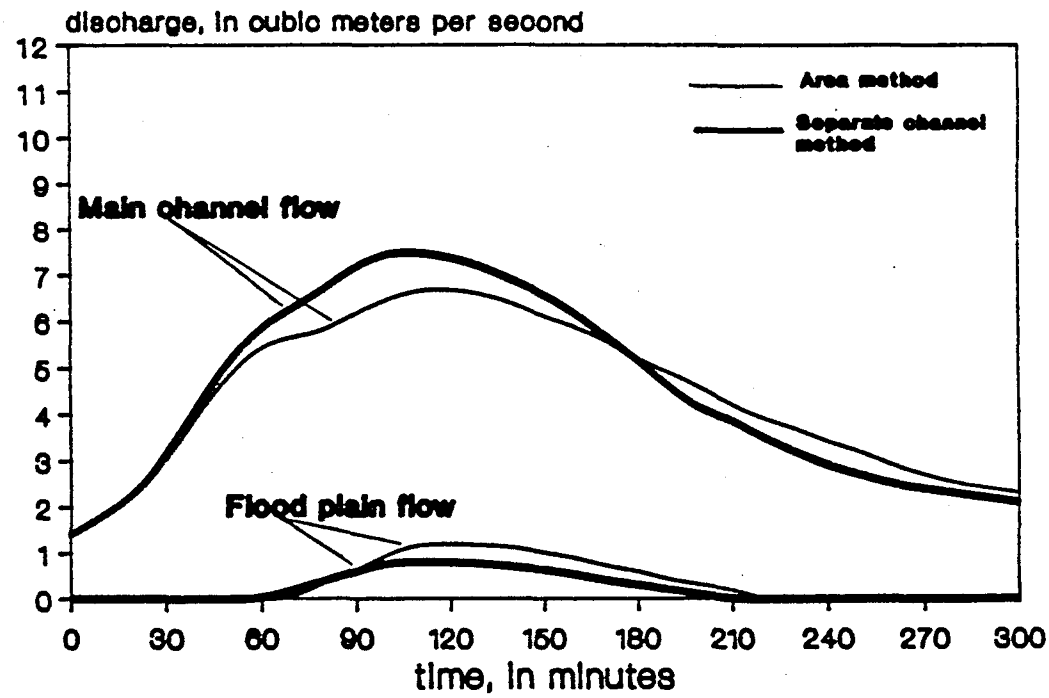

Figure 118. Error in the flow distribution in the main channel and flood plains - case study (low flows)

In conclusion, the analysis showed that the momentum exchange mechanism results in:

- An attenuation of the flowrate hydrograph at low depths.

- A delay in the falling of the water levels.

- A shift of the loop-rating curve.

- An increase in the flood plain flow and a decrease of the main channel carrying capacity.

8.8 SIGNIFICANCE OF THE MOMENTUM EXCHANGE MECHANISM IN THE UNSTEADY FLOW COMPUTATIONS

It is important to investigate the significance of the phenomenon in natural channels with dimensions which are different from the channel used and the range of applicability of the conventional models. The channel parameters were varied in an effort to determine the effect of the momentum transfer mechanism in relation to:

- Roughness
- Slope
- Flood plain width
- Scale effects

Assuming that the observed hydrograph is the one computed at the downstream end of the channel and the simulated hydrograph is the one computed with the separate channel model, two statistics were used in order to identify the accuracy of the assumption that most conventional models ignore this phenomenon in natural rivers. The two statistics are:

- The sum of absolute area/ordinate divergence $(SAAD)_n$
- The modified correlation coefficient MR_{so}

These statistics were selected as they highlight the difference in the shape of the two hydrographs, as outlined in Chapter 5. Values of MR_{so} close to 1, indicate that the difference in the shape of the two hydrographs is minimal, thus the effect of the momentum transfer mechanism can safely be ignored. Alternatively, an increase of $(SAAD)_n$ or a decrease of MR_{so}, in relation to the channel parameter, implies that the effect of the phenomenon with respect to the water level or the flowrate hydrograph shape becomes important.

It was found that the increasing of any of the pertinent parameters in the channel results in main channel/flood plain momentum exchange decreasing drastically. An increase in the roughness of the compound channel, keeping the flood plain/main channel roughness ratio constant (R_f/R_c=ct) reduces the discrepancy of the two hydrographs to a minimum (Figures 119, 120). For roughnesses in the main channel larger than 0,03 the MR_{so} is larger than 0,950 and the $(SAAD)_n$ becomes less than 0,50.

An increase of the river slope has a similar effect (Figure 123). This is to be expected as the parameter describing the turbulence intensity is the relative apparent shear stress ASSR-(τ_r). The ratio ASSR decreases with an increase in the slope. This has been verified experimentally (Wormleaton et al., 1983).

Increase of the flood plain width reduces the $(SAAD)_n$ of the computed water level hydrographs, but the MR_{so} does not become larger than 0,90, even for ratios W_f/W_c greater than 7 (Figures 121, 122). As the width ratio increases, the difference in the discharge hydrographs is minimised but the falling limb of the computed water level hydrograph, taking into account the momentum transferred, is delayed for more than an hour.

Increase of the channel scale (W_c/h) minimises the difference of the computed hydrographs (Figure 124). An increase in the main channel and flood plain widths, keeping their ratio constant, may not affect the turbulence intensity at the interface. The phenomenon is not significant, as the area subtracted or added to the main channel and flood plains, is small when compared to the total area of flow A_T. In other words, as the horizontal dimensions of the channel increase, relative to the main channel depth (h), the total conveyance K(Z) increases, while the change in K(Z) caused by the turbulence phenomenon remains the same or reduces. The increase in the friction slope caused by the main channel/flood plain interaction is therefore minimal.

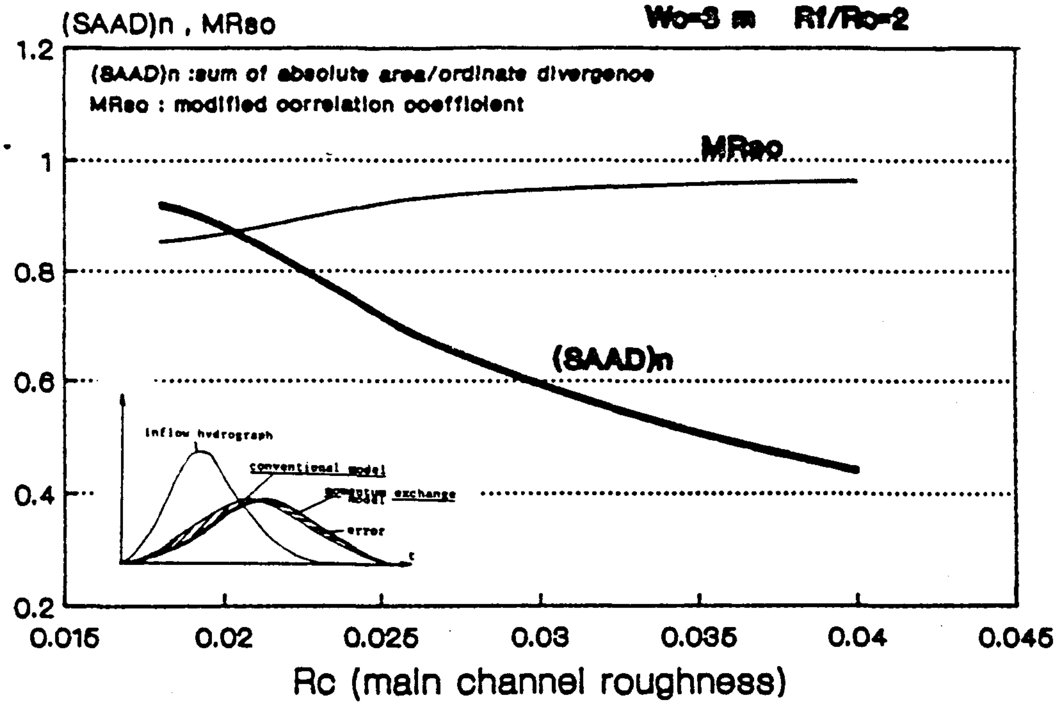

Figure 119. Water level error plot, comparing momentum exchange and conventional models for variations in roughness

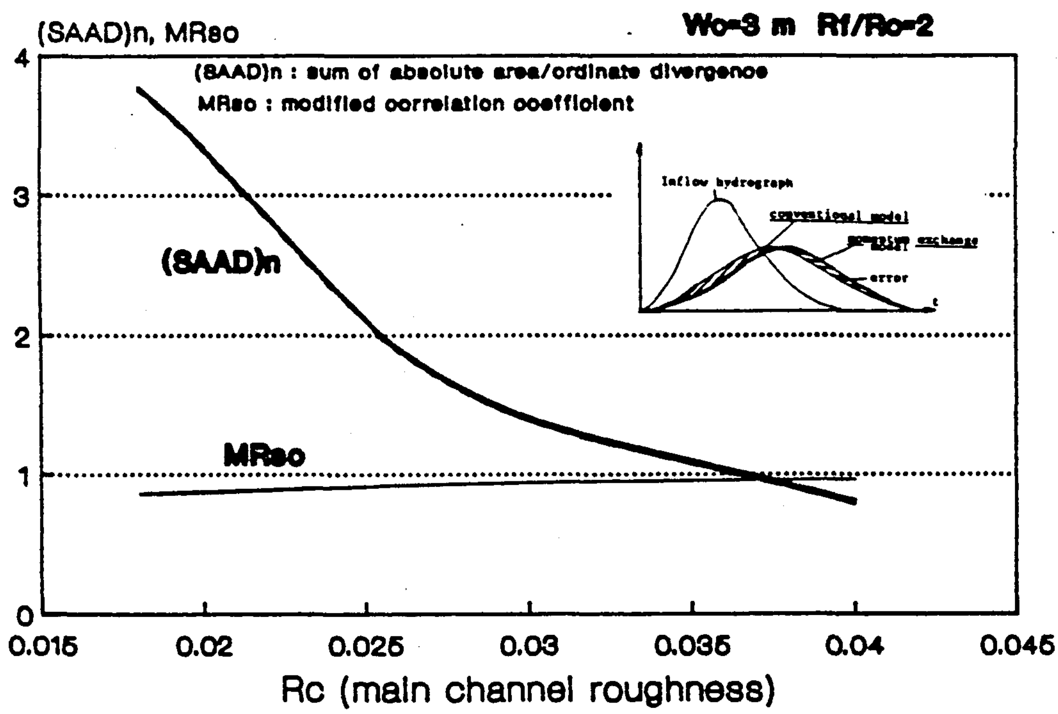

Figure 120. Flowrate error plot, comparing momentum exchange and conventional models for variations in roughness

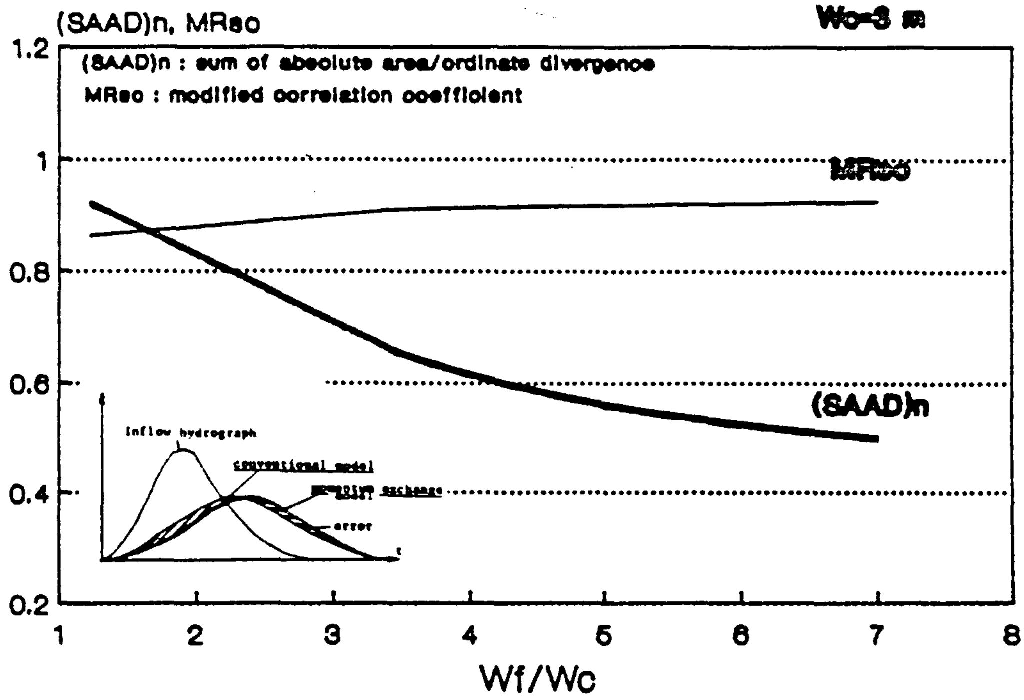

Figure 121. Water level error plot,comparing momentum exchange and conventional models for variations in the main channel/flood plain width ratio

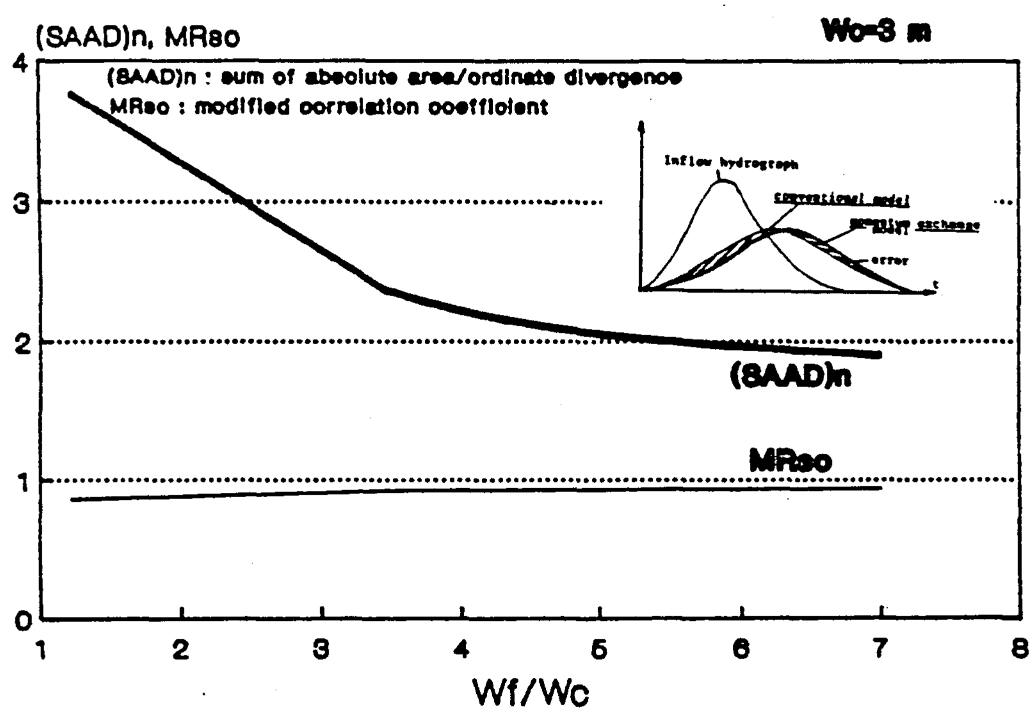

Figure 122. Flowrate error plot, comparing momentum exchange and conventional models for variations in the main channel/flood plain width ratio

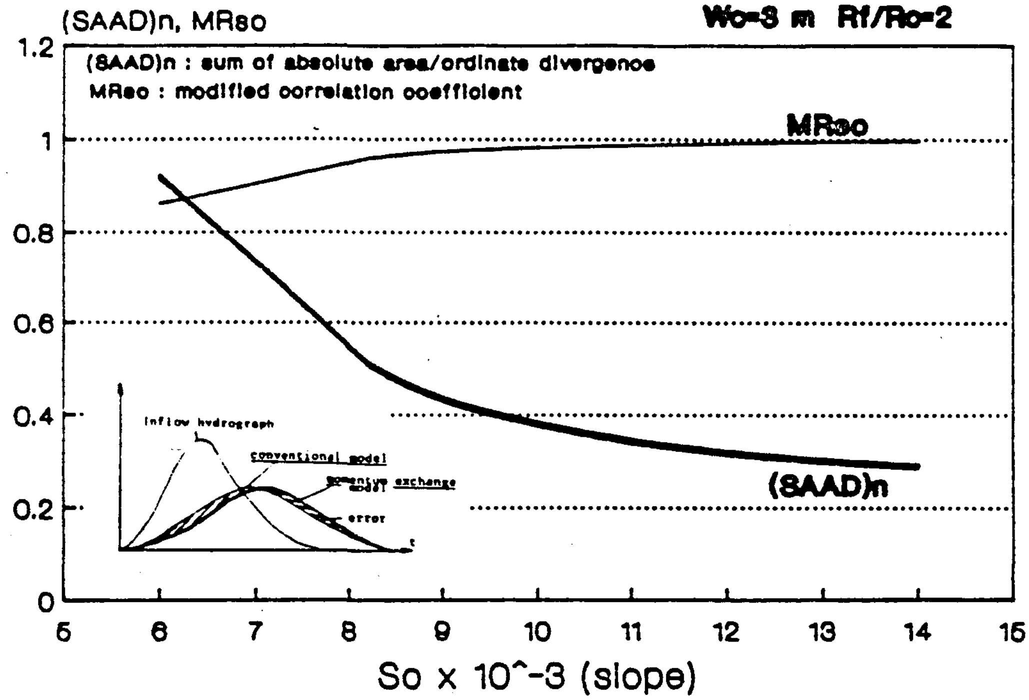

Figure 123. Water level error plot, comparing momentum exchange and conventional models for variations in slope

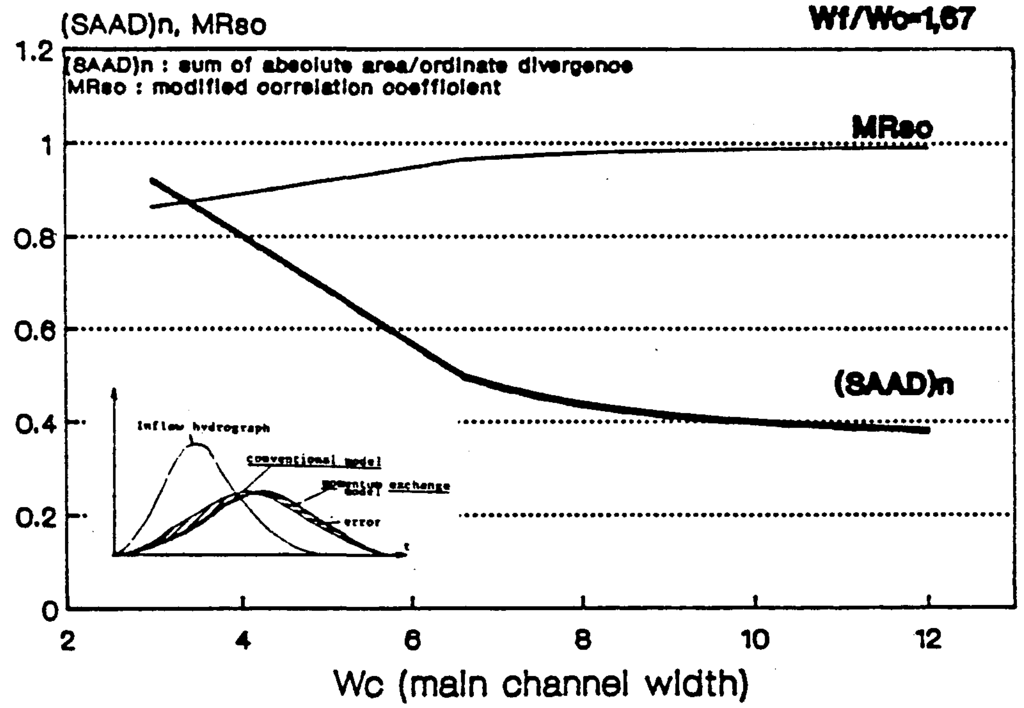

Figure 124. Water level error plot, comparing momentum exchange and conventional models for variations in the main channel width to depth ratio

Although general conclusions cannot be drawn, the above mentioned analysis indicates that:

- For steep rivers (slopes higher than 0,001) the turbulence phenomenon is drastically reduced.

- An increase in the roughness (keeping R_f/R_c constant) reduces the momentum exchange. Roughnesses in the main channel higher than 0,03 and in the flood plain of 0,06 or smaller, reduces the momentum exchange to very low levels.

- Increasing of the flood plain/main channel width ratio, does not reduce the momentum exchange, but results in a longer duration of the peak water levels and a marked increase in the delay of the falling limb of the water level hydrograph.

- The main channel width to depth ratio is a critical parameter (W_c/h - scale effects). For W_c/h ratios larger than 5 the momentum exchange mechanism is no longer significant.

These results were verified by routing hydrographs through the compound channel used in the comparisons of the off-channel storage and separate-channel models. The computed flowrate and water level hydrographs which take into account the momentum exchange (area model) and ignore it (separate-channel model) were identical. Therefore, in natural rivers with large width to depth ratios, the phenomenon of the main channel/flood plain interaction can safely be ignored and any of the conventional models can be used. However, the analysis showed that for flat rivers with smooth boundaries and relatively small main channel width to depth ratios, the conventional models give erroneous results for both the computed flowrates and the water levels.

The above mentioned results must be viewed cautiously with regard to compound channels with very wide flood plains. For rivers with large flood plains, the assumption of a uniform water level is questionable. As discharge decreases, the water level in the main channel tends to fall faster than that on the flood plains and there is a substantial lateral flow from the flood plains to the main channel. The retention of water on the flood plain when the water is falling has two effects:

- o The total discharge (when the water level is above bank full) is less than if the water was uniformly spread across the river at each section.

- o When the water level in the channel is at or below bank full, the drainage of the flood plain tends to increase the discharge along the river.

Therefore, for the simulation of flow in compound channels with very wide flood plains, the modeller must always take into account the accuracy of the assumptions of each model. If the flow is essentially one-dimensional then the "off-channel storage" model is preferable.

9.0 CONCLUSIONS - RECOMMENDATIONS

9.1 SUMMARY AND CONCLUSIONS

The recent floods in South Africa emphasise the need for an easy implemented and reliable model for simulating unsteady flows in natural river systems. The OSYRIS suite of models was developed in an attempt to fill this need. The shortcomings and disadvantages of the existing main-frame river flow simulation models were taken into consideration when formulating goals for the development of OSYRIS.

The model was based on the solution of a box scheme of the Preismann type using an implicit algorithm. Discretizations of the Saint Venant equations proposed by various researchers were examined and compared. Finally a new formulation of the finite difference equations was developed that ensures stability and maintains flexibility. Weighting factors can be specified to vary the implicit solution technique from box centred to fully forward.

The large storage requirements of the implicit schemes, coupled with the fact that the flow model should be capable of running on any common micro computer, made the selection of the model's solution algorithm a difficult task. Different computational procedures were tested in terms of accuracy, computational speed, storage requirements and flexibility. Finally, a looped algorithm technique was employed to reduce machine memory and execution time requirements.

The developed techniques for the solution of the looped network involve complicated procedures, however, the algorithm proved to be efficient in terms of speed and time requirements. The ability of the program to handle looped networks makes the system capable of simulating physical systems which could before, only be simulated by expensive and tedious to use, mainframe, two-dimensional programs.

The input-output formats of the model are designed for easy understanding of the simulation process and minimum data capture effort. The output is in the form of tables and graphics for quick visualisation of the variables involved in the simulation process.

The model was tested with eight examples representing different application problems. It was shown that the model is capable of simulating with minimal distortion, a wide range of unsteady flows, tidal flows, and regulated flows encountered in prototype channels. With regard to the actual time-series generated by the model, the overall performance of OSYRIS compared favourably with the observed data and was very similar to the output generated by other internationally accepted river simulation models (CARIBA). It was shown that the suite of models may simulate very complicated river configurations, i.e. St. Lawrence river, or very specialised flood routing problems, such as a dam failure.

In Chapter 5 a rational calibration and adjustment strategy was developed. The possible model parameters that have to be adjusted were identified and techniques for a sound model calibration were outlined. Based on this analysis the input of the model was designed to assist the modeller during trial and error adjustments and throughout the calibration process.

For model verification, a literature review of statistical goodness-of-fit criteria, relating simulated and observed events was undertaken. As no single statistical goodness-of-fit criterion is sufficient to adequately compare simulated time-series events with those observed, it was decided that the model should include a set of criteria for model verification.

These statistical methods and graphical aids for model verification were assembled into a statistical package. Application of the statistical package was provided for the model's verification in an ocean estuary situated at St. Lucia.

The model was used as a tool for the study of flood propagation in prismatic and compound channels. The unsteady flow model was modified to account for the routing of hydrographs when the downstream boundary condition is not a variable. The suite of models was coupled with a non-linear kinematic model for the routing of floods in natural branched channels. The development of the kinematic model became necessary, as it was shown in Chapter 7 that many flood routing problems can be solved quickly and accurately using a kinematic model, without having to resort to the full dynamic equations. The structure of the suite of models therefore gives the analyst the flexibility to apply any of the approximation models.

In order to clarify the confusion among practising engineers on the appropriateness of the diffusion and kinematic models, all the existing theories on wave subsidence were examined. Applying the small perturbation analysis the spectrum of shallow water waves were divided, taking into account the predominant physical mechanisms and the attenuation characteristics of the waves. The findings of the researchers were combined and tested and practical criteria for determining the applicability of each wave model were developed. Figures 81 to 84 assist the analyst in identifying, prior to the routing, the dominant mechanisms responsible for wave subsidence, the appropriate approximation model, or provide a qualitative knowledge of the quantity of subsidence expected.

In order to obtain a generalised picture of the damping of flood waves in prismatic channels, a parametric study was made to investigate the effect of wave parameters and waves of arbitrary shapes, in conjunction with the defined practical criteria. From the analysis, the following conclusions were drawn:

- o The pertinent parameters that affect the wave subsidence are the wave duration and the slope.
- o The developed criteria offer mainly qualitative guidance as the wave damping is affected by the model's numerical solution and the truncation errors.
- o Other factors such as the wave amplitude and the time to peak have a minor influence on subsidence.

The applicability criteria are a valuable indicator for the modeller in order to predict the wave subsidence in river channels.

In Chapter 8, the momentum transfer mechanism between main channel and flood plain was modelled under unsteady state conditions. From the extensive literature survey regarding research on the momentum transfer mechanism, it was concluded that:

- o There is an almost complete lack of field measurements.
- o All the formulae and methods that have been proposed, have been developed and tested under steady-state conditions.
- o Under certain conditions, the conventional methods of discharge calculation for compound channels may grossly underestimate or overestimate discharge capacity.

The mechanism of the momentum transfer was initially analysed under steady-state conditions. An important parameter that describes the phenomenon was identified; the force acting upon the interface between the main channel and the flood plain, termed the **apparent shear force**. The existing models for the prediction of the apparent shear stress were evaluated with sets of flume data. The Prinos equation was identified as the best model. Having decided on the model that describes the apparent shear stress the best, four existing steady-state discharge computation methods were assessed and compared based on published flume data, incorporating a fairly wide range of bed roughness and flood plain widths. From the evaluation, it was concluded that the most promising method is the **area method**, as it is conceptually sound, it is the most consistent and it does not need any criteria before application.

Since, in the unsteady flow, a steady-state empirical law for the calculation of the friction slope is used, it was logical to extrapolate the procedures of the proposed steady-state methods to develop a more accurate flood routing model. Therefore, the unsteady flow model was modified to incorporate a modified form of the Prinos equation for the calculation of the apparent shear stresses at the interfaces. The area method was then used for the computation of the total conveyance.

By incorporating these features in the model, the effect of the momentum transfer mechanism in flood routing was analysed. A range of hydrographs were routed through a compound channel with symmetrical flood plains. The analysis showed that the momentum exchange results in:

- An attenuation of the flowrate hydrographs at low depths.
- A delay in the falling of the water levels.
- A shift of the loop-rating curve.
- An increase in the flood plain flow and a decrease of the main channel carrying capacity.

These results were derived from the theoretical applications and the conclusions are applicable to channels with specific dimensions as shown in the comparisons. Therefore, it was necessary to investigate the significance of the phenomenon in natural channels with different dimensions from those in the specific channels used. The effect of the momentum transfer mechanism was studied in relation to the roughness, slope, flood plain width and scale effects. The parametric analysis showed that:

- In steep rivers (slopes higher than 0,001) and in rivers with main channel roughness higher then 0,03 the momentum exchange phenomenon is reduced drastically.
- The main channel width to depth ratio, was identified as the critical parameter. For ratios higher than 5, the phenomenon has no significant effect.

The results indicate that in most natural channels, the phenomenon of the main channel/flood plain interaction can safely be ignored and any of the conventional flood routing models can be used. However, for flat rivers with smooth boundaries and relatively small main channel width to depth ratios, the conventional models can give erroneous results.

In Chapter 8, an analysis of the existing conventional flood routing models was performed. The **separate channel** model and the **off-channel storage** model, were compared in terms of computed hydrograph peaks and attenuation times. It was concluded that:

- The assumption in the **off channel storage** model, of storage in the flood plain, can lead to a significant error in flood routing computations for the following reasons;

    - the flowrates are underestimated,
    - the water levels are overestimated,
    - a higher stage is estimated at the flood peak.

    Furthermore the model has theoretical drawbacks as it is not clear at what point the flood plain acts only as storage and no longer contributes to 'the momentum of the compound channel.

- The main reason for the wide application of the model is that it provides a more conservative approach to that of the separate channel model. This is desirable as the computation of the water levels is of the utmost importance in the calculation of flood lines.

All the models developed must be used with caution in regard to compound channels with very wide flood plains. In this case the assumption of a uniform water level is questionable. The flow is essentially two-dimensional as there is substantial lateral inflow from the flood plains to the main channel as discharge decreases.

The subject of compound channel flow simulation is far from being thoroughly understood by experts in the field. The analysis in Chapter 8 shows the complexities of flood routing in compound channels. All the models were included as options in the OSYRIS suite of models. The analyst must always be aware of the assumptions and limitations of each flood routing model. Therefore, it is left to his judgement to decide which of the models should be used.

9.2 RECOMMENDATIONS

Based on the research work carried out in the dissertation, the following recommendations can be listed. These recommendations are firstly valid for practical applications carried out on projects similar to that analysed in the dissertation and secondly, may be considered applicable to more general use of the model. The recommendations are:

- The model will become fully operational only through specific applications, by incorporating subroutines specifically built in for the simulation at hand. Such model improvements are:

- **Irrigation canal simulations**: Complicated structures are a source of instability for the model. Therefore subroutines must be included in the main program for the simulation of galleries, automatic level regulation structures and surge tanks. In this way, the model will be applicable in any system of irrigation canals.
- **Routing flood waves downstream of dam breaches**: Subroutines for the determination of the dam breach outflow hydrograph can be designed, so the analyst can directly generate a range of hydrographs as upstream model boundaries. The subroutines require information such as: reservoir geometry, dam-site cross-sections, dam breach size, tailwater conditions etc. More involved dam-break problems can be simulated by updating the model's structure, such as:
    - Sudden release in the form of instantaneous removal of the dam-barrier retaining the reservoir water.
    - Movement of the released wave by sudden, total opening on to a dry bed, with no flow in the recipient channel or valley for released wave, with a particular emphasis on the dry-bed wave tip or very small base flow.

- The model algorithm can be modified to account for **supercritical flows**. This requires an alternative algorithmic structure and a different formulation of the solution matrices. In such a case, the input to the program must also be updated, as two upstream boundary conditions for every upstream termini of the river network would then be needed.

- The model could be used for **flood forecasting, flood warning and reservoir management**. Various improvements can be directed to this area, such as:

    - Powerful time-series techniques, such as **recursive estimation** (Young, 1984) can be used in the identification, estimation and validation of the model. The recursive approach to estimation allows for continuous updating of the model parameter estimates and the possibility of more advanced "self adaptive" forecasting and control procedures.

- The deterministic hydrological flood routing model could be extended with a stochastic component, thereby describing the information contained in the forecast errors of the model. In such a case a simplified model can be conceived for use in the forecasting itself. Its coefficients are calibrated by repeated use of the full model. The statistical package can then be coupled with stochastical evaluation methods as spectral analysis.

o The model could be extended in order to account for **sediment transport routing**, degradation, and aggragation studies and long term channel development studies. Such a development will help in a better understanding of the dynamics of alluvial rivers. However, this upgrading will require major changes in the model's algorithms, structure and in the input and output subroutines.

o The concept of simulation modelling must include consideration of the **collection and processing of quality prototype data** with which to implement the numerical model and by which to subsequently test, calibrate and verify it. The model will not be fully operational if it is not coupled with a system that would organise and standardise the collection, processing, and filing of the various types of time-series raw data. Various subsystems may be built in, such as:

- A subsystem to process the raw data and load them into a database.

- A subsystem to detect and correct obvious errors, and to process the yielded data in a suitable format for inclusion in an indexed database system.
- A subsystem to analyse river cross-section data in order to transform them into a format directly applicable to the one-dimensional model.

A similar system for the collection and management of urban catchment hydrological data has been developed by the Water Systems Research Group (Lambourne, 1987). The system involves the use of a micro-computer with peripherals for digitising, EPROM (Erasable programmable read only memory), downloading, storage retrieval and archiving of data.

o Regarding the simulation of flow in compound channels and the main channel/flood plain interaction, the research should be directed to the collection of reliable field data, the results of the simulations performed could therefore be more thoroughly tested. Furthermore, flume experiments should be extended to the routing of hydrographs and into different channel shape sections. Promising models such as the λ-method and the area method could then be tested under unsteady flow conditions.

9.3 CONCLUDING REMARKS

An unsteady flow simulation suite of models has been developed that has all the capabilities of standard mainframe models and at the same time it is computationally efficient and accurate. The model has been tested in only a few rivers with encouraging results and it compares favourably with other internationally accepted simulation models. This does not however, prove that the model will perform with similar results in all cases, and more testing and validation is required. This point will be appreciated when one considers that SYSTEM 21 and CARIBA have undergone continuous updating and improvement since their inception more than 10 years ago. Exposure of OSYRIS to the engineering profession in South Africa has evoked some constructive criticism and suggestions for future improvements. It is the author's opinion that this type of exposure is essential in order to achieve as close a degree of perfection as possible.

The suite of programs incorporates all the models developed in this dissertation. The research findings can therefore help the analyst to:

- Select the appropriate wave model.
- Select the appropriate flood routing model.
- Have a qualitative knowledge of the amount of subsidence expected prior to the routing.
- Have a qualitative knowledge of the importance of the main channel/flood plain flow interaction in the specific application.

The OSYRIS suite of programs can be used in South Africa to determine flood levels along urban water courses which affects development along streams. All the above serves as the basis for economic analysis and a more accurate assessment of the consequence of flooding. The suite of models can also be used in research, as in Chapters 7 and 8. It offers an advanced tool for scientific assessment of the various flow parameters, for evaluating the effect of various simulation inputs and a better understanding of the simulation process in complex river systems.

APPENDIX A. REFERENCES

Abbot, M.B. and Ionescu, F., "*On the Numerical Computation of Nearly Horizontal Flows*," Jnl. Hydraulic Res. 5(2), 97-117, 1967.

Abbot, M.B. and Verwey, A., "*Four-Point Method of Characteristics*," Jnl. Hyd. Div. ,ASCE, HY12, Dec. 1970.

Abbot, M.B., "*Continuous flows, Discontinuous flows and Numerical Analysis*," Jnl. Hydr. Res. 12(4), 417-467, 1974.

Abbot, M.B. , "*Computational Hydraulics*," Pitman Publ. Ltd. London, 1979.

Aitken, A.P., "*Assessing Systematic Error in Rainfall-Runoff Models*," Jnl. of Hydrology, Vol. 20, pp. 121-136, 1973.

Akan, A.O. and Yen, B.C., "*A Non-linear Diffusion-Wave Model for Unsteady Open-Channel Flow*," Proceedings of the 17th Congress, International Association for Hydraulic Research, Vol. 2, pp. 181-190, August, 1977.

Amein, M., "*Streamflow Routing on a Computer by Characteristics*," Water Resources Research, Vol. 2, No. 1, pp. 123-130, 1966.

Amein, M., "*Field Application of an Implicit Numerical Method*," Proc. Int. Symp. Unsteady Flow Open Channels, Int. Assoc. Hydraulic Res., Newcastle-upon-Tyne, England, 1976.

Amein, M. and Fang, G.S., "*Implicit Flood Routing in Natural Channels*," Jnl. Hydraulics Division, ASCE, 96(HY12), pp. 2481-2500, Discussion, 97(HY5), pp. 761-762, 1970.

Amein, M. and Chu, H.L., "*Implicit Numerical Modelling of Unsteady Flows*," Jnl. of Hydraulics Division, ASCE, (HY6), June, 1975.

American Society of Agricultural Engineers, Number 5, "*Hydrological Modelling of Small Watersheds*," Edited by Haan C.T., Johnson H.P., and Brakensiek D.L, 1982.

ASCE Task Committe on Glossary of Hydraulic Modelling Terms of the Committee on Research of the Hydraulics Division, "*Modelling Hydraulic Phenomena: A Glossary of Terms*," Jnl. Hyd. Division, pp. 845-850, July, 1982.

Balloffet, A., Cole, E. and Balloffet, A.F., "*Dam Collapse Wave in a River*," Jnl. of Hydraulics Division, ASCE, No. 100, No.(HY5), May, 1974.

Baltzer, R.A. and Lai C., "*Computer Simulation of Unsteady Flow in Waterways*," ASCE Proceedings, Jnl. Hyd. Div., Vol. 94, no. HY4, pp 1083-1117, 1968.

Barishnikov and Ivanov, "*Role of Flood Plain in Flood Discharge of a River Channel*," Proceedings, 14th International Conference of the International Association for Hydraulic Research, Paris, France, 1971.

Basco, D.R., "*On Numerical Accuracy in Computational Hydraulics*," Proc. Ann. Hydr. Spec. Conf. ASCE, 25th, Texas A&M Univ., College Station, Texas, pp.179-186, 1977.

Bathhurst, C.J., "*Slope-area Discharge Gaging in Mountain Rivers*," Jnl. Hyd. Division, ASCE, Vol. 112, No.5, May, 1986.

Bhowmik, N.G. and Demissie, M., "*Carrying Capacity of Flood Plains*," Jnl. of Hydraulic Engineering, ASCE, 108, No. HY3, pp. 443-452, March, 1982.

Brent, R.P., *Algorithms for minimization without derivatives*," Englewood Cliffs, N.J., Prentice-Hall, 1973.

Chaudhry, Y.M. and Contractor, D.N., "*Application of the Implicit method to Surges in Open Channels*," Water Resources Research, 9(6), pp. 1605-1612, 1973.

Cheng, R.T., "*Modelling of Hydraulic Systems by Finite Element Methods*" In "Advances in Hydroscience," (V.T. Chow edition), Vol.11, pp.207-284, Academic Press, New-York, 1978.

Chervet, A. and Dalleves, P., "*Calcul de l' onde de submersion consecutive a la rupture d un barrage*," Schwiszerische Bauzeitung 88, No. 19, May, 1970.

Chow, V.T., *"Open Channel Hydraulics,"* McGraw-Hill, New York, 1959..

Clarke, R.T., *"Mathematical Models in Hydrology,"* Irrigation and Drainage Paper 19, Food and Agriculture Organisation of the United Nations, Rome, Italy, 1973.

Connor, J.J. and Brebbia, C.A., *"Finite Element Techniques for Fluid Flow"* NewsesButterworths, London, 1976.

Constantinides, C.A., *"Two Dimensional Kinematic Modelling of the Rainfall-Runoff Process,"* Report No.1/1982, Hydrological Research Unit, University of the Witwatersrand, 1982.

Cooley, R.L. and Moin, S.A., *"Finite Element Solution of Saint Vecant Equations,"* Jnl. Hydraulics Division, ASCE, HY6, June, 1976.

Corps of Engineers, *"HEC-2 Water Surface Profiles, Users Manual with Supplement,"* Hydrologic Engineering Centre, Corps of Engineers, U.S. Army, Davis, California, November 1976.

Courant, R., Friedriech, K.O and Lewy, H., *"Uber die Partiellen Differenzengleichnungen der Mathematischen Physic"* In Mathematisch Annalen, Vol.100, pp.32-74, 1928.

Cunge, J.A. and Wegner, M., *"Integration numerique des equations d' ecoulement de Barre de Saint-Venant par un schema implicite de differences finies,"* La Houille Blanche, pp. 33-39, 1964.

Cunge, J.A., Holly, F.M., and Verwey J.A., *"Practical Aspects of Computational River Hydraulics,"*, 1981.

Dekker, T.J., *Finding a zero by means of successive linear interpolation,"* in B. Dejon and P. Henrici (editors), Costructive aspects of the fundamental theorem of algebra, New York, Wiley-Interscience, 1969.

Dooge, J.C.L., *"Theory of Flood Routing,"* 3rd chapter from "River Flow Modelling and Forecasting," Edited by Kraijenhoff D.A., and Moll J.R., The Netherlands, 1986.

Dronkers, J.J., "*Tidal Computations in Rivers and Coastal Waters*," North Holland Publ., Amsterdam, 1964.

Dronkers, J.J., "*Tidal Computations for Rivers, Coastal areas, and Seas*," Jnl. Hydraul. Div. ASCE, 95 (HY1), 29-77, 1969.

Electricite de France, "*Tailwater discharge tunnels at Sisteron*," Region d' Equipement Hydraulique Alpes Sud, Marseilles, 1965.

Evangelisti, G., "*Analysis of Unsteady Flow in Open Channels by Characteristics*," NATO Advances Institute, Bressanone, 1966.

Favre, H., "*Ondes de translation dans les canaux decouverts*," Dunod, Paris, 1935.

Fread, D.L., "*Numerical Properties of Implicit Four-Point Finite-Difference Equations of Unsteady Flow*," NOAA Tech. Memo. NWS HYDRO-18. US National Weather Service, Silver Spring, Maryland 1974.

Fread, D.L., "*Flood Routing in Meandering Rivers with Flood Plains*," Rivers 76 - Volume I, Symposium on Inland Waterways for Navigation, Flood Control and Water Diversions, 3rd Annual Symposium of the Waterways, Harbors and Coastal Engineering Division, ASCE, Colorado State University, Fort Collins, Colorado, August, 10-12, 1976.

Friazinov, I.D., "*Solution algorithm for finite difference problems on directed graphs*," Jnl.Math. and Math. Phys., 10, No. 2 (in Russian), 1970.

Fletcher, I., Alan, G., and Hamilton, W.S., "*Flood Routing in an Irregular Channel*," Jnl. of the Engineering Mechanics Division, ASCE, Vol. 93, No. EM3, pp. 45-62, June, 1967.

Garrison, J.M., Granju, J.P., and Price, J.T., "*Unsteady Flow Simulation in Rivers and Reservoirs*," Jnl. of Hydraulics Division, ASCE, Vol. 95, No. HY5, pp. 1559-1576, Sept., 1969.

Gerritsen, F., "*Velocities on Very Long Weirs*," Proc. of the 6th General Meeting I.A.H.R., Vol. 4, 451, 1955.

Garrick, M., Cunnane, C. and Nash, J.E., "*A Criterion of Efficiency for Rainfall-Runoff Models*," Jnl. of Hydrology, Vol. 36, pp. 375-381, 1978.

Ghosh, S.N. and Jena, S.B., "*Boundary Shear Distribution in Open Compound Channel*," Proceedings, Institute of Civil Engineers, London, Vol. 49, pp. 417-430, August 1971.

Ghosh, S.N., "*Boundary Shear Distribution in Rough Compound Channel*," Synopsis, Proceedings of the Institution of Civil Engineers, London, England, Part 2, Research and Theory, Vol. 55, pp. 487, June, 1973.

Green, I.R.A., "*Computer Modelling of Urban Storm Runoff in South Africa*," PhD Thesis presented at the University of the Witwatersrand, 1985.

Green, I.R.A. and Stephenson, D. , "*Criteria for Comparison of Single Event Models*," Jnl. of Hydrological Sciences, 31, 3, pp. 395-411, September, 1986.

Hayami, S., "*On the Propagation of Flood Waves*," Bulletin No.1, Disaster Prevention Research Institute, Kyoto University, Japan, 1951.

Henderson, F.M., "*Open Channel Flow*," Macmillan, New York, 1966.

Herschy, R.W., "*Accuracy*," Hydrometry, R.W. Herschy, Ed. John Wiley and Sons Ltd., New York, N.Y., pp. 353-397, 1978.

Holden, A., "*Shear Stresses and Discharges in Compound Channels*," MSc thesis submitted in the University of the Witwatersrand, Johannesburg, 1986.

Hornberger, G.M., Ebert, J. and Remson, I., "*Numerical Solutions of the Boussinesq Equation for Stream Aquifer Interaction*," Water Resources Research, Vol. 6, No. 2, pp. 601-608, 1970.

Huber, W.C., Heaney, J.P., Nix, S.J., Dickenson, R.E. and Polman, D.J., "*Stormwater Management Model, User's Manual, Version III*," Dept. of Environmental Engineering Sciences, University of Florida, Gainesville, Florida, U.S.A., May, 1982.

Hutchison, I.P.G., "*Lake Staint Lucia- Mathematical Modelling and Evaluation of Ameliorative Measures*", Report no. 1/76, Hydrological Research Unit, 1976.

Isaacson, E., Stoker, J.J. and Troesch, A. "*Numerical Solution of Flow Problems in Rivers*," Jnl. Hyd. Division, ASCE, HY5, pp 1-18, 1958.

Ivanova, A.A., "*Analysis of Stage Discharge Relation in the Propagation of Release Waves in Prismatic Channels (a numerical experiment)*," GGI Trudy, No. 140, pp. 43-63, (in Russian), 1967.

James, C.S., "*Numerical Modelling of Gold Transport and Deposition*," Doctoral thesis, Civil Engineering Department, University of the Witwatersrand, Johannesburg, 1984.

James, C.S., "*Sediment Transfer to Overbank Sections*," Jnl. of Hydraulic Research, Vol. 23, no. 5, 1985.

Jewell, T.K., Nunno, T.J. and Adrian, D.D., "*Methodology for Calibrating Stormwater Models*," Jnl Environmental Division, ASCE, pp 485-501, 1978.

Kamphuis, J.W., "*Mathematical Model Study of the Propagation of Tides in the St. Lawrence River and Estuary*," National Research Council, Report DME MH 105, Ottawa, Canada, August, 1968.

Kamphuis, J.W., "*Mathematical Tidal Study of St. Lawrence River*," Jnl. of the Hydraulics Div., ASCE, Vol. 96, No. (HY3), March, 1970.

Katopodes, N.K., "*A Dissipative Galerkin Scheme for Open-Channel Flow*", Jnl. Hyd. Div., ASCE, pp.450-466, 1984.

Knight, D.W. and Demetriou, J.D., "*Flood Plain and Main Channel Flow Interaction*," Proceedings, ASCE, Journal of Hydraulics Division, Vol. 109, HY8, pp. 1073-1092, August 1983.

Knight, D.W., Demetriou, J.D. and Hamed, M.E., "*Hydraulic Analysis of Channels with Flood Plains*," Paper from International Conference on Hydraulic Aspects of Floods and Flood Control, Editors Stephens and Stapleton, pp. 129-144, London, 13-15 September 1983.

Knight, D.W and Hamed, M.E., "*Boundary Shear in Symmetrical Compound Channels*," Jnl. of Hydraulics Division, ASCE, Vol. 110, No. 10, pp. 1412-1426, October, 1984.

Knight, D.W. and Lai, C.J., "*Turbulent Flow in Compound Channels*," International Symposium on Refined Flow Modelling and Turbulence Measurements, USA, September 1985.

Kolovopoulos P., "*Modelling the Effect of Urbanization on Storm Flow in the Braamfontein Spruit*," MSc thesis submitted in the University of the Witwatersrand, Johannesburg, 1986.

Kolovopoulos P. and Stephenson D., *The Development of a Modelling System for the Routing of Floods*," Floods in Perspective, CSIR Conference, 20-21 October, 1988.

Kovacs, Z. P., *Regional maximum flood peaks in Southern Africa*," Department of Water Affairs, (in preparation), 1988.

Lai, C., "*Flows of Homogeneous Density in Tidal Reaches, Solution by the Implicit Method*," U.S. Geological Survey Open-File Rep., 1965.

Lai, C., "*Computation of Transients Flows in Rivers and Estuaries by the Multiple-Reach Implicit Method*," Geological Survey Research, Geol. Survey Prof. Paper 575-B, pp.B228-B232, 1967.

Lai, C., Schaffranek R.W., and Baltzer, A.R., "*An Operational System for Implementing Simulation Models: A Case Study*," Seminar on Computational Hydraulics the 26th Annual Specialty Conference, Hydraulics Division, ASCE, University of Maryland, August, 1978.

Lai, C., "*Procedures and Techniques for a Rational Model Adjustment in Numerical Simulation of Transient Open-Channel Flow*," International Conference on Numerical Modelling of River, Channel and Overland Flow for Water Resources and Environmental Applications, Bratislava, Czechoslovakia, May 4-8, 1981.

Lai, C., *"Numerical modelling of Unsteady Open Channel Flow,"* Advances in Hydroscience, Vol. 14, 1986.

Lambourne, J.J, *"Urban Catchment Data Management System,"* Fourth International Conference on Urban Storm Drainage, Lausanne, 1987.

Ligget, J.A. and Woolhiser, D.A., *"Difference Solutions of the Shallow Water Equations,"* Jnl. Eng. Mech. Div., ASCE, April 1967.

Ligget, J.A. and Cunge, J.A., *"Numerical Methods of Solution of the Unsteady Flow Equations,"* Unsteady Flow in Open Channels, edited by K. Mahmood and V. Yevjevich, Vol. I, Chapter 4, 89-182, Water Resour. Pub., Ft. Collins, Colorado, 1975.

Lighthill, M.J. and Whitham, G.B., *"On Kinematic Waves, I.-Flood Movement In Long Rivers,"* Proceedings, Royal Society of London, Series A, 229, pp. 281-316, 1955.

Manley, R.E., *"Improving the Accuracy of Flow Measurement of Open Channel Sites,"* Water Services, Vol. 81, No. 98, Dec. 2, 1977.

Manley, R.E., *bration of Hydrological Model Using Optimisation Technique,"* Jnl. of Hyd. Division, ASCE, Vol. 104, No. HY2, February 1978.

Martin, C.S. and DeFazio, G.F., *"Open Channel Simulation by Digital Computer,"* Jnl. Hyd. Division, ASCE, HY6, pp. 2049-2060, 1969.

Mayne, W.M., *"The use of Micro-Computers by Civil and Structural Engineering Consultants,"* Research Report, Graduate School of Business Administration, University of the Witwatersrand, May, 1984.

Meis, T. and Markowitz, U., *"Numerical Solution of Partial Differential Equations,"* Springer-Verlang 1981.

McCarthy, G.T., *"The Unit Hydrograph and Flood Routing,"* Unpublished manuscript presented at a Conference of the North Atlantic Division, US Army Corps of Engineers, 24 June, 1938.

McCuen, R.M. and Snyder, W.M., "*A Modified Weighted Pearson Coefficient*," Water Resources Research, Vol. 11, No.6, December, 1975.

McKenzie, R. S., "*Hydrology of Vaal Dam Catchment; Vaal River System Analysis*," Department of Water Affairs, Report 4161/04 October, 1985.

Menendez, A.N. and Norcini, R., "*Spectrum of Shallow Water Waves: An Analysis*," Jnl. of the Hydraulics Division, ASCE, Vol. 108, No. (HY1), January, 1982.

Miller, A.R., "*PASCAL programs for Scientists and Engineers*," Sybex, 1981.

Miller, W.A. and Cunge, J.A., "*Examples of One-dimensional Flow Modelling*," Unsteady Flow in Open Channels, edited by K. Mahmood and V. Yevjevich, Vol. I, Chapter 11, 407-484, Water Resour. Pub., Ft. Collins, Colorado, 1975.

Mozayeny, B. and Song, C.S., "*Propagation of Flood Waves in Open Channels*," Jnl. of the Hydraulics Division, ASCE, Vol.95, No. (HY3), Proc. Paper 6561, pp. 877-892, March, 1969.

Myers, W.R.C., "*Boundary Shear Stress and Momentum Transfer in Open Channels of Complex Cross-sections*," PhD. thesis, Queens University, Belfast, May 1973.

Myers, W.R.C., "*Momentum Transfer in a Compound Channel*," Jnl. of Hydraulic Research, Delft, Vol. 16, pp. 139-150, 1978.

Myers, W.R.C. and Elsawy, E.M., "*Boundary Shear in Channel with Flood Plain*," Proceedings, ASCE, Jnl. of Hydraulics Division, Vol. 110, (HY7), pp. 933-946, July 1975.

Myers, W.R.C., "*Velocity and Discharge in Compound Channels*," Jnl. of Hydraulic Engineering, Vol.113, No. 6, June, 1987.

Nash, J.E. and Sutcliffe, J.V., "*River flow forecasting through conceptual models, Part 1: A Discussion of Principles*," Jnl. of Hydrology, Vol. 10, pp.282-290, 1970.

Natural Environmental Research Council, *"Flood Studies Report - Volume III - Flood Routing Studies,"* London, 1975.

O' Brien, G.G., Hyman, M.A. and Kaplan, S., *"A Study of the Numerical Solution of Partial Differential Equations,"* Jnl. of Mathematics and Physics, Vol. 29, No. 4, pp. 223-251, 1950.

Pegram, G. and Adamson, P., *"Revised risk analysis for extreme storms and floods in Natal/KwaZulu,"* The Civil Engineer in South Africa, January 1988.

Perkins, F.E., *"Flood Plain Modelling,"* Water Resource Bull., 6 (3), pp. 375-383, 1970.

Perkins, F.E., *"The Role of Damping in Numerical Stability,"* presented at the ASCE National Meeting on Environmental Engineering, held at Chattanooga, Tennesse, May 13-17, 1967.

Pitman, W.V., *"A Mathematical Model for Generating Daily River Flows from Meteorological Data in South Africa,"* Report 2/76, Hydrological Research Unit, University of the Witwatersrand, Johannesburg, 1976.

Ponce, V.M. and Simons, D.R., *"Shallow Water Wave Propagation in Open Channel Flow,"* Jnl. of the Hydraulics Division, ASCE, Vol. 103, (HY12), Proc. Paper 13392, pp. 1461-1476, December, 1977.

Ponce, V.M., Li, R.M. and Simons, D.B., *"Applicability of Kinematic and Diffusion Models,"* Jnl. of the Hydraulics Division, ASCE, Vol. 104, No. (HY3), March, 1978.

Posey, C.J., *"Computation of Discharge Including Overbank Flow,"* Jnl. of Hydraulic Div., ASCE, pp. 62-63, April, 1967.

Prandle, D. and Crookshank, N., *"Numerical Model Studies of the St. Lawrence River,"* MH-109, Hydraulics Laboratory, National Research Council of Canada, Ottawa, Ontario, Canada, July, 1972.

Prandle, D. and Crookshank, N., *"Numerical Model of St. Lawrence River Estuary,"* Jnl. of the Hydraulics Division, ASCE, Vol. 100, No. (HY4), April, 1974.

Preissmann, A., "*Propagation des intumescences dans les canaux et rivières*," First Congress of the French Association for Computation, Grenoble, September 1961.

Preissmann, A. and Cunge, J.A., "*Calcul des intumescences sur machines electroniques*," IX meeting of the IAHRE, Dubrovnik 1961.

Prinos, P., Townsend, R. and Tavoularis, S., "*Structure of Turbulence in Compound Channel Flows*," Jnl. of Hydraulics Div., ASCE, Vol. 111, (HY9), pp. 1246-1261, September, 1985.

Radojkovic, "*Mathematical Modelling of Rivers with Flood Plains*," Rivers 76 - Volume I, pp. 56-64, Symposium on Inland Waterways for Navigation, Flood Control and Water Diversions, 3rd Annual Symposium of the Waterways, Harbors and Coastal Engineering Division, ASCE, Colorado State University, Fort Collins, Colorado, August, 10-12, 1976.

Rajaratnam, N. and Ahmadi, R., "*Hydraulics of Channels with Flood Plains*," Jnl. of Hydraulics Research, Vol. 19, No. 1, pp. 43-60, 1981.

Roache, P.J., "*Computational Fluid Dynamics*," Hermosa Publishers, Albuquerque, N.M, 1972.

Robbins, G.L., "*Suspended Sediment and Bed Material Studies on the Lower Mississippi River*," Vicksburg District, Vicksburg, Mississippi, (unpublished), 1976.

Sarma, P.B.S., Deleur J.W., and Rao A.P., "*A Program in Urban Hydrology*," Part 2, Technical Report 9, Water Resources Res. Centre, Purdue Univ., Lafayette, Ind., 1969.

Schaffranek, R.W. and Baltzer, R.A., and Goldberg, D.E., "*A Model for Simulation of Flow in Singular and Interconnected Channels*," Book 7, Chap.3. U.S. Geol. Survey Tech. of Water Resour. Inv., 1981.

Sellin, R.H., "*A Laboratory Investigation into the Interaction between the Flow in the Channel of a River and that over its Flood Plain*," La Houille Blanche, Grenoble, France, No. 7, pp. 793-802, 1964.

Smith, L.H. and Cheng, R.T., "*A Galerkin Finite Elemet Solution of the One-Dimensional Unsteady Flow Problems Using a Cubic Hermite Polynomial Basis Function*," Proc. International Conference on Coastal Engin., ASCE 15th, Honolulu, Hawaii, 1976.

Snyder W.M., Mills, W.C. and Stephens, J.C., "*A Method of Derivation of Non-constant Watershed Response Functions*," Water Resourses Res., 6(1), pp. 261-274, 1970.

Societe du Canal de Provence et d' amenagement de la region Provencale, "*Ecoulements trasitoires a Surface libre modele d' Hayami*," ref. FD/mp 40/84 - 240, 1984.

SOGREAH, "*Modelling of Unsteady Flow in River and Flood Plain Networks using the CARIMA System*,", 1978.

Stephenson, D., "*Direct Optimisation of Muskingum Routing Coefficients*," Jnl. of Hydrology, Vol. 41, pp 161-165, 1979.

Stoker, J.J, "*The Formation of Breakers and Bores*," Communications on Pure and Applied Mathematics, Vol. 1, pp. 1-87, 1948.

Stoker, J.J., "*Numerical Solution of Flood Prediction and River Regulation Problems: Report I. Derivation of Basic Theory and Formulation of Numerical Method of Attack*," Rep. No. IMM-200, Inst. of Mathematical Science, New York Univ., New York, 1953.

Stoker, J.J., "*Water Waves*," Wiley (Interscience), New York, 1957.

Strelkoff, T., "*Numerical Solution of the Saint-Venant Equations*," Jnl. Hyd. Div., ASCE, January, 1970.

Tingsanchali, T. and Ackerman, N.L., "*Effects of Overbank Flow in Flood Computations*," Jnl. of Hyd. Division, ASCE, July, 1976.

Toebes, G.H. and Sooky, A.A., "*Hydraulics of Meandering Rivers with Flood Plains*," Jnl. Wat. & Harbours Div., ASCE, (WW2), pp. 213-236, May, 1967.

Townsend, D.R., "*An Investigation of Turbulence Characteristics in a River Model of Complex Cross-section*," Proc. Institute ASCE, Vol. 40, pp. 155-175, June, 1968.

U.S. Dept. of Commerce - Bureau of Public Roads, "*Hydraulics of Bridge Waterways*," First Edition, 1960.

U.S. Dept. of Transportation, "*Hydraulics of Bridge Waterways*," Hydraulic Design Series No. 1, Second Edition, Revised March, 1978.

Vasilief, O.F., "*Numerical Solution of the Non-linear Problems of Unsteady Flow in Open Channels*," Proceedings of the 2nd International Conference on Numerical Methods in Fluid Dynamics, Berkley, 1970.

Verwey, A., "*Mathematical Model for Flow in Rivers with Realistic Configuration*," Report series No.12, International Courses in Hydraulic and Sanitary Engineering, Delft, 1971.

Viessman, W., Jr., Harbaugh, T.E. and Knapp, J.W., "*Introduction to Hydrology*," Intext Educational Publishers, New York, N.Y., 1972.

Wallis, J.R. and Todini, E., "*Comment Upon the Residual Mass-Curve Coefficient*," Jnl. of Hydrology, Vol. 24, pp. 201-205, 1975.

Weiss, H.W. and Midgley, D.C., "*Suite of Mathematical Flood Plain Models*," Jnl. Hyd. Division, (HY3), pp. 361-375, March, 1978.

Wignyosukarto, B., "*Ecoulement trasitoire en canal- Application a la regulation*," Rapport de D.E.A. de Mecanique des Fluides, Ecole Nationale Superieure de Grenoble, 1983.

Wilkinson, J.H. and Reisch, C., "*Handbook for Automatic Computation*" Vol II, Linear Algebra, Springer-Verlang, 1971.

Wormleaton, P.R., Allen, J. and Hadjipanos, P., "*Discharge Assessment in Compound Channel Flow*," Jnl. of Hydraulics Div., ASCE, Vol. 108, (HY9), pp. 975-994, September, 1982.

Wormleaton, P.R. and Karmegam, M., "*Parameter Optimisation in Flood-Routing*," Jnl. of Hydraulics Division, ASCE, Vol. 110, No. 12, pp no. 19352, December, 1984.

Wormleaton, P.R. and Hadjipanos, P., "*Flow Distribution in Compound Channels*," Jnl. of Hydraulics Division, ASCE, Vol. 111, No. 2, February, 1985.

Wright, R.R. and Carstens, H.R., "*Linear Momentum Flux to Overbank Sections*," Jnl. of the Hydraulics Division, ASCE, Vol. 96, No. (HY9), pp. 1781-1793, September, 1970.

Wylie, E.B. and Streeter, V.L., "*Fluid Transients*," McGraw-Hill, New York, 1978.

Yen, B.C., "*Open Channel Flow Equations Revisited*," Jnl. of Environ. Eng., ASCE, October, 1973.

Yen, B.C. and Overton, D.E., "*Shape Effects on Resistance in Flood Plain Channels*," Jnl. of Hydraulics Div., ASCE, Vol. 99, (HY1), pp. 219-238, January, 1973.

Young, P.C., "*Recursive Estimation and Time-series Analysis: An Introduction*," Springer Verlag: Berlin, 1984.

Zheleznyakov, G.V., "*Relative Deficit of Mean Velocity of Unstable River Flow; Kinematic Effect in River Beds with Flood Plains*," Proceedings of the 11'th International Association for Hydraulic Research, Leningrad, USSR, 1966.

APPENDIX B. USER'S MANUAL

B.1 INTRODUCTION

OSYRIS-Version I is an interactive micro-computer orientated suite of programs for simulation of flow in channel networks. It may be used for:

- Steady-state (backwater) calculations
- Flood routing
- Unsteady flow simulation

The suite of programs is able to simulate a river, its tributaries, inundated plains, and hydraulic structures (e.g. bridges etc.). Information on the development and background theory of the models employed in the suite of programs is contained in Chapters 2 to 5 of Volume I.

The model is intended to be used on any stream network where the flow can be regarded as one dimensional (Figure B.1). The ability of the program to handle looped networks makes the system capable of simulating physical systems which could previously only be simulated by expensive and non-user-friendly two-dimensional programs. The engineer using an operational system such as OSYRIS, is concerned only with the physical aspects of the problem, as with the user of a scale model. The 'OSYRIS' suite of programs should not however be treated as a 'black box' giving answers, with the engineer being unaware of its limitations and constraints. The engineer must always be familiar with the **logic**, **assumptions** and the **range of applicability** of the program.

An experienced modeller with knowledge of computational hydraulics can apply 'OSYRIS' to his individual research needs. Using 'OSYRIS' the attenuation and dispersion characteristics of waves, the physical characteristics, the steepening of the kinematic wave and the associated kinematic shock phenomena may be analysed. Although the suite of programs is capable of modelling very complicated situations, its application to simple problems requires minimal input and user knowledge.

The 'OSYRIS' suite of programs can be used to determine flood-levels along urban water-courses which will in turn control development along streams. The above elements serve as the basis for economic analysis and a more accurate assessment of the consequences of flooding.

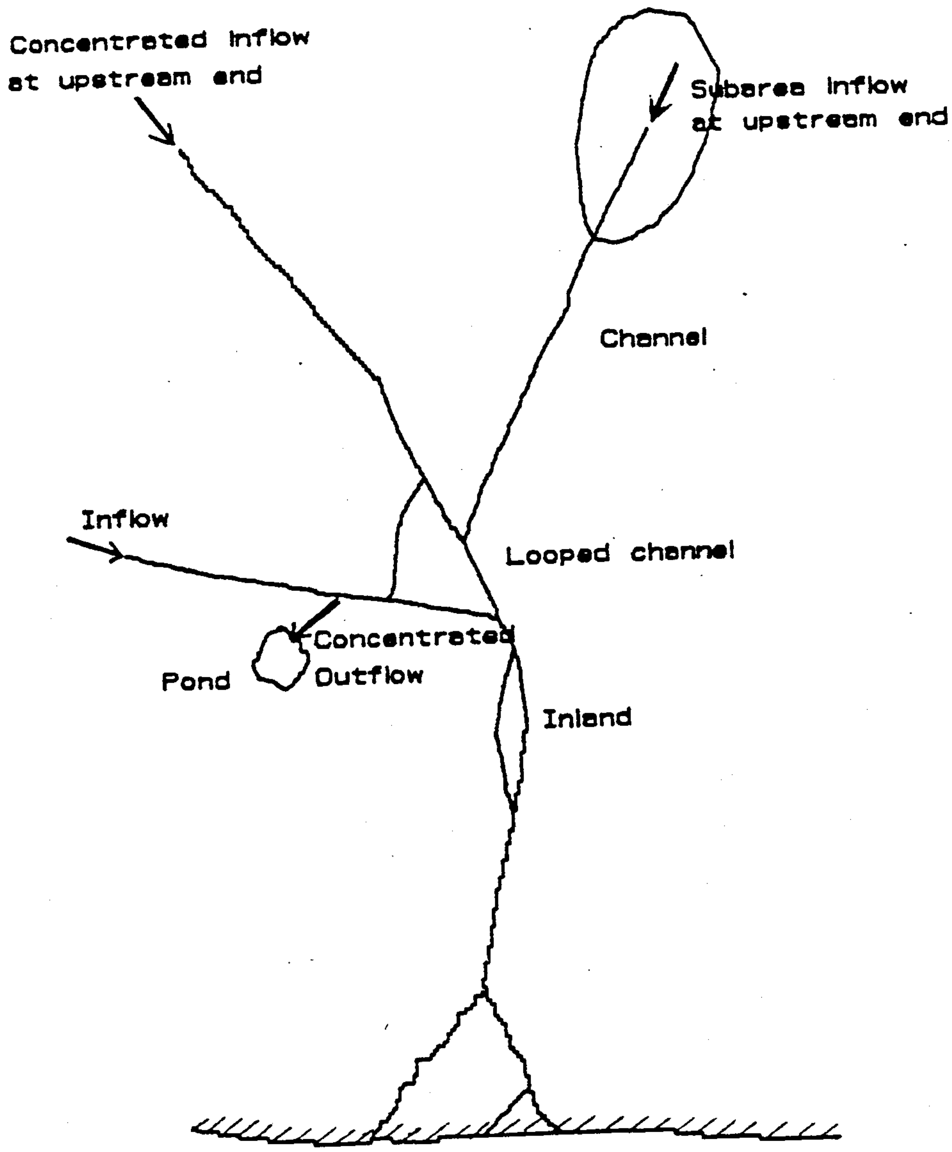

Figure B.1 - An example of a complex river system

B.2 REPRESENTATION OF STREAM SYSTEMS

B.2.1 STREAM CHANNEL NETWORK REPRESENTATION

'OSYRIS' represents an actual channel network by a series of branches. Any form of channel network may be modelled, including single streams, convergent, divergent and looped networks, and any combination of these (Figure B.2). The direction of flow is not important as the model is based on the solution of the full Saint Venant equations and therefore backwater effects are always considered.

The program is dimensioned to accommodate 20 branches, and each branch can accommodate 20 cross-sections. The definition of 'branch' adopted in the program is very broad: Any single channel with less than 20 cross-sections describing it, may be defined by the user as a branch. Figure (B.2) illustrates a river network and two possible schematizations. The two schematizations are equivalent. With regard to the numbering system of the branches there are no restrictions. The program prompts the user to enter the numbers of the upstream and downstream branches for each new branch, and rearranges the branches automatically from upstream to downstream.

Subdivision of the channel network into branches serves the following purposes:

- It provides for runoff hydrographs from catchments to enter the channel system at various points.

- It provides for representation of concentrated inflow/outflow hydrographs entering the channel system at any point.

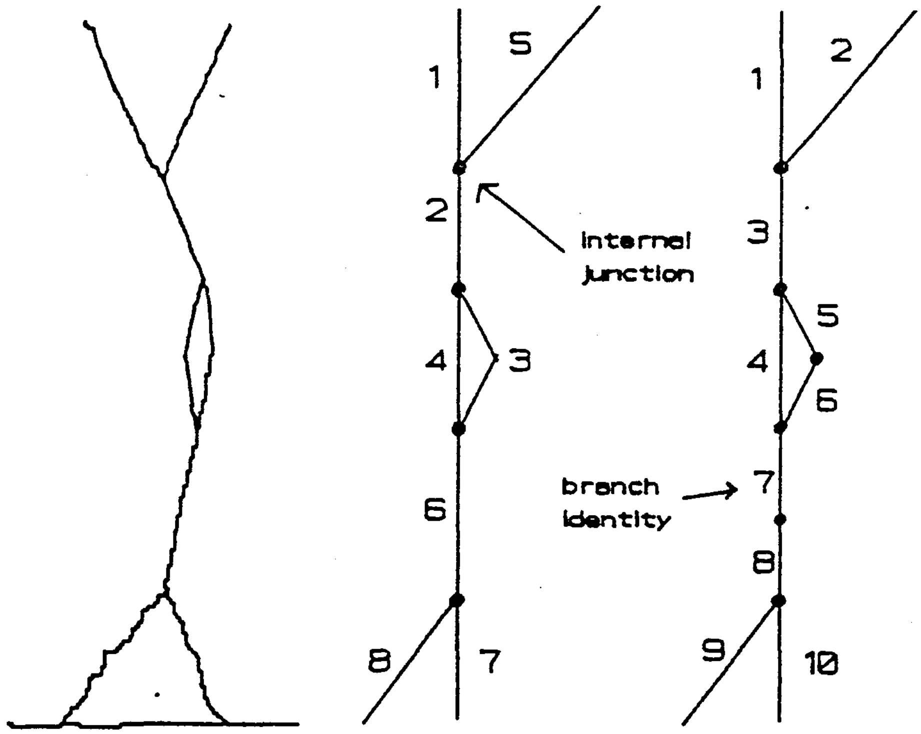

Figure B.2 Possible schematizations of a river network.

- It gives the programmer flexibility in the representation of the various topographical features and allows for the schematization of branched and looped networks.

It must be remembered that the cross-sections that a branch can accommodate may not exceed 20. Thus, it might be necessary for a single connectivity channel to be represented by more than one branch. The degree of subdivision of the channel network is a matter demanding subjective judgement by the user and definite advice can not be given other than to stress avoiding excessively fine subdivision if the data available (topographical and boundary data) are not very accurate.

B.2.2 CONCENTRATED CHANNEL INFLOW/OUTFLOW

This is representative of many cases in practise such as streamflow from a tributary not modelled, diversion into the channel from an off-stream storage (inflow) or a controlled diversion into a man-made channel (outflow) etc. Concentrated inflow/outflow must be allowed for during the schematization as it is permitted only at a confluence of branches. Therefore the channel in Figure (B.3) must be represented by two branches.

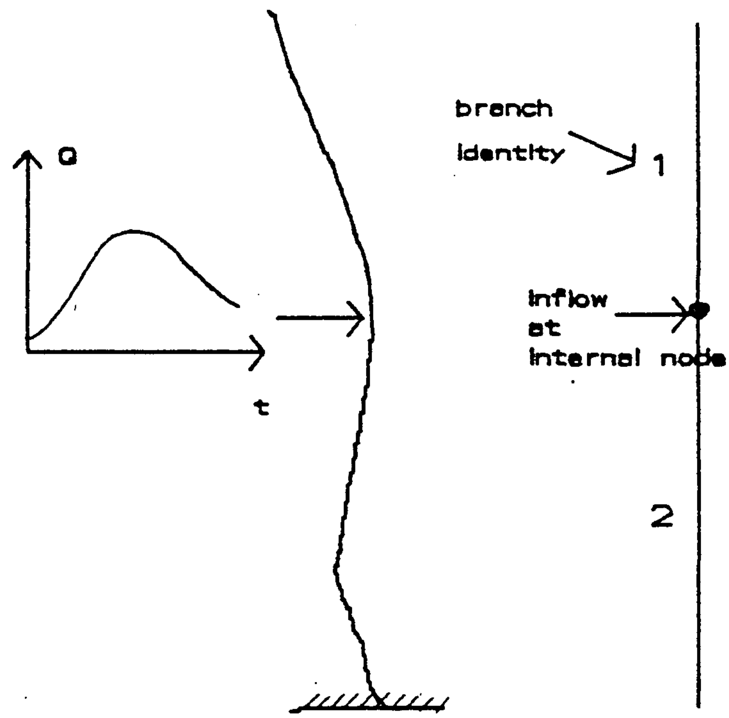

Figure B.3 Schematization of a single channel with concentrated inflow.

B.2.3 BRANCH REPRESENTATION/CROSS-SECTIONS

Transformation of the topographical data, as represented by a contour plan, into a form suitable for computer manipulation is accomplished through the use of ground surface profiles (cross-sections) and the measured distances between them (reach length).

The cross-section should extend across the entire flood-plain and should be perpendicular to the contour lines. The cross-section data requirements are identical to those of the more standard backwater programs such as HEC-2 etc.

However, the following points are important:

- Cross-sectional data is orientated looking downstream as the program considers the left side of the stream to have the lowest station numbers and the right side the highest.

- In each branch the cross-sections are numbered in increasing order from downstream to upstream.

- The cross-sections are represented by two numbers, the first representing the branch and the latter the cross-section, e.g. (2.1) is the first downstream cross-section of the second branch.

- Where abrupt changes occur, several cross-sections should be used to describe the change regardless of the distance between them.

A further feature to be explained is the subdivision of a cross-section into segments. Thus:

- Each cross-section may be subdivided into three segments (main channel, left overbank, right overbank) and roughness coefficients must be specified for each segment.

- Different reach lengths may be entered for each segment for any reach. Overbank reach lengths should be measured along the anticipated path of the centre of the mass of the overbank flow. Often these values are equal. There are, however, conditions where they will differ, such as at river bends, or where the channel meanders considerably and the overbanks are straight (Corps of Engineers, 1976; HEC-2 User's manual).

- Caution and careful schematization is necessary in cases of divided flow. It is to the judgement and experience of the modeller to decide if the divided flow will be schematized in the same branch as different cross-sectional segments, or as different branches in a looped network.

B.2.4 BOUNDARY DATA REPRESENTATION

Boundary conditions are required at all external junctions, that is junctions which are connected to only one branch. The various types of boundary data input are described below and depend on the type of simulation and the channel network.

- **Boundary data for steady-state calculations**

  Flowrates are required at all upstream external junctions of the network and starting water-levels at the downstream external junction. Thus, for the network in Figure (B.4), the following boundary data are required:

  1. Flowrates at the upstream ends of branches (1) and (2).

2. Water-level at the downstream end of branch (6).

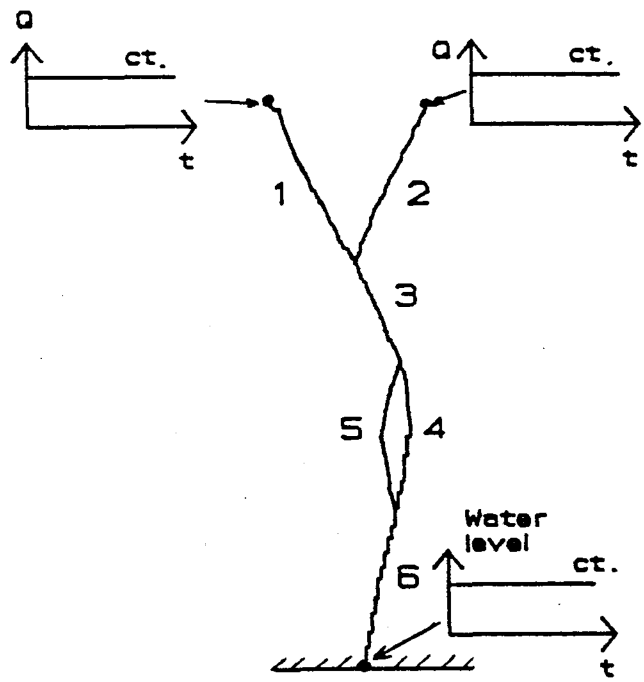

Figure B.4 Example of boundary conditions for steady-state simulation

- **Boundary data for unsteady flow simulation.**

Boundary-value data for use in simulation of unsteady flow requires the establishment and operation of a network of data stations throughout the prototype system. In selecting suitable station locations a thorough understanding of the hydrological system being modelled, a familiarity with the time-dependent data requirements of modelling, coupled with a general familiarity of operational field techniques for obtaining hydrological information are necessary.

The boundary value data requirements of the model can be divided into two categories:

1. External boundary data or boundary conditions that are the forcing functions of the flow.

2. Hydrographs at intermediate points of the network used for model calibration and adjustment.

The program checks the connectivity of the branched network and prompts the user to enter the boundary conditions at all the external junctions of the network. The compulsory boundary-value data may be:

1. **Stage recorded hydrograph.**
2. **Flowrate recorded hydrograph.**
3. **Stage-discharge relation.**
4. **Stage-discharge graph.**

The program accepts stage-discharge relations at the boundaries of the following form only:

$$Q = (a)\ Z^{(m)} + (b)$$

where

Q, Z any flowrate and water-level at the boundary respectively.

a, b, m :constants specified by the user.

If the stage-discharge relationship does not conform with the above relationship the user may enter the flowrates that correspond to incremental stage-elevations. It should be noted that a rating curve relationship Q(Z) cannot be used as an upstream boundary condition.

Any boundary condition at internal branch junctions may be specified by the user after the completion of the compulsory external boundary conditions. An example of boundary-value data for the network of Figure (B.4) is given in Figure (B.5).

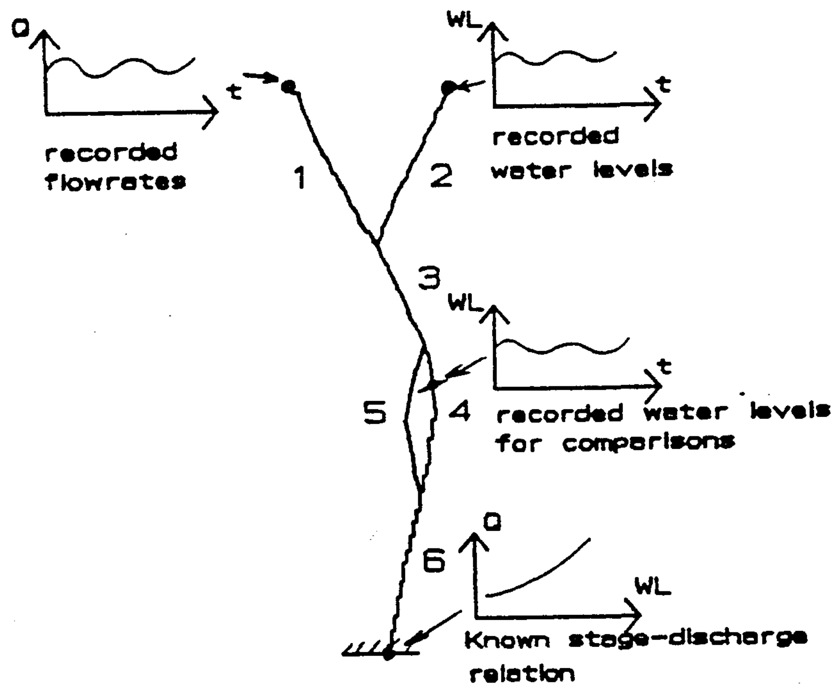

Figure B.5 Example of boundary conditions for unsteady flow simulation for the network of Figure (B.4).

- **Boundary value data for hydrograph routing**

The program will route any inflow hydrograph entering the system at the upstream external junctions. The inflow hydrograph can be in flowrates (m^3/sec) or water-levels (m) recorded or generated by a catchment routing program such as WITWAT, ILLUDAS etc.

B.3 MODEL STRUCTURE

The 'OSYRIS' suite of programs is composed of programs controlling the input data, the output data and the main computational procedures. The main menus include the following programs:

I N P U T - C O N T R O L   P R O G R A M S

"INSTAL" :Program for disk configuration.
"OSYRIS" :Introductory program.
"INPUT" :Input-Editing program
All the cross-sectional data and boundary value data are inputted and edited through this program.

M A I N   C O M P U T A T I O N   P R O G R A M S

"BACKWATER":This program is used for steady-state calculations or for the computation of initial conditions for the unsteady flow simulation.
"IMPLICIT" :Unsteady flow simulation program for branched and looped networks using the IMPLICIT method. The background theory for the development of this program is given in Chapter 4.

O U T P U T - C O N T R O L   P R O G R A M S

"BACKWRES" :This program prints and/or plots the results of the steady-state computations to the screen or the printer.
"UNRES" :This program prints and/or plots the results of the unsteady flow simulation program.
"GRPLOT ":Utility plotting the results on the screen

and sending them to the plotter.

"UNSTAT" :Utility for time-series statistical comparisons.

"GRSTAT" :Utility plotting the graphical aids used for the model calibration and adjustment.

"DATAPR" :Utility for the printing of data & result files.

The operational arrangement of the programs is given in Figure (B.6).

The 'OSYRIS' programs are arranged on four floppy disks as follows:

D I S K 1	D I S K 2	D I S K 3	D I S K 4
INSTAL.EXE	BACKWATE.EXE	BACKWATE.EXE	DATAPR.EXE
OSYRIS.EXE	IMPLICIT.EXE	IMPLICIT.EXE	GRPLOT.EXE
INPUT.EXE	BACKWRES.EXE	UNRES.EXE	UNSTAT.EXE
			GRSTAT.EXE

The programs on the fourth disk are loaded by the user by typing the name of the program. All other programs are loaded during execution and are brought in as needed by chaining procedures. Examples of the file-sequence for different simulation runs are:

a. **Backwater computations**

```
OSYRIS-->INPUT----->BACKWATE----->BACKWRES
    D I S K  1     |     D I S K  2
```

b. **Unsteady flow simulation using the 'IMPLICIT" method**

```
OSYRIS-->INPUT----->BACKWATE---->IMPLICIT---->UNRES
    D I S K  1     |       D  I  S  K  3
```

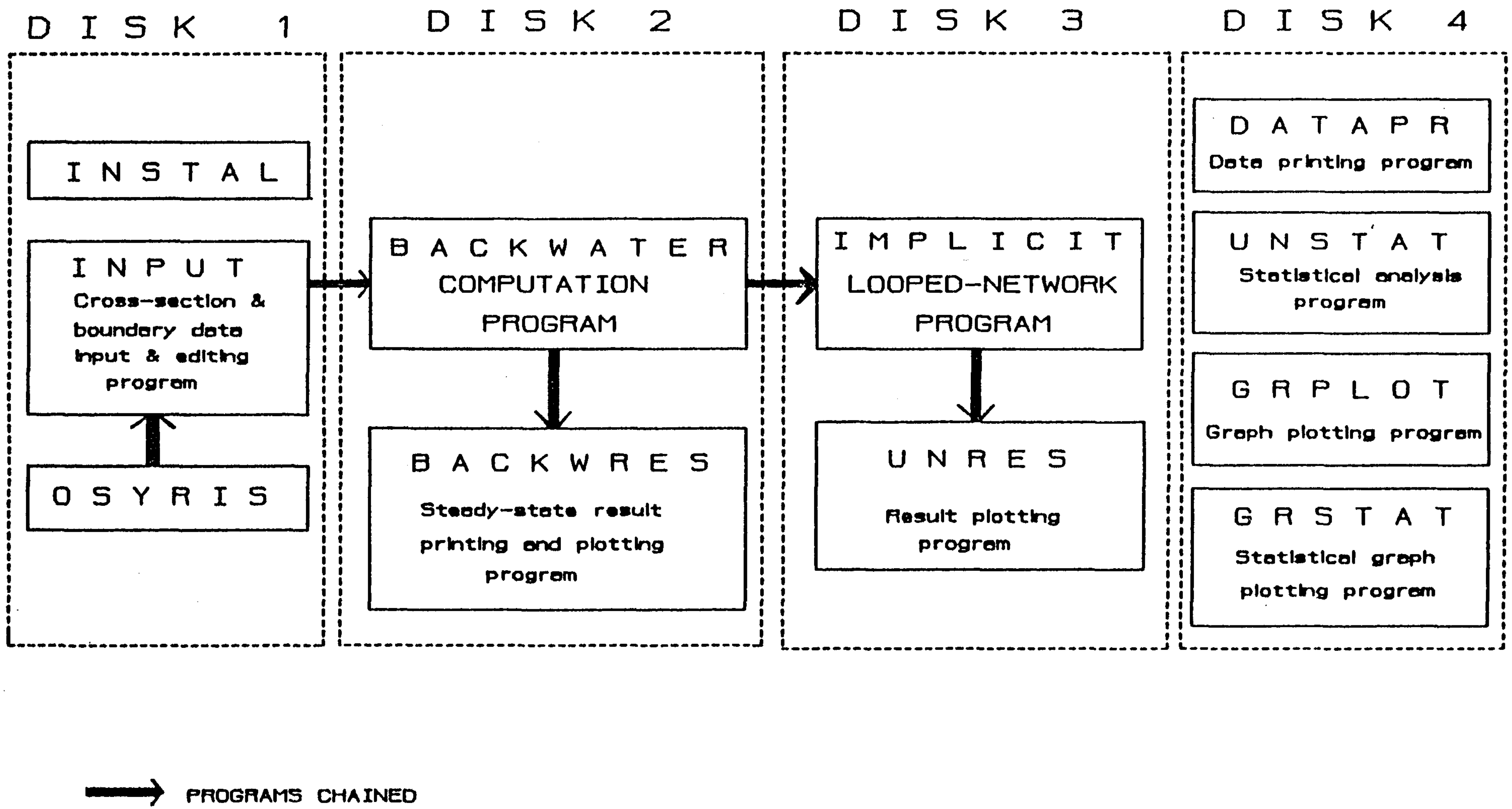

Figure B.6 'OSYRIS' - Operational System for RIver flow SImulation - sequence of operations.

The data and the results of each simulation run are stored in files with names specified by the user. It is not necessary that the user be familiar with the sequence of operations as messages are printed during the simulation explaining which file is loaded, which run is in progress, the disk that must be loaded into the disk drive and so on. The following points are important:

- The cross-sectional data and the boundary data are kept in separate files. This setup creates greater flexibility as the same cross-sectional data files can be combined with different boundary data files (different events for simulation). Thus, the sequence of functions performed by the user must be in the following order:

  1. **Enter the cross-sectional data.**: This data will be stored in a file of the type (filename.CRS).

  2. **Enter the boundary value data (if required).**: This data is stored in a file of the type (filename.BND).

  3. **Call the simulation program.**

- The results of the simulation are also stored in files. In this way important result files need never be erased, and can be stored indefinitely. For unsteady flow simulation three types of result files are created ending with the prefixes .RS1, .RS2, .RS3 respectively. Their file-name is specified by the user at the beginning of the simulation run. After the completion of the simulation the user can call any of the result files through the use of the programs on the 4th disk. Thus, the user can view the results, send them to the printer, or analyse them using the statistical programs "GRSTAT" and "UNSTAT". During program execution dummy files are created which may be erased at the end of the simulation.

B.4 USER'S GUIDE - INPUT DATA

B.4.1 GENERAL

This version of 'OSYRIS' has been developed for IBM-compatible micro computers. Although the program was developed on an "M-24 Olivetti" micro computer, special attention was taken in order not to use commands and features specific to this type of micro computer. Thus, the system can be used on any new and more advanced micro, as long as the system is compatible with the standard IBM-AT micro-computer.

B.4.2 INSTALLING THE SYSTEM - GETTING STARTED

The 'OSYRIS' suite of programs is stored on magnetic disks and requires a separate disk for storage of data and result files. Thus the user may generate as many data files as he wishes, new data disks being used when necessary. Before any of the programs are run, the user must make sure that the 'OSYRIS' suite of programs can locate all the files it needs. The first disk of the four contains the program 'INSTAL' which can be used to set up the drive definitions. To set up the programs complete the following steps:

1. Make sure that DISK 1 is in the current disk drive.

2. Type 'INSTAL' and press 'ENTER' to carry out the command.

The screen should look like this:

```
          WATER LEVEL CALCULATION SUITE OF PROGRAMS
                  INSTALLATION PROGRAM


>Program Disk Drive Designation ( A: B: C: or D:).: c:

>Data Disk Drive Designation    ( A: B: C: or D:).: c:

>Parallel Printer Designation   (LPT1: LPT2: etc).: LPT1:

>Screen type....monochrome(1)  or colour (2)......: 2

            ------------------help------------------
              Use the arrow keys to select parameter
                          to change

  Enter information and press ←┘ to continue or <ESC> to exit
```

Figure B.7 Installing the system - selecting directories

For a system with two floppy-disk drives the following disk setup is proposed:

Program disk drive: (A:)
Data disk drive : (B:)

If the hardware system has a hard disk, it is possible to place the executable and data files on the hard disk. In this case type:

Program disk drive: (C:)
Data disk drive : (C:)

Pressing 'ENTER" the screen in Figure (B.8) appears. At this time you enter the subdirectories of the source and data files in the shown format. In the case of a hard disk set up, it is a good practise to keep the data files in different subdirectories from the source files.

WATER LEVEL CALCULATION SUITE OF PROGRAMS
INSTALLATION PROGRAM

>Program Disk Drive Path................: \osyris\

>Data Disk Drive Path................: \osyris\data\

————————help————————
Enter the path in the format \xxxxx\xxxx\.

Enter information and press ←┘ to continue or <ESC> to exit

Figure B.8 Installing the system - selecting subdirectories

After installing the program on the micro to start the 'OSYRIS' program type:

'OSYRIS' and press ENTER

'OSYRIS' is a pre-program that loads the 'INPUT' program while displaying the name of the program on the screen. 'INPUT' (the data input and editing program) acts as a steering program and always precedes simulation. It allows the user to either input new cross-sectional or boundary data files or immediately call the simulation program.

All of the input-editing system responds interactively with the user. To choose a command from the keyboard, perform the following steps:

- Use the direction keys to highlight the command

- Press ENTER to carry out the command.

In case of a mistake (e.g pressing ENTER to wrong command), the user returns to the initial steering menu by pressing 'ESCAPE'.

After a few seconds the input-editing program 'INPUT' is loaded and the following menu appears on the screen.

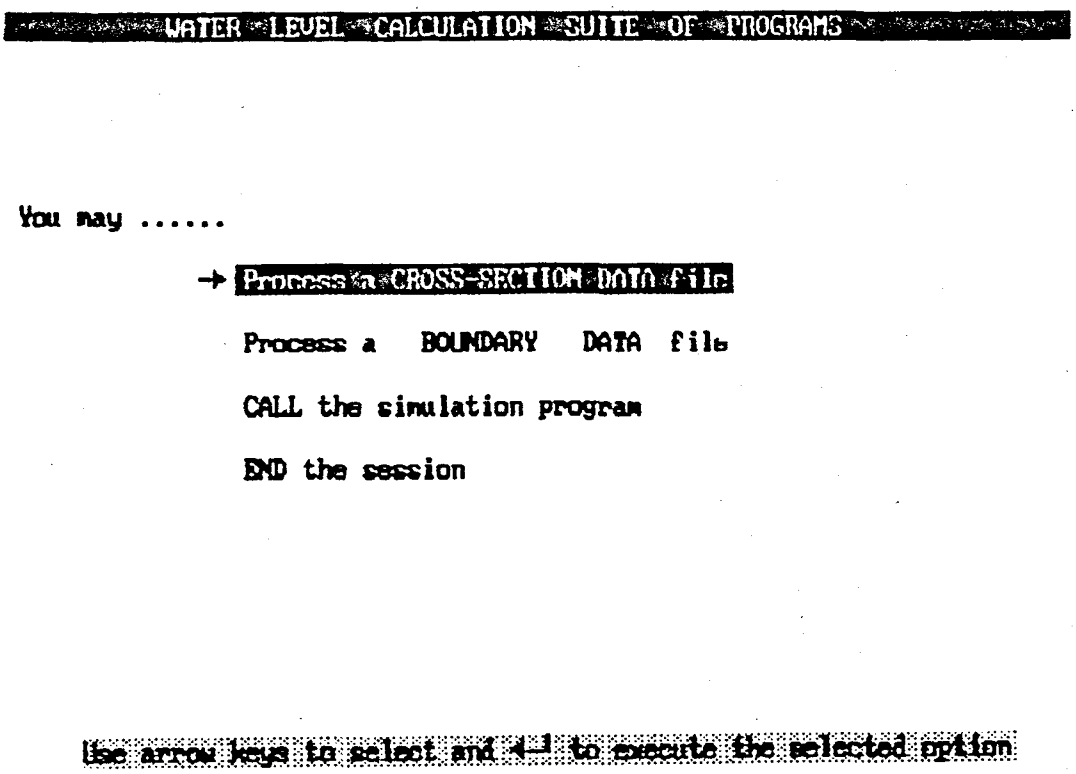

Figure B.9 Main steering menu of program 'INPUT'

B.4.3 CROSS-SECTION DATA INPUT

If the user selects to "Process a CROSS-SECTION data file" the following screen appears:

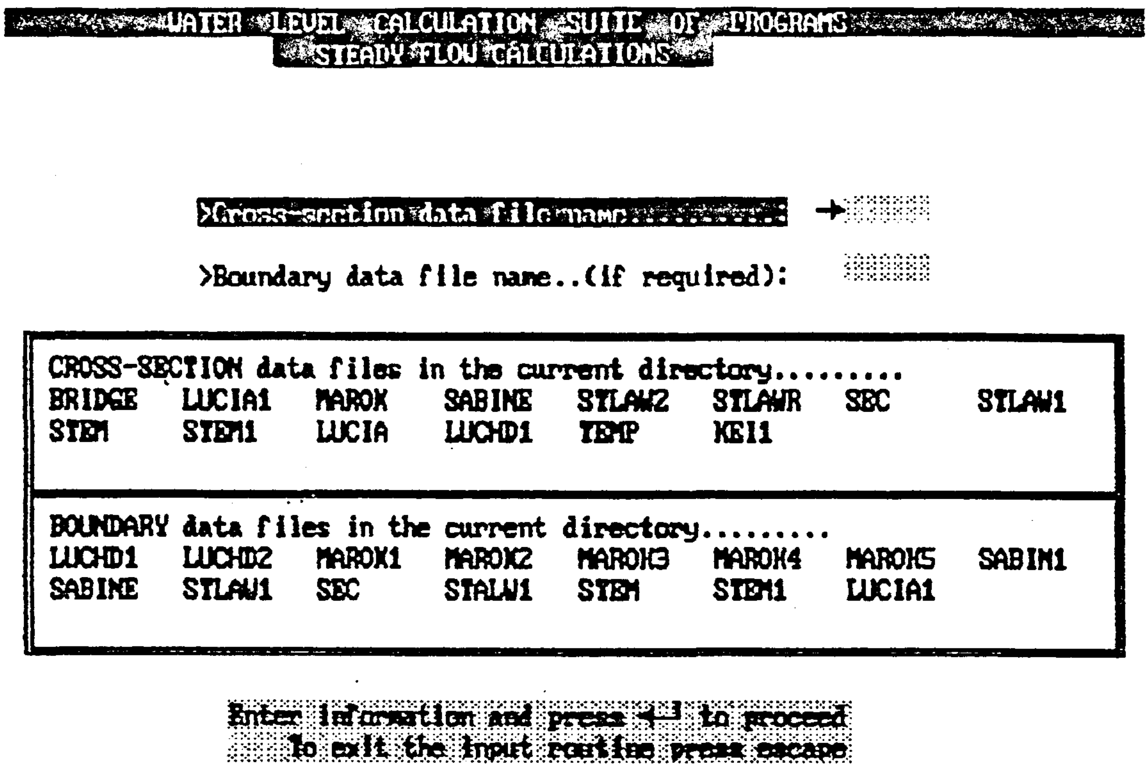

Figure B.10 Cross-section data handling steering menu.

The program searches on the data disk and lists all the existing cross-section data files. In order to create a NEW file or EDIT an existing data file, type the name of the file into the box. After creating a NEW cross-section data file, the program prompts the user for "the number of branches" (Figure B.11):

WATER LEVELS COMPUTATION SUITE OF PROGRAMS
I N P U T M O D E --->CROSS SECTION DATA FILE:tmep

>Number of branches..........:

help

Each branch may contain up to 20 cross-sections. The cross-sections may have up to 20 points and are represented by 2 numbers (n.n). The numbering of the cross-sections proceeds upstream in increasing order. i.e. 2.3--> is the third cross-section in the second branch.

Enter information and press ←┘ to proceed
To exit the INPUT routine press escape

Figure B.11 Input mode - Entering the number of branches

WATER LEVELS COMPUTATION SUITE OF PROGRAMS
I N P U T M O D E --->CROSS SECTION DATA FILE:temp

BRANCH : 1

Enter........

>Number of cross-sections.....: →

>Upstream branches...........:

>Downstream branches.........:

help

Enter the identities of the upstream and downstream branches

Enter information and press ←┘ to proceed
To exit the INPUT routine press escape

Figure B.12 Input mode - Entering branch data

The data for each branch are entered and stored individually in the same file. For each branch the program prompts the user for the following data (Figure B.12):

- **Number of cross-sections.**

- **Upstream branches.**

- **Downstream branches.**

For branch (3) in Figure (B.5) the user should enter the following connectivity data:

- **Upstream branches.** :1,2

- **Downstream branches.** :4,5

The identities of the branches upstream or downstream of the current-input branch, may be separated by a comma or a space. The cross-sections are entered in ascending order (1.1,1.2,1.3 etc) from downstream to upstream. An example of the screen with the data entries for a cross-section is shown in Figure (B.13). The following data are required for each cross-section:

- **Expansion & Contraction coefficients** : (Entry in the form X,Y or X Y) The coefficients should be entered only if the user performs steady-state computations.

- **Number of points in cross-section:** Every cross-section can accommodate up to 20 points. Initially only input boxes for the coordinates of the first 10 points are shown on the screen. However, if the user presses the direction arrow '-->' when the pointer is at the 10th point the input boxes for the following 10 points will appear on the screen.

WATER LEVELS COMPUTATION SUITE OF PROGRAMS
I N P U T M O D E >CROSS SECTION DATA FILE:lucia1

CROSS SECTION 1 - 1

Expansion and Contraction coef ..(steady-state): +
Number of points in cross-section..............: 17
Points where flood-plain begins.........(M1,M2): 3,15
Roughness......(Channel, left & right overbank): .021,.021,.021
Reach length...(Channel, left & right overbank): 0,0,0
Reach lateral inflow (+) or outflow (-)........:
Is upstream a Bridge(B) ?......................:

Coordinates of the cross-section.......:

	Point 1	Point 2	Point 3	Point 4	Point 5	Point 6	Point 7	Point 8	Point 9	Point10
X axis	0	5	7.5	16.5	40.50	70	92.5	94	100	106
Y axis	2	1	0	-.50	-1.50	-2	-3	-3.5	-3.25	-3.5

Enter information and press ↵ to proceed
To exit the EDIT routine press escape

Figure B.13 Cross-section data input

- **Reach lengths (Channel, left and right overbanks):** If there are no flood-plains the user may only enter the length of the main channel. The data should again be separated by a comma or space.

- **Roughness:** The same format as for the reach lengths.

- **Points where flood-plain begins:** For compound channels the points where the flood-plains begin must be specified in order for the program to distinguish between the segments of the cross-section. The cross-section can consist of a flood-plain either on the left hand-side or the right hand-side of the main channel. In the case of a flood-plain on the left hand-side, instead of the point where the right flood-plain begins the user must enter a -1, and vice versa, e.g. for the Figure (B.14) the entry should be -1,7. If there are no flood-plains the box should be blank.

Entries:

Number of cross-section points: 10

Points where flood plain begins: -1, 7

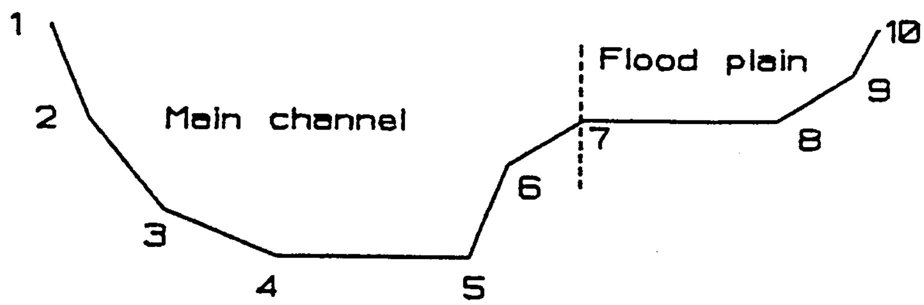

Figure B.14 Example of a channel with only the right flood-plain.

- **Reach lateral inflow(+) or outflow(-):** The program accepts continuous inflow/outflow in the reach. However, this option should be used only for steady-state calculations. For unsteady flow calculations the lateral inflow/outflow should be represented as point input.

- **Is upstream a (B)ridge ?:** If there is a bridge upstream of the cross-section, it must be indicated, by entering the initial of the structure type e.g. enter 'B'.

- **Coordinates of the cross-section:** The elevation and the distance from the origin are entered for each point.

In case of a bridge cross-section the input screen shown in Figure (B.15) appears. The data required are depicted in the example in Figure (B.16). An analysis of the types of piers and abutments

WATER LEVELS COMPUTATION SUITE OF PROGRAMS
I N P U T M O D E -->CROSS SECTION DATA FILE:temp

B R I D G E CROSS SECTION 1 . 2

Enter.........

Soffit elevation..........................:
Invert length and elevation............:
Bridge invert location (station points):
Abutments (slope,type and direction)...:
Road width and elevation...............:
Degree of skewness.....................:
Length of the reach....................:

If the bridge has piers, enter......

Number and type of the piers...........:
Width of the piers.....................:

Enter information and press ↵ to proceed
To exit the INPUT routine press escape

Figure B.15 Input mode - Bridge data

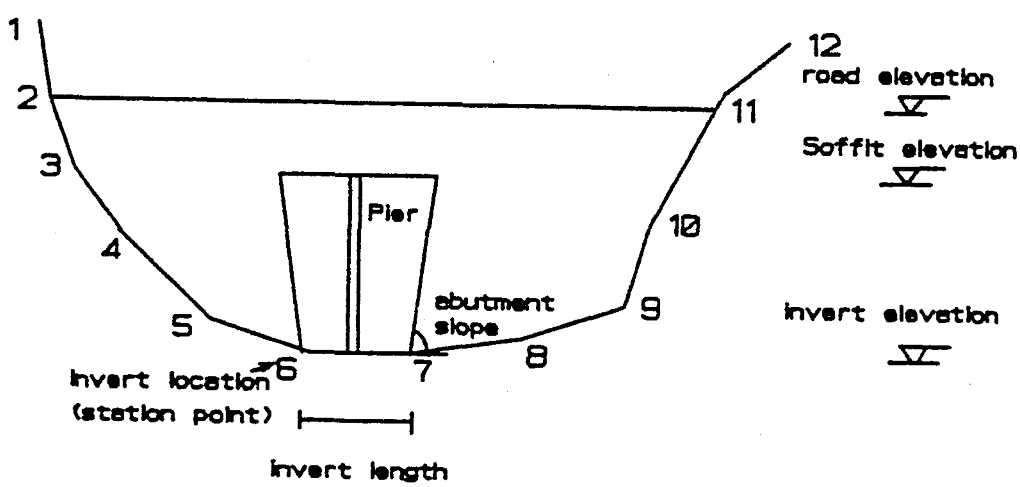

Figure B.16 Example of bridge data

and the bridge computations is given in Appendix (D). The following points are important to note:

- The bridge computations require cross-sections immediately downstream and upstream of the bridge.

- The program assumes that the cross-section entered immediately downstream from the bridge is repeated in the bridge-section. The location of the bridge within the cross-section is specified as "BRIDGE INVERT LOCATION" and the station point of the previous cross-section, where the left of the invert starts, is entered.

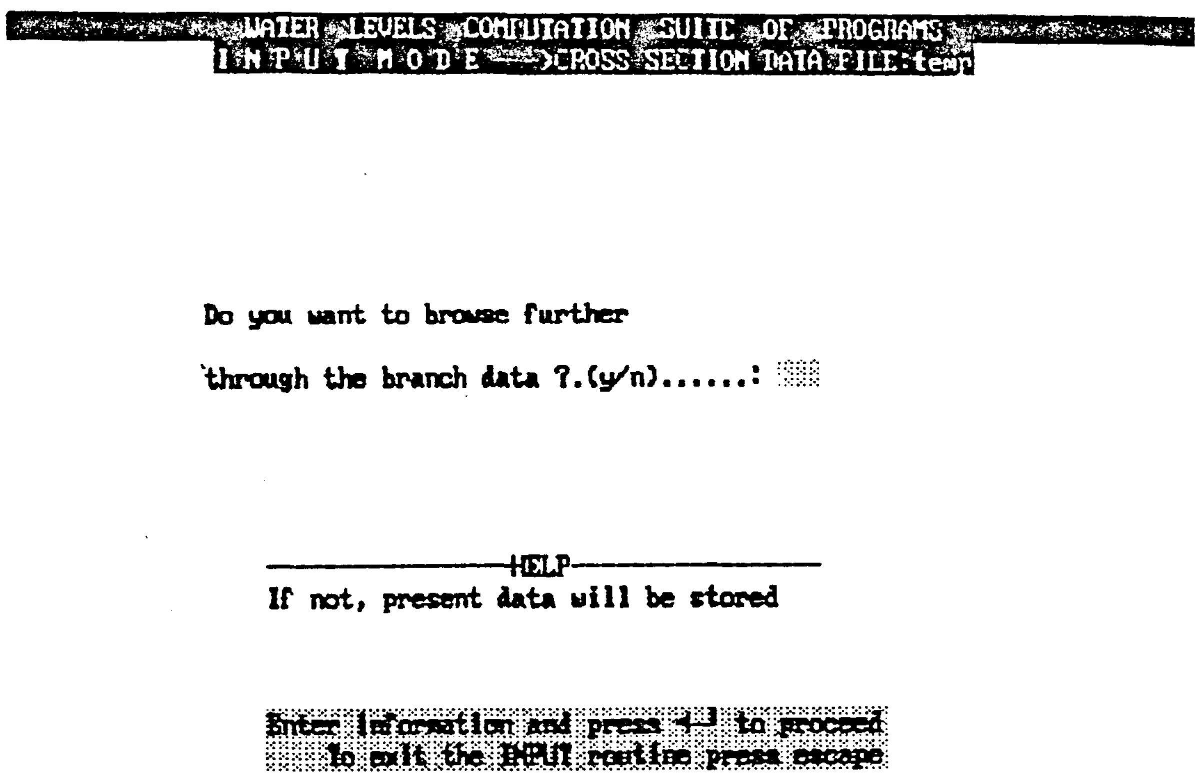

Figure B.17 Screen after the completion of the input of each branch

After the completion of the branch data input the screen in Figure (B.17) appears. The user may browse through the branch data or type 'n' and store the branch data. In this way, while in INPUT mode, the user can correct a mistake without having to wait for the completion of the input of the whole network. The input of the other branches proceeds in exactly the same manner.

B.4.4 CROSS-SECTION DATA EDITING

Once a cross-section data file exists, the data contained therein can be edited by means of routines in the INPUT program. When data are echoed to the screen for either updating or re-acceptance, the user either enters new data or, should the echoed data be acceptable, the ENTER key is pressed thereby retaining the existing data. At any stage in the edit mode the user may exit the routine by pressing ESCAPE.

The unsteady flow simulation has extensive data requirements. Therefore the system is provided with a powerful editing system. It is able to store and retrieve up to 400 cross-sections. Any cross-section in a network may be addressed, corrected, and re-stored. On entering the edit mode, the user is presented with the main Edit menu shown in Figure (B.18).
The editing facility can:

- **BROWSE through the data file:** This routine allows the user to view the entire cross-section data file, branches and cross-sections appearing in exactly the same sequence as in the INPUT mode. To edit the data the user need only move the cursor to the relevant position on the coloured boxes, overtype the value and press ENTER.

- **UPDATE a branch or a cross-section:** This routine allows the user to immediately access all the data pertinent to a specific cross-section or branch for updating.

- **INSERT a branch or a cross-section:** The same subroutine is employed as in input mode. The format for entering a new cross-section should be noted. Referring to Figure (B.18), assume that the third branch has 12 cross-section and the user wants to enter a cross-section between cross-sections '3.3' and '3.4'. The user types in the box '3.3.1' and presses ENTER.

```
                    WATER LEVELS COMPUTATION SUITE OF PROGRAMS
              E D I T  M O D E   >CROSS SECTION DATA FILE lucia1

You may........
     UPDATE a branch or a cross section.....:    →
     INSERT a branch or a cross-section.....:
     DELETE a branch or a cross-section.....:
     COPY   a  cross-section..(from,to).....:
          BROWSE through the data file
               END the EDIT
----------------------help------------------------
Enter the number of the branch or the cross-section to be
inserted or deleted.i.e. I-->1.3.1 insert a CRS between CRS
3 and 4. You may copy cross-sections only in the same branch
i.e. (1.3,1.6) copy CRS 1.3 to 1.6

          Enter information and press ←┘ to proceed
             To exit the EDIT  routine press escape
```

Figure B.18 Main edit menu for cross-sectional data.

The program will identify the newly entered cross-section as 3.4 and will renumber all the upstream cross-sections. The old identity of cross-section 3.5 will now become 3.6 and so on.

- **DELETE a branch or a cross-section:** The identity number of the branch or cross-section to be deleted must be entered, e.g. by entering '3.5' the routine will delete cross-section '3.5' and will renumber all the upstream cross-sections. Thus, cross-section '3.10' will now be identified as '3.9' and so on.

- **COPY a cross-section:** Cross-sections may be copied only within the same branch. Thus to copy cross-section '3.5' on to cross-section '3.7' the user need only enter '3.5,3.7'.

The identities of the cross-sections must be separated by commas.

- **END the edit:** After the completion of the cross-section data editing, the user may return to the main steering menu, depicted in Figure (B.10), by highlighting this option and pressing ENTER.

B.4.5 BOUNDARY VALUES DATA INPUT

After the input of the cross-sectional data the user may enter the boundary data by selecting the option "**Process a BOUNDARY data file**" from the main steering menu. In only one case is the creation of a separate boundary data file not necessary and the user may proceed directly to the simulation program. The two requirements for this case are:

1. The network should be composed of only a single channel (single connectivity).

2. The user performs steady-state computations.

In all other cases, the creation of a boundary data file is compulsory.

The boundary data requirements depend on the type of simulation and the network configuration. **Before creating a boundary data file the user must have already created the cross-sectional data file.** Thus the user at the beginning of the routine selects the type of simulation for which he wants to enter boundary data and the corresponding data file name (Figure B.19). After completing the screen in Figure (B.19), the main menu for the selection of input or editing of boundary data appears (Figure B.20). The user in a similar manner as in cross-sectional data input, writes the file name of the new boundary data file and presses ENTER. The created boundary data file is distinguished by the extention **.BND**.

The routine then checks the connectivity of the channel network and depending on the type of simulation, specifies the boundary data requirements of the network. In the case of unsteady flow simulation or channel routing the program prompts the user to enter inflow flowrates at the upstream external junctions of the

WATER LEVEL CALCULATION SUITE OF PROGRAMS
BOUNDARY DATA PROCESSING PROGRAM

You may enter boundary data for...

>STEADY state computations.......:

>UNSTEADY flow simulation........:

>Hydrograph ROUTING..............:

>END this session

help
In the box enter the name of the file containing
the river gometry data to be processed

Enter information and press ←┘ to continue

Figure B.19 Menu for selecting type of boundary data and relevant cross-section data file

WATER LEVEL CALCULATION SUITE OF PROGRAMS
PROCESSING OF RIVER DATA FILE lucia1

You may ....
>Create a NEW boundary data file....:

>EDIT an existing data file.........:

>END this session

BOUNDARY data files in the current directory.........

LUCHD1	LUCHD2	MAROK1	MAROK2	MAROK3	MAROK4	MAROK5	SABIN1
SABINE	STLAW1	SEC	STALW1	STEM	STEM1	LUCIA1	

help
In the box enter the name of the file containing the boundary data

Enter information and press ←┘ to continue

Figure B.20 Main menu for boundary data handling network and water-levels at the downstream external junctions. These data are used in the backwater program in order to calculate the initial conditions (water-levels and flowrates) at all the cross-sections of the network. While reasonable initial conditions are desirable, estimates can be used for starting conditions if a sufficient amount of 'warm up' time is provided for the model to dissipate the errors and converge to the true solution. For initial values that are in error by as much as 100% the convergence time of the model has been found to be roughly 1-2 hours. Two hours after the start of the simulation, all computed discharges are within 2-3% of the true values. For a single connectivity channel the screen would be as shown in Figure (B.21).

For steady state simulation (backwater computations) the control of the program returns to the menu in Figure (B.20) after the completion of data entry, in a screen similar to that shown in Figure (B.21) For unsteady flow simulation pressing ENTER results in the screen in Figure (B.22) appearing. This screen provides information regarding the boundary data input process. In the next screen (Figure B.23) the order of the hydrograph input for a single connectivity channel is displayed. The first two hydrographs are compulsory boundary conditions that are the forcing functions of the flow. If the user was entering data for channel routing then only one hydrograph would be compulsory at the upstream termini of the channel.

For each boundary condition two pieces of information are necessary:

- **Method of input:** (manually or digitizer input).

- **Type of boundary conditions:** (recorded water-levels or flowrates, stage-discharge relation, stage-discharge graph).

WATER LEVEL CALCULATION SUITE OF PROGRAMS
PROCESSING OF RIVER DATA FILE LUCIA1
INITIAL CONDITIONS UNSTEADY FLOW MODEL

	BRANCH	FLOWRATE
Enter the inflow flowrate to the upstream end of the relevant branch.	1	→
		WATER LEVEL
Enter the water-levels downstream of the relevant branch.	1	

Enter information and press ↵ to continue
To exit the INPUT routine press escape

Figure B.21 Input of initial conditions for unsteady flow simulation

WATER LEVEL CALCULATION SUITE OF PROGRAMS
PROCESSING THE BOUNDARY DATA FILE:TEMP OF THE RIVER DATA FILE: LUCIA1

YOU MAY PROCEED

You may enter up to 10 hydrographs with a maximum of 300 coordinates. The program automatically prompt the user for boundary conditions at all the external junctions, that is junctions that are connected with only one branch. Any boundary conditions at internal branch junctions may be specified by the user after the completion of the compulsory external boundary conditions.

Press any key to continue

Figure B.22 Information screen for unsteady flow simulation

WATER LEVEL CALCULATION SUITE OF PROGRAMS
PROCESSING THE BOUNDARY DATA FILE TEMP OF THE RIVER DATA FILE: LUCIA1
BOUNDARY DATA FILE INFORMATION SHEET =>HYDROGRAPH NUMBERING

HYDROGRAPH INDEX	HYDROGRAPH DESCRIPTION
1	INFLOW HYDROGRAPH UPSTREAM OF BRANCH 1
2	OUTFLOW HYDROGRAPH DOWNSTREAM OF BRANCH 1
3	ADDITIONAL HYDROGRAPHS
4	,,
5	,,
6	,,
7	,,
8	,,
9	,,
10	,,

The input of the hydrographs will proceed in the above order. Any corrections or editing of the hydrographs should be carried out by referring index numbers desplayed above.

Press any key to continue

Figure B.23 Boundary data order input display screen

These options are selected from the screens in Figures (B.24) and (B.25).

If the boundary conditions are recorded water-levels or flowrates the following data are required:

- **Station site:** Only for printing or reference purposes.
- **Time (starting, ending)**
- **Date (starting, ending):** It is important to enter the dates and the times in the correct format. If the recording of the hydrograph started at 16.30 on the 10th of July 1976 and it ended at 6.30 on the 15th of July 1976 the two entries should be:

WATER LEVEL CALCULATION SUITE OF PROGRAMS
PROCESSING THE BOUNDARY DATA FILE:TEMP OF THE RIVER DATA FILE:LUCIA1
BRANCH 1 => UPSTREAM BOUNDARY CONDITIONS HYDR. INDEX 1

You may enter the boundary data.....

→ MANUALLY

THROUGH DIGITIZER

Use arrow keys to select and ↵ to execute the selected option

Figure B.24 Menu for the selection of boundary input

WATER LEVEL CALCULATION SUITE OF PROGRAMS
PROCESSING THE BOUNDARY DATA FILE:TEMP OF THE RIVER DATA FILE:LUCIA1
BRANCH 1 => UPSTREAM BOUNDARY CONDITIONS HYDR. INDEX 1

The boundary conditions are....

→ Recorded WATER-LEVELS

Recorded FLOWRATES

STAGE-DISCHARGE relation

STAGE-DISCHARGE graph

Use arrow keys to select and ↵ to execute the selected option

Figure B.25 Menu for the selection of type of the boundary input

Date (starting, ending): 10/7/76,15/7/76
Time (starting, ending): 16.30, 6.30

It is important that the starting date and time of each hydrograph coincide with the starting date and time of the simulation and the starting date and times of all the other hydrographs. The use of improperly timed dates will lead to an invalid simulation.

- **Time-step:** The hydrographs are at a constant spacing of one time increment. The time-step is specified in minutes.

- **Hydrograph Coordinates:** The maximum number of coordinates is restricted to 300.

Depending on the method of input, selected in the screen of Figure (B.24), the following options are possible:

- **Manually:** In this case the data are entered manually through the input screen as depicted in Figure (B.26). After entering all the values and pressing the right arrow the program automatically generates the timing of each coordinate and specifies the number of coordinates required.

- **Through Digitizer:** If the hydrograph is to be read in from a recorded chart the screen in Figure (B.27) with additional data is shown.

As regards the type of boundary conditions allowed, the following options are supported by the system:

- **Water level or flowrate hydrographs.**

- **Stage-discharge relation:** If the boundary data is a stage-discharge relation the user must specify the three

WATER LEVEL CALCULATION SUITE OF PROGRAMS
PROCESSING THE BOUNDARY DATA FILE:LUCHD1 OF THE RIVER DATA FILE: LUCIA1

RECORDED HYDROGRAPH

Station.................→[illegible]

Date (starting,ending): 15/7/72,15/7/72

Time.(starting,ending): 16.30,6,30

Stage correction .(cm):

Time-step.(min).......: 30

Number of coordinates.:

help

Date: DD/MM/YY,DD/MM/YY Time: HH.MM,HH.MM
Time-step in minutes (integer)
You may enter up to 300 coordinates.

To enter more coordinates press↵
If you are finished, press↵to continue

INDEX	TIME	WATER-LEVELS
1	16.30	9.8E-02
2	17.00	.129317
3	17.30	.177841
4	18.00	.223483
5	18.30	.249716
6	19.00	.264939
7	19.30	.281592
8	20.00	.281679
9	20.30	.252974
10	21.00	.224531
11	21.30	.168644
12	22.00	.180353
13	22.30	9.8E-02
14	23.00	.107543
15	23.30	.100782
16	24.00	9.6E-02
17	.30	9.2E-02
18	1.00	8.4E-02

Figure B.26 Manual input of boundary data

WATER LEVEL CALCULATION SUITE OF PROGRAMS
HYDROGRAPH INPUT FROM DIGITIZER

>Graph units in S.I (1) or U.S. (2).......: →

>Minimum W.level in the chart............:

>Maximum W.level in the chart............:

>Maximum duration in hours in the chart...:

>Enter the digitizer address.............:

help

Default digitizer address:COM1:9600,E,7,1

Enter information and press ↵ to change page

Figure B.27 Input through digitizer additional data constants (a), (b) and (c) that satisfy a relation of the form:

$$Q = (a)\ Z^{(m)} + (b)$$

- **Stage-discharge graph:** If the stage-discharge relation cannot be written in the above form, then the user may manually enter the stage-discharge graph Q(Z) as shown in Figure (B.26), where the starting and ending times are replaced by starting and ending elevations, and the time-step is replaced by a stage-increment in meters. Pressing the right arrow, incremental stage elevations are automatically created by the program and the user need only enter the corresponding flow-rates.

After the completion of the boundary data, the user may enter additional hydrographs either for comparison and calibration purposes, or point lateral inflow/outflow at branch junctions. Thus, three types of additional hydrographs may be specified:

- **Comparison hydrographs**

- **Inflow hydrographs**

- **Outflow hydrographs**

The location of the recorded comparison hydrograph is entered by specifying the identity of the relevant cross-section e.g 2.3. The joint where the lateral inflow is recorded is specified by entering the identity of any branch downstream of the relevant junction. This information is entered in a screen as shown in Figure (B.28). After the identification of the type of additional hydrograph, the sequence of entries is the same as described for the compulsory hydrographs.

WATER LEVEL CALCULATION SUITE OF PROGRAMS
PROCESSING THE BOUNDARY DATA FILE:LUCHD1 OF THE RIVER DATA FILE:LUCIA1
HYDROGRAPH INPUT AT INTERNAL JUNCTIONS OR REACHES HYDR. INDEX

>Hydrograph type.................................: →3

>REACH where the hydrograph is recorded..: 1.5

help

Hydrograph types: (1) Reach inflow (2) Reach outflow
(3) Simulation comparisons
Inflow/outflow hydrographs are allowed only at branch junctions. To specify an internal junction enter the number of any of the downstream of the junction branches. To specify a comparison hydrograph enter the reach number.

Enter information and press ↵ to continue
To exit the EDIT routine press escape

Figure B.28 Screen for the input of additional hydrographs

B.4.6 BOUNDARY DATA EDITING

Once the boundary data are stored, the user can call the boundary data file and correct it by selecting the command 'EDIT an existing data file' in the main menu, Figure (B.20), by entering the data file name. The following screen then appears:

WATER LEVEL CALCULATION SUITE OF PROGRAMS
PROCESSING THE BOUNDARY DATA FILE:LUCHD1 OF THE RIVER DATA FILE: LUCIA1

You may.....

>UPDATE a hydrograph...............:

>DELETE a hydrograph..............:

>INSERT a new hydrograph

>BROWSE through the data file

>UPDATE the INITIAL conditions

>END the EDIT

help

Enter the index number of the hydrograph.
You may delete or insert only non-compulsory hydrographs.

Enter information and press ↵ to continue
To exit the EDIT routine press escape

Figure B.29 Menu for editing boundary data files

The program reads the boundary data file and provides a data file information sheet displaying the existing stored hydrographs on the file. For a single channel with two additional hydrographs the boundary data information would be as shown the screen in Figure (B.30).

```
WATER LEVEL CALCULATION SUITE OF PROGRAMS
PROCESSING THE BOUNDARY DATA FILE LUCHD1 OF THE RIVER DATA FILE: LUCIA1
BOUNDARY DATA FILE INFORMATION SHEET  >HYDROGRAPH NUMBERING

HYDROGRAPH INDEX          HYDROGRAPH DESCRIPTION

      1            INFLOW HYDROGRAPH UPSTREAM OF BRANCH  1
      2            OUTFLOW HYDROGRAPH DOWNSTREAM OF BRANCH  1
      3            COMPARISON HYDROGRAPH  AT REACH 1.5
      4            COMPARISON HYDROGRAPH  AT REACH 1.1


Any corrections or editing of the hydrographs should be done
by referring to the index number desplayed above. The
first 2 hydrographs are compulsory, and refer
      to the external junctions of the network.

            Press any key to continue
```

Figure B.30 Information page for a single channel with two additional hydrographs

---

Pressing any key the editing menu of Figure (B.29) appears on the screen. The user can update, and delete hydrographs by entering their index numbers. However;

- Only additional hydrographs may be inserted or deleted.

- The compulsory boundary conditions at the external boundaries may only be updated.

Ending the edit the user returns to the menu in Figure (B.20).

B.4.7 CALLING THE SIMULATION PROGRAM

Once the cross-sectional and boundary data are stored, the user can complete the simulation process by calling the simulation program. Selecting the option "CALL the simulation program" a series of menus appear on the screen which allow the user to enter the various run parameters prior to the actual simulation. The type of simulation run is selected from the following menu of Figure (B.31).

WATER LEVEL CALCULATION SUITE OF PROGRAMS

You may perform......

→ **STEADY-STATE computations**

UNSTEADY flow computations

CHANNEL ROUTING

Use arrow keys to select and ↵ to execute the selected option

Figure B.31 Menu for the selection of the type of the simulation run

---

For each type of simulation run a different set of data is required. For a **backwater simulation** the following data must be entered:

- Cross-section data file name and boundary data file name (if required).

- Type of network connectivity (single, branched or looped).

- **Downstream water-level, upstream flowrate**: These data are required only in the case of a single connectivity channel where a boundary data file is not created.

- **Output parameters** : Results file name, printing and plotting options. The results of the steady-state computations are stored in a file and the program "BACKWRES" handles the output. After the completion of the simulation run this program is chained and according to the variables initially specified by the user, it sends the results to the screen or to the printer. The following results may be printed or plotted:

  - The cross-sectional data.

  - The run parameters.

  - The results (water-level, head, losses etc.) for each cross-section.

  - Plots of the longitudinal profile of each branch.

  - Plots of the cross-sections with the computed water-levels.

  The "BACKWRES" program can be called directly by the user by typing 'BACKWRES'. Exactly the same output options are available. In this way important result files can be kept separately and it is not necessary to run the simulation program each time the same output is required.

If an **unsteady flow simulation** or **Channel routing** is performed, additional data have to be specified by the user through a series of screens. These screens are depicted in Figures (B.32) to (B.38). The following **run parameters** are required:

- **Type of model:** This option gives the user the flexibility to study separately the effect of each term of the full Saint Venant equation on the simulation. Five different models can be selected, namely, the **Full Saint Venant equation model**, the **Gravity model**, the **Quasi-steady dynamic model**, the **Diffusion model**, and the **Kinematic model**. In this way the predominant characteristics of the wave can be analysed and the applicability of each model for simulation can be analysed.

- **Simulation starting date and time:** The starting date and time of the simulation must coincide with the starting dates and times of the boundary hydrographs entered in the boundary data file. The format of the entry is similar to the other entries. Thus, if the simulation starts on the 6th of December 1987 at 16.30 the entry must be **6/12/1987,16.30.**

- **Simulation duration and time-step:** The simulation duration must be entered in hours and the time-step in minutes. The two entries must be separated by a space or comma.

- **Wind direction, wind speed, surface drug coefficient and water density:** The entry of this data is optional and depends on their availability.

- **Chart datum or Mean sea level:** The mean sea level or any other arbitrary datum specified, will be used by the program

WATER LEVEL CALCULATION SUITE OF PROGRAMS
UNSTEADY FLOW CALCULATIONS
C A L L M O D E >DATA FILE:LUCIA1

You may use...........

→ The FULL DYNAMIC equations

The GRAVITY wave model

The QUASI-STEADY DYNAMIC equations

The DIFFUSION wave model

The KINEMATIC wave model

Enter information and press ←┘ to proceed
To exit the RUN routine press escape

Figure B.32 Input of run parameters - Selection of simulation model

WATER LEVEL CALCULATION SUITE OF PROGRAMS
UNSTEADY FLOW CALCULATIONS
C A L L M O D E >DATA FILE:LUCIA1
ROUGHNESS OPTIONS

>Change the roughness(%) (n1,n2,n3)..........: →

>Steady roughness(n1,n2,n3)..................:

>Roughness relation.(a,b,c,)................:

help

You may increase or decrease or assume steady roughness.
i.e. (-20,10,10) —> decrease the roughness of the main channel 20%, and increase the roughness of the banks 10%.

Enter information and press ←┘ to proceed
To exit the RUN routine press escape

Figure B.33 Input of run parameters - Roughness options

```
WATER LEVEL CALCULATION SUITE OF PROGRAMS
UNSTEADY FLOW CALCULATIONS
FLOOD PLAIN MODELLING      'COMPOSITE CHANNEL' MODEL OPTIONS

You may use the.........

          → SEPARATE-CHANNEL method

            OFF-CHANNEL STORAGE  method

            DIAGONAL interface method

            AREA  method  .

            -K-  method


Enter information and press ↵ to proceed
  To exit the RUN routine press escape
```

Figure B.34 Input of run parameters - Flood plain modelling options

```
WATER LEVEL CALCULATION SUITE OF PROGRAMS
UNSTEADY FLOW CALCULATIONS
CALI MODE          >DATA FILE:LUCIA1
ADDITIONAL DATA ———— >RUN VALUES

          >Starting Date(DY/MO/YR) & Hour(hr.min).....: →

          >Simulation duration(hours) & Time-step(min):

          >Surface drag coeff. & water density........:

          >Wind direction & wind speed................:

          >Chart datum or Mean Sea Level(MSL).........:

          >Iteration  accuracy  (water-level,flowrate):
IMPLICIT
 MODEL    >Theta,Xi & Yi values (0<Th,Xi,Yi<1)........:
VARIABLES

          ————————HELP—> DEFAULT VALUES————————
              Theta=.66     Xi=.66    Yi=0.58
           Enter information and press ↵ to proceed
             To exit the RUN routine press escape
```

Figure B.35 Input of run parameters (Main data) as the reference datum for all the elevation entries of the cross-section data stations and for the calculation of the stage. In addition, all the plots in the output are automatically referenced to this datum.

- **Iteration accuracy (water-level, flowrate):** The results at each time-step are refined by additional iterations until the difference between water-levels or flowrates of subsequent iterations meet the requirements of the user. The default values for the water levels and flowrates are 0,01 and 0,1 respectively.

- **Values for the implicit model parameters (θ, χ, ψ) :** The significance of these parameters is analysed in Chapters 5 and 6. The default values are θ=0,66, χ=0,66, ψ=0.50.

- **Roughness options:** These options may be used for the calibration by trial-and-error of the most important parameter in the unsteady flow simulation, the roughness. An analysis of the options and an overall approach to a rational calibration and verification of the model is given in Chapter 6.

- **Flood-plain modelling options:** The subject of the flood-plain and main-channel interaction was analysed in Chapter 8. It is suggested that an inexperienced user use the "off channel storage method", as it the most conservative and it is widely applied in unsteady flow simulation.

- **Printing and plotting options:** The massive output that can be generated by the model is handled by the three screens depicted in Figures (B.36) to (B.38). The cross-sections for which information will be requested are specified in the first screen (Figure B.36). The present version of the program, because of storage and flexibility limitations, can only generate information for up to 10 cross-sections. The type of output required for these cross-sections is entered in the screens of Figures (B.37) and (B.38) by identifying the correct cross-section.

Figure (B.37) shows the information which will be sent to the printer during the simulation and any data will is optionally printed at the beginning of the simulation. The plots required are specified in Figure (B.38). The following plotting options are currently supported by the system:

- Cross-section plotting
- Stage-versus time graphs
- Discharge-versus time graphs
- Velocity-versus time graphs
- Mass-curve graphs
- Longitudinal profiles

Entering an animation time-step the user can view the changes in the water-levels in animation form at the end of the simulation. The plotting of the graphs is performed by the program 'UNRES'. The 'UNRES' program can also be called directly by the user by typing **UNRES**, exactly the same plotting options are available.

In order to adjust the graph to his individual needs (different ticks, axis etc.) or to plot additional graphs as loop-rating curves, the user may call the 'GRPLOT' program, described in the next section.

WATER LEVEL CALCULATION SUITE OF PROGRAMS
UNSTEADY FLOW CALCULATIONS
C A L L M O D E >DATA FILE:LUCIA1
UNSTEADY FLOW MODEL OUTPUT OPTIONS

>Results file name......................→

Enter the reaches where graphs plotting or results printing will be requested

INDEX	CROSS-SECTIONS
1	
2	
3	
4	
5	
6	
7	
8	
9	
10	

Enter information and press ↵ to proceed
To exit the RUN routine press escape

Figure B.36 Selection of cross-sections for output purposes

WATER LEVEL CALCULATION SUITE OF PROGRAMS
UNSTEADY FLOW CALCULATIONS
C A L L M O D E >DATA FILE:LUCIA1
UNSTEADY FLOW MODEL OUTPUT PRINTING OPTIONS

>Is results printing required?..........(y/n): →

>Cross-section data..... (* or branch number):

>Boundary data..........................(y/n):

>Reach results at every time-step..(only one):
OR
>Water-levels & discharg. at every time-step.:

HELP

To print reach results (at one reach) or water-levels & discharges (at max. 3 reaches) during the simulation enter the index number of the relevant reach.

Enter information and press ↵ to proceed
To exit the RUN routine press escape

Figure B.37 Output-printing options for unsteady flow simulation

WATER LEVEL CALCULATION SUITE OF PROGRAMS
UNSTEADY FLOW CALCULATIONS
C A L L M O D E >DATA FILE:LUCIA1
UNSTEADY FLOW MODEL OUTPUT PLOTTING OPTIONS

>Results plotting on screen(1) or printer(2): →

PLOTTING OPTIONS

>Cross-sections.........(* or branch number):

>Longitudinal profile ......(branch number):
Animation time-step.......................:

>Stage versus time graphs..................:
>Discharge & velocity versus time graphs....:
>Mass-curve graphs.........................:

HELP

To plot the graphs enter the index number of the relevant cross-section. Enter (*) if you want all the cross-sections plotted otherwise the branch number.

Enter information and press ↵ to proceed
To exit the RUN routine press escape

Figure B.38 Output-plotting options for unsteady flow simulation

B.5 SUPPORTING PROGRAMS

Four additional programs have been developed for the analysis and handling of the output. The input format of these programs is not described as it is straightforward and similar to the previously discussed programs. These supporting programs are called directly by typing their name from the subdirectory of the source files. The programs and their use is shown in Table (B.1).

PROGRAM	USE
DATAPR	Print on the screen or the printer: A. Cross-section data B. Boundary data C. Result hydrographs (flowrates, water levels & velocities)
GRPLOT	1 . Plot on the screen or the plotter: A. Water levels versus time graphs B. Flowrates versus time graphs C. Velocities versus time graphs D. Mass-curve plots E. Loop rating curves 2. The user may combine on the same plot up to 10 hydrographs. 3. The axis, ticks, graph limits may be changed according to the user's individual needs.
UNSTAT	Statistical comparison of two time-series hydrographs (observed & simulated)
GRSTAT	Plotting on the screen or the plotter: A. Scattergrams of the simulated magnitude B. Absolute errors of simulated magnitudes C. Relative errors of simulated magnitudes D. Cumulative sum of departures from the mean

Table B.1 Supporting programs

APPENDIX C. BACKWATER COMPUTATIONS

C.1 THEORETICAL BACKGROUND

Calculation of the water surface profile for subcritical flow proceeds in the upstream direction. The upstream unknown water surface elevation is calculated by solving iteratively the following equation:

$$Z_2 + \frac{\alpha_2 V_2^2}{2g} = Z_1 + \frac{\alpha_1 V_1^2}{2g} + \Delta h_e \qquad \text{(C1)}$$

in which

Z_1, Z_2 = water-surface elevation at ends of reach (Figure C.1)

V_1, V_2 = mean velocities at the ends of the reach

α_1, α_1 = velocity coefficients

g = acceleration of gravity

Δh_e = energy head loss

and

$$\Delta h_e = LS_f + C \left| \frac{\alpha_2 V_2^2}{2g} - \frac{\alpha_1 V_1^2}{2g} \right| \qquad \text{(C2)}$$

where

S_f = friction slope of the reach

C = expansion or contraction loss coefficients

L = discharge-weighted reach length

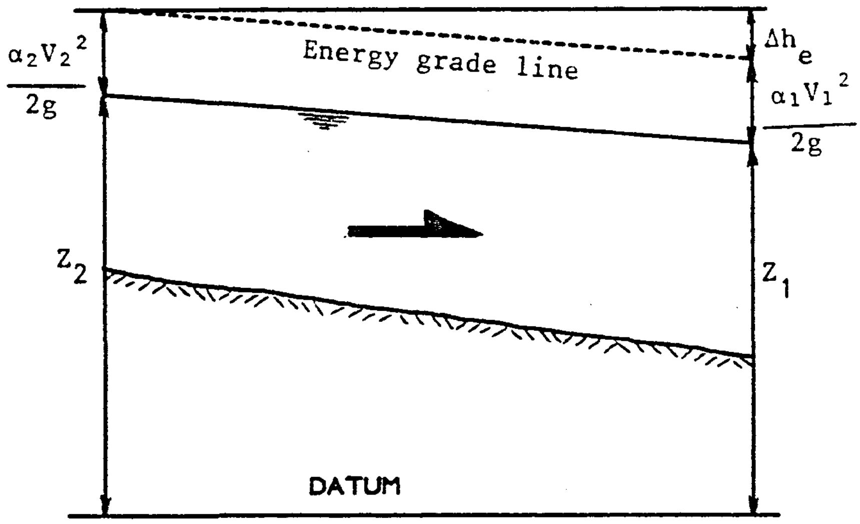

Figure C.1 Definition sketch for the energy equation

The discharge-weighted reach length is:

$$L = \frac{L_1Q_1 + L_2Q_2 + L_3Q_3}{Q_1 + Q_2 + Q_3} \tag{C3}$$

where

L_1, L_2, L_3 = reach lengths of the main channel, left and right overbanks, respectively.

Q_1, Q_2, Q_3 = flows of the reach for the main channel the left and the right overbank, respectively.

The determination of the proportion of flow in the main channel and in the flood-plains is discussed separately.

C.2 COMPUTATIONAL PROCEDURE

The unknown upstream water-level is determined by an iterative solution of equations (C1) and (C2). The procedure is initiated by the step method as described by Henderson (1966). The third and subsequent iterations are based on the computer algorithm, called ZEROIN, for finding a real zero of a single function. The algorithm combines the certainty of bisection with the speed of the secant method for smooth functions (Dekker, 1969; Brent, 1973). A listing of the algorithm is included in Appendix (H).

If the calculated water-level is below the critical level, critical depth is assumed, and the program proceeds to the next upstream reach. The critical depth and the Froude number are calculated for all the reaches irrespective of the flow regime.

C.3 DATA REQUIREMENTS

The program is designed for subcritical flow. In the case of supercritical flow it assumes the flow is critical. This assumption is conservative and adequate for most practical applications. The basic data requirements are:

- **Downstream Starting elevation:** The water-surface elevation for the starting cross-section may be one of three options:

  - Known elevation
  - Critical water-level: By entering (-1) in the field.
  - Normal water-level: By entering (+1) in the field.

- **Discharge:** If the network is of dendroid type then the user must adopt the following procedure:

- Create a file with the cross-sectional data
- Create a file with the boundary data (the flowrates at the upstream termini of the branches, and the downstream water-elevation).
- Call the simulation program

If the network is of single connectivity (only one upstream boundary condition) the user creates the file with the cross-sectional data and then calls the simulation program directly. The program requires the upstream flowrate and the downstream water-elevation.

- **Contraction and expansion coefficients:** These coefficients are used to compute the energy losses associated with changes in the shape of the river cross-section. Typical values are:

	Contraction coef.	Expansion coef.
Gradual transition	0,1	0,3
Bridge sections	0,3	0,5
Abrupt transitions	0,6	0,8

APPENDIX D. BRIDGE BACKWATER COMPUTATIONS (STEADY STATE CONDITIONS)

D.1 INTRODUCTION

D.1.1 NATURE OF BRIDGE BACKWATER

Constriction or expansion of flow causes a loss of energy, the greater portion occurring in the downstream expansion. Energy losses occur in the form of entry loss, increased friction loss due to increased velocity through the constriction, and an expansion loss downstream. This loss of energy is reflected by a rise in both the water surface elevation and the energy line upstream from the bridge.

D.1.2 TYPES OF FLOW ENCOUNTERED

There are three types of flow which may be encountered in bridge waterway design. These are labelled types I through III on Figure (D.1).

- **Type I flow:** The normal water surface is above critical depth (subcritical flow) everywhere. This is the most common type of flow encountered in practice.

- **Type IIA flow:** The flow remains subcritical in the unconstricted channel but the water surface passes through

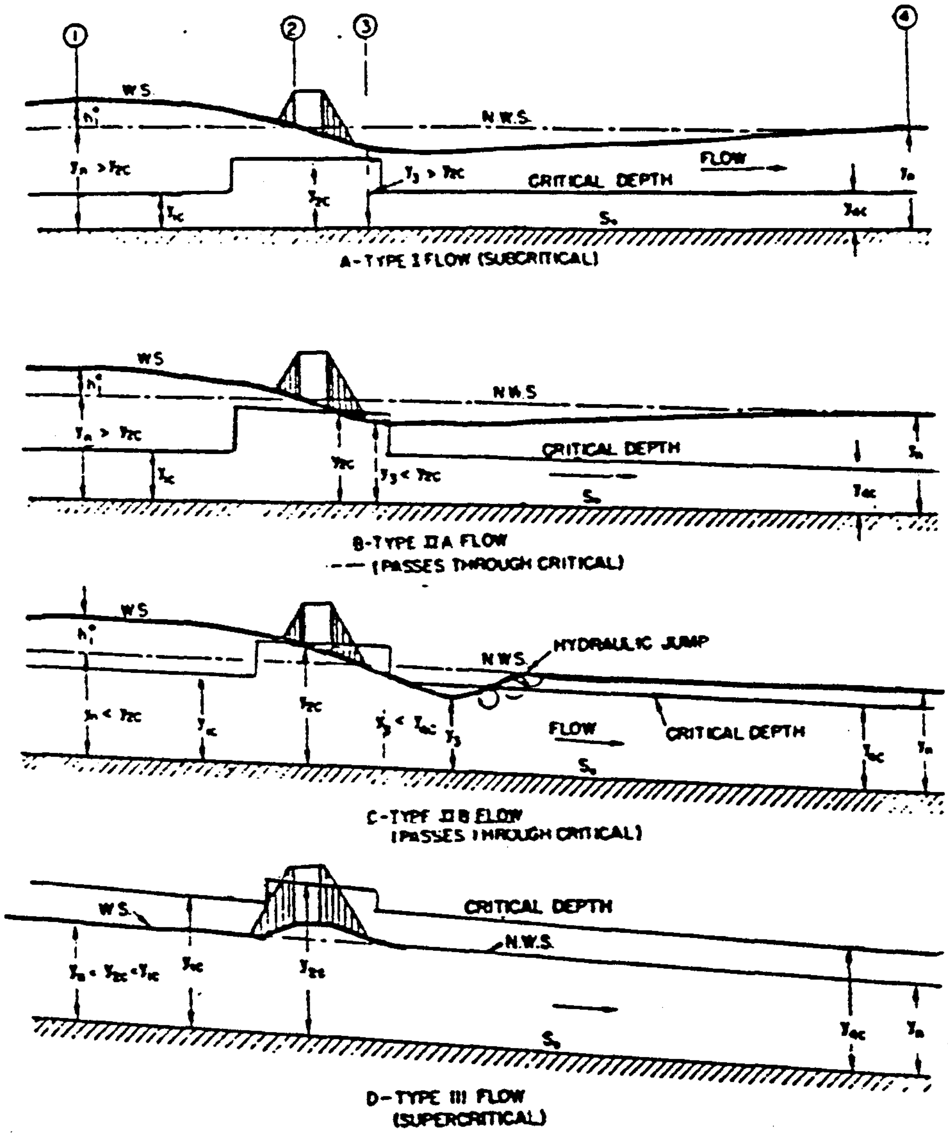

Figure D.1 Types of flow encountered (U.S. Dept. of Transportation, 1978) critical depth in the constriction. In this case, the upstream backwater is independent of downstream conditions.

- **Type IIB flow:** The water surface starts subcritical upstream, passes through critical depth in the constriction, dips below critical depth immediately downstream of the constriction and then returns to normal depth via a hydraulic jump downstream of the constriction.

- **Type III flow:** The flow is supercritical throughout. This is an unusual case requiring a very steep gradient.

D.2 METHOD USED FOR BRIDGE BACKWATER COMPUTATIONS

The computational procedures for the calculation of the backwater are based on the research findings of the U.S. Department of Transportation (1978). This method is preferred to other methods ("Contracted opening" method, Yarnell's empirical method) as it is the most updated and has been tested for a large number of cases. The method was based principally on the results of hydraulic model studies (U.S. Dept. of Commerce, Bureau of Public Roads, 1960) and was limited in its range of application. After the collection of field data and measurement of the hydraulics of many different sizes of bridges during floods, the model results were reevaluated. Design curves were then completed and revised (U.S. Dept. of Transportation, 1978). The OSYRIS model incorporates all the design curves, and other more recent research findings of the U.S.Geological Survey on backwater computations.

Several terms that are frequently used, and are calculated by the program are:

- **Normal stage:** Normal stage is the normal water surface elevation of a stream at a bridge site, for a particular discharge, prior to constricting the stream (Figure D.2).

- **Abnormal stage:** is the stage resulting from backwater effects of structures downstream e.g. bridges, dams or any other constriction downstream. The water surface with abnormal stage is not parallel to the bed.

- **Bridge opening ratio (M):** The bridge opening ratio, M, defines the degree of stream constriction, expressed as the ratio of the flow which can pass unimpeded through the bridge constriction to the total flow of the river. The bridge opening ratio, M, is most easily explained in terms of discharges, but it is usually determined from conveyance relations.

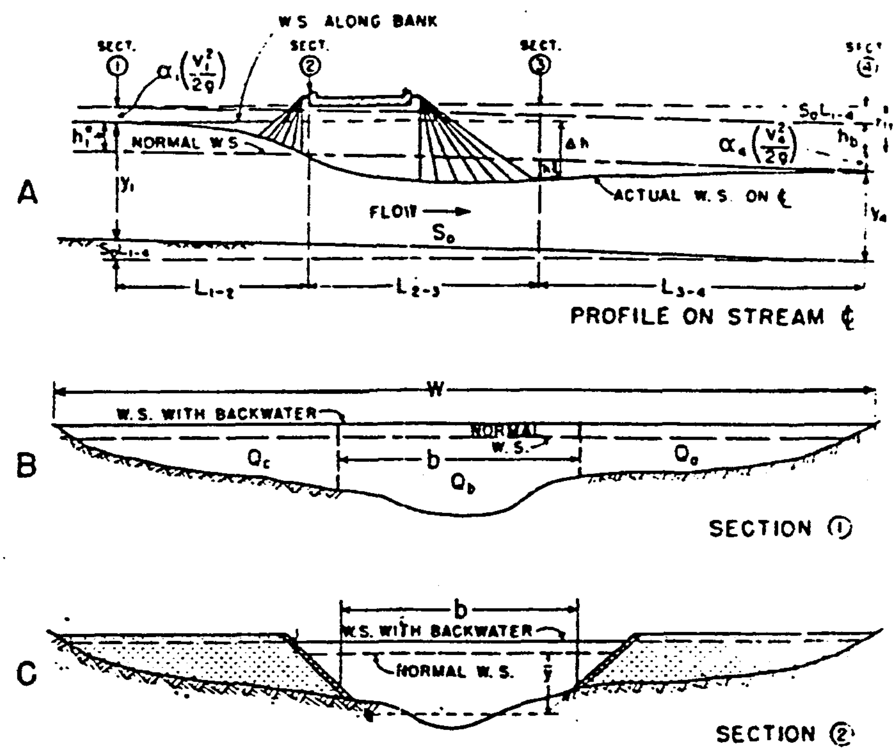

Figure D.2 Normal crossing (U.S. Dept. of Transportation, 1978)

D.3 COMPUTATION OF BACKWATER

The expression for computation of backwater upstream from a bridge constricting the flow is as follows:

$$h_1 = K \alpha_2 \frac{V_{n2}^2}{2g} + \alpha_1 \left| \left(\frac{A_{n2}^2}{A_4}\right) - \left(\frac{A_{n2}^2}{A_1}\right) \right| \frac{V_{n2}^2}{2g} \qquad \text{(D1)}$$

where

h_1 = total backwater

K = total backwater coefficient

α_1, α_2 = kinetic energy correction coefficients

A_1 = total water area at section 1 (Figure D.2)

A_4 = water-level at section 4 where normal stage is reestablished

A_{n2} = gross water area in constriction measured below normal stage

V_{n2} = average velocity in constriction for flow at normal stage

The value of the overall backwater coefficient, K, is likewise dependent on the value of M but also affected by:

- Number, size, shape and orientation of piers in the constriction.

- Eccentricity or asymmetric position of bridge with respect to the valley cross-section, and

- Skewness of bridge (bridge crosses stream at other than 90° angle).

Thus the total backwater coefficient is:

$$K = K_b + K_p + K_e + K_s \qquad \text{(D2)}$$

where

K_b = base coefficient (dependent on the opening ratio M)

K_e = incremental coefficient to account for eccentricity

K_p = incremental coefficient to account for piers

K_s = incremental coefficient to account for skewness

If the stage at a bridge site is not normal but is increased by unnatural backwater conditions from downstream, then the above computation of the backwater is not strictly applicable. An approximate solution is obtained from the following expression:

$$h_{1A} = K \alpha_2 \frac{V^2_{2A}}{2g} \qquad \text{(D3)}$$

where

V_{2A} = the velocity at abnormal stage at section 2

H_{1A} = backwater for abnormal stage

K = is evaluated in the same manner as for flow at normal stage.

Cases arise in which it is desirable to compute the backwater upstream from a bridge or the discharge under a bridge when flow is in contact with the girders. Once flow makes contact with the upstream girder of a bridge, orifice flow is established, the discharge then varies as the square root of the effective head. The result is a rather rapid increase in discharge for a moderate rise in upstream stage. Two cases can exist:

o Upstream girder in contact with flow: (Figure D.3)

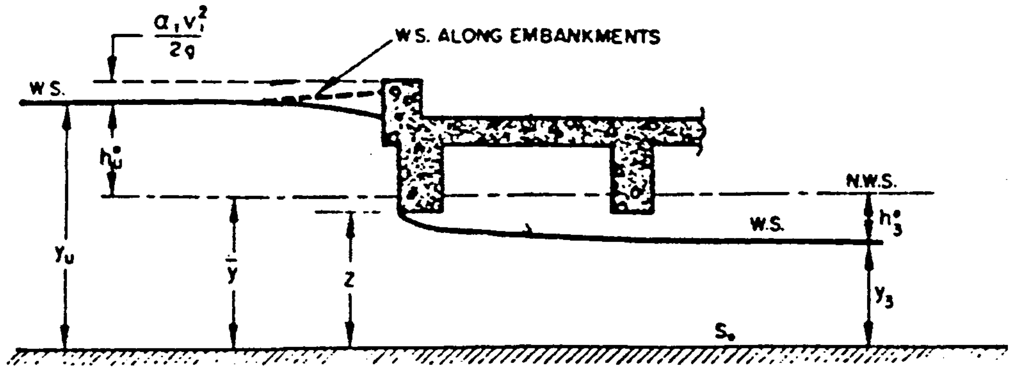

Figure D.3 Upstream girder in contact with the flow (U.S. Dept. of Transportation, 1978)

The flow condition is treated as a sluice gate problem (extreme case), thus:

$$Q = c_d b_N Z \; |2g \; (Y_u - \frac{Z}{2} + \alpha_1 V^2{}_1/2g)|^{1/2} \qquad \text{(D4)}$$

where

Q = total discharge

c_d = coefficient of discharge

b_N = net width of the waterway

Z = vertical distance from bottom of upstream girder to mean riverbed level

Y_u = vertical distance from upstream water level to mean riverbed level o All girders in contact with the flow: (Figure D.4)

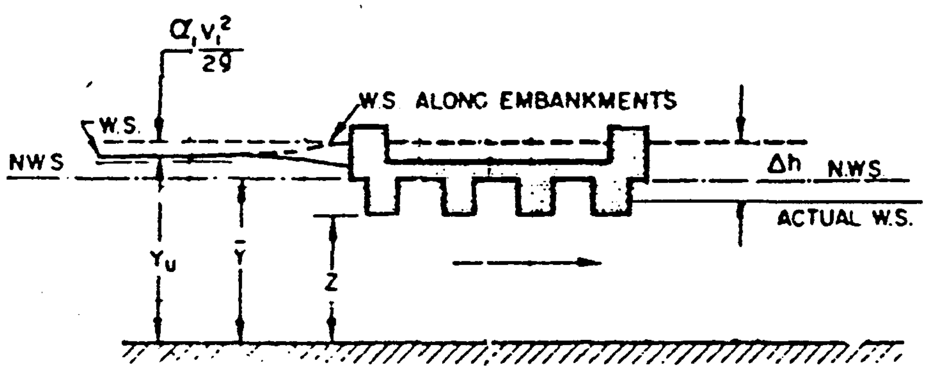

Figure D.4 All girders in contact with the flow (U.S. Dept. of Transportation, 1978)

Where the entire bridge soffit is swamped by the flow, the computation is handled in a different manner. The equation recommended is:

$$Q = 0.80 b_N Z (2g\Delta h)^{1/2} \qquad \text{(D5)}$$

where

Δh = drop in water surface across roadway embankment

In cases where bridge superstructure becomes submerged it is likely that flow will also occur over the approach embankments. To determine the discharge or the upstream water level, the flow over the embankment roadway is treated as flow over a broad-crested weir. The coefficient of free discharge is determined from a design curve and is then corrected for submergence.

The computation of backwater for bridges on streams with fairly steep gradients, using the method above may result in unrealistic values. When this occurs, it is a sign that the flow encountered is probably of type II and the backwater analysis for subcritical or type I flow no longer applies. The backwater for type II flow, with no allowance for piers, eccentricity and skewness is then:

$$h_1 = \alpha_2 \frac{V_{2c}^2}{2g} (C_b+1) - \alpha_1 \frac{V_1^2}{2g} + Y_{2c} - Y \qquad \text{(D6)}$$

where

Y = mean depth in the constriction

Y_{2c} = critical depth in the constriction

D.3.1 RECOGNITION OF FLOW TYPE AND DECISION LOGIC

The prime difficulty in the computation of bridge backwater is to determine which type of flow will occur. The decision logic is based on the guidelines of the U.S. Dept. of Transportation, 1978 and on the HEC-2 computer program approach. The first step is to assume low flow conditions and estimate the water surface elevation on the other side of the bridge. The program determines the total backwater coefficient K , and computes the backwater by using equation (D1). The estimated upstream energy elevation is then compared with the soffit elevation. If the low flow energy elevation is less than the soffit elevation the program concludes that low flow controls. If the low flow energy elevation is greater than the soffit elevation the program will check if the flow is orifice flow. If it is not, an energy elevation assuming that the flow is pressure flow will be calculated. With either type of flow (low or pressure) the program then checks the mimimum top of road elevation to determine if weir flow also exists. The higher energy elevation is assumed to control. If the energy elevation is greater than the top road elevation, a trial and error solution is followed to determine the distribution of the flow under and over the bridge. The flowchart for the bridge method is shown in Figure (D.5).

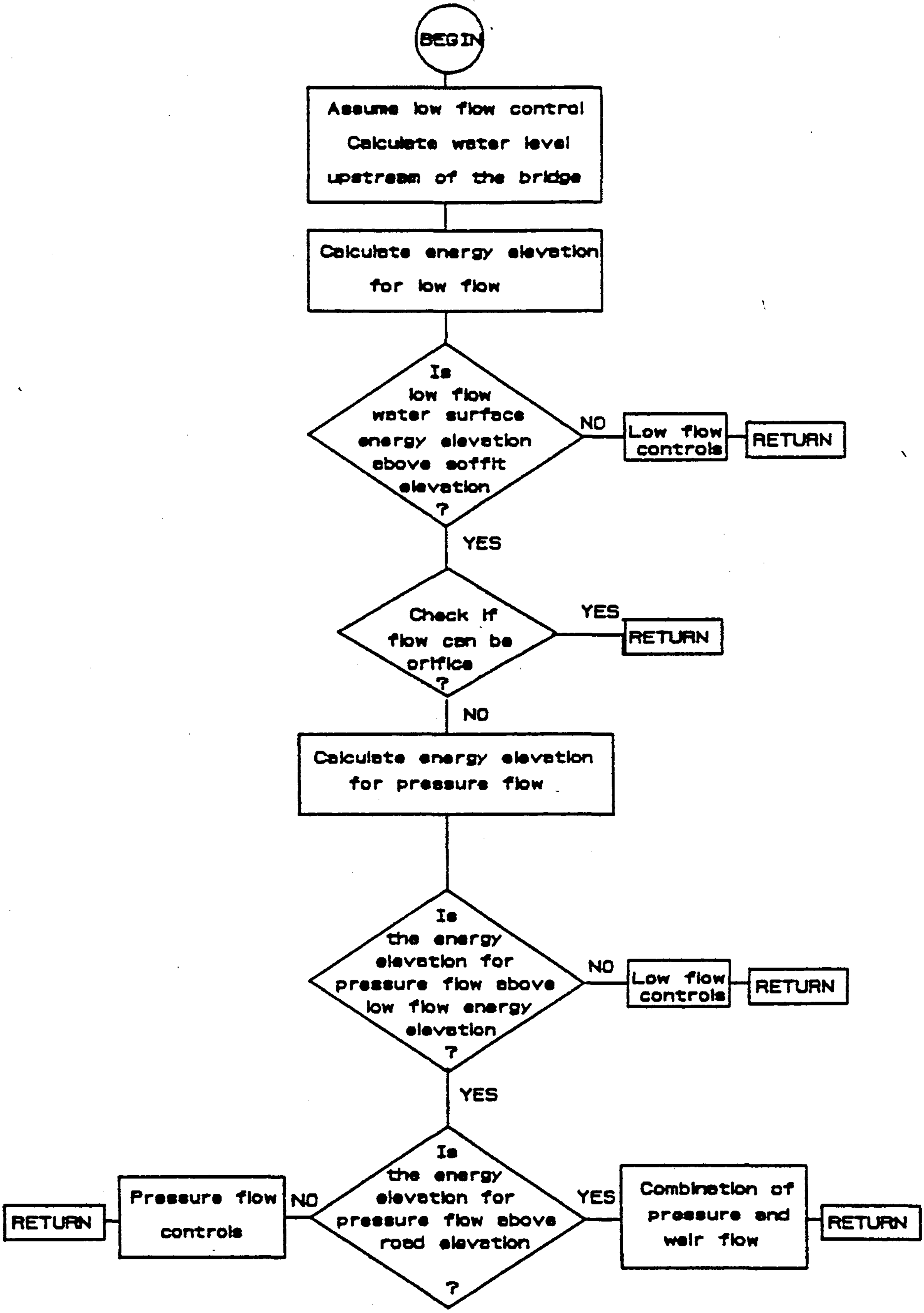

Figure D.5 Bridge method - Logic diagram

D.4 MODELLING GUIDELINES AND BRIDGE INPUT PARAMETERS

The value of the overall backwater coefficient is dependent on the opening ratio, the type of piers, the eccentricity and the skewness of the bridge. For all these factors design curves have been developed and the equations are incorporated in the program for the calculation of the total backwater coefficient.

The user can describe the bridge configuration with the following coefficients in each case:

- **Abutment shape:** Three types of abutments can be modelled:

Coefficient	Abutment shape
1	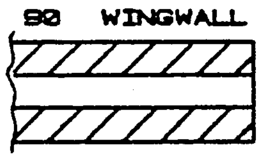
2	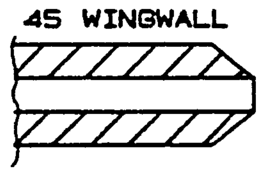
3	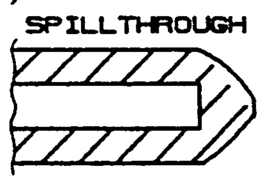

- **Pier shape:**

Coefficient	Pier shape
1	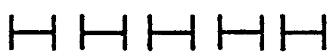
2	
3	

4

5

6

7

8

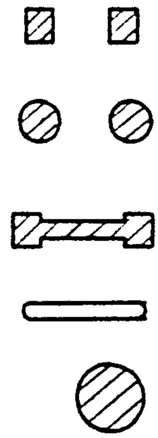

o **Skewed crossing:** The user is only required to input the angle of the bridge abutments to the direction of flow, as indicated in Figure (D.6).

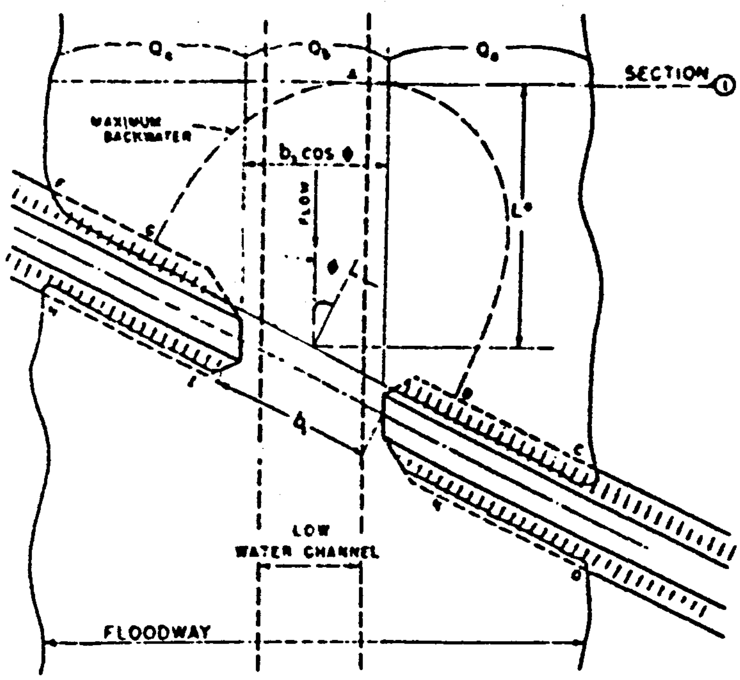

Figure D.6 Skewed crossing (U.S. Dept. of Transportation, 1978)

The modelling of the cross-sections in the vicinity of the bridge needs careful consideration. The location of the cross-sections is shown in Figure (D.7).

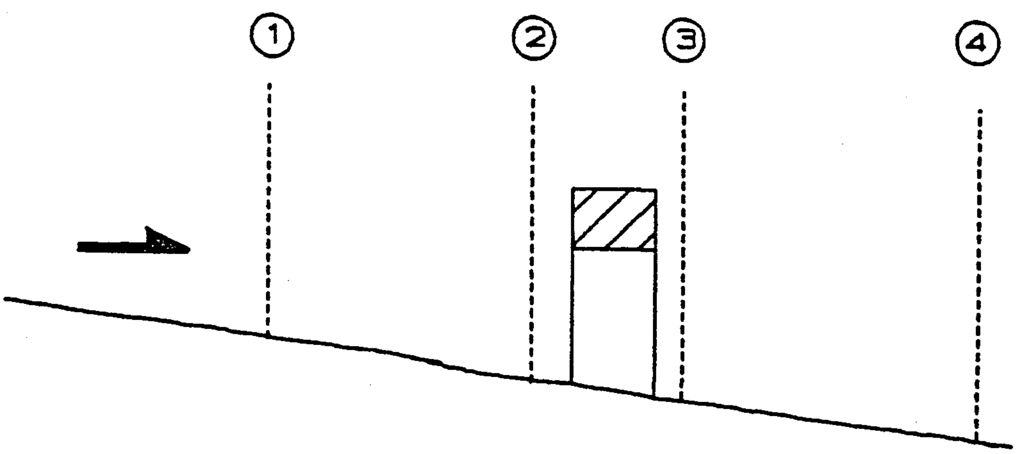

Figure D.7 Location of cross-section in vicinity of bridge

- **Section 4:** must be sufficiently downstream of the bridge so that flow is no longer affected by the bridge.

- **Section 2, 3:** are river cross-sections immediately downstream and upstream from the bridge. The sections should represent the flow area just outside the bridge and their location could be at the downstream and upstream faces of the bridge.

- **Section 1:** is a cross-section upstream of the bridge where the backwater will be calculated. The reach lengths between sections three and four should be equal to the average opening between the abutments.

APPENDIX E. WORKED EXAMPLES

E.1 INTRODUCTION

In the following pages print-outs and photographs of the application of the model in two river reaches and for different flow conditions are presented. Example I is a bridge computation under steady state conditions. Example II is the unsteady flow simulation of the St. Lucia estuary, described in Chapter 5.

The photographs presented in this Appendix illustrate the importance of the use of computer graphics in the numerical modelling of unsteady open channel flow. The graphic representation assist in the handling of the input and output data in an easily understandable form.

E.2 EXAMPLE I - STEADY STATE COMPUTATIONS

Figures (E.1) and (E.2) present the data input and data output generated by the program 'BACKWRES'. Figure (E.3) presents the information appearing on the screen during the steady state simulation. As the computation proceeds to the next upstream section, the user is informed of the water level computed in the present section.

Figure (E.4) depicts the longitudinal profiles computed. Information as to the head level and the critical depth can immediately be visualised. Figures (E.5) and (E.6) depict various cross-sections and the water level computed in order to identify the flood lines.

```
==========================================================================
U N S T E A D Y  F L O W  S I M U L A T I O N  S U I T E  O F  P R O G R A M S
     O N E  D I M E N S I O N A L  F L O W  I N  B R A N C H E D  A N D
              L O O P E D  R I V E R  N E T W O R K S
                  P R I N T I N G   U T I L I T Y
                   Developed by P.KOLOVOPOULOS
                          Version 1.02
==========================================================================

 Cross-section data file name:BRIDGE
 ----------------------------------------


Print-out  selected:                    CROSS-SECTION DATA


                       CONNECTIVITY
=====================================================================
     BRANCH          UPSTREAM BRANCHES          DOWNSTREAM BRANCHES
---------------------------------------------------------------------

       1                  -



=========================================================
                CROSS-SECTION  DATA ECHO
---------------------------------------------------------


CROSS-SECTION NO.  1 . 1
--------------------------

Expansion & Contraction coefficients.......:  0.30,   0.10
Number of cross-section points.............:    11
Reach length of the main channel...........:  0.00
Manning's (n) of the main channel..........: 0.035

 Coordinates
 -------------
      1      2      3      4      5      6      7      8      9     10
X   0.00  20.00  40.00  60.00  80.00 100.00 120.00 140.00 160.00 180.0
Y  93.10  92.50  92.00  92.00  90.15  90.00  89.90  93.20  92.50  93.9
     11
X 200.00
Y  95.51
```

Figure E.1   Bridge example - Cross-sectional data

CROSS-SECTION NO. 1 . 2

Expansion & Contraction coefficients.......: 0.30, 0.10
Number of cross-section points.............: 11
Reach length of the main channel...........: 250.00
Manning's (n) of the main channel..........: 0.035

Coordinates

	1	2	3	4	5	6	7	8	9	10
X	0.00	20.00	40.00	60.00	80.00	100.00	120.00	140.00	160.00	180.0
Y	94.80	94.20	93.70	93.70	91.85	91.70	91.60	94.90	94.20	95.6
	11									
X	200.00									
Y	97.21									

CROSS-SECTION NO. 1 . 3

Expansion & Contraction coefficients.......: 0.30, 0.10
Number of cross-section points.............: 11
Reach length of the main channel...........: 250.00
Manning's (n) of the main channel..........: 0.035

Coordinates

	1	2	3	4	5	6	7	8	9	10
X	0.00	20.00	40.00	60.00	80.00	100.00	120.00	140.00	160.00	180.0
Y	96.50	95.90	95.40	95.40	93.55	93.40	93.30	96.60	95.90	97.3
	11									
X	200.00									
Y	98.91									

CROSS-SECTION NO. 1 . 4

Expansion & Contraction coefficients.......: 0.30, 0.10
Number of cross-section points.............: 11
Reach length of the main channel...........: 250.00
Manning's (n) of the main channel..........: 0.035

Coordinates

	1	2	3	4	5	6	7	8	9	10
X	0.00	20.00	40.00	60.00	80.00	100.00	120.00	140.00	160.00	180.0
Y	98.20	97.60	97.10	97.10	95.25	95.10	95.00	98.30	97.60	99.0
	11									
X	200.00									
Y	100.61									

Figure E.1 (Continued)

CROSS-SECTION NO. 1 . 5

Expansion & Contraction coefficients.......: 0.50, 0.30
Number of cross-section points.............: 11
Reach length of the main channel...........: 250.00
Manning's (n) of the main channel..........: 0.035

Coordinates

	1	2	3	4	5	6	7	8	9	10
X	0.00	20.00	40.00	60.00	80.00	100.00	120.00	140.00	160.00	180.0
Y	99.90	99.30	98.80	98.80	96.95	96.80	96.70	100.00	99.30	100.7

	11
X	200.00
Y	102.31

CROSS-SECTION NO. 1 . 6 -BRIDGE

Soffit elevation.......................: 98.70
Invert length & elevation..............: 40.00, 96.80
Bridge invert location (station points): 5, 5
Abutments (slope,type,direction).......: 90, 1, 1
Road width & elevation.................: 10.00, 99.75
Length of the reach....................: 5.00
Piers (number, type, width)............: 1, 8, 1.00

CROSS-SECTION NO. 1 . 7

Expansion & Contraction coefficients.......: 0.50, 0.30
Number of cross-section points.............: 11
Reach length of the main channel...........: 20.00
Manning's (n) of the main channel..........: 0.035

Coordinates

	1	2	3	4	5	6	7	8	9	10
X	0.00	20.00	40.00	60.00	80.00	100.00	120.00	140.00	160.00	180.0
Y	100.00	99.40	98.90	98.90	97.05	96.90	96.80	100.10	99.40	100.8

	11
X	200.00
Y	102.41

Figure E.1 (Continued)

CROSS-SECTION NO. 1 . 8

Expansion & Contraction coefficients.......: 0.30, 0.10
Number of cross-section points.............: 11
Reach length of the main channel...........: 50.00
Manning's (n) of the main channel..........: 0.035

Coordinates

	1	2	3	4	5	6	7	8	9	10
X	0.00	20.00	40.00	60.00	80.00	100.00	120.00	140.00	160.00	180.0
Y	100.32	99.72	99.22	99.22	97.37	97.22	97.12	100.42	99.72	101.1

	11
X	200.00
Y	102.73

Figure E.1 (Continued)

==

B A C K W A T E R   S I M U L A T I O N   P R O G R A M

COMPUTED WATER SURFACE PROFILES

Developed by: P.KOLOVOPOULOS

==

Data file name:BRIDG2

The results are set in the following order for each cross-section:

----

(1) Computed water surface elevation (2) Critical water surface elevation
(3) Energy elevation (4) Channel slope (5) Depth of flow (6) Velocity head
(7) Energy loss due to friction (8) Cross-section area
(9) Minimum elevation (10) Width at the calculated water-surface elevation
(11) Froude number (12) Velocity head coefficient
(13)(14)(15) Amount of flow in the channel, the left and the right overbanks
(16)(17)(18) Mean velocity in the channel, the left and the right overbanks

----

CROSS-SECTION NO. 1 . 1

----

(1)	91.01	(2)	90.88	(3)	91.28	(4)	0.00680	(5)	1.11	(6)	0.28
(7)	0.000	(8)	47.45	(9)	89.90	(10)	55.97	(11)	0.65	(12)	1.23
(13)	100.00	(14)	0.00	(15)	0.00	(16)	2.11	(17)	0.00	(18)	0.00

CROSS-SECTION NO. 1 . 2

----

(1)	92.71	(2)	92.58	(3)	92.98	(4)	0.00680	(5)	1.11	(6)	0.28
(7)	1.700	(8)	47.46	(9)	91.60	(10)	55.97	(11)	0.65	(12)	1.23
(13)	100.00	(14)	0.00	(15)	0.00	(16)	2.11	(17)	0.00	(18)	0.00

CROSS-SECTION NO. 1 . 3

----

(1)	94.41	(2)	94.28	(3)	94.68	(4)	0.00680	(5)	1.11	(6)	0.28
(7)	1.700	(8)	47.45	(9)	93.30	(10)	55.97	(11)	0.65	(12)	1.23
(13)	100.00	(14)	0.00	(15)	0.00	(16)	2.11	(17)	0.00	(18)	0.00

Figure E.2 Results from the steady-state simulation

```
CROSS-SECTION NO.  1 . 4
------------------------------

 (1)  96.11 ¦ (2)  95.98  ¦ (3)  96.38 ¦ (4)0.00680 ¦ (5)   1.11 ¦ (6)   0.28
 (7)  1.700 ¦ (8)  47.47  ¦ (9)  95.00 ¦(10)  55.98 ¦(11)   0.65 ¦(12)   1.23
(13) 100.00 ¦(14)   0.00  ¦(15)   0.00 ¦(16)   2.11 ¦(17)   0.00 ¦(18)   0.00


CROSS-SECTION NO.  1 . 5
------------------------------

 (1)  97.35 ¦ (2)  97.68  ¦ (3)  98.19 ¦ (4)0.00680 ¦ (5)   1.15 ¦ (6)   0.34
 (7)  1.803 ¦ (8)  40.87  ¦ (9)  96.70 ¦(10)  38.99 ¦(11)   0.65 ¦(12)   1.11
(13) 100.00 ¦(14)   0.00  ¦(15)   0.00 ¦(16)   2.45 ¦(17)   0.00 ¦(18)   0.00


CROSS-SECTION NO.  1 . 6  - B R I D G E
---------------------------------------------
```

The results for the bridge are set in the following order:

(1) Amount of flow through opening
(2) Water surface elevation at bridge (downstream embankment)
(3) Water surface elevation without bridge
(4) Critical water surface elevation
(5) Total weir flow (6) Total weir length

```
 (1) 100.00  (2)  97.85  (3)  97.81  (4)  97.68  (5)   0.00  (6) 144.55
```

FLOW THROUGH BRIDGE IS LOW FLOW

```
CROSS-SECTION NO.  1 . 7
------------------------------

 (1)  97.87 ¦ (2)  97.75  ¦ (3)  98.23 ¦ (4)0.00600 ¦ (5)   1.07 ¦ (6)   0.36
 (7)  0.138 ¦ (8)  39.88  ¦ (9)  96.80 ¦(10)  38.99 ¦(11)   0.70 ¦(12)   1.11
(13) 100.00 ¦(14)   0.00  ¦(15)   0.00 ¦(16)   2.51 ¦(17)   0.00 ¦(18)   0.00


CROSS-SECTION NO.  1 . 8
------------------------------

 (1)  98.33 ¦ (2)  98.10  ¦ (3)  98.55 ¦ (4)0.00600 ¦ (5)   1.21 ¦ (6)   0.22
 (7)  0.317 ¦ (8)  53.57  ¦ (9)  97.12 ¦(10)  57.79 ¦(11)   0.47 ¦(12)   1.24
(13) 100.00 ¦(14)   0.00  ¦(15)   0.00 ¦(16)   1.87 ¦(17)   0.00 ¦(18)   0.00
```

Figure E.2 (Continued)

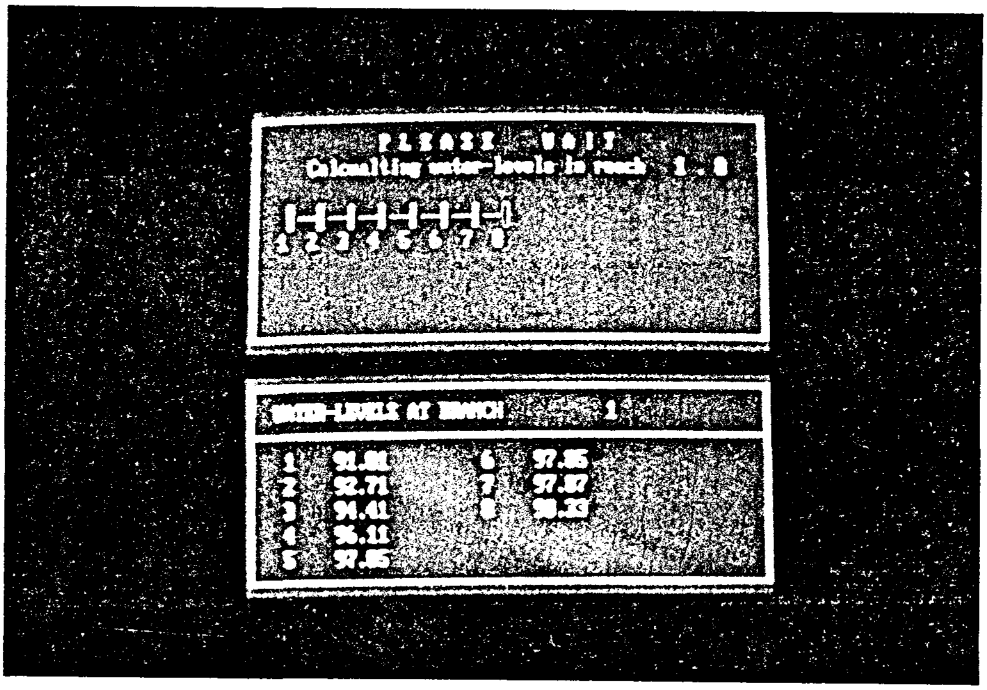

Figure E.3 Photograph of information shown during steady-state simulation

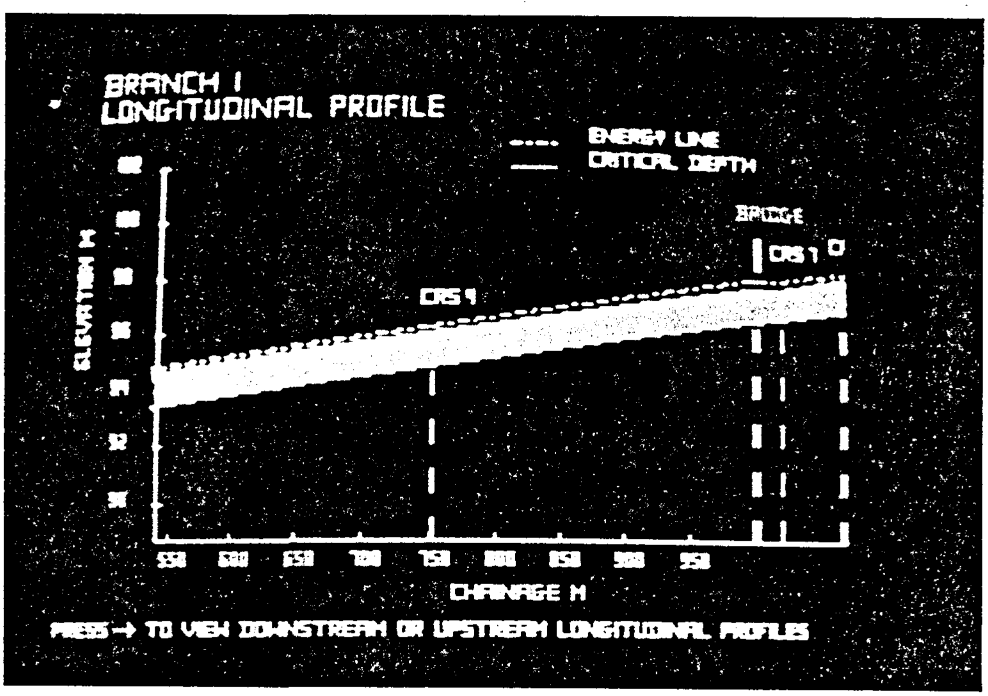

Figure E.4 Photograph of Longitudinal profile - (BACKWRES program)

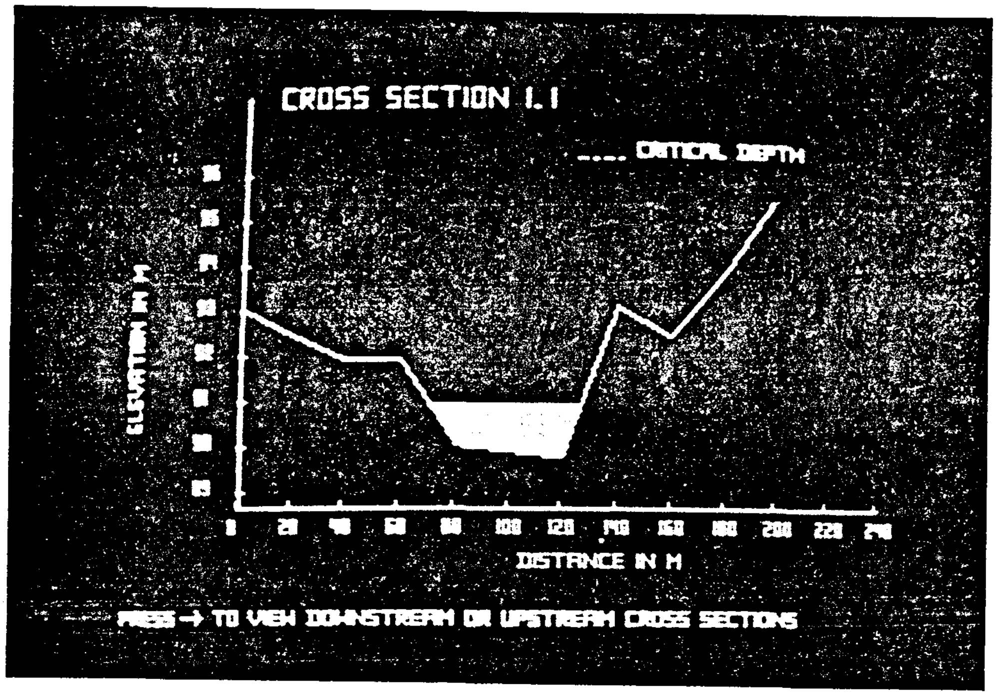

Figure E.5 Photograph of the plot of cross-section 1.1

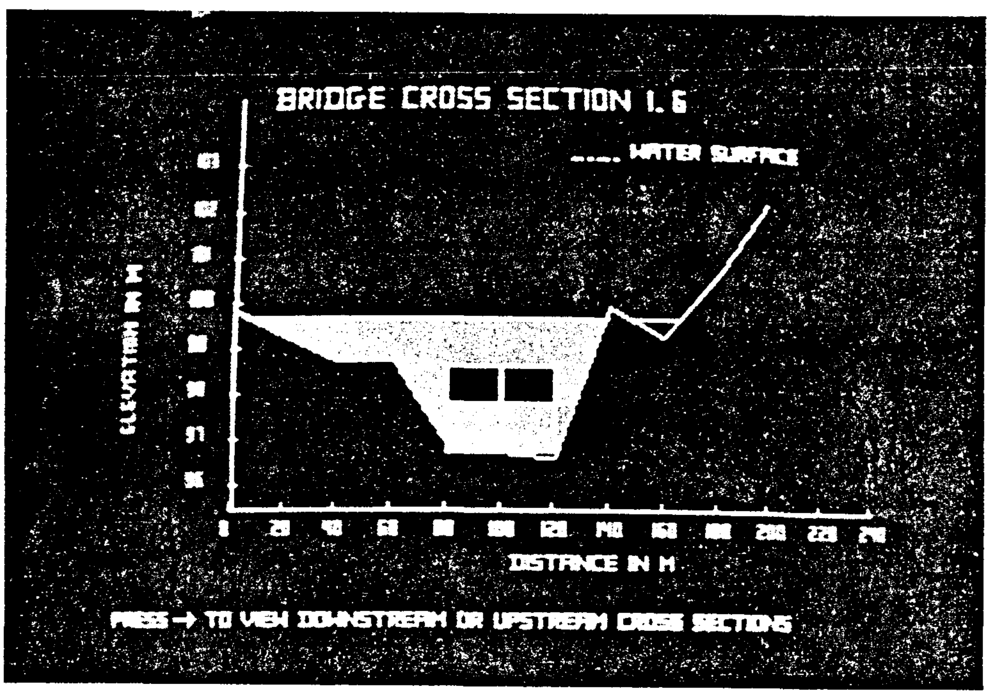

Figure E.6 Photograph of the plot of bridge-section 1.6

E.3 EXAMPLE II - UNSTEADY FLOW CONDITIONS

Figure (E.7) illustrates the cross-sectional data used for the St. Lucia estuary simulation. Figure (E.8) presents the output generated for the selected reach (1.1). Water levels, flowrates and velocities are printed for each time step. Both outputs were generated by the program "DATAPR".

Figures (E.9) and (E.10) depict examples of the cross-section and boundary data input. Figure (E.11) shows the screen during the unsteady flow simulation. Information as to the iteration accuracy is shown in every time step so the user is aware of the stability and progress of the simulation. Figures (E.12) to (E.14) depict the screens showing the computed water levels and flowrates at cross-sections (1.1) and (1.5). Figure (E.15) is a plot of cross-section (1.1) with the minimum and maximum water levels computed during the simulation. Figure (E.16) is a mass-curve plot for cross-section (1.1). All screens are generated by the program "UNRES". They can assist the modeller to analyse the results and immediately visualise the important factors.

```
========================================================================
U N S T E A D Y   F L O W   S I M U L A T I O N   S U I T E  OF  P R O G R A M S
     O N E  D I M E N S I O N A L  F L O W   I N   B R A N C H E D  A N D
              L O O P E D  R I V E R  N E T W O R K S
                  P R I N T I N G    U T I L I T Y
               . Developed by P.KOLOVOPOULOS
                         Version 1.02
========================================================================

 Cross-section data file name:LUCIA1
 --------------------------------------


Print-out  selected:                    CROSS-SECTION DATA



                    CONNECTIVITY
==================================================================
    BRANCH         UPSTREAM BRANCHES          DOWNSTREAM BRANCHES
------------------------------------------------------------------

       1                  -



=======================================================
              CROSS-SECTION  DATA ECHO
-------------------------------------------------------



CROSS-SECTION NO.  1 . 1
-------------------------

Number of cross-section points............:     17
Reach length of the main channel..........:   0.00
Points where flood-plains begin...........:   3,15
Manning's (n) of the main channel.........:  0.021
Manning's (n) of the left & right overbanks:  0.021, 0.021

 Coordinates
 ------------
      1       2       3       4       5       6       7       8       9      10
X   0.00    5.00    7.50   16.50   48.50   78.00   92.50   94.00  100.00  106.0
Y   2.00    1.00    0.00   -0.50   -1.50   -2.00   -3.00   -3.50   -3.75   -3.5
     11      12      13      14      15      16      17
X 107.50  122.00  151.50  183.50  192.50  195.00  200.00
Y  -3.00   -2.00   -1.50   -0.50    0.00    1.00    2.00
```

Figure E.7   St. Lucia estuary - Cross-sectional data

CROSS-SECTION NO. 1 . 2

Number of cross-section points.............: 17
Reach length of the main channel...........:1470.00
Reach lengths of the left & right overbanks:1470.00,1470.00
Manning's (n) of the main channel..........: 0.021
Manning's (n) of the left & right overbanks: 0.021, 0.021

Coordinates

	1	2	3	4	5	6	7	8	9	10
X	0.00	43.50	46.00	48.50	155.50	199.00	253.50	271.00	283.50	296.0
Y	2.00	0.70	0.00	-0.30	-0.50	-0.90	-1.30	-2.00	-2.15	-2.0
	11	12	13	14	15	16	17			
X	313.50	368.00	411.50	518.50	521.00	523.50	567.00			
Y	-1.30	-0.90	-0.50	-0.30	0.00	0.70	2.00			

CROSS-SECTION NO. 1 . 3

Number of cross-section points.............: 15
Reach length of the main channel...........:1280.00
Reach lengths of the left & right overbanks:1280.00,1280.00
Manning's (n) of the main channel..........: 0.021
Manning's (n) of the left & right overbanks: 0.021, 0.021

Coordinates

	1	2	3	4	5	6	7	8	9	10
X	0.00	52.50	64.50	70.50	77.00	81.00	95.00	125.00	155.00	169.0
Y	2.00	0.40	0.00	-0.50	-1.00	-1.50	-2.00	-2.20	-2.00	-1.5
	11	12	13	14	15					
X	173.00	179.50	185.50	197.50	250.00					
Y	-1.00	-0.50	0.00	0.40	2.00					

CROSS-SECTION NO. 1 . 4

Number of cross-section points.............: 17
Reach length of the main channel...........: 720.00
Reach lengths of the left & right overbanks: 720.00, 720.00
Manning's (n) of the main channel..........: 0.021
Manning's (n) of the left & right overbanks: 0.021, 0.021

Coordinates

	1	2	3	4	5	6	7	8	9	10
X	0.00	53.50	55.50	58.00	80.00	103.50	113.00	133.00	150.00	167.0
Y	2.00	0.40	0.00	-0.20	-0.50	-1.00	-1.50	-2.00	-2.15	-2.0
	11	12	13	14	15	16	17			
X	187.00	196.50	220.00	242.00	244.50	246.50	300.00			
Y	-1.50	-1.00	-0.50	-0.20	0.00	0.40	2.00			

Figure E.7 (Continued)

CROSS-SECTION NO. 1 . 5

Number of cross-section points.............: 17
Reach length of the main channel...........:1170.00
Reach lengths of the left & right overbanks:1170.00,1170.00
Manning's (n) of the main channel..........: 0.021
Manning's (n) of the left & right overbanks: 0.021, 0.021

Coordinates

	1	2	3	4	5	6	7	8	9	10
X	0.00	16.00	31.50	38.50	67.00	80.50	88.00	109.50	127.50	145.5
Y	2.00	1.00	0.00	-0.30	-0.50	-1.00	-1.50	-2.00	-2.10	-2.0

	11	12	13	14	15	16	17
X	167.00	174.50	188.00	216.50	223.50	239.00	255.00
Y	-1.50	-1.00	-0.50	-0.30	0.00	1.00	2.00

CROSS-SECTION NO. 1 . 6

Number of cross-section points.............: 19
Reach length of the main channel...........: 860.00
Reach lengths of the left & right overbanks: 860.00, 860.00
Manning's (n) of the main channel..........: 0.021
Manning's (n) of the left & right overbanks: 0.021, 0.021

Coordinates

	1	2	3	4	5	6	7	8	9	10
X	0.00	17.50	25.00	138.00	171.00	305.00	330.50	336.50	370.50	375.5
Y	2.00	1.00	0.30	0.00	-0.20	-0.50	-1.00	-1.50	-2.00	-2.5

	11	12	13	14	15	16	17	18	19
X	380.50	414.50	420.50	446.00	580.00	613.00	726.00	733.50	751.00
Y	-2.00	-1.50	-1.00	-0.50	-0.20	0.00	0.30	1.00	2.00

CROSS-SECTION NO. 1 . 7

Number of cross-section points.............: 15
Reach length of the main channel...........:1070.00
Reach lengths of the left & right overbanks:1070.00,1070.00
Manning's (n) of the main channel..........: 0.021
Manning's (n) of the left & right overbanks: 0.021, 0.021

Coordinates

	1	2	3	4	5	6	7	8	9	10
X	0.00	2.50	5.50	15.50	22.50	36.50	51.50	65.50	79.50	94.5
Y	2.00	1.00	0.00	-0.50	-1.00	-1.50	-2.00	-2.10	-2.00	-1.5

	11	12	13	14	15
X	108.50	115.50	125.50	128.50	131.00
Y	-1.00	-0.50	0.00	1.00	2.00

Figure E.7 (Continued)

CROSS-SECTION NO. 1 . 8

Number of cross-section points.............: 17
Reach length of the main channel...........:1080.00
Reach lengths of the left & right overbanks:1080.00,1080.00
Manning's (n) of the main channel..........: 0.021
Manning's (n) of the left & right overbanks: 0.021, 0.021

Coordinates

	1	2	3	4	5	6	7	8	9	10
X	0.00	5.00	11.50	13.50	108.00	189.00	215.50	240.50	262.50	284.5
Y	2.00	1.00	0.00	-0.10	-0.30	-0.50	-1.00	-1.40	-1.60	-1.4

	11	12	13	14	15	16	17
X	309.50	336.00	417.00	511.50	513.50	520.00	525.00
Y	-1.00	-0.50	-0.30	-0.10	0.00	1.00	2.00

CROSS-SECTION NO. 1 . 9

Number of cross-section points.............: 15
Reach length of the main channel...........: 480.00
Reach lengths of the left & right overbanks: 480.00, 480.00
Manning's (n) of the main channel..........: 0.021
Manning's (n) of the left & right overbanks: 0.021, 0.021

Coordinates

	1	2	3	4	5	6	7	8	9	10
X	0.00	36.00	38.00	45.00	59.50	75.00	90.00	100.00	110.00	125.0
Y	2.00	1.00	0.00	-0.50	-1.00	-1.50	-2.00	-2.05	-2.00	-1.5

	11	12	13	14	15
X	140.50	155.00	162.00	164.00	200.00
Y	-1.00	-0.50	0.00	1.00	2.00

CROSS-SECTION NO. 1 . 10

Number of cross-section points.............: 15
Reach length of the main channel...........: 650.00
Reach lengths of the left & right overbanks: 650.00, 650.00
Manning's (n) of the main channel..........: 0.021
Manning's (n) of the left & right overbanks: 0.021, 0.021

Coordinates

	1	2	3	4	5	6	7	8	9	10
X	0.00	40.50	62.00	72.00	218.00	250.50	252.50	288.00	310.50	325.5
Y	2.00	1.00	0.00	-0.20	-0.50	-1.00	-1.50	-1.70	-1.50	-1.0

	11	12	13	14	15
X	358.00	504.00	514.00	535.50	576.00
Y	-0.50	-0.20	0.00	1.00	2.00

Figure E.7 (Continued)

CROSS-SECTION NO. 1 . 11

Number of cross-section points.............: 15
Reach length of the main channel...........:2050.00
Reach lengths of the left & right overbanks:2050.00,2050.00
Manning's (n) of the main channel..........: 0.021
Manning's (n) of the left & right overbanks: 0.021, 0.021

Coordinates

	1	2	3	4	5	6	7	8	9	10
X	0.00	68.00	95.50	105.50	114.00	123.00	162.00	200.00	238.00	277.0
Y	2.00	1.00	0.50	0.00	-0.50	-0.80	-1.10	-1.50	-1.10	-0.8

	11	12	13	14	15
X	286.00	294.50	304.50	332.00	400.00
Y	-0.50	0.00	0.50	1.00	2.00

Figure E.7 (Continued)

UNSTEADY FLOW SIMULATION SUITE OF PROGRAMS
ONE DIMENSIONAL FLOW IN BRANCHED AND
LOOPED RIVER NETWORKS
PRINTING UTILITY
Developed by P.KOLOVOPOULOS
Version 1.02

Result file name:LUCIA

Print-out selected: RESULT FILE

REACH 1. 1

TIME(hours)	WATER LEVEL	FLOWRATE	VELOCITY
18. 00	0.316	63.487	0.178
18. 30	0.375	-31.116	-0.085
19. 00	0.401	-101.803	-0.274
19. 30	0.411	-82.864	-0.222
20. 00	0.384	-49.940	-0.136
20. 30	0.269	36.728	0.106
21. 00	0.141	116.953	0.362
21. 30	0.065	113.750	0.368
22. 00	0.029	94.381	0.311
22. 30	0.007	84.975	0.284
23. 00	-0.016	78.237	0.266
23. 30	-0.078	91.320	0.322
0. 00	-0.138	90.717	0.333
0. 30	-0.185	85.741	0.325
1. 00	-0.208	74.981	0.288
1. 30	-0.211	64.432	0.249
2. 00	-0.209	58.103	0.224
2. 30	-0.201	52.210	0.200
3. 00	-0.054	-20.770	-0.072
3. 30	0.075	-75.474	-0.242
4. 00	0.070	-20.073	-0.065
4. 30	0.168	-88.069	-0.268
5. 00	0.292	-145.388	-0.413
5. 30	0.420	-173.368	-0.462
6. 00	0.482	-149.839	-0.387
6. 30	0.519	-133.026	-0.338
7. 00	0.534	-114.756	-0.289
7. 30	0.511	-74.824	-0.191
8. 00	0.402	17.965	0.048
8. 30	0.330	60.423	0.168

Figure E.8 St. Lucia estuary - Simulation results at cross-section (1.1)

REACH 1. 1

TIME(hours)	WATER LEVEL	FLOWRATE	VELOCITY
9. 00	0.241	117.095	0.342
9. 30	0.165	118.463	0.361
10. 00	0.117	110.019	0.344
10. 30	0.048	119.488	0.390
11. 00	0.004	105.729	0.354
11. 30	-0.023	94.404	0.322
12. 00	-0.073	99.589	0.351
12. 30	-0.109	90.816	0.327
13. 00	-0.134	82.611	0.302
13. 30	-0.159	78.067	0.291
14. 00	-0.182	74.048	0.280
14. 30	-0.203	70.701	0.271
15. 00	-0.213	63.665	0.246
15. 30	-0.117	11.475	0.042
16. 00	-0.041	-12.627	-0.043
16. 30	-0.001	-14.806	-0.050
17. 00	0.077	-57.266	-0.184
17. 30	0.334	-251.340	-0.699
18. 00	0.456	-175.879	-0.460
18. 30	0.526	-172.478	-0.437
19. 00	0.584	-166.768	-0.411
19. 30	0.623	-159.106	-0.385
20. 00	0.606	-112.889	-0.276
20. 30	0.447	19.733	0.052
21. 00	0.387	26.860	0.073
21. 30	0.326	61.991	0.173
22. 00	0.255	101.563	0.295
22. 30	0.186	103.637	0.312
23. 00	0.114	101.785	0.319
23. 30	0.026	108.500	0.359
0. 00	-0.016	87.101	0.295
0. 30	-0.052	80.591	0.280
1. 00	-0.098	82.208	0.294
1. 30	-0.146	82.163	0.303
2. 00	-0.183	76.271	0.288
2. 30	-0.204	68.180	0.262
3. 00	-0.217	61.416	0.238
3. 30	-0.224	55.728	0.217
4. 00	-0.135	7.493	0.027
4. 30	-0.023	-43.677	-0.149
5. 00	0.055	-69.915	-0.227
5. 30	0.183	-133.998	-0.404
6. 00	0.272	-128.471	-0.369
6. 30	0.345	-134.250	-0.371
7. 00	0.447	-167.471	-0.440
7. 30	0.565	-200.734	-0.499
8. 00	0.521	-96.029	-0.244
8. 30	0.444	-31.937	-0.084
9. 00	0.364	15.673	0.043
9. 30	0.247	97.349	0.284
10. 00	0.198	95.555	0.286
10. 30	0.095	121.687	0.386

Figure E.8 (Continued)

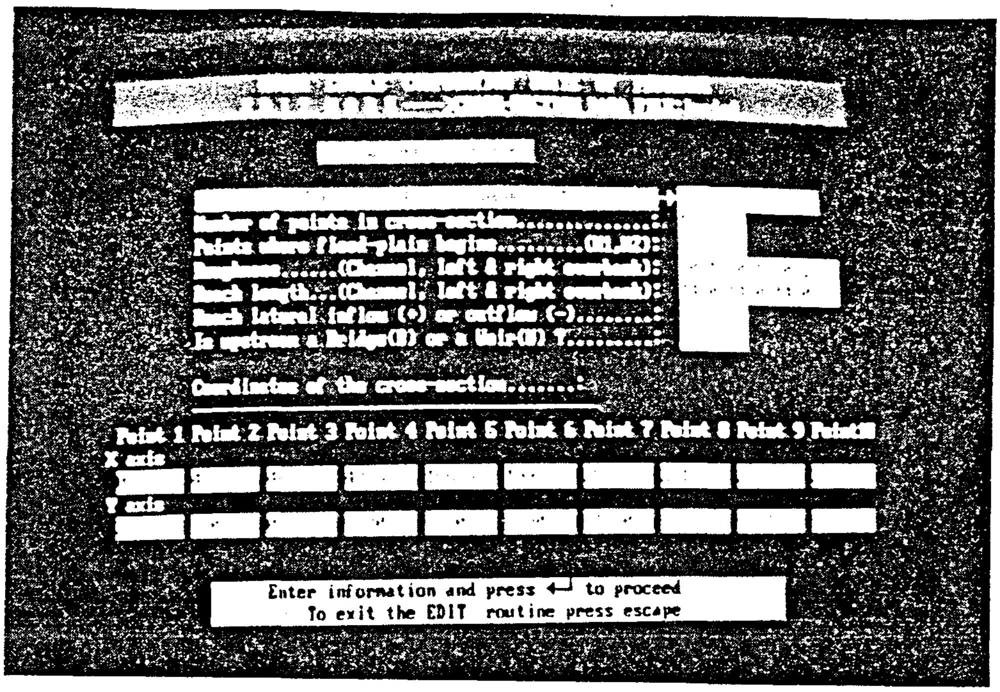

Figure E.9 Photograph of cross-sectional data input screen

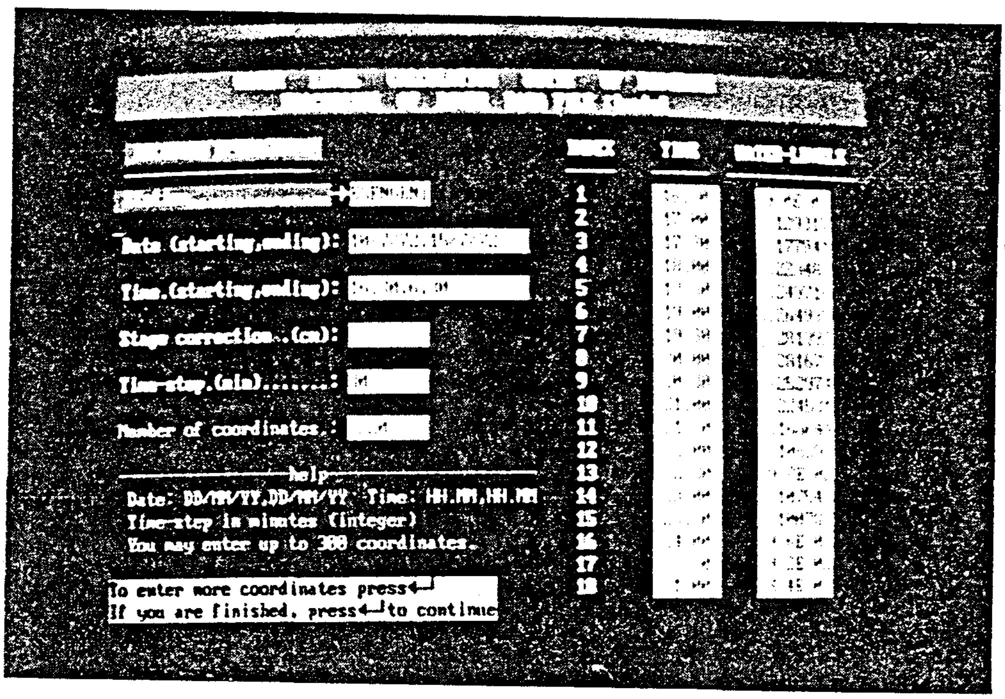

Figure E.10 Photograph of boundary data input screen

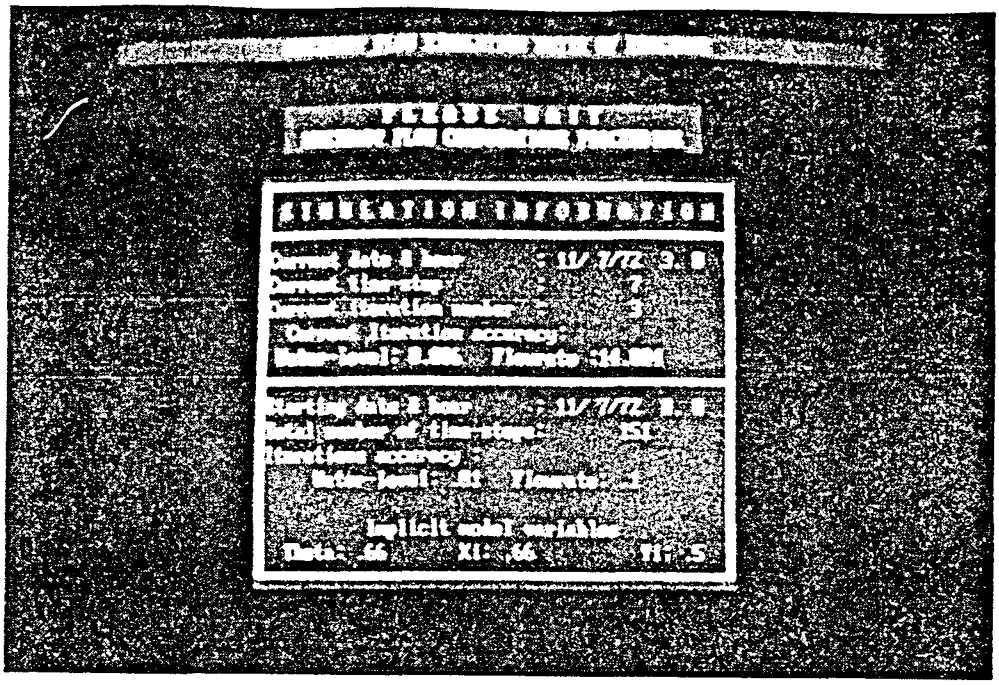

Figure E.11 Photograph of information printed during unsteady-state simulation

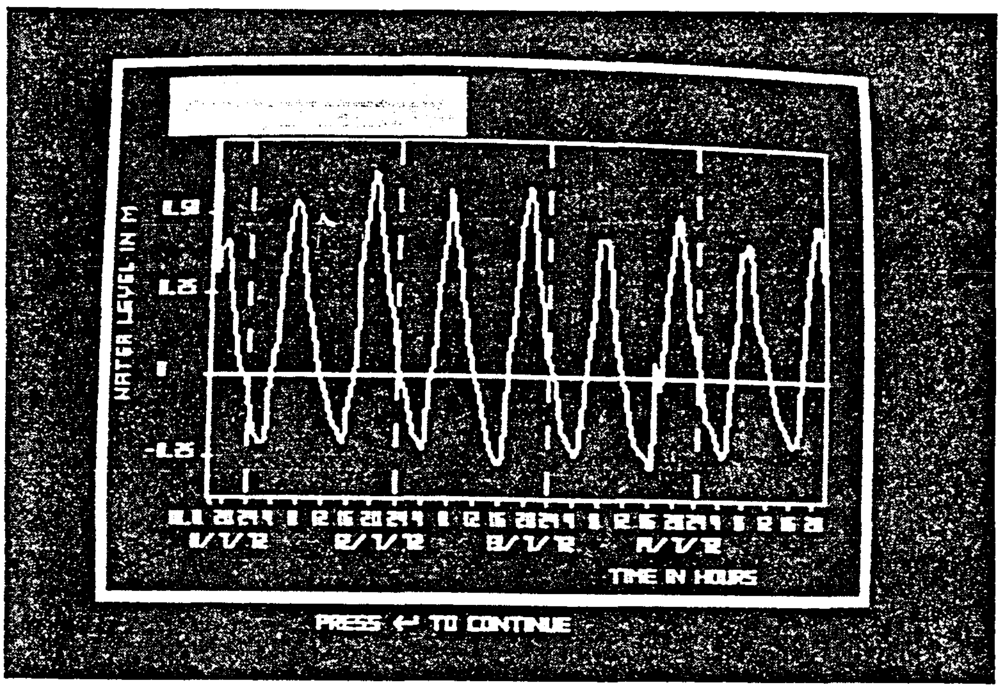

Figure E.12 Photograph of water level plot at cross-section (1.1)

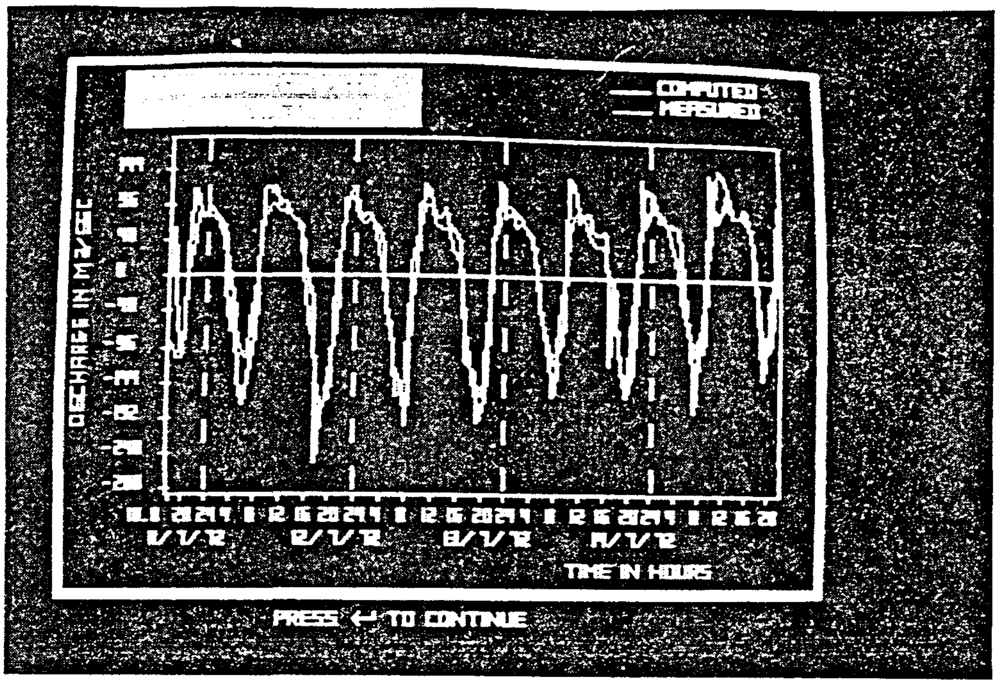

Figure E.13 Photograph of flowrate plot at cross-section (1.1)

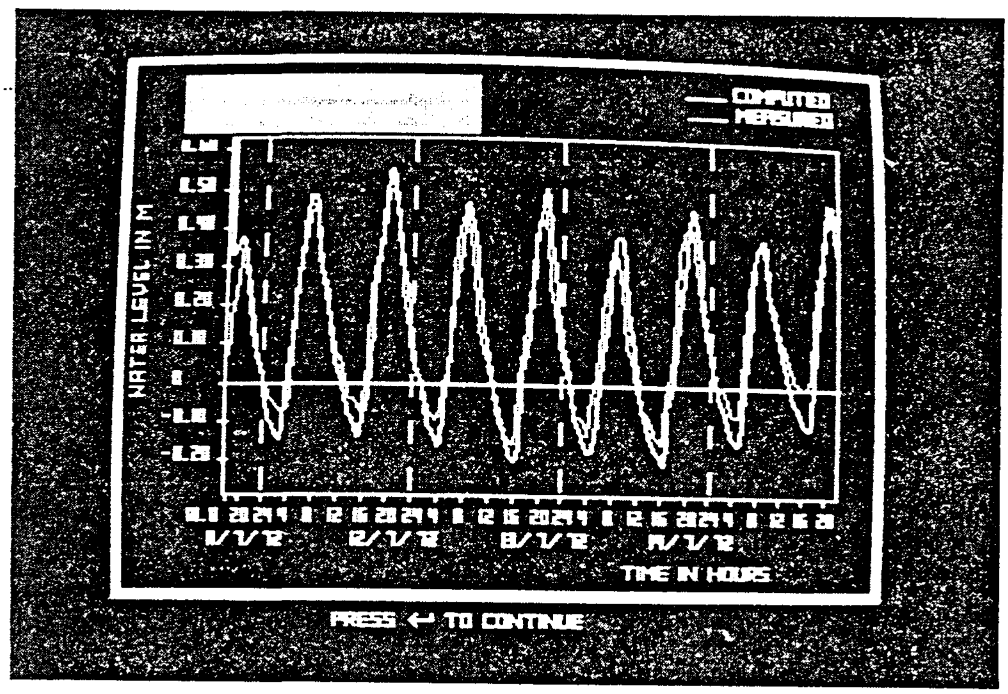

Figure E.14 Photograph of water level plot at cross-section (1.5)

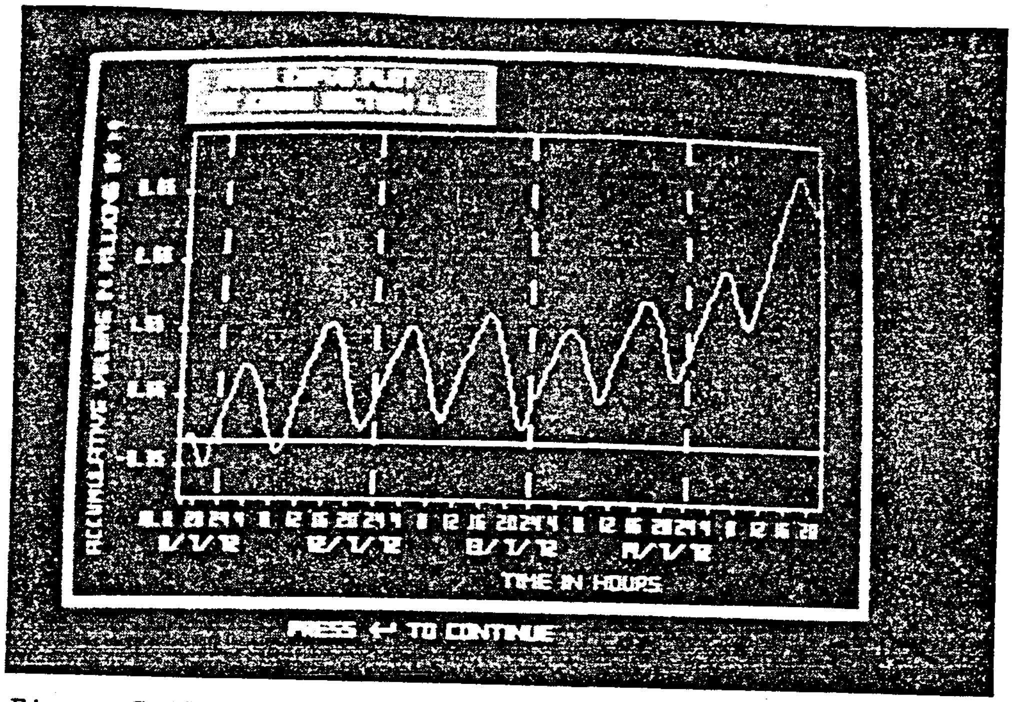

Figure E.15 Photograph of mass-curve plot at cross-section (1.1)

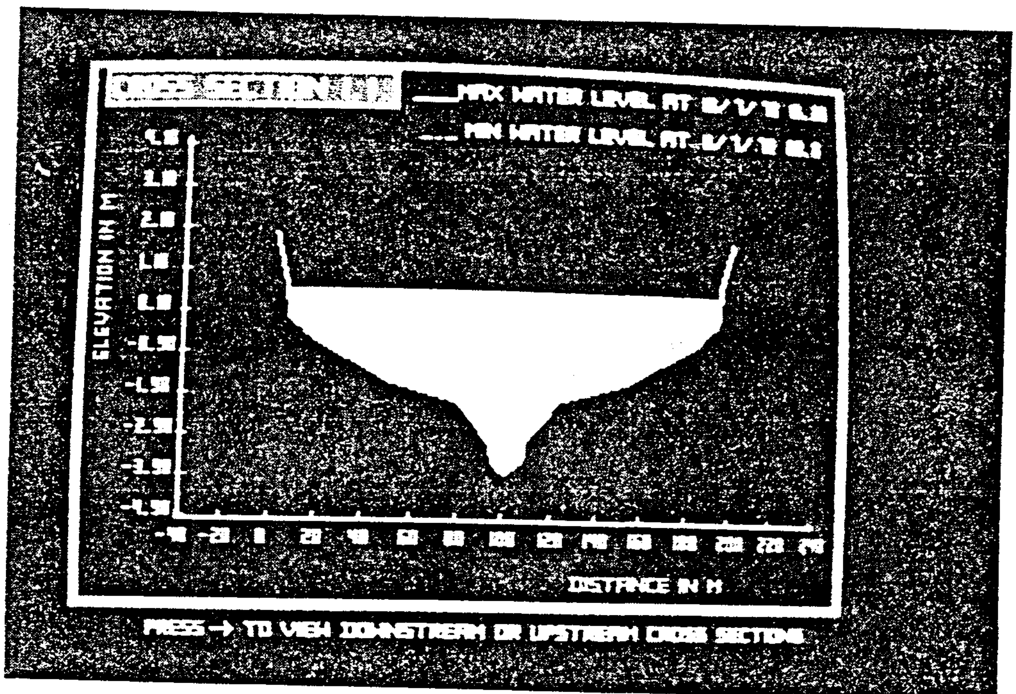

Figure E.16 Photograph of the plot of cross-section (1.1)